HMGB proteins, lncRNAs, and their interaction in epithelial ovarian cancer

Martín Salamini Montemurri

Doctoral Thesis

2023

Supervisors: Dr. Mª Esperanza Cerdán Villanueva and Dr. Mónica Lamas Maceiras Programa Oficial de Doutoramento en Bioloxía Celular e Molecular

UNIVERSIDADE DA CORUÑA

El autor de este trabajo ha disfrutado durante la realización de esta tesis doctoral de un contrato a cargo del proyecto de Consolidación de Grupos de Referencia Competitiva de la Xunta de Galicia (ref. ED431C 2016-012) por la Universidade da Coruña (enero 2019 - mayo 2019) cofinanciado por el Fondo Europeo de Desarrollo Regional (FEDER), una ayuda de apoyo a la etapa predoctoral en las universidades del Sistema Universitario de Galicia de la Xunta de Galicia de la convocatoria de 2019, modalidad A (junio 2019 - septiembre 2019) cofinanciado por el Fondo Social Europeo, y una ayuda predoctoral para la Formación del Profesorado Universitario (FPU) de la convocatoria de 2018 (octubre 2019 - mayo 2023). Como complemento formativo se realizó una estancia en la Facultad de Medicina de la Universidad Católica de Leuven (Leuven, Bélgica) entre junio y septiembre de 2021 en el *Laboratory for RNA Cancer Biology*, financiada por el programa In-Motion (INDITEX-Universidade da Coruña). Parte del trabajo se realizó en el *National Institute on Aging* (Baltimore, Estados Unidos de América) en una estancia realizada entre agosto y noviembre de 2022 en el grupo *RNA Regulation Section*, y que fue financiada por el programa de ayudas para estancias de corta duración de la *European Molecular Biology Organization* (EMBO).

La realización de este trabajo ha sido posible gracias a la financiación obtenida del proyecto del Instituto de Salud Carlos III con referencia PI18/01714 y de los proyectos de la Xunta de Galicia de Consolidación de Grupos de Referencia Competitiva, Contratos ED431C 2016-012 y ED431C 2020-08, cofinanciados por el FEDER.

A mis padres y mi hermana

"*All things are difficult before they are easy.*"-
Thomas Fuller

Quiero comenzar esta sección más informal de la tesis agradeciendo a mis directoras, Esperanza Cerdán y Mónica Lamas, por haberme dado la oportunidad de empezar con aquella beca de colaboración y, años más tarde, de poder realizar la tesis en el grupo Exprela, lo cual me ha permitido aprender mucho y empezar mi carrera investigadora. Agradeceros además por toda vuestra ayuda, disponibilidad, paciencia y compresión.

Me gustaría agradecer a toda la gente que está y estuvo en el laboratorio de Bioquímica y Biología Molecular de la UDC desde que entré hasta ahora: Ángel, Aída, Juanjo, Mariu, Esther (profe), Marián, Ana, Isabel, Manuel, Thamer, Almudena, María, Lidia, Cora, Natalia, Carmen, Esther (alumna), Lucía, Anahir, Josema, Andrea, Isma, Simón, Maya, Flor, Moussa (perdón si me dejo a alguien en el tintero). Dentro de los momentos más destacables, no puedo dejar de mencionar las sobremesas en la salita del café de la facultad hablando de Juego de tronos (sin yo haberla visto) o política, las frases de los Simpson y memes, o teniendo debates de la ciencia y de los científicos, sin olvidarme de las comidas y cenas de Navidad.

Tengo que hacer especial mención a María (o Mary Austin), la pollita jefa, con quien tuve el placer de coincidir estando de prácticas y después al empezar la tesis, y Lidia, la verdadera primera pollita, que llegaste un año después de que yo empezara y fue maravilloso poder compartir poyata contigo y con María, los tres juntos. Gracias a las dos por ser así de buenas conmigo, por aguantarme, por la complicidad, por las risas, por los cotilleos a puerta cerrada, por los memes que buscamos y pegamos en laboratorio, por las carreras, por los truquitos, por las sesiones de terapia entre nosotros, por el karaoke de la ciencia (temazo adaptado de Pokémon), por esperar a que calentara el tupper hasta que quemara las manos, entre otras muchas cosas lindas. Las dos sois bellísimas personas y extraordinarias científicas, valéis mucho, de eso no tengo ninguna duda. Cora, me da pena no haber coincidido más contigo, pero lo bueno si breve, dos veces bueno, y por lo menos pudimos compartir el intenso congreso en Lisboa con “tito” Juanjo y Ángel, te deseo todo lo mejor. Mencionar también a los cracks de los pollitos

del corral de Exprela (Esther, Lucía, Anahir, Josema) que, a pesar de que unos se quedan y otros se van, estoy seguro de que os va a ir a todos fenomenal. También quiero desear mucha suerte y ánimo a Thamer y Almudena, que están ya cerca del fin del doctorado, y a Natalia, Carmen, que están empezando.

Tengo que agradecer enormemente a toda la gente tan maja que he conocido en el CICA, con los que se han forjado grandes amistades y he compartido momentos increíbles: Lucía, Paula, Iago, Jorge Salgado, Diana, Javi Cisneros, Lili, Ana, Javi García, Alberto García, Alberto Cuquejo, Anabel, María Camacho, Jorge Lado, Carol, Amit, Raquel, Rosalía, Pablo, Esteban, Gus, Diego, Junquera, Alex (Vila), Mauro, Antía, Natalia, Fabio, Rocío, Charlene, Gonzalo, Iván, Claudia (perdón si me olvido de alguien otra vez). Sería imposible describir aquí todas esas experiencias, pero de las más destacables, me quedo con mi primer *Science expression*, donde hicimos grupito y comenzamos la tradición de jueves de cañas a 1€; aquel finde en Santiago por todo lo alto; el QuimBioQuim y todo el juego que dio; todas las fiesteCICAs de navidad y verano; las sobremesas jugando al UNO, jenga o sushi go; los festivales de O Son do Camiño (pre y post pandemia); las videollamadas durante el confinamiento; las escapadas a Cedeira; las salidas por el Mi Habana (asere) o el Miracle, entre otros; las tardes perdidas en la “verba baleira” o en “el cursito del CUFIE”; o las tardes de vóley playa. Debo hacer especial mención a Iago, Jorge Salgado, Lucía y Paula por haber tenido el placer de compartir y disfrutar con ellos de “verbas baleiras”, actuaciones musicales, clases de body combat o incluso piso, entre muchas otras cosas. Gracias por tanto. También agradecer al personal de gestión, limpieza y conserjería del CICA por su trabajo.

I switch to English because this thesis would not have been the same if I did not have the chance to go abroad, learn from new cultures, and meet amazing and great scientists. I want to thank Eleonora Leucci and her team for hosting in her lab in Leuven (Belgium) during summer 2021. That experience was great because I was lucky to had met Rocío, Andrés, Eleonora, Cristina, Rocco, Donatela, Denis, and also my residence

roomies Íñigo, Paulino, Alessandro, and Paula. I also want to thank Myriam Gorospe and her team for hosting me in her lab in Baltimore (USA) during fall 2022. Again, that experience was amazing and exciting thanks to having met and spent time inside and outside the lab with Carlos and Gisela.

Me gustaría agradecer por la ayuda técnica prestada a Eloísa, Mónica y Victoria de la unidad de Genómica del CABIMER y a Yulan y Krystyna del laboratorio de Myriam Gorospe con los RNA-Seq, y a Nani y Miriam de la unidad de Biología Molecular de los Servicios de Apoyo a la investigación de la UDC, con quienes empecé realmente mis andanzas en la biología molecular con aquellas prácticas de verano de 2016.

También me gustaría agradecer a la gente con la que he tenido la oportunidad de aprender muchísimo de ciencia y de la vida en laboratorios en los que había estado antes de empezar la tesis, en concreto a Mónica Folgueira, Julián Yáñez y Óscar Lenis, del laboratorio de Biología Celular de la UDC, y, por otro lado, a Ignacio Pérez-de-Castro, Alberto Martín y el resto del grupo del grupo de Terapia Génica del ISCIII, así como a Ujué Moreno por ejercer de mentora a la distancia, escucharme y darme consejos.

Agradecer, como no, a mis amigos ajenos al CICA, Lucas, Yago, Simón, Luciano, Sara, Oscar, Lorenzo, Picos, Alba, Iván, Ocampo, Jerry, por todos los momentos y experiencias compartidas durante estos años, y las que vendrán.

Por último y más importante, agradecer a mi familia, mamá, papá y Georgi, por vuestro apoyo y ánimo incondicional en todo lo que me he propuesto, por vuestros consejos, por vuestra compañía, por haberme dado todo el cariño que un hijo y hermano pueda recibir. Por haberme llevado a ensayos, conciertos, entrenamientos, partidos, clases y viajes, por sembrar la semilla de la curiosidad, creatividad, el gusto por las ciencias, la música y los idiomas y por educarme en valores.

Contents

CONTENTS

ABBREVIATIONS

λ	wavelength
µg	microgram
µL	microliter
ºC	degree Celsius
ATCC	American Type Culture Collection
bp	base pair
CCLE	Cancer Cell Line Encyclopedia
cDNA	complementary DNA
cm	centimeter
DFS	disease-free survival
DNA	deoxyribonucleic acid
DTT	dithiothreitol
eCLIP	enhanced crosslinking immunoprecipitation
EDTA	ethylenediaminetetraacetic acid
EMBO	European Molecular Biology Organization
EMT	epithelial to mesenchymal transition
ENA	European Nucleotide Archive
EOC	epithelial ovarian cancer
FBS	fetal bovine serum
FIGO	Federation of Gynecology and Obstetrics
FDR	false discovery rate
g	gravity acceleration
GEO	Gene Expression Omnibus
GO	Gene Ontology
GTEx	Genotype-Tissue Expression
GSEA	Gene Set Enrichment Analysis
HMGB	High Mobility Group B
HRP	horseradish peroxidase
IAA	isoamyl alcohol
IgG	immunoglobulin G
IP	immunoprecipitation
kDa	kilodalton
L	liter
lncRNA	long non-coding RNA

M	molar
min	minute
miRNA	microRNA
mJ	millijoule
mL	milliliter
mm	millimeter
mM	millimolar
mRNA	messenger RNA
ncRNA	non-coding RNA
ng	nanogram
nm	nanometer
nM	nanomolar
OS	overall survival
(D)PBS	(Dulbecco's) phosphate-buffered saline
(q)PCR	(quantitative) polymerase chain reaction
PAGE	polyacrylamide gel electrophoresis
pH	hydrogen potential
PLB	polysome lysis buffer
RBP	RNA-binding protein
PVDF	polyvinylidene fluoride
RIP	RNA immunoprecipitation
RNA	ribonucleic acid
ROC	receiver operating characteristic
rpm	revolutions per minute
RPM	reads per million mapped reads
ROS	reactive oxygen species
RT	room temperature
s	second
SDS	sodium dodecyl sulfate
siRNA	small interfering ribonucleic acid
snoRNA	small nucleolar RNA
ssDNA	single-stranded DNA
TCGA	The Cancer Genome Atlas
UV	ultraviolet
WB	Western blot

Short Abstracts

Abstract

Ovarian cancer is one of the most lethal gynecological malignancies worldwide due to the lack of early diagnostic methods. In this regard, HMGB family members, HMGB1 and HMGB2, as well as long non-coding RNAs (lncRNAs), participate in the malignant transformation by regulating gene expression and, therefore, their study represents an opportunity to progress towards a better understanding of the disease and the development of novel clinical strategies. The main objective of this work was to identify lncRNAs in epithelial ovarian cancer that are deregulated and/or associated with HMGB1 and/or HMGB2 because of their potential value as novel diagnostic biomarkers and therapeutic targets. The determination of new RNA interactions of these proteins would allow a better understanding of their mechanism of action and their role in ovarian cancer pathology.

We performed a meta-analysis on transcriptomic profiling expression data from epithelial ovarian cancer patients that are publicly available. By this approach, we identified several lncRNAs previously unrelated to epithelial ovarian cancer, with diagnostic and prognostic values, and associated with metastasis, chemoresistance, or histological subtype.

Then, the RNA interactome of HMGB1 and HMGB2 was determined by applying *in silico* binding predictions, as well as two immunoprecipitation-based techniques, RIP-Seq and eCLIP in a high-grade serous epithelial ovarian cancer cell line, PEO1. The identified lncRNAs and messenger RNAs (mRNAs) are related to previous information present in scientific literature and gene ontologies regarding biological processes, respectively.

Finally, HMGB1 and HMGB2 silencing was carried out using an siRNA-based approach and their effects on PEO1 transcriptome were analyzed. Their role in signaling pathways and biological processes in addition to the HMGB-regulated lncRNAs were assessed.

Resumen

El cáncer de ovario es uno de los cánceres ginecológicos más letales en todo el mundo debido a la falta de métodos de diagnóstico precoz. En este sentido, los miembros de la familia *High Mobility Group Box* (HMGB), HMGB1 y HMGB2, así como los ARNs largos no codificantes (lncRNAs), participan en el proceso de malignización regulando la expresión génica y, por tanto, su estudio representa una oportunidad para avanzar hacia una mejor comprensión de la enfermedad y el desarrollo de nuevas estrategias clínicas. El objetivo principal de este trabajo consistió en identificar lncRNAs en cáncer de ovario epitelial que estén desregulados y/o asociados a HMGB1 y/o HMGB2, debido a su potencial valor como nuevos biomarcadores diagnósticos y dianas terapéuticas. La determinación de nuevas interacciones de estas proteínas con ARNs permitirá una mejor comprensión de su mecanismo de acción y su papel en la patología del cáncer de ovario.

Realizamos un metaanálisis de datos disponibles públicamente de transcriptomas de pacientes con cáncer de ovario epitelial. Mediante esta aproximación, identificamos varios lncRNAs que no estaban previamente relacionados con el cáncer de ovario epitelial, y que tienen valor diagnóstico y pronóstico, o están asociados a metástasis, resistencia a quimioterapia o subtipo histológico.

A continuación, se determinó el interactoma de ARN para HMGB1 y HMGB2 aplicando predicciones de unión *in silico*, así como dos técnicas basadas en inmunoprecipitación, RIP-Seq y eCLIP en la línea celular de cáncer de ovario epitelial seroso de alto grado, PEO1. Los lncRNAs y ARN mensajeros (ARNm) identificados se relacionaron con información previa presente en la bibliografía científica y ontologías génicas relativas a procesos biológicos, respectivamente.

Por último, se llevó a cabo el silenciamiento de HMGB1 y HMGB2 utilizando una aproximación basada en siRNA y se estudiaron sus efectos en el transcriptoma de PEO1. Se evaluó su papel en vías de señalización y procesos biológicos, así como los lncRNAs regulados por HMGBs.

Resumo

O cancro de ovario é un dos cancros xinecolóxicos máis letais en todo o mundo debido á falta de métodos de diagnóstico precoz. Neste senso, os membros da familia *High Mobility Group Box* (HMGB), HMGB1 e HMGB2, así como os ARNs longos non codificantes (lncRNAs) participan no proceso de malignización regulando a expresión xénica e, por tanto, o seu estudo representa unha oportunidade para avanzar cara a unha mellor comprensión da enfermidade e o desenvolvemento de novas estratexias clínicas. O obxectivo principal deste traballo consistiu en identificar lncRNAs en cancro de ovario epitelial que estean deregulados e/ou asociados a HMGB1 e/o HMGB2, debido ao seu potencial valor como novos biomarcadores diagnósticos e dianas terapéuticas. A determinación de novas interaccións destas proteínas con ARNs permitirá unha mellor comprensión do seu mecanismo de acción e o seu papel na patoloxía do cancro de ovario.

Realizamos unha meta-análise de datos dispoñibles publicamente de transcriptomas de pacientes con cancro de ovario epitelial. Mediante esta aproximación, identificamos varios lncRNAs que non estaban previamente relacionados co cancro de ovario epitelial, e que teñen valor diagnóstico e prognóstico, ou están asociados a metástase, resistencia á quimioterapia ou subtipo histolóxico.

A continuación, determinouse o interactoma de ARN para HMGB1 e HMGB2 aplicando predicións de unión *in silico*, así como dúas técnicas baseadas en inmunoprecipitación, RIP-Seq e eCLIP na liña celular de cancro de ovario epitelial seroso de alto grao, PEO1. Os lncRNAs e ARN mensaxeiros (ARNm) identificados relacionáronse con información previa presente na bibliografía científica e ontoloxías xénicas relativas a procesos biolóxicos, respectivamente.

Por último, levouse a cabo o silenciamento de HMGB1 e HMGB2 utilizando unha aproximación baseada en siRNA e se estudaron os seus efectos no transcriptoma de PEO1. Avaliouse o seu papel nas vías de sinalización e os procesos biolóxicos, así como os lncRNAs regulados por HMGBs.

Introduction

1.- Ovarian cancer

Ovarian cancer (OC), also known as ovarian malignant neoplasm or malignant tumor, is a group of diseases in which abnormal cells in the ovaries, or the related areas of the fallopian tubes and the peritoneum, grow out of control, invade adjacent parts of the body and/or metastasize to other organs (Centers for Disease and Control Prevention, 2022; World Health Organization, 2023). It is the second most common cause of death worldwide due to gynecological cancers. There were approximately 314,000 new cases and 205,000 deaths around the globe in 2020, of which 3,500 and 2,100, respectively, occurred in Spain, with increasing trends predicted (Sung et al., 2021).

According to the type of cell in which the tumor originates, OC can be classified into germinal (3-5%), stromal (2-3%), and epithelial (90%), whereas the remaining 2-5% correspond to tumors originated elsewhere that metastasize in the ovaries (Sankaranarayanan & Ferlay, 2006). Epithelial ovarian cancer (EOC), also known as ovarian carcinoma, adenocarcinoma, or cystadenocarcinoma, consists of five subtypes that can be distinguished according to their histological structure, mutations in certain tumor suppressors or proto-oncogenes, chemosensitivity, spreading behavior, patient prognosis, and frequency (indicated within the parentheses): High-Grade Serous (70%), Low-Grade Serous (>5%), Endometrioid (10%), Clear Cell (10%), and Mucinous (3%) (Gilks & Prat, 2009).

Little is known about the etiology of the disease, although some genetic and environmental risk factors have been identified, e.g., *BRCA1/2* mutations, and low or null parity, respectively, or even certain cell states such as oxidative stress (reviewed in Barreiro-Alonso et al., 2016). OC, and EOC patients particularly, are usually diagnosed at an advanced stage of the disease owing to the asymptomatic character of the tumor during its onset and initial development, leading to a five-year overall survival rate below 40% (Reid et al., 2017). In contrast, early diagnosis correlates with a much better prognosis, however, there are currently no efficient, approved, and routine methods or

biomarkers for an early diagnosis of OC. Only in a minority of cases, wherein the condition is suspected based on either unspecific symptoms or familial antecedents, can preventive measures be taken, such as gynecological explorations, imaging techniques like transvaginal sonography, or blood tests to measure cancer antigen 125 (CA-125) or HE4, as it was implemented in ROMA, OV1, and Overa diagnostic kits only for women with pelvic mass (Ueland, 2017). If a tumor is detected, further and more sophisticated explorations are conducted: imaging techniques such as computed tomography or positron emission tomography, and laparotomy or surgery to (i) extract a sample for biopsy/histology-based diagnosis, (ii) study the extent of the disease (localized or generalized-staging) and/or (iii) proceed with therapeutic surgical debulking/cytoreductive surgery of the tumor (Cortez et al., 2018). These techniques are either non-OC-specific or only valid for late detection (Ueland, 2017).

The extent of OC in patients is classified into four stages according to the International Federation of Gynecology and Obstetrics (FIGO), which in addition to tumor size and histological grade (tissue structure loss), negatively correlates with patient prognosis (Prat, 2014). FIGO stage 0 is considered *in situ* carcinoma, FIGO I is when the tumor is confined in the ovary, FIGO II is when the invasion of surrounding organs or tissue occurs, and FIGO III and IV are when close or distant metastasis occur, respectively.

After surgery, the first-line treatment of OC consists in the administration of platinum derivatives, taxanes, and/or bevacizumab, which is a monoclonal antibody targeting vascular endothelial cell growth factor (VEGF). Additionally, olaparib, which is an inhibitor of poly (ADP-ribose) polymerase (PARPi), was authorized as a first-line maintenance treatment for BRCA-mutated High-Grade Serous OC patients who have shown complete or partial response to platinum. Despite the benefits of these therapies, most patients experience relapses, and the tumor eventually becomes resistant to the treatment. As a second-line treatment, PARPi, doxorubicin, or gemcitabine are administered (Cortez et al., 2018). In November 2022 the U.S. Food and Drug

Administration approved the use of a monoclonal antibody targeting FOLR1 (mirvetuximab) conjugated with a cytotoxic maytansinoid drug (soravtansine) (US Food and Drug Administration, 2022). Anti-PD-1 immunotherapy monoclonal antibodies Pembrolizumab and Dostarlimab, as well as CAR-T therapies, gene therapy, or anti-cancer vaccines, are currently only under clinical trials (Áyen et al., 2018; Palaia et al., 2020).

2.- Long non-coding RNAs and EOC

Long non-coding RNAs (lncRNAs) are transcripts identified in genomic studies during the late 1990s and 2000s that are defined as RNAs longer than 200 nucleotides, mainly transcribed by RNA polymerase II, often 5′-capped, spliced and polyadenylated, that are presumed not to encode proteins, although there is evidence that some can encode for short biologically active peptides (K. C. Wang & Chang, 2011). Within the cell, they are present in the nucleus and/or the cytoplasm and are able to regulate gene expression at different levels, taking part in many physiological processes. Therefore, their deregulation contributes to the aberrant functioning of the cell leading to different diseases. They actively participate in all the events involved in tumor development and spread, and even in treatment resistance in bladder cancer, colorectal cancer, multiple myeloma, and others, including EOC (J. Wang et al., 2019). The study of lncRNAs is an emerging field. According to GENCODE Release 43 (Frankish et al., 2021), the number of known lncRNA genes in the human genome so far is 19,928, of which 1,054 need to be experimentally confirmed. LncRNAs have not been as deeply studied as their counterparts, microRNAs (miRNAs), and many questions remain about their mechanisms of action and effects in the context of cancer, including OC.

In the process of developing new, specific, differential molecular markers for EOC, lncRNAs are proposed as a new generation of clinical tools. They have been studied in OC patient samples using reverse-transcription quantitative polymerase chain reaction (RT-qPCR), microarray hybridization, and (fluorescence) *in situ* hybridization ((F)ISH), mainly from cancerous tissue, and compared with adjacent normal tissue or samples

from healthy patients. Differentially expressed lncRNAs in EOC patients can correlate with clinicopathological parameters, such as histological subtype, tumor size, presence and extent of metastasis, and therefore FIGO stage, as well as tumor invasion depth, patient prognosis (progression-free and disease-free survival periods), and radio- and/or chemotherapy sensitivity. LncRNAs can be detected in tumor-derived small extracellular vesicles as well as in blood serum and plasma samples from EOC patients. Circulating lncRNA levels can correlate to those found in tumor tissue, increasing its importance as an object of study for applying them in liquid biopsy, with ongoing clinical trials (reviewed in Salamini-Montemurri et al., 2020).

There is experimental evidence in the context of OC, using cell and animal models, that lncRNAs are involved in proliferation, tumor growth *in vivo*, cell cycle control, several types of cell death, migration, invasion, epithelial-to-mesenchymal transition (EMT), metastasis *in vivo*, angiogenesis, cell metabolism, inflammation, and immunomodulation (reviewed in Salamini-Montemurri et al., 2020), all of them related to the hallmarks of cancer (Hanahan, 2022).

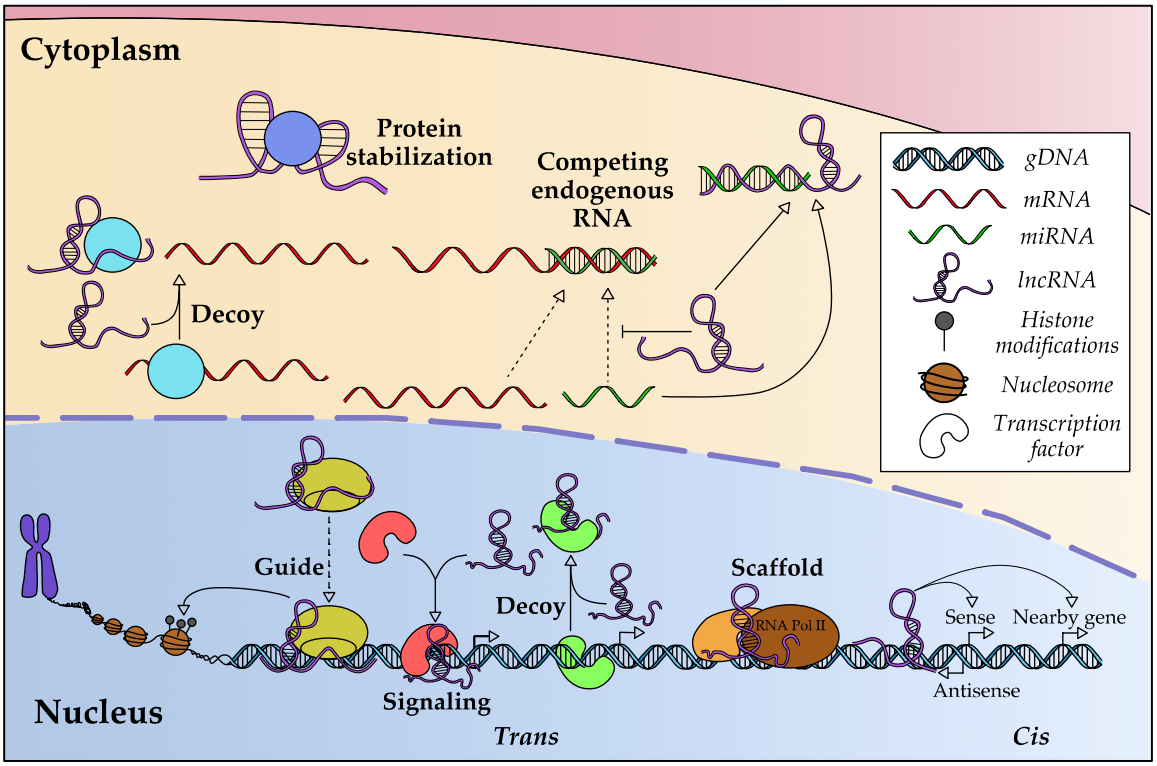

Figure 1. Scheme of gene expression regulatory mechanisms by lncRNAs in EOC. Adapted from Salamini-Montemurri et al. 2020.

The described phenotypes are a consequence of lncRNA-driven target gene regulation by different (and not mutually exclusive) mechanisms, affecting gene expression at the transcriptional, post-transcriptional, and post-translational levels in OC, as reviewed in Salamini-Montemurri et al. (2020) and depicted in Figure 1.

LncRNAs can regulate transcription either at a nearby locus, i.e., in *cis*, or at distant sites on the same or different chromosomes, i.e., in *trans*, mainly in two different ways. One mechanism consists in the association with proteins to change their capacity to bind DNA, what is called “signaling” if it promotes, or “decoy” if it inhibits the binding of the protein to the regulatory DNA sequence of a target gene. They can also promote the formation of protein complexes, a process called “scaffolding”, which will also act on their target DNA sequence. The other transcriptional regulatory mechanism consists in guiding DNA or chromatin modifiers, such as Polycomb Repressive Complexes (PRC), to a certain locus based on DNA-RNA complementarity, leading to nucleotide or histone modifications.

Post-transcriptional regulation by lncRNAs takes place in several ways. The most studied by far is acting as competing endogenous RNAs (ceRNA) of miRNAs, meaning that lncRNAs sequester miRNAs to prevent them from binding their target mRNAs, thus regulating the fate of protein-coding mRNAs that can be involved in cancer. Several lncRNAs can act on the same miRNA targets and numerous lncRNA/miRNA/mRNA axes have been identified in the context of OC. Besides binding miRNAs, some lncRNAs can generate miRNAs or other small RNAs, such as small nuclear (snRNAs) or small nucleolar (snoRNAs), by cleavage and/or processing. Additionally, lncRNAs can affect alternative splicing by sequestering RNA processing factors.

Finally, the gene expression regulation mediated by lncRNAs can happen at the post-translational level in a variety of mechanisms, such as interacting with proteins implicated in the translation process, modulating the half-lives of the proteins they bind by stabilizing them or serving as a scaffold between two proteins to trigger the activation, translocation, or degradation of one of them.

3.- HMGB proteins

High mobility group box proteins are a highly conserved eukaryotic protein family characterized by the presence of an HMG-box domain that consists of 3 alpha helices in an L shape (Weir et al., 1993). Four canonical human HMGB protein members have been described (Štros, 2010), namely, HMGB1, HMGB2, HMGB3, and HMGB4, which present a short N-terminal fragment, two in-tandem HMG-box domains joined by a small linker, and a C-terminal acidic tail, except for HMGB4 which lacks the acidic tail. This tail is an intrinsically disordered region (Mensah et al., 2023) and enables HMGB1/2/3 to interact with positively charged proteins, such as histones (Watson et al., 2014), and autoinhibition through intramolecular electrostatic interaction with the HMGB domains (X. Wang et al., 2021; Watson et al., 2007).

HMGB1 and HMGB2 are the most ubiquitously expressed and abundant proteins of the family. They were originally described as non-histone chromatin architectural proteins due to their high proportion in the nucleus where they participate in nucleosome structure maintenance, DNA bending, DNA recombination, DNA repair, and chromatin remodeling. They also act as transcriptional regulators by interacting with transcription factors, although HMGB1 and HMGB2 cannot be considered traditional transcription factors since they lack sequence specificity and rather bind specific DNA structures like distorted DNA or DNA adducts (Reeves, 2015). Depending on their redox status, they can translocate to the cytoplasm to promote autophagy, prevent apoptosis, regulate mitochondrial morphology, and act as a sensor for ROS species (Tang et al., 2011) or immunogenic nucleic acids (Yanai et al., 2009). They can even be released by damaged or immune cells, mainly during oxidative stress, to the extracellular milieu where they act as cytokines to promote inflammation by triggering several signaling pathways, like NF-kB, through the interaction with RAGE and TLRs (reviewed in Barreiro-Alonso et al., 2016).

HMGB1 and HMGB2 act in physiological conditions such as tissue homeostasis (Straino et al., 2008; Taniguchi et al., 2009), cell differentiation (Chen et al., 2021; B.

Wang et al., 2016), pluripotency maintenance, or senescence (Aird et al., 2016; Sofiadis et al., 2021). To study the role of HMGB1 and HMGB2 in the development of multicellular organisms, genetic mouse models were created, with no embryonic lethality observed, resulting in a marked lifespan reduction for HMGB1, but not HMGB2, knockouts (Calogero et al., 1999), whereas HMGB2 knockouts lead to an impairment in fertility in male mice (Ronfani et al., 2001). They can also play a role in pathological conditions, such as ischemic brain damage, neurodegenerative disorders, obesity, diabetes, autoimmune, inflammatory diseases, and of course, cancer, conditions in which they are commonly upregulated. Despite the high percent identity in amino acid sequence between these two proteins, which accounts for more than 80%, some of their functions can be different and non-overlapping (reviewed in Cámara-Quílez et al., 2020).

The effects of HMGB1 and HMGB2 in cancer have been studied in several models, including colorectal (Ohmori et al., 2011; Z. Wang et al., 2016), hepatocellular (Tohme et al., 2017), pancreatic (Cai et al., 2017), gastric (Cui et al., 2019), hypopharyngeal (Y. Li et al., 2017), prostate (Gnanasekar et al., 2009), lung (Liu et al., 2010), glial (Wu et al., 2013), and ovarian (H. Li et al., 2018) cancers. They promote *in vitro* and *in vivo* cell proliferation and viability, as well as migration and invasion, by modulating epithelial-to-mesenchymal transition and metalloproteinase expression. They are involved in reactive oxygen species response (reviewed in Barreiro-Alonso et al., 2016), and their absence leads to increased apoptosis (Gnanasekar et al., 2009; Yang et al., 2020). In the case HMGB1, it promotes autophagy (Tang et al., 2010), DNA repair (Ito et al., 2015; Lange et al., 2008), and, depending on its redox state, modulates the positive or negative immune response to cancer; for instance, by inducing thymic stromal lymphopoietin expression in other tumor cells that leads to a dendritic cell-mediated regulatory T cell immunosuppression (Zhang et al., 2018). HMGB1 and HMGB2 are implicated in radioresistance (H. Ma et al., 2019; Shin et al., 2013) and chemoresistance to 5-fluorouracil, taxanes, cis-, carbo-, and oxaliplatin (Bernardini et al., 2005; Syed et al.,

2015; Varma et al., 2005). HMGB1 and HMGB2 also contribute to the maintenance of cancer stem cells (Bagherpoor et al., 2020; Conti et al., 2013).

Data of HMGB RNA expression from Pan-Cancer Analysis of Whole Genomes (analyzed by Cámara-Quílez et al., 2020) shows that both HMGB1 and HMGB2 expression is increased by a fold change of 3.4 and 4.5, respectively, in cancer compared to normal human tissues (Cámara-Quílez et al., 2020). HMGB1 and HMGB2 serve as prognostic factors in EOC patients, as their expression levels positively correlate with reduced overall survival periods (H. Li et al., 2018; Machado et al., 2017).

4.- Interactions between HMGBs and (lnc)RNAs

Mechanisms of action explaining the functions of HMGB proteins are normally mediated by their interaction with DNA and chromatin (Štros, 2010), or other proteins (Barreiro-Alonso et al., 2019; Cámara-Quílez et al., 2020). However, their interaction with RNAs in the cell context has been less studied, although there are some examples on this topic.

Several *in vitro* studies observed the binding of recombinant human HMGB1, HMGB2, HMGB3, or their corresponding fruit fly, rat, and mouse orthologs, with different kinds of RNAs, such as 5S rRNA from *E. coli* and the group I intron ribozyme from *Azoarcus* bacteria pre-tRNA^{Ile} (Bell et al., 2008), double-stranded viral RNA (Arimondo et al., 2000; Khoury et al., 2021; Yu et al., 2016), small interference RNA (Choi et al., 2020; Lee et al., 2012; Oh & Lee, 2014), and double-stranded poly(I:C) and single-stranded poly(U) RNA (Yanai et al., 2009). Such RNA interaction ability was also confirmed *in cellula* by several studies trying to identify or expand the RNA-binding proteome, in which HMGB1, HMGB2, and/or HMGB3 were revealed as RBPs in various human and mouse cell types, including differentiated, embryonic stem, and cancer cells (Hamilton et al., 2023).

Despite these examples are merely descriptive, several studies have deciphered some of the biological implications of these interactions in different contexts for HMGB1 and HMGB2 proteins, but not for HMGB3 yet. It is not surprising to find examples in

which these proteins regulate transcriptional processes due to their mainly nuclear location.

Human HMGB1 and mouse Hmgb2 interact with antisense lncRNAs *CFTR-AS1* and *Lrp1-AS*, respectively, to regulate the transcription of their corresponding sense transcripts, i.e., *cis* regulation. HMGB1 and *CFTR-AS1* regulation consists of a negative epigenetic transcriptional regulation mediated by the additional interaction with other non-chromatin proteins, leading to chromatin remodeling at the *CFTR* locus (Saayman et al., 2016). Instead, *Lrp1*-AS recruits Hmgb2 to dock the transcription factor Srebp1 to the *Lrp1* promoter (Yamanaka et al., 2015). Similarly, mouse *Linc-Tnfaip3* serves as a molecular scaffold that allows the assembly of NF-κβ-Hmgb1 complex to modulate the transcription of its sense transcript *Tnfaip3* (*cis* regulation), as well as inflammation-related genes by chromatin remodeling (*trans* regulation); specifically by histone H3 modification, and bringing the transcription factor NF-κβ to the regulatory sequences of the target genes (S. Ma et al., 2017).

Interaction with lncRNAs can also affect transcriptional regulation mediated by HMGB1 and HMGB2 by controlling their subcellular location, allowing or not their presence in the nucleus. *SEMA3B-AS1* favors the translocation of HMGB1 into the nucleus to transcriptionally activate FBXW7, which belongs to the ubiquitin protein ligase complex and leads to the ubiquitination and degradation of the oncogenic BGN protein (Huang et al., 2022). Oppositely, *CRCMSL* (Han et al., 2019) and *LINC00341* (S. Li et al., 2020), physically bind to HMGB2 in the cytoplasm to prevent its translocation to the nucleus, where HMGB2 exerts its transcriptional regulation on target genes.

HMGB interaction with RNAs can also affect expression at post-transcriptional levels. HMGB1 binds mRNA and ncRNA precursors to regulate their alternative splicing, regulating the senescence-associated secretory phenotype in a model of cell senescence (Sofiadis et al., 2021).

Besides, HMGB1 levels can be affected by the interaction with the lncRNA *MALAT1*, whose binding reduces its degradation, promoting autophagy and inhibition of apoptosis in a model of human multiple myeloma (Gao et al., 2017).

Apart from gene expression, these HMGB-RNA interactions can have an impact on cell integrity, as is the case of the lncRNA *BS-DRL1*, which guides HMGB1 to DNA-damaged chromatin regions to participate in the repair event and trigger the DNA damage response in a mouse model with neurodegeneration (Lou et al., 2021).

There are many issues yet to be addressed to fully understand the role of these proteins, in connection with their interaction with RNA and their cellular mechanisms and implications.

In this Ph.D. Thesis we study lncRNAs, HMGB1/2 proteins and their interaction as an approach to find biomarkers in epithelial ovarian cancer. In the first chapter, we carry out a meta-analysis of gene expression profiling in 46 ovarian cancer patient cohorts available online to identify previously unrelated, differentially expressed lncRNAs genes in ovarian cancer with potential clinical value. In the second chapter, we present an interactome study of HMGB1 and HMGB2 RNA partners in EOC cancer cell lines, by applying predictive (catRAPID) and experimental (RIP-Seq and eCLIP) techniques. In the third chapter, we analyze the effects of silencing HMGB1 and HMGB2 independently in an ovarian cancer cell line, followed by RNA-Seq in order to identify biological processes and hallmarks in which they are implicated, as well as to identify lncRNAs regulated by these proteins.

REFERENCES

Aird, K. M., Iwasaki, O., Kossenkov, A. V., Tanizawa, H., Fatkhutdinov, N., Bitler, B. G., Le, L., Alicea, G., Yang, T.-L., Johnson, F. B., Noma, K., & Zhang, R. (2016). HMGB2 orchestrates the chromatin landscape of senescence-associated secretory phenotype gene loci. *Journal of Cell Biology*, *215*(3), 325–334. https://doi.org/10.1083/jcb.201608026

Arimondo, P. B., Gelus, N., Hamy, F., Payet, D., Travers, A., & Bailly, C. (2000). The chromosomal protein HMG-D binds to the TAR and RBE RNA of HIV-1. *FEBS Letters*, *485*(1), 47–52. https://doi.org/10.1016/S0014-5793(00)02183-9

Áyen, Á., Jiménez Martínez, Y., Marchal, J., & Boulaiz, H. (2018). Recent Progress in Gene Therapy for Ovarian Cancer. *International Journal of Molecular Sciences*,

19(7), 1930. https://doi.org/10.3390/ijms19071930

Bagherpoor, A. J., Kučírek, M., Fedr, R., Sani, S. A., & Štros, M. (2020). Nonhistone Proteins HMGB1 and HMGB2 Differentially Modulate the Response of Human Embryonic Stem Cells and the Progenitor Cells to the Anticancer Drug Etoposide. *Biomolecules*, *10*(10), 1450. https://doi.org/10.3390/biom10101450

Barreiro-Alonso, A., Cámara-Quílez, M., Salamini-Montemurri, M., Lamas-Maceiras, M., Vizoso-Vázquez, Á., Rodríguez-Belmonte, E., Quindós-Varela, M., Martínez-Iglesias, O., Figueroa, A., & Cerdán, M.-E. (2019). Characterization of HMGB1/2 Interactome in Prostate Cancer by Yeast Two Hybrid Approach: Potential Pathobiological Implications. *Cancers*, *11*(11), 1729. https://doi.org/10.3390/cancers11111729

Barreiro-Alonso, A., Lamas-Maceiras, M., Rodríguez-Belmonte, E., Vizoso-Vázquez, Á., Quindós, M., & Cerdán, M. E. (2016). High Mobility Group B Proteins, Their Partners, and Other Redox Sensors in Ovarian and Prostate Cancer. *Oxidative Medicine and Cellular Longevity*, *2016*, 1–17. https://doi.org/10.1155/2016/5845061

Bell, A. J., Chauhan, S., Woodson, S. A., & Kallenbach, N. R. (2008). Interactions of recombinant HMGB proteins with branched RNA substrates. *Biochemical and Biophysical Research Communications*, *377*(1), 262–267. https://doi.org/10.1016/j.bbrc.2008.09.131

Bernardini, M., Lee, C.-H., Beheshti, B., Prasad, M., Albert, M., Marrano, P., Begley, H., Shaw, P., Covens, A., Murphy, J., Rosen, B., Minkin, S., Squire, J. A., & Macgregor, P. F. (2005). High-Resolution Mapping of Genomic Imbalance and Identification of Gene Expression Profiles Associated with Differential Chemotherapy Response in Serous Epithelial Ovarian Cancer. *Neoplasia*, *7*(6), 603–613. https://doi.org/10.1593/neo.04760

Cai, X., Ding, H., Liu, Y., Pan, G., Li, Q., Yang, Z., & Liu, W. (2017). Expression of HMGB2 indicates worse survival of patients and is required for the maintenance of Warburg effect in pancreatic cancer. *Acta Biochimica et Biophysica Sinica*, *49*(2), 119–127. https://doi.org/10.1093/abbs/gmw124

Calogero, S., Grassi, F., Aguzzi, A., Voigtländer, T., Ferrier, P., Ferrari, S., & Bianchi, M. E. (1999). The lack of chromosomal protein Hmg1 does not disrupt cell growth but causes lethal hypoglycaemia in newborn mice. *Nature Genetics*, *22*(3), 276–280. https://doi.org/10.1038/10338

Cámara-Quílez, M., Barreiro-Alonso, A., Rodríguez-Bemonte, E., Quindós-Varela, M., Cerdán, M. E., & Lamas-Maceiras, M. (2020). Differential Characteristics of HMGB2 Versus HMGB1 and their Perspectives in Ovary and Prostate Cancer. *Current Medicinal Chemistry*, *27*(20), 3271–3289. https://doi.org/10.2174/0929867326666190123120338

Cámara-Quílez, M., Barreiro-Alonso, A., Vizoso-Vázquez, Á., Rodríguez-Belmonte, E., Quindós-Varela, M., Lamas-Maceiras, M., & Cerdán, M. E. (2020). The HMGB1-2 Ovarian Cancer Interactome. The Role of HMGB Proteins and Their Interacting Partners MIEN1 and NOP53 in Ovary Cancer and Drug-Response. *Cancers*, *12*(9), 2435. https://doi.org/10.3390/cancers12092435

Centers for Disease and Control Prevention. (2022). *Basic Information About Ovarian Cancer*. https://www.cdc.gov/cancer/ovarian/basic_info/index.htm

Chen, K., Zhang, J., Liang, F., Zhu, Q., Cai, S., Tong, X., He, Z., Liu, X., Chen, Y., & Mo, D. (2021). HMGB2 orchestrates mitotic clonal expansion by binding to the promoter of C/EBPβ to facilitate adipogenesis. *Cell Death & Disease*, *12*(7), 666. https://doi.org/10.1038/s41419-021-03959-3

Choi, M., Jeong, H., Kim, S., Kim, M., Lee, M., & Rhim, T. (2020). Targeted delivery of Chil3/Chil4 siRNA to alveolar macrophages using ternary complexes composed of HMG and oligoarginine micelles. *Nanoscale*, *12*(2), 933–943. https://doi.org/10.1039/C9NR06382J

Conti, L., Lanzardo, S., Arigoni, M., Antonazzo, R., Radaelli, E., Cantarella, D., Calogero, R. A., & Cavallo, F. (2013). The noninflammatory role of high mobility group box

1/toll-like receptor 2 axis in the self-renewal of mammary cancer stem cells. *The FASEB Journal*, *27*(12), 4731–4744. https://doi.org/10.1096/fj.13-230201

Cortez, A. J., Tudrej, P., Kujawa, K. A., & Lisowska, K. M. (2018). Advances in ovarian cancer therapy. *Cancer Chemotherapy and Pharmacology*, *81*(1), 17–38. https://doi.org/10.1007/s00280-017-3501-8

Cui, G., Cai, F., Ding, Z., & Gao, L. (2019). HMGB2 promotes the malignancy of human gastric cancer and indicates poor survival outcome. *Human Pathology*, *84*, 133–141. https://doi.org/10.1016/j.humpath.2018.09.017

Frankish, A., Diekhans, M., Jungreis, I., Lagarde, J., Loveland, J. E., Mudge, J. M., Sisu, C., Wright, J. C., Armstrong, J., Barnes, I., Berry, A., Bignell, A., Boix, C., Carbonell Sala, S., Cunningham, F., Di Domenico, T., Donaldson, S., Fiddes, I. T., García Girón, C., … Flicek, P. (2021). GENCODE 2021. *Nucleic Acids Research*, *49*(D1), D916–D923. https://doi.org/10.1093/nar/gkaa1087

Gao, D., Lv, A., Li, H.-P., Han, D.-H., & Zhang, Y.-P. (2017). LncRNA MALAT-1 Elevates HMGB1 to Promote Autophagy Resulting in Inhibition of Tumor Cell Apoptosis in Multiple Myeloma. *Journal of Cellular Biochemistry*, *118*(10), 3341–3348. https://doi.org/10.1002/jcb.25987

Gilks, C. B., & Prat, J. (2009). Ovarian carcinoma pathology and genetics: recent advances. *Human Pathology*, *40*(9), 1213–1223. https://doi.org/10.1016/j.humpath.2009.04.017

Gnanasekar, M., Thirugnanam, S., & Ramaswamy, K. (2009). Short hairpin RNA (shRNA) constructs targeting high mobility group box-1 (HMGB1) expression leads to inhibition of prostate cancer cell survival and apoptosis. *International Journal of Oncology*, *34*(2), 425–431. https://doi.org/10.3892/ijo_00000166

Hamilton, D. J., Hein, A. E., Wuttke, D. S., & Batey, R. T. (2023). The DNA binding high mobility group box protein family functionally binds RNA. *WIREs RNA*, *14*(5), e1778. https://doi.org/10.1002/wrna.1778

Han, Q., Xu, L., Lin, W., Yao, X., Jiang, M., Zhou, R., Sun, X., & Zhao, L. (2019). Long noncoding RNA CRCMSL suppresses tumor invasive and metastasis in colorectal carcinoma through nucleocytoplasmic shuttling of HMGB2. *Oncogene*, *38*(16), 3019–3032. https://doi.org/10.1038/s41388-018-0614-4

Hanahan, D. (2022). Hallmarks of Cancer: New Dimensions. *Cancer Discovery*, *12*(1), 31–46. https://doi.org/10.1158/2159-8290.CD-21-1059

Huang, G., Xiang, Z., Wu, H., He, Q., Dou, R., Yang, C., Song, J., Huang, S., Wang, S., & Xiong, B. (2022). The lncRNA SEMA3B-AS1/HMGB1/FBXW7 Axis Mediates the Peritoneal Metastasis of Gastric Cancer by Regulating BGN Protein Ubiquitination. *Oxidative Medicine and Cellular Longevity*, *2022*(4), 1–26. https://doi.org/10.1155/2022/5055684

Ito, H., Fujita, K., Tagawa, K., Chen, X., Homma, H., Sasabe, T., Shimizu, J., Shimizu, S., Tamura, T., Muramatsu, S., & Okazawa, H. (2015). HMGB1 facilitates repair of mitochondrial DNA damage and extends the lifespan of mutant ataxin-1 knock-in mice. *EMBO Molecular Medicine*, *7*(1), 78–101. https://doi.org/10.15252/emmm.201404392

Khoury, G., Lee, M. Y., Ramarathinam, S. H., McMahon, J., Purcell, A. W., Sonza, S., Lewin, S. R., & Purcell, D. F. J. (2021). The RNA-Binding Proteins SRP14 and HMGB3 Control HIV-1 Tat mRNA Processing and Translation During HIV-1 Latency. *Frontiers in Genetics*, *12*(June), 1–18. https://doi.org/10.3389/fgene.2021.680725

Lange, S. S., Mitchell, D. L., & Vasquez, K. M. (2008). High mobility group protein B1 enhances DNA repair and chromatin modification after DNA damage. *Proceedings of the National Academy of Sciences*, *105*(30), 10320–10325. https://doi.org/10.1073/pnas.0803181105

Lee, S., Song, H., Kim, H. A., Oh, B., Lee, D. Y., & Lee, M. (2012). The box a domain of high mobility group box-1 protein as an efficient siRNA carrier with anti-inflammatory effects. *Journal of Cellular Biochemistry*, *113*(1), 122–131. https://doi.org/10.1002/jcb.23334

Li, H., Zhang, H., & Wang, Y. (2018). Centromere protein U facilitates metastasis of ovarian cancer cells by targeting high mobility group box 2 expression. *Am J Cancer Res*, *8*(5), 835–851.

Li, S., Chen, S., Wang, B., Zhang, L., Su, Y., & Zhang, X. (2020). The long noncoding RNA LINC00341 suppresses colorectal carcinoma by preventing cell migration and apoptosis. *Cell Biochemistry and Function*, *38*(3), 266–274. https://doi.org/10.1002/cbf.3473

Li, Y., Wang, P., Zhao, J., Li, H., Liu, D., & Zhu, W. (2017). HMGB1 attenuates TGF-β-induced epithelial–mesenchymal transition of FaDu hypopharyngeal carcinoma cells through regulation of RAGE expression. *Molecular and Cellular Biochemistry*, *431*(1–2), 1–10. https://doi.org/10.1007/s11010-017-2968-2

Liu, P.-L., Tsai, J.-R., Hwang, J.-J., Chou, S.-H., Cheng, Y.-J., Lin, F.-Y., Chen, Y.-L., Hung, C.-Y., Chen, W.-C., Chen, Y.-H., & Chong, I.-W. (2010). High-Mobility Group Box 1–Mediated Matrix Metalloproteinase-9 Expression in Non–Small Cell Lung Cancer Contributes to Tumor Cell Invasiveness. *American Journal of Respiratory Cell and Molecular Biology*, *43*(5), 530–538. https://doi.org/10.1165/rcmb.2009-0269OC

Lou, M.-M., Tang, X.-Q., Wang, G.-M., He, J., Luo, F., Guan, M.-F., Wang, F., Zou, H., Wang, J.-Y., Zhang, Q., Xu, M.-J., Shi, Q.-L., Shen, L.-B., Ma, G.-M., Wu, Y., Zhang, Y.-Y., Liang, A., Wang, T.-H., Xiong, L.-L., … Wang, W.-Y. (2021). Long noncoding RNA BS-DRL1 modulates the DNA damage response and genome stability by interacting with HMGB1 in neurons. *Nature Communications*, *12*(1), 4075. https://doi.org/10.1038/s41467-021-24236-z

Ma, H., Zheng, S., Zhang, X., Gong, T., Lv, X., Fu, S., Zhang, S., Yin, X., Hao, J., Shan, C., & Huang, S. (2019). High mobility group box 1 promotes radioresistance in esophageal squamous cell carcinoma cell lines by modulating autophagy. *Cell Death & Disease*, *10*(2), 136. https://doi.org/10.1038/s41419-019-1355-1

Ma, S., Ming, Z., Gong, A.-Y., Wang, Y., Chen, X., Hu, G., Zhou, R., Shibata, A., Swanson, P. C., & Chen, X.-M. (2017). A long noncoding RNA, lincRNA-Tnfaip3, acts as a coregulator of NF-κB to modulate inflammatory gene transcription in mouse macrophages. *The FASEB Journal*, *31*(3), 1215–1225. https://doi.org/10.1096/fj.201601056R

Machado, L. R., Moseley, P. M., Moss, R., Deen, S., Nolan, C., Spendlove, I., Ramage, J. M., Chan, S. Y., & Durrant, L. G. (2017). High mobility group protein B1 is a predictor of poor survival in ovarian cancer. *Oncotarget*, *8*(60), 101215–101223. https://doi.org/10.18632/oncotarget.20538

Mensah, M. A., Niskanen, H., Magalhaes, A. P., Basu, S., Kircher, M., Sczakiel, H. L., Reiter, A. M. V., Elsner, J., Meinecke, P., Biskup, S., Chung, B. H. Y., Dombrowsky, G., Eckmann-Scholz, C., Hitz, M. P., Hoischen, A., Holterhus, P.-M., Hülsemann, W., Kahrizi, K., Kalscheuer, V. M., … Hnisz, D. (2023). Aberrant phase separation and nucleolar dysfunction in rare genetic diseases. *Nature*, *614*, 564–571. https://doi.org/10.1038/s41586-022-05682-1

Oh, B., & Lee, M. (2014). Combined delivery of HMGB-1 box A peptide and S1PLyase siRNA in animal models of acute lung injury. *Journal of Controlled Release*, *175*(1), 25–35. https://doi.org/10.1016/j.jconrel.2013.12.008

Ohmori, H., Luo, Y., & Kuniyasu, H. (2011). Non-histone nuclear factor HMGB1 as a therapeutic target in colorectal cancer. *Expert Opinion on Therapeutic Targets*, *15*(2), 183–193. https://doi.org/10.1517/14728222.2011.546785

Palaia, I., Tomao, F., Sassu, C. M., Musacchio, L., & Benedetti Panici, P. (2020). Immunotherapy For Ovarian Cancer: Recent Advances And Combination Therapeutic Approaches. *OncoTargets and Therapy*, *13*, 6109–6129. https://doi.org/10.2147/OTT.S205950

Prat, J. (2014). Staging classification for cancer of the ovary, fallopian tube, and peritoneum. *International Journal of Gynecology & Obstetrics*, *124*(1), 1–5. https://doi.org/10.1016/j.ijgo.2013.10.001

Reeves, R. (2015). High mobility group (HMG) proteins: Modulators of chromatin structure and DNA repair in mammalian cells. *DNA Repair*, *36*, 122–136. https://doi.org/10.1016/j.dnarep.2015.09.015

Reid, B. M., Permuth, J. B., & Sellers, T. A. (2017). Epidemiology of ovarian cancer: a review. *Cancer Biology & Medicine*, *14*(1), 9–32. https://doi.org/10.20892/j.issn.2095-3941.2016.0084

Ronfani, L., Ferraguti, M., Croci, L., Ovitt, C. E., Schöler, H. R., Consalez, G. G., & Bianchi, M. E. (2001). Reduced fertility and spermatogenesis defects in mice lacking chromosomal protein Hmgb2. *Development*, *128*(8), 1265–1273. https://doi.org/10.1242/dev.128.8.1265

Saayman, S. M., Ackley, A., Burdach, J., Clemson, M., Gruenert, D. C., Tachikawa, K., Chivukula, P., Weinberg, M. S., & Morris, K. V. (2016). Long Non-coding RNA BGas Regulates the Cystic Fibrosis Transmembrane Conductance Regulator. *Molecular Therapy*, *24*(8), 1351–1357. https://doi.org/10.1038/mt.2016.112

Salamini-Montemurri, M., Lamas-Maceiras, M., Barreiro-Alonso, A., Vizoso-Vázquez, Á., Rodríguez-Belmonte, E., Quindós-Varela, M., & Esperanza Cerdán, M. (2020). The challenges and opportunities of lncRNAs in ovarian cancer research and clinical use. *Cancers*, *12*(4), 1–25. https://doi.org/10.3390/cancers12041020

Sankaranarayanan, R., & Ferlay, J. (2006). Worldwide burden of gynaecological cancer: The size of the problem. *Best Practice & Research Clinical Obstetrics & Gynaecology*, *20*(2), 207–225. https://doi.org/10.1016/j.bpobgyn.2005.10.007

Shin, Y.-J., Kim, M.-S., Kim, M.-S., Lee, J., Kang, M., & Jeong, J.-H. (2013). High-mobility group box 2 (HMGB2) modulates radioresponse and is downregulated by p53 in colorectal cancer cell. *Cancer Biology & Therapy*, *14*(3), 213–221. https://doi.org/10.4161/cbt.23292

Sofiadis, K., Josipovic, N., Nikolic, M., Kargapolova, Y., Übelmesser, N., Varamogianni-Mamatsi, V., Zirkel, A., Papadionysiou, I., Loughran, G., Keane, J., Michel, A., Gusmao, E. G., Becker, C., Altmüller, J., Georgomanolis, T., Mizi, A., & Papantonis, A. (2021). HMGB1 coordinates SASP-related chromatin folding and RNA homeostasis on the path to senescence. *Molecular Systems Biology*, *17*(6), 1–17. https://doi.org/10.15252/msb.20209760

Straino, S., Di Carlo, A., Mangoni, A., De Mori, R., Guerra, L., Maurelli, R., Panacchia, L., Di Giacomo, F., Palumbo, R., Di Campli, C., Uccioli, L., Biglioli, P., Bianchi, M. E., Capogrossi, M. C., & Germani, A. (2008). High-Mobility Group Box 1 Protein in Human and Murine Skin: Involvement in Wound Healing. *Journal of Investigative Dermatology*, *128*(6), 1545–1553. https://doi.org/10.1038/sj.jid.5701212

Štros, M. (2010). HMGB proteins: Interactions with DNA and chromatin. *Biochimica et Biophysica Acta (BBA) - Gene Regulatory Mechanisms*, *1799*(1–2), 101–113. https://doi.org/10.1016/j.bbagrm.2009.09.008

Sung, H., Ferlay, J., Siegel, R. L., Laversanne, M., Soerjomataram, I., Jemal, A., & Bray, F. (2021). Global Cancer Statistics 2020: GLOBOCAN Estimates of Incidence and Mortality Worldwide for 36 Cancers in 185 Countries. *CA: A Cancer Journal for Clinicians*, *71*(3), 209–249. https://doi.org/10.3322/caac.21660

Syed, N., Chavan, S., Sahasrabuddhe, N. A., Renuse, S., Sathe, G., Nanjappa, V., Radhakrishnan, A., Raja, R., Pinto, S. M., Srinivasan, A., Prasad, T. S. K., Srikumar, K., Gowda, H., Santosh, V., Sidransky, D., Califano, J. A., Pandey, A., & Chatterjee, A. (2015). Silencing of high-mobility group box 2 (HMGB2) modulates cisplatin and 5-fluorouracil sensitivity in head and neck squamous cell carcinoma. *PROTEOMICS*, *15*(2–3), 383–393. https://doi.org/10.1002/pmic.201400338

Tang, D., Kang, R., Livesey, K. M., Cheh, C.-W., Farkas, A., Loughran, P., Hoppe, G., Bianchi, M. E., Tracey, K. J., Zeh, H. J., & Lotze, M. T. (2010). Endogenous HMGB1 regulates autophagy. *Journal of Cell Biology*, *190*(5), 881–892. https://doi.org/10.1083/jcb.200911078

Tang, D., Kang, R., Zeh, H. J., & Lotze, M. T. (2011). High-Mobility Group Box 1, Oxidative Stress, and Disease. *Antioxidants & Redox Signaling*, *14*(7), 1315–1335.

https://doi.org/10.1089/ars.2010.3356
Taniguchi, N., Caramés, B., Kawakami, Y., Amendt, B. A., Komiya, S., & Lotz, M. (2009). Chromatin protein HMGB2 regulates articular cartilage surface maintenance via β-catenin pathway. *Proceedings of the National Academy of Sciences*, *106*(39), 16817–16822. https://doi.org/10.1073/pnas.0904414106
Tohme, S., Yazdani, H. O., Liu, Y., Loughran, P., van der Windt, D. J., Huang, H., Simmons, R. L., Shiva, S., Tai, S., & Tsung, A. (2017). Hypoxia mediates mitochondrial biogenesis in hepatocellular carcinoma to promote tumor growth through HMGB1 and TLR9 interaction. *Hepatology*, *66*(1), 182–197. https://doi.org/10.1002/hep.29184
Ueland, F. (2017). A Perspective on Ovarian Cancer Biomarkers: Past, Present and Yet-To-Come. *Diagnostics*, *7*(1), 14. https://doi.org/10.3390/diagnostics7010014
US Food and Drug Administration. (2022). *FDA grants accelerated approval to mirvetuximab soravtansine-gynx for FRα positive, platinum-resistant epithelial ovarian, fallopian tube, or peritoneal cancer*. https://www.fda.gov/drugs/resources-information-approved-drugs/fda-grants-accelerated-approval-mirvetuximab-soravtansine-gynx-fra-positive-platinum-resistant
Varma, R., Hector, S., Clark, K., Greco, W., Hawthorn, L., & Pendyala, L. (2005). Gene expression profiling of a clonal isolate of oxaliplatin-resistant ovarian carcinoma cell line A2780/C10. *Oncology Reports*, *14*(4), 925–932. https://doi.org/10.3892/or.14.4.925
Wang, B., Li, F., Zhang, C., Wei, G., Liao, P., & Dong, N. (2016). High-mobility group box-1 protein induces osteogenic phenotype changes in aortic valve interstitial cells. *The Journal of Thoracic and Cardiovascular Surgery*, *151*(1), 255–262. https://doi.org/10.1016/j.jtcvs.2015.09.077
Wang, J., Lu, A., & Chen, L. (2019). LncRNAs in ovarian cancer. *Clinica Chimica Acta*, *490*(October 2018), 17–27. https://doi.org/10.1016/j.cca.2018.12.013
Wang, K. C., & Chang, H. Y. (2011). Molecular Mechanisms of Long Noncoding RNAs. *Molecular Cell*, *43*(6), 904–914. https://doi.org/10.1016/j.molcel.2011.08.018
Wang, X., Greenblatt, H. M., Bigman, L. S., Yu, B., Pletka, C. C., Levy, Y., & Iwahara, J. (2021). Dynamic Autoinhibition of the HMGB1 Protein via Electrostatic Fuzzy Interactions of Intrinsically Disordered Regions. *Journal of Molecular Biology*, *433*(18), 167122. https://doi.org/10.1016/j.jmb.2021.167122
Wang, Z., Wang, X., Li, J., Yang, C., Xing, Z., Chen, R., & Xu, F. (2016). HMGB1 knockdown effectively inhibits the progression of rectal cancer by suppressing HMGB1 expression and promoting apoptosis of rectal cancer cells. *Molecular Medicine Reports*, *14*(1), 1026–1032. https://doi.org/10.3892/mmr.2016.5340
Watson, M., Stott, K., Fischl, H., Cato, L., & Thomas, J. O. (2014). Characterization of the interaction between HMGB1 and H3--a possible means of positioning HMGB1 in chromatin. *Nucleic Acids Research*, *42*(2), 848–859. https://doi.org/10.1093/nar/gkt950
Watson, M., Stott, K., & Thomas, J. O. (2007). Mapping Intramolecular Interactions between Domains in HMGB1 using a Tail-truncation Approach. *Journal of Molecular Biology*, *374*(5), 1286–1297. https://doi.org/10.1016/j.jmb.2007.09.075
Weir, H. M., Kraulis, P. J., Hill, C. S., Raine, A. R., Laue, E. D., & Thomas, J. O. (1993). Structure of the HMG box motif in the B-domain of HMG1. *The EMBO Journal*, *12*(4), 1311–1319. https://doi.org/10.1002/j.1460-2075.1993.tb05776.x
World Health Organization. (2023). *Cancer*. https://www.who.int/health-topics/cancer
Wu, Z. B., Cai, L., Lin, S. J., Xiong, Z. K., Lu, J. L., Mao, Y., Yao, Y., & Zhou, L. F. (2013). High-mobility group box 2 is associated with prognosis of glioblastoma by promoting cell viability, invasion, and chemotherapeutic resistance. *Neuro-Oncology*, *15*(9), 1264–1275. https://doi.org/10.1093/neuonc/not078
Yamanaka, Y., Faghihi, M. A., Magistri, M., Alvarez-Garcia, O., Lotz, M., & Wahlestedt, C. (2015). Antisense RNA Controls LRP1 Sense Transcript Expression through Interaction with a Chromatin-Associated Protein, HMGB2. *Cell Reports*, *11*(6), 967–

976. https://doi.org/10.1016/j.celrep.2015.04.011
Yanai, H., Ban, T., Wang, Z., Choi, M. K., Kawamura, T., Negishi, H., Nakasato, M., Lu, Y., Hangai, S., Koshiba, R., Savitsky, D., Ronfani, L., Akira, S., Bianchi, M. E., Honda, K., Tamura, T., Kodama, T., & Taniguchi, T. (2009). HMGB proteins function as universal sentinels for nucleic-acid-mediated innate immune responses. *Nature*, *462*(7269), 99–103. https://doi.org/10.1038/nature08512
Yang, S., Ye, Z., Wang, Z., & Wang, L. (2020). High mobility group box 2 modulates the progression of osteosarcoma and is related with poor prognosis. *Annals of Translational Medicine*, *8*(17), 1082–1082. https://doi.org/10.21037/atm-20-4801
Yu, R., Yang, D., Lei, S., Wang, X., Meng, X., Xue, B., & Zhu, H. (2016). HMGB1 Promotes Hepatitis C Virus Replication by Interaction with Stem-Loop 4 in the Viral 5′ Untranslated Region. *Journal of Virology*, *90*(5), 2332–2344. https://doi.org/10.1128/JVI.02795-15
Zhang, Y., Liu, Z., Hao, X., Li, A., Zhang, J., Carey, C. D., Falo, L. D., & You, Z. (2018). Tumor-derived high-mobility group box 1 and thymic stromal lymphopoietin are involved in modulating dendritic cells to activate T regulatory cells in a mouse model. *Cancer Immunology, Immunotherapy*, *67*(3), 353–366. https://doi.org/10.1007/s00262-017-2087-7

Objectives

HMGB1, HMGB2, and lncRNAs have been described to be involved in the onset and progression of cancer, including epithelial ovarian cancer (EOC). The general objective of this doctoral thesis was to identify lncRNAs that are deregulated and/or associated with HMGB1 and/or HMGB2 as potential novel diagnostic biomarkers and therapeutic targets. To this purpose, we established the following objectives:

1) To identify the deregulated lncRNAs in epithelial ovarian cancer patients from gene expression profiling studies.
2) To analyze the RNA interactome of HMGB1 and HMGB2 in epithelial ovarian cancer cell lines.
3) To study the effects of silencing HMGB1 and HMGB2 at the transcriptomic level in the epithelial ovarian cancer cell line PEO1.

Chapter 1.

Identification of lncRNAs deregulated in epithelial ovarian cancer based on a gene expression profiling meta-analysis

INTRODUCTION

LncRNAs, as well as mRNAs and other types of RNAs, can be studied individually or by omic techniques thanks to the development and popularization of transcriptomic approaches, such as expression microarrays and RNA deep sequencing (Negi et al., 2022). These high-throughput techniques produce a large amount of information that is shared with the scientific community thanks to online repositories, such as the Gene Expression Omnibus (GEO) or the European Nucleotide Archive (ENA) (Negi et al., 2022). There are many gene expression profiling studies in the context of epithelial ovarian cancer (EOC), which also provide clinical information about patients and, depending on the cohort size, are able to capture the patient-to-patient variability, thereby allowing the validation and discovery of biological markers and the advance of precision medicine (Pleasance et al., 2022). Several transcriptomic meta-analyses have been previously published analyzing these data in EOC; however, they either used a small number of studies, those available at the moment (Y. Chen et al., 2019; Ma et al., 2019; Shen & Zhu, 2019; J. Wang et al., 2019) or were focused on protein-coding genes and neglected lncRNAs (H. Dong et al., 2010; Fridley et al., 2018; W. Li et al., 2018; L. Zhao et al., 2020). The work carried out in this chapter is the first lncRNA meta-analysis in EOC comprising a high and significant number of studies, specifically 46 independent cohorts, and the first to integrate information from expression microarrays and bulk RNA sequencing. The objective of this work is to reanalyze and compare all of the EOC-patient-derived microarray and RNA sequencing studies available to date, in order to find lncRNAs that highly correlate to clinical aspects and that might have clinical application in the management of EOC patients.

MATERIALS AND METHODS

Selection of suitable gene expression datasets for meta-analysis

Microarray- and bulk RNA-Seq-based gene expression profiling studies for ovarian cancer were identified in PubMed and the Gene Expression Omnibus (GEO - https://www.ncbi.nlm.nih.gov/geo/ accessed on 15 January 2023) (Barrett et al., 2012). The search terms included “ovarian cancer” AND (“microarray” OR “RNA-Seq”) AND “patients”. Eligible studies and datasets had to fulfill the following requirements: (i) include case and control human studies, (ii) perform transcriptomic analyses, and (iii) have available raw and/or processed microarray or RNA-Seq data. Studies were not considered if they were (i) letters, abstracts, and human case reports, i.e., not full, and original research studies; (ii) studies based only on cell lines as a model of study; (iii) RT-qPCR-based studies only; (iv) studies neglecting ncRNAs, specifically lncRNAs; or (v) only focused on stromal or germinal ovarian cancer.

Data extraction and processing

Microarray intensity files (CEL or text), probe information tables, and RNA-Seq read count tables, along with the experimental metadata included in the series matrix files, were downloaded from the GEO Accession Display for each selected dataset, whereas FASTQ files were downloaded from the European Nucleotide Archive (ENA) browser. It is worth noting that we only considered genes with Ensembl IDs, as their GENCODE annotation is manually supervised and, therefore, updated and reliable. Because of this, some lncRNAs with only RefSeq Gene IDs were not considered, although they were perhaps still interesting for EOC; thus, we may have underestimated our results for the sake of a more confident annotation. The version of the annotation was Ensembl 108 (GRCh38.p13).

Microarray.- Microarray data were processed using BRB-ArrayTools (version 4.6.2), developed by Dr. Richard Simon (Biometric Research Program, National Cancer Institute, Bethesda, Rockville, MD, USA) and the BRB-ArrayTools Development Team.

Affymetrix CEL files were imported with the Data Import Wizard option, using the JustRMA normalization method and standard Affymetrix probe set IDs. The text files were imported using the General Format Importer option, adjusting the red and green thresholds to 10 and 100, respectively, and the background intensity and spot flag information were considered when available. Regardless of the importing option, the experiment descriptor files, which were created from the corresponding series matrix files, were also imported and, in all cases, the option “Average the replicate spots within an array” was selected. Affymetrix Human Genome U133 Plus “1.0” and 2.0 arrays were annotated with chip-specific Bioconductor packages, whereas the rest were annotated using information included in the intensity file or the probe information table, both resulting in RefSeq ID, UniGene ID, and/or GenBank Nucleotide Accession Number lists. These IDs were converted to Ensembl Gene IDs using bioDBnet (Mudunuri et al., 2009), unified in one list, and annotated by merging with the human genome information (hg38, GRCh38.p13) using RStudio (v4.1.0)’s merge function from the data.table package.

RNA-Seq.- RNA-Seq data were processed using RStudio (version 2022.12.0 Build 353), R (version 4.1.0), Bioconductor (version 3.14), and DESeq2 (version 1.34) (Love et al., 2014). For GSE190688, GSE98281, and GSE115573 studies, read count files were not available; hence, after concatenating the GSE115573 files belonging to each sample, we mapped the three of them and quantified the reads using Kallisto (Bray et al., 2016) against human (hg38) cDNA and ncRNA transcriptomes obtained from Ensembl FTP (January 2023). After merging both cDNA and ncRNA abundance files, they were imported into RStudio using tximport and implemented into DESeq2 using the function DESeqDataSetFromTximport. For the rest of the cases, read counts for each Ensembl Gene ID and sample were imported to R in a single file, including the experimental design. Gene filtering and normalization were carried out using DESeq2. In the case of GSE189553, read counts were rounded to the closest integer so that they could be analyzed by DESeq2.

When using datasets from Gene Expression Profiling Interactive Analysis (GEPIA2) (Tang et al., 2019), gene expression profiling was compared between ovarian cancer patients from the Cancer Genome Atlas (TCGA) and normal ovarian tissues from Genotype-Tissue Expression (GTEx). Specifically, in the “FUNCTIONS”, “Expression Analysis”, and “Differential Genes” tab, the “OV” dataset, which corresponds to ovarian adenocarcinoma, was selected. Moreover, from GEPIA2, the top differential genes affecting prognostic variables were downloaded. Specifically, in the “FUNCTIONS”, “Survival Analysis”, and “Most Differential Survival Genes” tab, the “OV” dataset was again selected. Additionally, GTEx normal ovary read counts were downloaded from https://gtexportal.org/home/datasets (accessed on 15 January 2023), and TCGA ovarian adenocarcinoma read counts and raw survival information were downloaded from UCSC Xena (https://xenabrowser.net/datapages/ (accessed on 15 January 2023)).

Cell line RNA-Seq read count data generated by RNA-Seq by Expectation-Maximization (RSEM), along with metadata related to the histological subtype and metastatic or nonmetastatic origin of the cell lines, were downloaded from the Cancer Cell Line Encyclopedia (Ghandi et al., 2019). We filtered the information from 57 epithelial ovarian cancer cell lines and 1 immortalized, non-cancerous ovarian epithelium cell line (OELE). There are 74 cell lines derived from the ovaries, but COLO704, HEY, OVMIU, DOV13, OC315, JHOS3, OVCA420, and OVCA433 do not have transcriptomic information available, and OVCAR5, HSKTC, SNU840, KGN, PA1, COV434, BIN67, and SCCOHT1 were not considered in our meta-analysis because they are not models of epithelial ovarian cancer. RSEM counts were rounded to the closest integer and then normalized using DESeq2.

Data analysis

Five different types of comparisons were carried out to identify differentially expressed lncRNA genes in EOC: (I) “Diagnostic category”, cancer samples *versus* normal samples; (II) “Metastasis category”, peritoneal metastasis *versus* primary tumor,

peritoneal metastasis *versus* cancer cells from ascites or effusion, or cancer cells from ascites or effusion *versus* primary tumor; (III) high expression patients *versus* low expression patients and their correlation with survival periods; (IV) “Drug resistance category”, resistant *versus* sensitive or partial responders *versus* complete responders; and (V) “Subtype category”, samples with one histological subtype samples *versus* the remaining ones. An additional comparison was carried out between metastasis-derived cell lines and primary tumor-derived cell lines using data from cell line transcriptomes.

Differential expression in microarray.- To identify differentially expressed genes between ovarian cancer patients and women free of the disease, class comparisons between groups of arrays were carried out using the function “Class comparison”. Two-tailed *t*-tests were used, setting the significance threshold of univariate tests as 0.01, assuming (when possible) a random variance model, and blocking by patient or sample (when matched samples were available).

Differential expression in RNA-Seq.- Differential expression was run with DESeq2 and, finally, annotated to the human genome hg38, as previously described for microarray data. The false discovery rate (FDR) cutoff was set as 0.05 and |Log2FC| as 0.585, blocking by patient or sample when matched samples were available. In the case of GEPIA2, the differential gene expression was calculated using the LIMMA method, with the |Log2FC| cutoff set as 0.585, and the *q*-value cutoff set as 0.01, selecting both overexpressed and underexpressed genes.

Differential survival in microarray.- Overall survival (OS) and disease-free survival (DFS) gene lists were generated using BRB-ArrayTools “Survival analysis” and “Genes affecting survival”. This option carries out Cox proportional hazards model (Wald statistic) univariate tests, and the *p*-value was set to 0.01.

Differential survival in RNA-Seq (GEPIA2).- OS and DFS gene lists were generated based on gene expression by applying the Log-rank test (Mantel-Cox test). The OV TCGA cohort threshold between the “high” and “low” groups was set to the median, the confidence interval to 95%, and the *p*-value to 0.01.

Pairwise lncRNA analyses

Significantly deregulated lncRNAs with Ensembl IDs from microarray or RNA-Seq studies were selected and separated into “upregulated” or “downregulated” lists, respectively, for each individual study according to their fold change in the previously described comparisons.

All possible pairwise comparisons between studies of each category were carried out within the “upregulated” and “downregulated” lists, separately, using the Excel match function between Ensembl Gene IDs. As an exclusion criterion for all of the categories, genes that had contradictory trends (that is, upregulated in some studies but downregulated in others) were considered to be ambiguous and were discarded. For the “Diagnostic category”, only lncRNA genes that were differentially expressed in at least three independent studies were selected. For the “Survival category”, lncRNAs were separated into those positively correlated with favorable patient prognosis or unfavorable prognosis. Finally, selected lncRNA genes for each category were further compared pairwise with the remaining categories, again with the Excel match function (version 2305).

ROC analysis

Receiver operating characteristic (ROC) curve analysis was performed using easyROC (version 1.3.1) (http://www.biosoft.hacettepe.edu.tr/easyROC/ (accessed on 15 January 2023)) (Goksuluk et al., 2016).

Figures and Venn diagrams

Figures were created with GraphPad Prism version 8.0.2. Venn diagrams were generated using InteractiVenn (http://www.interactivenn.net/# (accessed on 15 January 2023)) (Heberle et al., 2015).

Nomenclature

Novel transcripts that do not have yet a gene symbol, are identified by their Ensembl Gene ID.

RESULTS

In this meta-analysis, we analyzed publicly available independent transcriptomic datasets from EOC-patient-derived samples, which contain lncRNA expression data as well as associated clinical data from patients included in the studies. They are representative of the actual clinical knowledge of EOC and integrate the wide variability between individuals and cohorts.

In our search for gene expression profiling data in ovarian cancer, we initially found a total of 63 studies, of which 51 and 12 accounted for microarray and bulk RNA-Seq technologies, respectively. In terms of the type of analyzed sample, 48 studies used tissue, 2 blood, 2 blood serum, 1 urine, and 1 saliva, whereas 9 worked with cell lines (2 of them including their derived exosomes). All of the studies were considered epithelial ovarian cancer cases, although four of them contained additional data from tumor stromal cells that were not used in this meta-analysis. Seventeen studies restrained the cancer samples to one specific subtype, such as high-grade serous or clear cell; another six compared several subtypes within the same study, while the remaining thirty-eight studies did not specify the EOC subtype. Those samples named in the original studies as “serous”, “high-grade serous”, or “low-grade serous” were jointly considered. Out of the 51 studies with cancer patients (excluding cell line studies) who were naïve to treatment at the time of sample extraction, 22 of them did not include samples from healthy tissue for comparison, but 7 of these 22 studies included either cancer cells from ascites and/or peritoneal metastatic samples matched to the primary tumor. There were 11 studies with prognostic information, including survival and/or progression over time. Twelve studies only considered miRNAs, due to the selected microarray platform. The full list of initially identified studies, including the cohort size of each study, can be found in the Supplementary Materials (Table S1).

Our objective was to identify lncRNAs (antisense, sense, intronic, intergenic, divergent, overlapping, and non-overlapping) with clinical value related to epithelial

ovarian cancer. Thus, we kept 46 studies from the 63 initially identified according to the criteria specified in the materials and methods section, thereby excluding 17 studies with information only from miRNAs and/or carried out only with cell lines. Due to the heterogeneity of clinical information available in each study, we performed different rounds of analyses focusing on different studies, which included information of relevance in diagnosis or prognosis, correlation to metastasis, chemotherapy resistance, and histological EOC subtypes. Therefore, in the following sections, we use the same criteria to present the results of the different analyses performed.

Analysis of lncRNAs with putative diagnostic value in EOC

In this first round of our analysis, we sought to identify differentially expressed lncRNAs, either upregulated or downregulated, in EOC compared with healthy samples. For this category, we considered 24 studies that used both cancer and control samples; however, EGAD00001000877 data are not publicly available, and the RNA-Seq libraries from GSE192410 were prepared from circular RNA only; therefore, these data were discarded. We analyzed the remaining 22 studies, whose metadata and results for the differential expression analyses are available in the Supplementary Materials (Table S2). The RNA analyzed in these studies was derived from tissue samples, except for GSE29220, whose RNA was derived from saliva samples. Only one study, GSE137238, presented matched cancer and normal ovarian tissue from the same woman, whereas in the rest, the case and control samples came from different women.

A summary from these 22 analyses is shown in Figure 1, in which the number of up- and downregulated lncRNAs in EOC is depicted, as well as the sum of the other gene biotypes (protein-coding genes, pseudogenes, micro-RNA genes, T-cell receptor genes, immunoglobulin genes, small nuclear RNA genes, small nucleolar RNA genes, small Cajal body-specific RNA genes, ribosomal RNA genes, and ribozyme genes). The study generating the highest number of deregulated targets was GSE190688, with 6,934

upregulated and 5,325 downregulated, of which 1,691 and 1,497 were lncRNAs, respectively. For GSE29220, statistically significant deregulation was not identified.

After obtaining the list of differentially expressed genes for each study, we carried out multiple pairwise comparisons to determine which lncRNAs were deregulated across the different cohorts with the same trend (up or down). A total of 271 lncRNAs with contradictory trends among different studies (that is, upregulated in some studies but downregulated in others) were excluded, but they are listed in the Supplementary Materials (Table S3). There were 247 upregulated and 243 downregulated lncRNAs that were statistically significant in at least three of the analyzed studies (listed in Tables 1 and 2, respectively); the majority of which (200 and 209, respectively) were not previously related to EOC (Supplementary Materials, Table S4).

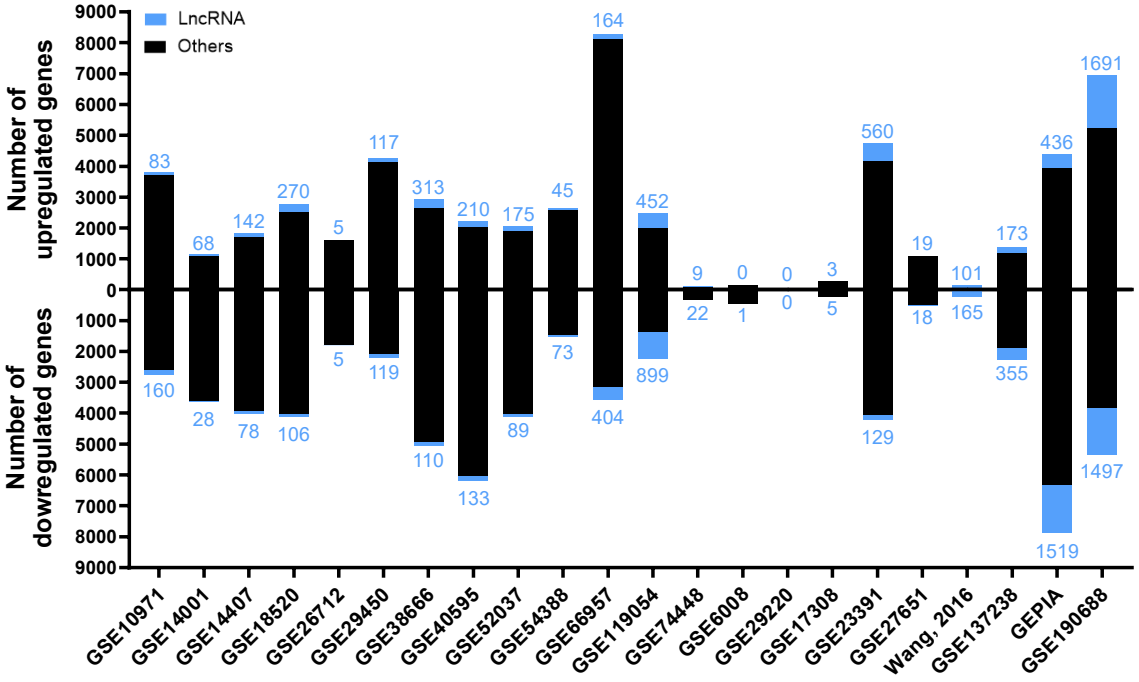

Figure 1.- The number of deregulated genes in each selected study in the "Diagnostic" analysis. The bar graph shows the absolute frequency of upregulated (upper part) and downregulated (lower part) genes, depicting the fraction corresponding to lncRNA genes in blue at the ends of the bars.

The most frequently upregulated lncRNAs were *RNF157-AS1* and *BBOX1-AS1*, both in 12 different studies, whereas *MAGI2-AS3* was the most frequently downregulated lncRNA, in 15 different studies. The lncRNAs that showed significant upregulation and that were more frequently found in different cohorts, but that had not been previously related to EOC diagnosis, were *ENSG00000187951*, *MIR205HG*, *ZNF232-AS1*,

ENSG00000285756, *LINC01297*, *TFAP2A-AS1*, *LINC01977*, and *LINC01770*, as shown in Figure 2A. The lncRNAs that were more frequently downregulated in different cohorts but that had not been previously related to EOC diagnosis were *PGM5-AS1*, *ENSG00000267058*, *EPM2A-DT*, *NR2F1-AS1*, *KLF3-AS1*, *GLIDR*, *ERVK13-3*, and *CLN8-AS1*, as shown in Figure 2B.

There were several lncRNAs that we considered to be contradictory from the results that we found in the meta-analyses (Supplementary Materials, Table S3) and that were related to EOC in the literature, such as *PART1* (H. Li et al., 2022) or *XIST* (R. Jiang et al., 2021). This fact does not invalidate the experimental evidence collected about their role in EOC, although it downplays their importance as diagnostic biomarkers for the disease since different trends are observed in different cohorts.

Once we had obtained these two lists, we checked whether these lncRNAs were also deregulated in 57 epithelial ovarian cancer cell lines when compared with OELE*,* a non-cancerous human ovarian epithelium cell line, as a criterion for further validation. We obtained raw read counts from RNA sequencing of each of these cell lines from the Cancer Cell Line Encyclopedia (CCLE), rounded them to the closest integer, and normalized them using DESeq2. After that, we sorted the 58 cell lines in ascending normalized read counts for each gene, annotating the position and quartile in which OELE was present. We considered that deregulation in patients was consistent with the cell line data when OELE occupied a position within the first quartile (lower expression) for upregulated genes or the fourth quartile (higher expression) for downregulated genes. There were 42 upregulated and 57 downregulated lncRNAs that fulfilled these criteria (in bold in Tables 1 and 2, and reported, together with position and quartile information, in the Supplementary Materials (Table S4).

Table 1.- Upregulated lncRNAs in ovarian cancer tissue in at least three different transcriptomic studies from the "Diagnostic" analysis. For genes in bold, the position of the non-cancerous cell line OELE matches the first quartile when sorting the cell lines in ascending normalized counts.

# of studies	Gene count	Gene name
12	2	*RNF157-AS1, BBOX1-AS1*
11	1	*DUXAP8*
10	6	*ATP2A1-AS1,* ***ENSG00000187951****, FOXP4-AS1, MIR205HG,* ***UCA1****, ZNF232-AS1*
9	2	***LINC00664****,* ***LINC01503***
8	10	***ENSG00000285756****, ESRG, HAGLR, LINC00665, LINC01297, LINC01770,* ***LINC01977****, PRKCQ-AS1, TFAP2A-AS1, TIAM1-AS1*
7	8	*ASH1L-AS1, HAGLROS, LINC00839, LINC01135, LINC01558, MRPL20-AS1,* ***SPINT1-AS1****, VPS13B-DT*
6	11	*C10orf95-AS1,* ***DLX6-AS1****, ENSG00000286546, FZD10-AS1, KLHDC7B-DT, LINC03014, NCK1-DT, PCAT6,* ***PP7080****, RNASEH1-AS1, TDRKH-AS1*
5	25	*CCDC140, CDKN2B-AS1, DLEU1, DPP3-DT, ELFN1-AS1, WDR35-DT,* ***PPP1R3B-DT****, ENSG00000256802, KDM7A-DT, KIAA1614-AS1, KIF25-AS1, LBX2-AS1, LINC00853, LINC00884, LINC01142, LINC01215, LINC01532, LINC02159, LINC02387, LYRM4-AS1, MIR155HG, MYCNOS,* ***OBSCN-AS1****, TLR8-AS1,* ***TNFRSF10A-DT***
4	46	*ATP11A-AS1, CLMAT3,* ***DSP-AS1****,* ***ENSG00000231119****, ENSG00000260418, ENSG00000267665, EPHA1-AS1, EPIC1,* ***EXOSC10-AS1****, GAPLINC, ITGB2-AS1, LAMA5-AS1, LINC00943, LINC00944,* ***LINC00958****, LINC01224, LINC01271,* ***LINC01315****, LINC01333, LINC01342, LINC01356, LINC01362, LINC01410, LINC01545, LINC01547, LINC02041, LINC02043, LINC02492, LINC03011, LINGO1-AS1, MINCR,* ***MIR1915HG****, MIR200CHG, NAV2-AS5, PCAT4,* ***PPP1R14B-AS1****, PPP1R26-AS1, PRRT3-AS1, PRRX2-AS1, PSORS1C3, RALY-AS1, SLC2A1-DT, SNHG4, ZNF503-AS1, ZNF687-AS1, ENSG00000215022*
3	136	*ANKRD44-IT1,* ***BISPR****, BRWD1-AS2, C6orf99,* ***C8orf31****, CA3-AS1, CARD8-AS1, CASC9, CSMD2-AS1, CT69, CTB-178M22.2, DHCR24-DT, DHX35-DT, EGFLAM-AS4, ENSG00000224504, ENSG00000226527, ENSG00000259540,* ***ENSG00000260912****, ENSG00000261095,* ***ENSG00000261924****, ENSG00000273523, ENSG00000289161, ENSG00000290993, ENSG00000291232, FAM151B-DT, FZD4-DT, GNAS-AS1,* ***GPRC5D-AS1****, HMMR-AS1, IQCF5-AS1, KANSL1-AS1, KCNMB2-AS1,* ***LCAL1****,* ***LCMT1-AS2****, LINC00308, LINC00354, LINC00461, LINC00513, LINC00589, LINC00620, LINC00656, LINC00668, LINC00858, LINC00868, LINC00896, LINC00907, LINC01049, LINC01111,* ***LINC01123****,* ***LINC01127****, LINC01144, LINC01512, LINC01737, LINC01812,* ***LINC01833****, LINC01904, LINC02064, LINC02152, LINC02223, LINC02240, LINC02257, LINC02517, LINC02580, LINC02712, LINC02837, LNCOC1, LZTS1-AS1,* ***MAP3K9-DT****, MAPT-AS1, MIR3681HG, MIR3945HG, MIR4458HG, MRPL20-DT, NDUFB2-AS1,* ***NEBL-AS1****,* ***NINJ2-AS1****, NUP50-DT, NUTM2A-AS1,* ***OGFRP1****, PARTICL, PIK3CD-AS2, POU2F2-AS1, PSLNR, PTPRN2-AS1, RAPGEF4-AS1, RFX5-AS1,* ***RHPN1-AS1****, RNASE11-AS1,* ***SAMD12-AS1****, SCIRT, SLC8A1-AS1, STAU2-AS1, TIPARP-AS1, TRPM2-AS, TYMSOS, UBAC2-AS1, UBR5-DT,* ***ENSG00000236529****,* ***ENSG00000261211****,* ***ENSG00000268204****,* ***ENSG00000272275****,* ***AQP5-AS1****,* ***LINC03057****,* ***ENSG00000261068****, ENSG00000261135, ENSG00000261061, ENSG00000272872, ENSG00000224272, ENSG00000275216, ENSG00000225335, ENSG00000236924, ENSG00000250899, ENSG00000269155, ENSG00000245719, ENSG00000256234, ENSG00000259163, ENSG00000225489, ENSG00000260920, ENSG00000255114, ENSG00000270460, ENSG00000278238, ENSG00000267698, ENSG00000233461, ENSG00000270174, ENSG00000253174, ENSG00000269968, ENSG00000231295, ENSG00000232386, ENSG00000269399, ENSG00000226334, ENSG00000265415, ENSG00000234694, ENSG00000243224, ENSG00000267512, ENSG00000244184, ENSG00000261071*

Table 2.- Downregulated lncRNAs in ovarian cancer tissue in at least three different transcriptomic studies from the "Diagnostic" analysis. For genes in bold, the position of the non-cancerous cell line OELE matches the fourth quartile when sorting the cell lines in ascending normalized counts.

# of studies	Gene count	Gene name
15	1	***MAGI2-AS3***
13	2	*ADAMTS9-AS2,* ***HAND2-AS1***
12	4	*CRNDE, GAS1RR, MIR22HG,* ***PGM5-AS1***
11	4	*ADAMTS9-AS1, ENSG00000267058, EPM2A-DT,* ***NR2F1-AS1***
10	4	***GATA6-AS1***, ***GIHCG***, *KLF3-AS1, WDFY3-AS2*
9	6	*ATP2B1-AS1, ERVK13-1, GLIDR,* ***HHIP-AS1***, *HYMAI,* ***SNHG8***
8	9	*C2orf27A,* ***CLN8-AS1***, *DPP10-AS1, ENSG00000272447, EPB41L4A-AS1, FGF14-AS2,* ***MIR100HG***, *RASSF8-AS1, SP2-AS1*
7	6	*ID2-AS1,* ***LINC00667***, ***LINC00842***, *LINC02941, LINC03013, ZFAS1*
6	12	***CKMT2-AS1***, *DUBR, EGOT, FGD5-AS1, GABPB1-AS1,* ***LINC00924***, *LINC01616, PAN3-AS1, SDCBP2-AS1,* ***SLC25A21-AS1***, ***SNHG18***, ***ZEB1-AS1***
5	13	*CERNA1, CPVL-AS2, ENSG00000204814,* ***FRMD6-AS2***, *LINC00342,* ***LINC00526***, *LINC00683, LINC02754,* ***MEF2C-AS1***, *NIFK-AS1, PAXBP1-AS1, PWRN1, VLDLR-AS1*
4	44	*ADD3-AS1, ANXA2R-AS1,* ***ARHGEF26-AS1***, *CRIM1-DT, DPH1-AS1, ENSG00000145075, ENSG00000204666,* ***ENSG00000230393***, *ENSG00000244953, ENSG00000245025, ENSG00000248115, ENSG00000253123, ENSG00000255495, ENSG00000258181, ENSG00000259976, ENSG00000261305, ENSG00000261671, ENSG00000270589, FGF13-AS1,* ***FLRT2-AS1***, *GASK1B-AS1, KLRK1-AS1, LETR1, LINC00324, LINC00926, LINC00997, LINC01018, LINC01391,* ***LINC02360***, *LNCRNA-IUR, MIR3936HG,* ***MRGPRF-AS1***, *NPEPPSP1,* ***NR2F2-AS1***, *NR4A1AS, OR2A1-AS1, PCAT19, PTPRD-AS1, RPH3AL-AS1, SNHG26, TMEM220-AS1, TPT1-AS1,* ***TRHDE-AS1***, ***WARS2-IT1***
3	139	*CAVIN2-AS1, CEROX1,* ***CNN3-DT***, *DHDDS-AS1, DNAJC27-AS1,* ***ELOA-AS1***, *ENSG00000226622, ENSG00000226862, ENSG00000227733, ENSG00000231609, ENSG00000232934, ENSG00000233178, ENSG00000233760, ENSG00000233894,* ***ENSG00000234394***, *ENSG00000234699,* ***ENSG00000235159***, ***ENSG00000235563***, *ENSG00000238018,* ***ENSG00000243004***, *ENSG00000246250,* ***ENSG00000249679***, *ENSG00000249849, ENSG00000250286, ENSG00000250326, ENSG00000254141, ENSG00000254855, ENSG00000256139, ENSG00000256973,* ***ENSG00000257894***, *ENSG00000259275, ENSG00000259359, ENSG00000259367, ENSG00000259969,* ***ENSG00000260269***, ***ENSG00000260277***, ***ENSG00000260563***, *ENSG00000260583, ENSG00000260645, ENSG00000260686, ENSG00000260693, ENSG00000260859, ENSG00000261167, ENSG00000261269, ENSG00000261292,* ***ENSG00000266677***, *ENSG00000267042, ENSG00000267082, ENSG00000267636,* ***ENSG00000267774***, *ENSG00000268047, ENSG00000268912, ENSG00000269068, ENSG00000269194, ENSG00000269210, ENSG00000270096, ENSG00000270140, ENSG00000270640, ENSG00000271730, ENSG00000271930, ENSG00000272158,* ***ENSG00000272159***, ***ENSG00000272823***, *ENSG00000272831, ENSG00000273650, ENSG00000274719, ENSG00000275120, ENSG00000277351, ENSG00000277954, ENTPD1-AS1, FAM167A-AS1, FAM182A, FAM53B-AS1, FAM66A, FAM85B, FOXO6-AS1, GARS1-DT,* ***GCC2-AS1***, *HOXA-AS2,* ***HSD11B1-AS1***, *INE2, IRS4-AS1, JAZF1-AS1, LINC00602, LINC00844,* ***LINC00847***, *LINC00886, LINC00891,* ***LINC00921***, *LINC01229, LINC01402, LINC01474, LINC01560, LINC01619, LINC01625,* ***LINC01852***, *LINC02126, LINC02145,* ***LINC02202***, *LINC02308, LINC02345, LINC02613, LINC02691, LINC02731, LINC03007, LRRC8C-DT,* ***LRRK2-DT***, *MAFTRR, MAP3K4-AS1, MEG8, MIMT1, MIOS-DT, MIR223HG,* ***MIR497HG***, *MRPS30-DT, MSC-AS1,* ***NALT1***, ***PACERR***, ***PGM5P3-AS1***, ***PGM5P4-AS1***, *PRR34-AS1, PRSS23-AS1, PSMG3-AS1, RASGRF2-AS1, RBPMS-AS1, RORA-AS1, SAP30-DT, SEMA6A-AS1, SMC5-DT, SNHG5, TICAM2-AS1,* ***TMC3-AS1***, *TSPEAR-AS1, TTC3-AS1, XPC-AS1,* ***ZEB2-AS1***, *ZNF300P1, ZNF594-DT*

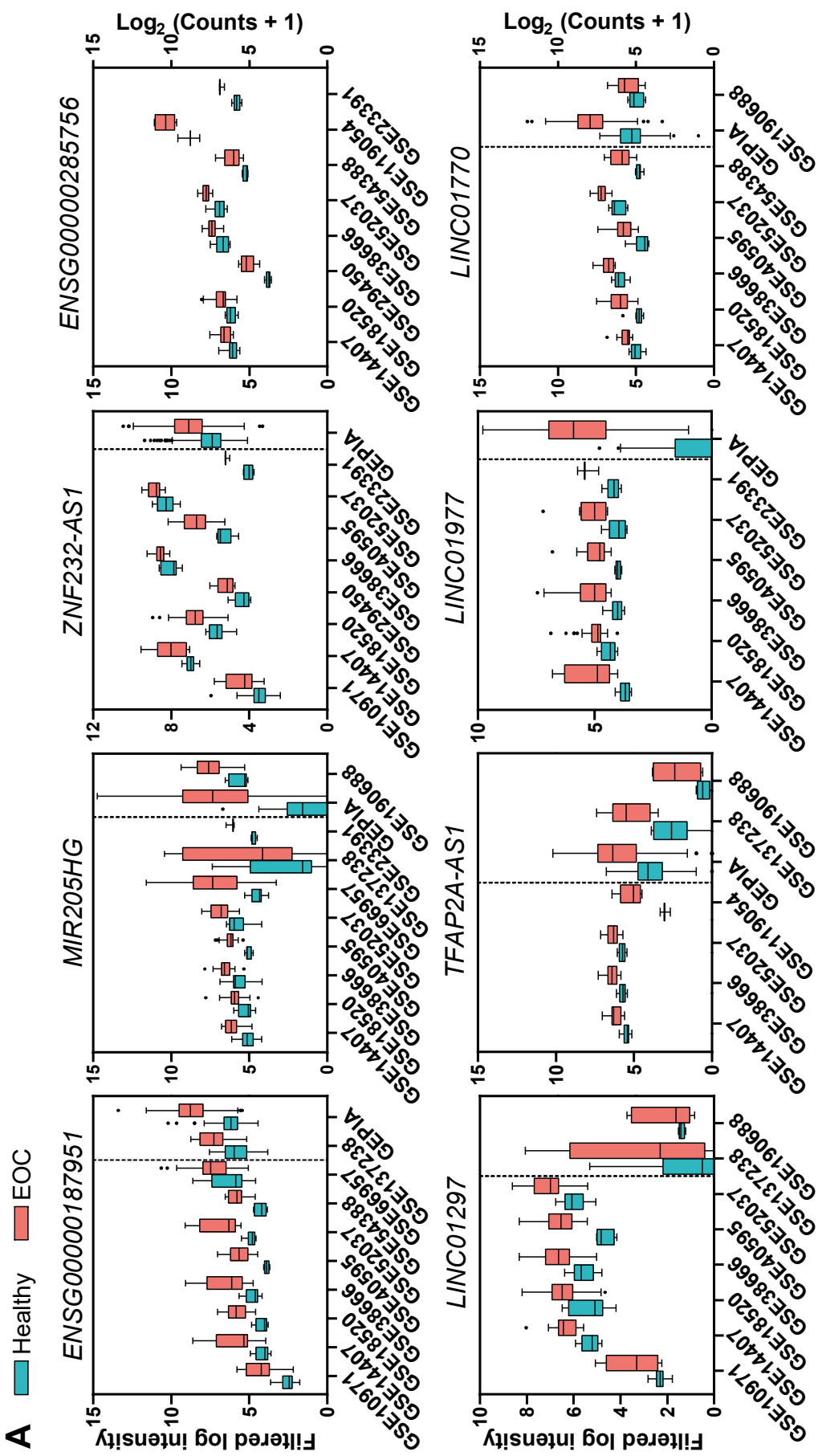

Figure 2.- Expression levels in EOC and normal ovary tissues of the top deregulated lncRNAs that were discovered in the EOC meta-analysis. (A, B) Panels correspond to upregulated and downregulated genes, respectively. The middle line in each boxplot represents the median value, and the black dots are the outlier values. Comparisons from the dotted line to the left are from microarray studies, and comparisons from the dotted line to the right are from RNA-Seq studies, except for *GLIDR* and *ENSG00000285756*, for which all comparisons are from microarrays. *ZNF232-AS1*, *ATP2A1-AS1*, *LINC01977*, *TFAP2A-AS1*, and *NR2F1-AS1* are not represented in this figure, because only fold changes and *p*-values are available in this study (H. Wang et al., 2016). All comparisons are $p \leq 0.01$.

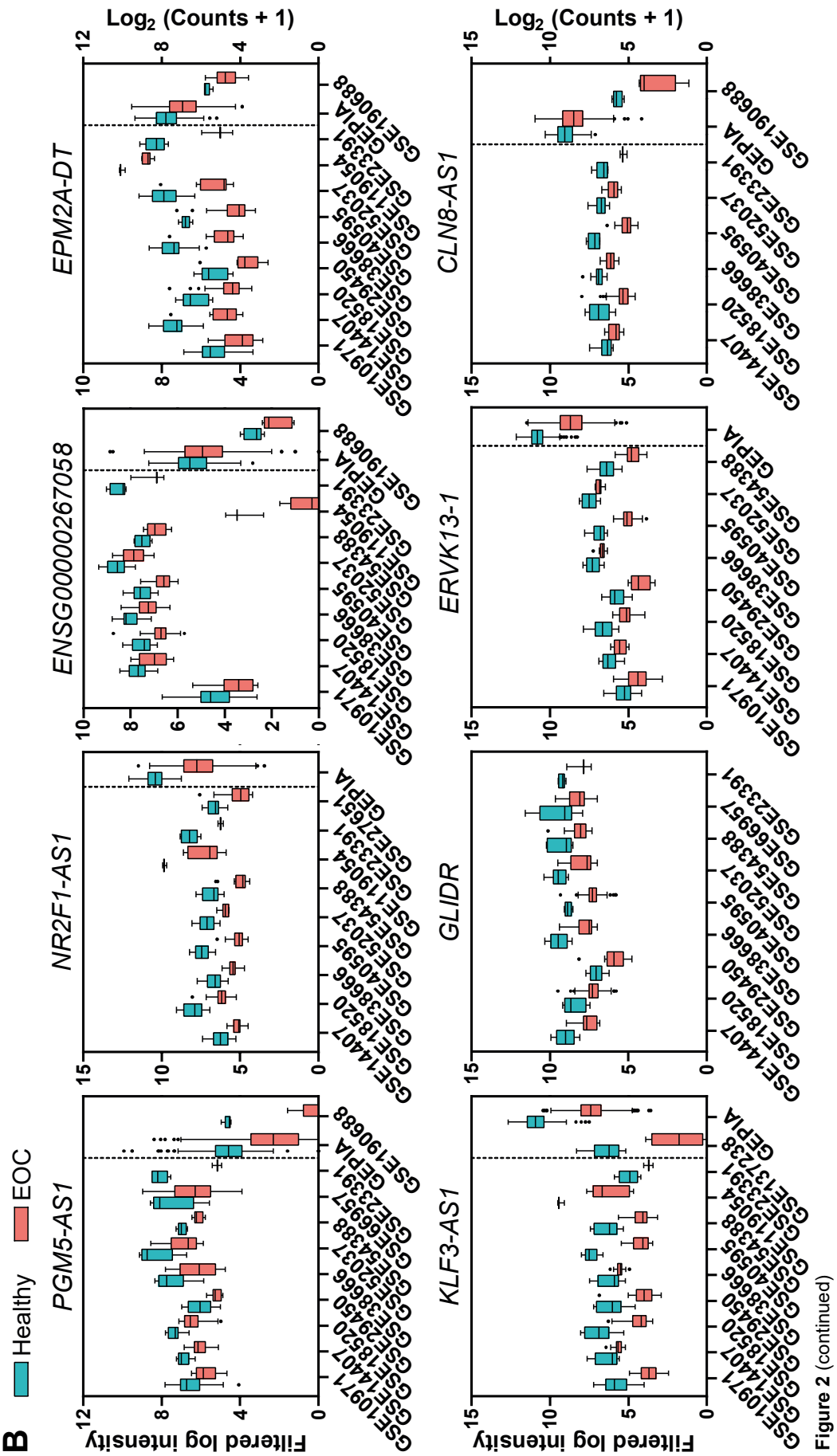

Figure 2 (continued)

Analysis of lncRNAs with putative prognostic value in EOC

This second analysis consisted of differentially expressed lncRNAs showing a significant correlation with favorable or unfavorable prognosis, meaning increased or decreased, respectively, overall survival (OS) and/or disease-free survival (DFS) periods after diagnosis or time without relapse after being treated or surgically debulked. In this category, we selected 11 studies containing information about death and relapse events over time. The metadata information of each study and the results from our meta-analysis can be found in the Supplementary Materials (Table S5). The numbers of genes resulting from the Cox proportional hazards model affecting OS and DFS for each study are depicted in Figure 3.

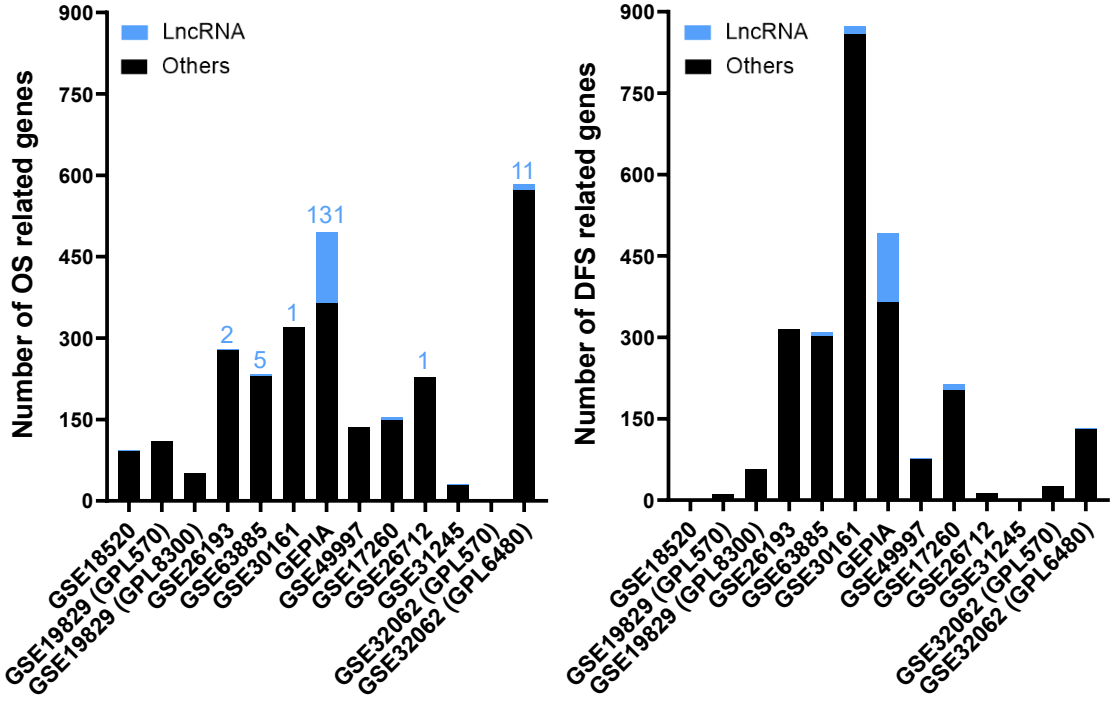

Figure 3.- The numbers of genes affecting OS (left) and DFS (right) in each selected study for the "Prognostic" analysis. The bar graph shows the absolute frequency of genes; the portion in blue at the ends of the bars is the fraction corresponding to lncRNA genes. NA (not applicable) means that there is no patient information about DFS for those studies, whereas 0 means that there are no statistically significant genes.

These analyses yielded 123 and 32 lncRNAs positively correlated with longer or shorter OS periods, respectively, as listed in Table 3. We also found 125 lncRNAs that were positively correlated with longer DFS periods and 34 lncRNAs with shorter DFS periods, as presented in Table 4. The references from the genes that were previously associated with EOC in the literature can be found in the Supplementary Materials (Table

S6). When comparing the resulting gene lists from each analysis pairwise, only six lncRNAs (in bold in Tables 3 and 4) were confirmed in two different studies: *RNF157-AS1*, *AQP5-AS1*, *CRNDE*, and *ZFAS1* in OS studies, and *MALAT1* and *SNHG8* in DFS studies. However, *SNHG8* showed opposed trends in the two studies; therefore, we excluded it from the final lists of this category (but it is included in the Supplementary Materials (Table S3)). Figure 4 shows the survival periods of three selected lncRNAs.

Table 3.- LncRNA genes positively correlated with longer (left) or shorter (right) OS periods in EOC patients identified in the studies from the "Prognosis" analysis. LncRNAs in bold are present in two different studies.

LncRNAs correlating with longer OS	LncRNAs correlating with shorter OS
RNF157-AS1, ***AQP5-AS1***, *AKAP1-DT, ANKRD44-AS1, ARHGAP28-AS1, BMPR1B-DT, CD2AP-DT, CEACAM16-AS1, DCTN6-DT, DNAJC9-AS1, DNM1P35, DTD1-AS1, EBLN3P, FAM27C, FOXP4-AS1, FZD4-DT, GPRC5D-AS1, HAGLROS, HCG14, HCP5, HLA-L, IFNG-AS1, IL6R-AS1, JARID2-DT, LINC00467, LINC00488, LINC00592, LINC00664, LINC01431, LINC01635, LINC01695, LINC01829, LINC01970, LINC02006, LINC02073, LINC02091, LINC02167, LINC02321, LINC02346, LINC02629, LINC02754, LINC02777, LUNAR1, MIR762HG, MYCNOS, MYL12-AS1, NUTM2A-AS1, PCAT18, POLH-AS1, RAB11B-AS1, RFX5-AS1, RGMB-AS1, RMST, RNASEH1-AS1, SCIRT, SNHG10, SRD5A3-AS1, TRBV11-2, TWSG1-DT, USP30-AS1, ENSG00000228863, ENSG00000259834, ENSG00000235021, ENSG00000273221, ENSG00000232739, ENSG00000270087, ENSG00000255135, ENSG00000256101, ENSG00000256948, SLC38A4-AS1, ENSG00000275769, ENSG00000276727, ENSG00000277863, ENSG00000258521, ENSG00000278022, ENSG00000259772, ENSG00000276408, ENSG00000263063, ENSG00000263427, ENSG00000265840, ENSG00000274213, ENSG00000277597, ENSG00000266149, ENSG00000267627, ENSG00000273368, ENSG00000268555, ENSG00000268650, ENSG00000230432, ENSG00000235319, ENSG00000273063, ENSG00000276517, ENSG00000281920, ENSG00000277901, ENSG00000273210, ENSG00000272858, ENSG00000250039, ENSG00000272626, ENSG00000272986, ENSG00000272203, ENSG00000272417, ENSG00000261071, ENSG00000272209, ENSG00000228506, ENSG00000261189, ENSG00000272009, ENSG00000272243, ENSG00000272379, ENSG00000231794, ENSG00000214870, ENSG00000237773, ENSG00000260997, ENSG00000273391, ENSG00000253982, PPP1R3B-DT, ENSG00000253369, ENSG00000254812, ENSG00000260484, ENSG00000253400, ENSG00000232412, ENSG00000290574, ENSG00000290689, ENSG00000290796*	***CRNDE***, ***ZFAS1***, *C2orf27A, DUXAP8, FLG-AS1, GUSBP11, LINC00484, LINC01127, LINC02881, MAGI2-AS3, MIR600HG, MIR924HG, NRSN2-AS1, PAXBP1-AS1, PCAT4, PIK3R5-DT, RP9P, ENSG00000260917, ENSG00000257545, ENSG00000259341, ENSG00000261069, ENSG00000271725, ENSG00000270020, ENSG00000275438, ENSG00000266709, LINC02958, ENSG00000213963, ENSG00000229839, ENSG00000270696, ENSG00000240057, ENSG00000230074, ENSG00000290659*

Table 4.- LncRNA genes positively correlated with longer (left) or shorter (right) DFS periods in EOC patients identified in the studies from the "Prognosis" analysis. LncRNAs in bold are present in two different studies.

LncRNAs related to longer DFS	LncRNAs related to shorter DFS
ADCY10P1, ANO1-AS1, ATXN2-AS, B4GALT1-AS1, C1orf21-DT, C6orf223, CRTC3-AS1, CT62, CXXC5-AS1, DIAPH2-AS1, DLGAP1-AS1, DNM1P35, EIF1B-AS1, EML2-AS1, FAM111A-DT, FAM27C, FOXP4-AS1, FZD4-DT, HCG15, IFNG-AS1, JARID2-DT, LINC00221, LINC00243, LINC00582, LINC00592, LINC00927, LINC01003, LINC01144, LINC01825, LINC02298, LINC02397, LINC02541, LINC02601, LINC02875, LL22NC03-63E9.3, LUNAR1, MAN2A1-DT, MIAT, MIR3142HG, NCKAP5-AS2, NDUFV2-AS1, NIFK-AS1, NR2F2-AS1, NSMCE1-DT, OLMALINC, PKP4-AS1, POLG-DT, PP2672, PPP1R21-DT, PPP1R26-AS1, RNF157-AS1, RORA-AS1, RPH3AL-AS1, SBF2-AS1, SLC25A5-AS1, SUGCT-AS1, TAX1BP1-AS1, THOC7-AS1, TRBV11-2, XIAP-AS1, ZSCAN5A-AS1, ENSG00000224152, ENSG00000226334, ENSG00000226889, ENSG00000228021, ENSG00000228084, ENSG00000228863, ENSG00000229311, ENSG00000230912, ENSG00000231081, ENSG00000231098, ENSG00000231519, ENSG00000231794, ENSG00000232533, ENSG00000233230, ENSG00000233242, ENSG00000234134, ENSG00000235586, ENSG00000236140, ENSG00000254290, ENSG00000254343, ENSG00000255440, ENSG00000257042, ENSG00000257327, AQP5-AS1, ENSG00000258534, ENSG00000258572, ENSG00000258904, ENSG00000259802, ENSG00000259834, ENSG00000260038, ENSG00000260352, ENSG00000260369, ENSG00000261071, ENSG00000261204, ENSG00000261320, ENSG00000261655, ENSG00000262115, ENSG00000263063, ENSG00000266830, ENSG00000267255, ENSG00000267666, ENSG00000269951, ENSG00000270115, ENSG00000270265, ENSG00000271367, ENSG00000272172, ENSG00000272209, ENSG00000272456, ENSG00000272672, ENSG00000272831, ENSG00000273004, ENSG00000273104, ENSG00000273162, ENSG00000273210, ENSG00000273456, ENSG00000273989, ENSG00000275155, ENSG00000275202, ENSG00000275297, ENSG00000275484, ENSG00000276408, ENSG00000277901, ENSG00000278022, ENSG00000291006, ENSG00000291136	*GUSBP11, **MALAT1**, AQP4-AS1, DSG2-AS1, HLA-F-AS1, HOTAIRM1, LINC00452, LINC00472, LINC00565, LINC01140, LINC02328, LINC02432, LINC-PINT, LNCOC1, MIR924HG, PHACTR2-AS1, RRP7BP, TMEM161B-AS1, ZNF295-AS1, ZNF503-AS2, ENSG00000233834, ENSG00000243004, ENSG00000248268, ENSG00000249476, ENSG00000258603, ENSG00000259065, ENSG00000260412, ENSG00000261292, ENSG00000265975, ENSG00000266283, ENSG00000270074, ENSG00000272632, ENSG00000278668, ENSG00000280604*

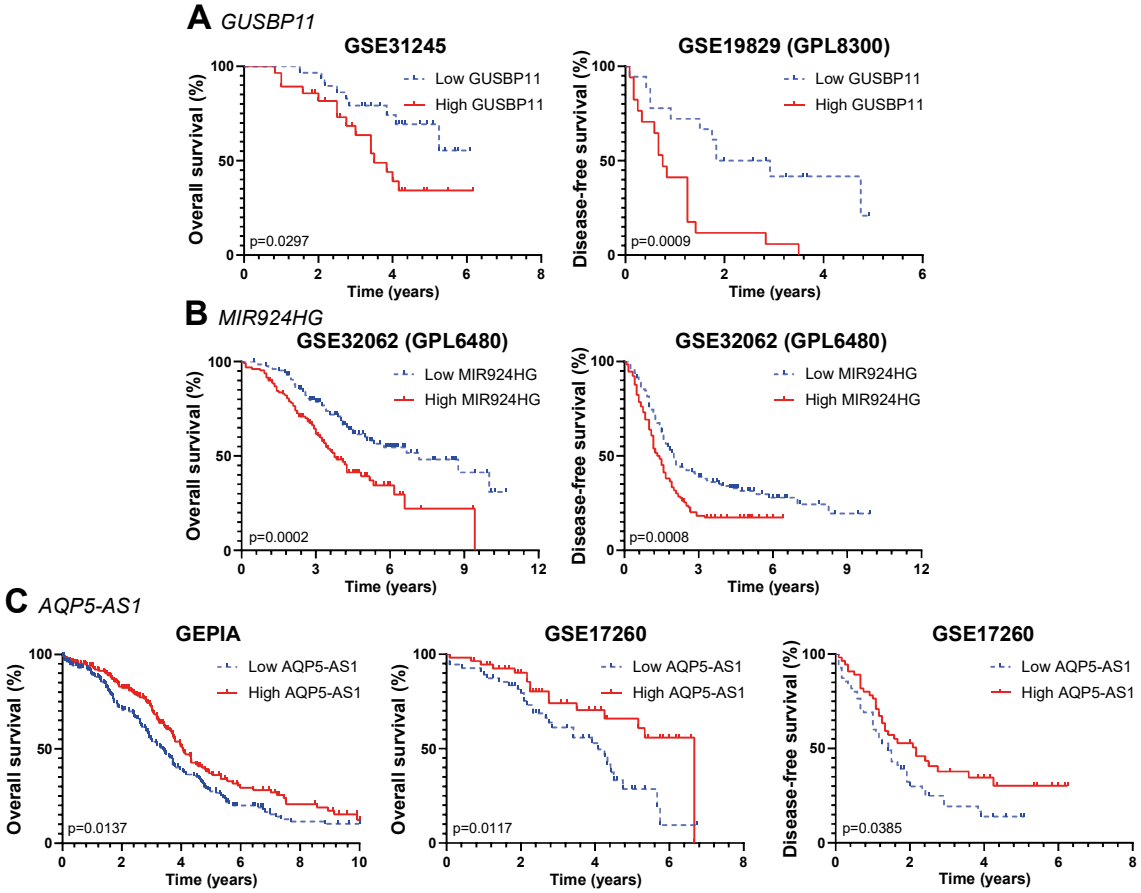

Figure 4.- Kaplan Meier curves for three lncRNAs affecting survival periods in EOC patients: *GUSBP11* (A), *MIR924HG* (B), and *AQP5-AS1* (C). Graph titles indicate each corresponding study.

Analysis of lncRNAs deregulated in EOC metastasis

The third analysis comprised seven different studies (summarized in the Supplementary Materials (Table S7)) containing transcriptomic information derived from the primary tumor, cancer cells from the ascitic fluid, and/or peritoneal solid metastasis samples, matched for each patient.

We analyzed the seven studies individually to look for differentially expressed lncRNA genes related to the metastatic process by comparing (i) peritoneal solid metastasis versus cancer cells from the ascitic fluid, (ii) peritoneal solid metastasis versus primary tumor, and (iii) cancer cells from the ascitic fluid versus primary tumor, using the variable “patient” as a blocking factor. A summary of the differentially expressed genes for each comparison and study is shown in Figure 5. The two studies that yielded the highest numbers of differentially expressed genes were GSE133296 and GSE137237.

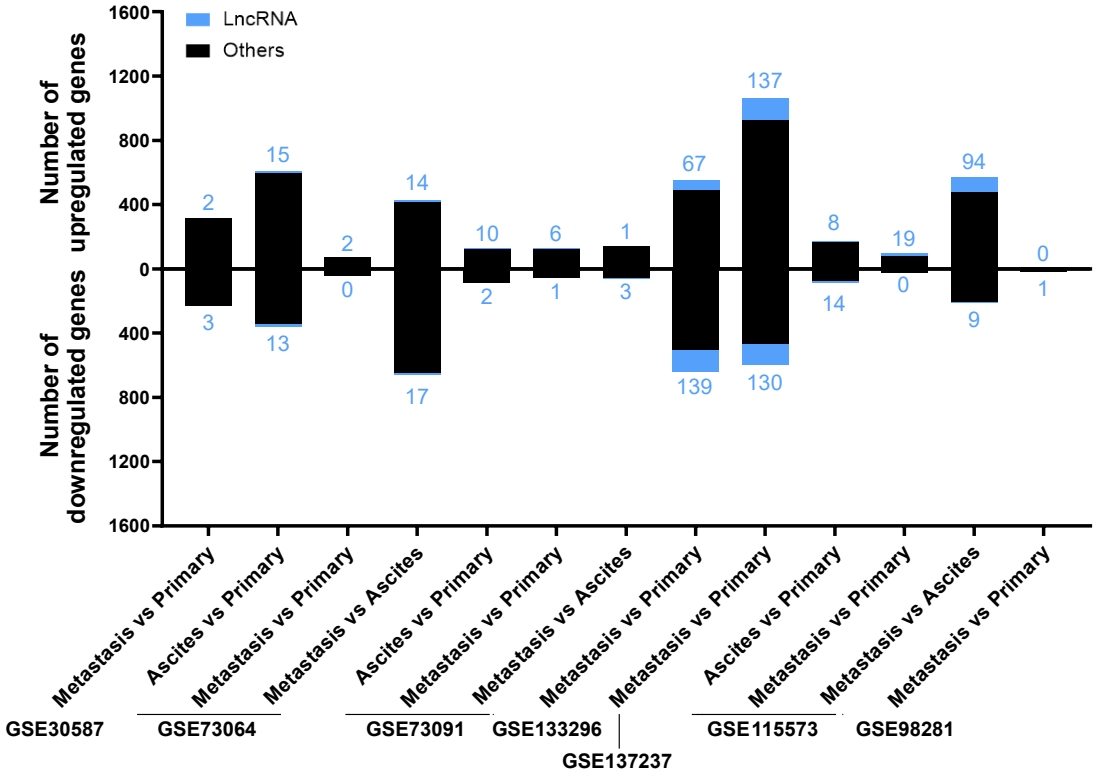

Figure 5.- The number of deregulated genes in each comparison within the selected studies for the "Metastatic" category. The bar graph shows the absolute frequency of upregulated (upper part) and downregulated (lower part) genes, depicting the fraction corresponding to lncRNA genes in blue at the ends of the bars.

After carrying out the individual analyses, we found 287 upregulated and 287 downregulated lncRNAs, of which 30 and 8, respectively, were found in two or three different studies carried out with patients, or in one study carried out with patients and differentially expressed in EOC cell lines from a metastatic origin when comparing them with those originating from primary tumors (Tables 5 and 6). Additionally, we identified 26 lncRNAs that were upregulated or downregulated in cancer cells from ascites but did not change their levels between primary tumor and solid peritoneal metastasis, which we named "switch" (Table 7). The full lists, including references from genes previously associated with EOC, can be found in the Supplementary Materials (Table S8). Those lncRNAs whose expression was contradictory between different analyzed studies were excluded from Table S8 but included in the Supplementary Materials (Table S3).

After obtaining these lists, we tested again whether we could correlate these results with cell lines using CCLE expression data, since there are 32 and 25 epithelial ovarian cancer cell lines that are derived from primary tumors and metastases,

respectively. We first looked for differentially expressed genes between the primary and metastatic cell line groups using DESeq2 and obtained three upregulated–*ENSG00000227496*, *ENSG00000282057*, and *LNCOG*– and one downregulated–*ENSG00000225649*– lncRNAs ($|\log_2$ fold change > 0.585 and *p*-value < 0.05) that were present in the upregulated and downregulated lists obtained from the analyses of the patient studies. The second approach was to carry out receiver operating characteristic (ROC) curve analyses to see if the genes outlined from the patient analyses also showed differences in the comparison between the metastatic and primary tumor cell line groups. We obtained five upregulated–*TENM3-AS1*, *LINC01678*, *ENSG00000250410*, *UNC5C-AS1*, and *ENSG00000261604*–and seven downregulated–*ENSG00000260604*, *ENSG00000267284*, *LINC01508*, *LINC01138*, *FAM160A1-DT*, *ENSG00000255118*, and *ENSG00000249049*–lncRNAs (area under the curve > 0.5 and *p*-value < 0.05) contained in the lists obtained from the analyses of the metastatic patient studies. The results for both DESeq2 and ROC for the metastasis category can be found in the Supplementary Materials (Table S8).

In terms of the influence of lncRNAs in EOC metastasis, upregulation of *LINC02544*, *LINC01235*, *HECW2-AS1*, and *MIR31HG* in relation to this process was derived from this meta-analysis (Figure 6), and since it has not been previously found in EOC, this deserves special mention.

Table 5.- Upregulated lncRNAs in metastasis in two or three patient transcriptomic studies, or in one patient transcriptomic study and also in metastatic versus primary tumor cell line groups from CCLE. Genes in bold coincide with significant differentially expressed (DE) lncRNAs between the primary and metastatic cell line groups using DESeq2, and underlined genes coincide with those that were significant in the receiver operating curve analyses.

# of studies	# of comparisons	Gene count	Gene name
3	4	2	*LINC02544*, *LINC01235*
2	3	2	*HECW2-AS1, MIR31HG*
2	2	20	***ENSG00000282057***, *UNC5C-AS1*, *ENSG00000261327*, *ENSG00000259807*, *MEG9*, *LINC01561*, *SNHG18*, *HOTAIRM1*, *LINC00922*, *LINC01619*, *FAM225A*, *HOXA-AS3*, *LINC00968*, *ENSG00000271811*, *ENSG00000272755*, *ENSG00000233682*, *ENSG00000248540*, *ENSG00000259663*, *LINC02593*, *HOXA-AS2*
1 + cell line	1	6	*TENM3-AS1*, *LINC01678*, *ENSG00000250410*, *ENSG00000261604*, ***ENSG0000022749***, ***LNCOG***

Table 6.- Downregulated lncRNAs in one patient transcriptomic study and also in metastatic versus primary tumor cell line groups from CCLE. Genes in bold coincide with significant DE lncRNAs between the primary and metastatic cell line groups using DESeq2, and underlined genes coincide with those that were significant in the receiver operating curve analyses.

# of studies	# of comparisons	Gene count	Gene name
1 + cell line	1	8	*ENSG00000260604*, *ENSG00000267284*, *LINC01508*, *LINC01138*, *FAM160A1-DT*, *ENSG00000255118*, *ENSG00000249049*, ***ENSG00000225649***

Table 7.- "Switch" lncRNAs in metastasis patient transcriptomic studies.

Status in ascites	Gene count	Gene name
Up	13	*TP53TG1*, *ENSG00000253982*, *MIR210HG*, *LINC00667*, *ATP2B1-AS1*, *ENSG00000275210*, *LINC00847*, *ENSG00000259153*, *ENSG00000243655*, *FCGR1BP*, *LINC00888*, *ENSG00000291107*, *ENSG00000291230*
Down	13	*MEG3*, *PCBP1-AS1*, *ENSG00000223774*, *FLJ16779*, *ENSG00000263065*, *SNHG12*, *IGFBP7-AS1*, *IDI2-AS1*, *PSMA3-AS1*, *NUTM2B-AS1*, *SNHG3*, *MALAT1*, *SMG1P5*

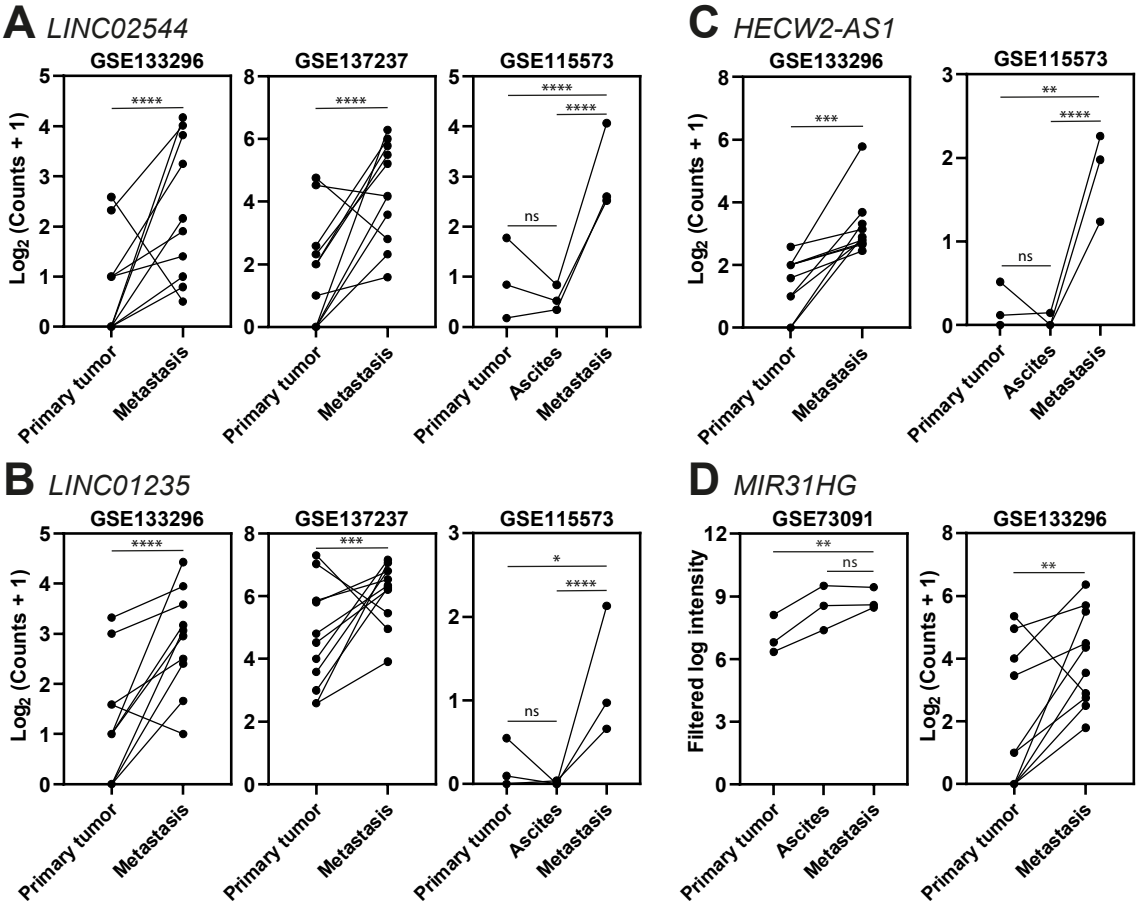

Figure 6. Expression levels of four lncRNAs upregulated in metastases: *LINC02544* (**A**), *LINC01235* (**B**), *HECW2-AS1* (**C**), and *MIR31HG* (**D**). Dots represent tissue samples and lines join the samples from each patient. * $p \leq 0.05$, ** $p \leq 0.01$, *** $p \leq 0.001$, **** $p \leq 0.0001$, ns $p > 0.05$.

Looking for outstanding lncRNAs related in common to diagnosis, prognosis, and metastasis in EOC

At this point of the analysis, we decided to overlap the final lists for the first three categories to highlight the most interesting lncRNAs in terms of clinical value. We generated two different intersections, as represented in Figure 7: one comparing the upregulated lncRNAs, which represent the ones that would be putative oncogenes, and another one comparing the downregulated lncRNAs, which represent the ones that could be considered tumor suppressors.

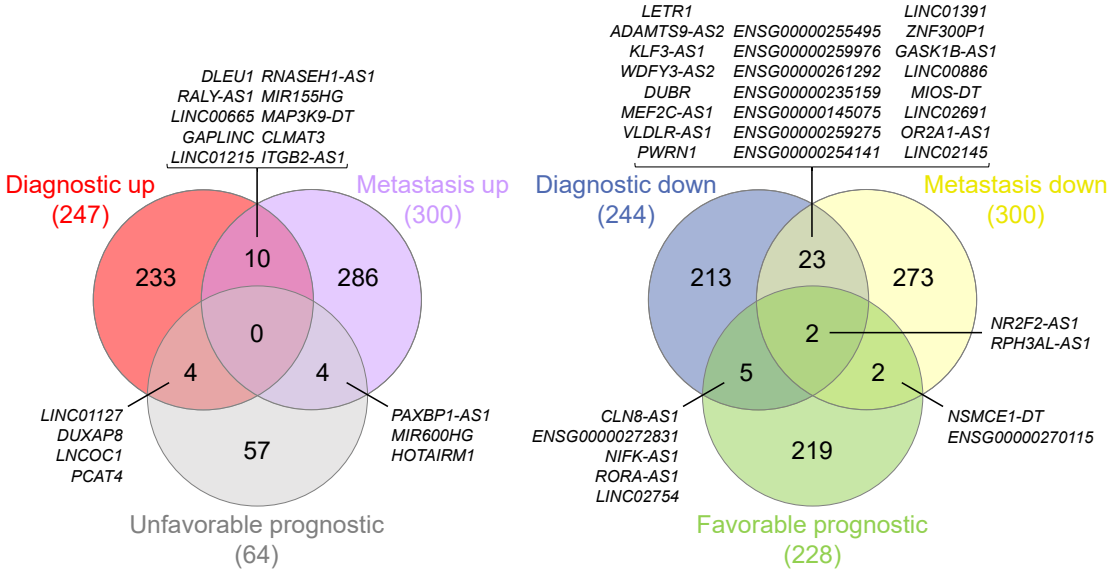

Figure 7. Venn diagrams represent the intersections between the final lists of the diagnostic, prognostic, and metastasis analyses, specifically potential oncogenes (**left**) and potential tumor suppressors (**right**). Diagrams were generated using interactivenn.net.

We only obtained results in the intersection of the three lists for the potential tumor suppressor comparison, whereas in the other comparison, the intersections found were only pairwise. The lncRNAs considered to be probable tumor suppressors in EOC were *NR2F2-AS1* and *RPH3AL-AS1*, and their data from the diagnostic, metastasis, and prognostic analyses are represented in Figure 8 (see also Figure S1).

NR2F2-AS1 and *RPH3AL-AS1* were both downregulated in EOC in comparison with healthy tissues in four independent studies (*NR2F2-AS1* was also downregulated in EOC cell lines) and in one study of metastatic tumors, correlating with a favorable prognosis (specifically, with improved disease-free survival), as shown in Figure 8.

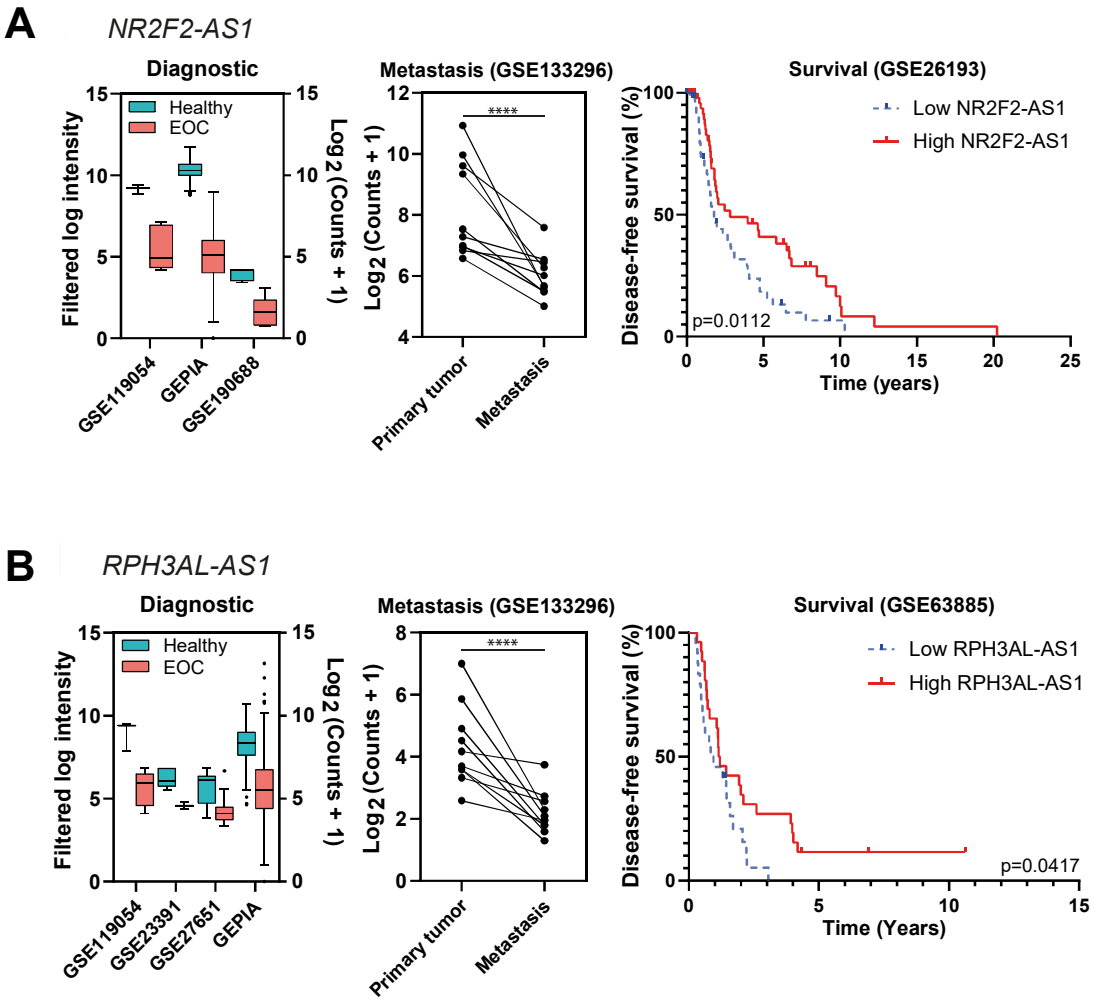

Figure 8. "Diagnostic" and "Metastasis" differential expression results, and survival plots of the potential tumor suppressors *NR2F2-AS1* (**A**) and *RPH3AL-AS1* (**B**). In the left panels, all the comparisons are $p \leq 0.01$. In the middle panels, dots represent tissue samples and lines join the three samples from each patient. In the case of *RPH3AL-AS1*, one study from the diagnostic category has not been represented because raw information from (H. Wang et al., 2016) is not available, only fold changes and *p*-values. **** $p \leq 0.0001$, ns $p > 0.05$.

Analysis of lncRNAs with putative influence in resistance to chemotherapy

Next, we aimed to identify lncRNAs related to standard chemotherapy resistance (jointly considering cisplatin or carboplatin and/or a taxane or cyclophosphamide) by comparing expression levels from partial or non-responder and responder patients. In this case, only three studies (all microarrays) had information regarding the response to treatment, and they are listed together with the results from the individual analyses in the Supplementary Materials (Table S9). We could only find six upregulated and nine downregulated lncRNAs, as shown in Figure 9. As expected, due to the low number of

deregulated genes in this category, multiple pairwise comparisons did not produce any overlap between studies. The references from previous associations between these genes and EOC can be found in the Supplementary Materials (Table S10).

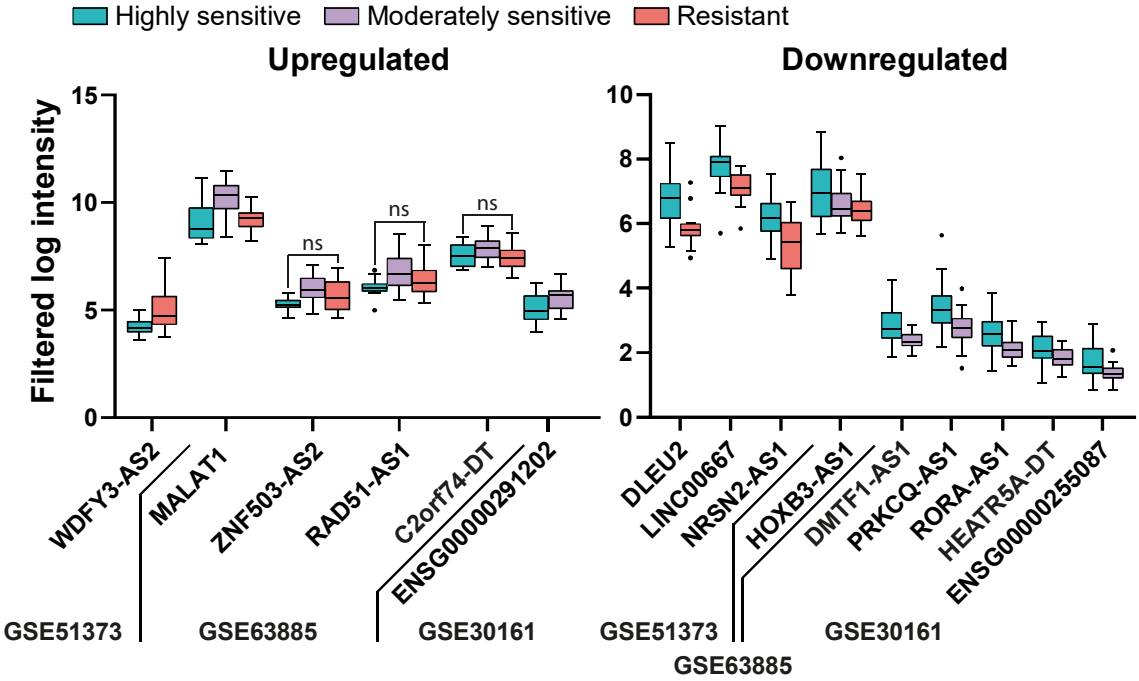

Figure 9.- Deregulated lncRNAs in tissue from patients according to the sensitivity to standard chemotherapy. All the comparisons are $p < 0.05$ except for those indicated with ns indicating $p > 0.05$.

Although there have been few transcriptomic studies considering the influence of lncRNAs in resistance to chemotherapy in EOC, our meta-analysis confirmed the influence of two lncRNAs previously associated with resistance to chemotherapy in EOC —*WDFY3-AS2* (Wu et al., 2021), and *MALAT1* (Mao et al., 2021) — as well as revealing the influence of other lncRNAs that have been associated with EOC, but not with chemoresistance until now, i.e., *LINC00667* (Y. Chen et al., 2019), *NRSN2-AS1* (Q. Chen et al., 2022), and *RAD51-AS1* (X. Zhang et al., 2017). Others had not been associated with EOC but had been associated with other cancers, i.e., *DLEU2* with endometrial (P. Dong et al., 2021) and prostate cancers (P. Li et al., 2022), *LINC00667* with breast cancer (Ren et al., 2022), and *PRKCQ-AS1* with multiple myeloma (Malek et al., 2016).

Analysis of lncRNAs with a putative specific value associated with histological EOC subtypes

Epithelial ovarian cancer can be further classified into five subtypes according to histological structure, mutations in certain tumor suppressors or proto-oncogenes, chemosensitivity, spreading behavior, and patient prognosis (Gilks & Prat, 2009). These five subtypes and their relative frequencies are high-grade serous (HGSOC, 70%), low-grade serous (LGSOC, >5%), endometrioid (ENOC, 10%), clear cell (CCOC, 10%), and mucinous (MOC, 3%) (Gilks & Prat, 2009). As there were six studies with the subtype information available (Supplementary Materials, Table S11), in the last analysis, we looked for lncRNAs whose expression was specific for each EOC subtype.

The results of each analysis for the subtype category are contained in the Supplementary Materials (Table S11) and summarized in Figure 10. Regarding HGSOC and LGSOC, we did not consider LGSOC independently, because there was only information about this subtype in two studies (GSE14001 and GSE26751), in which there were HGSOC and healthy individuals and no other subtypes available for comparison.

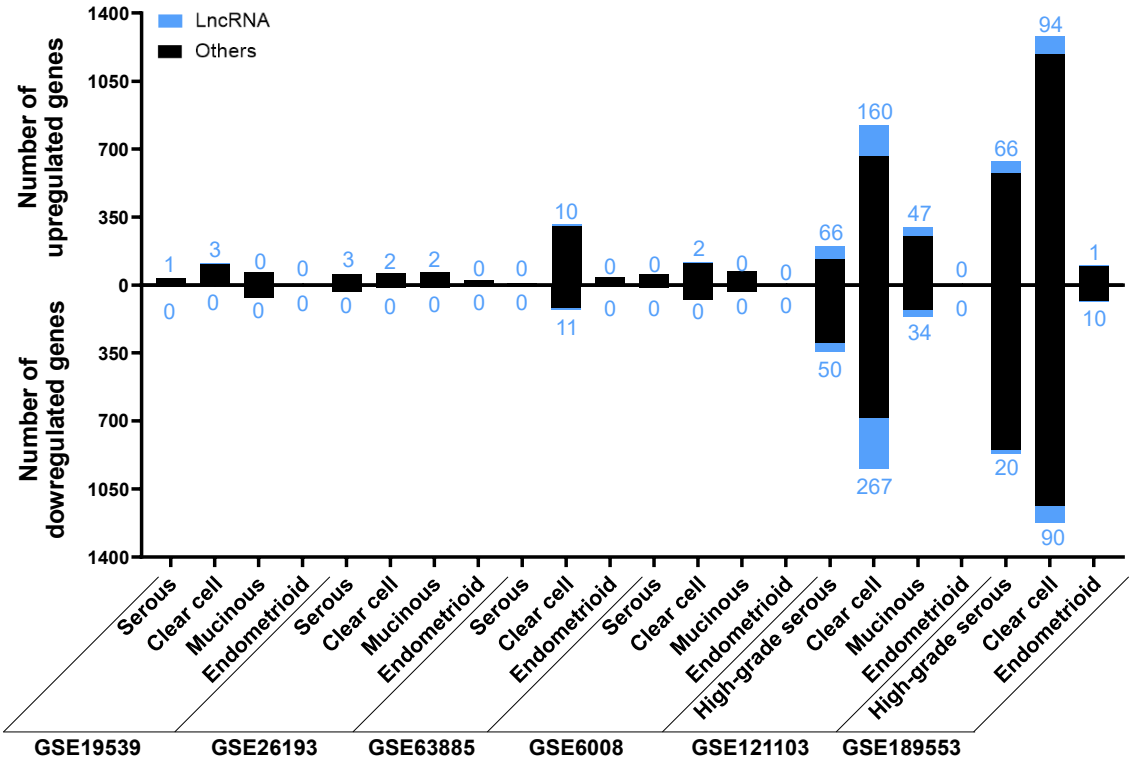

Figure 10.- The number of deregulated genes in each study selected for the "Subtype" category. The bar graph shows the absolute frequency of upregulated (upper part) and downregulated (lower part) genes, depicting the fraction corresponding to lncRNA genes in blue at the ends of the bars.

We did not find any ambiguous lncRNAs within any of the subtypes across different studies. Those lncRNAs that were present in two or three studies of HGSOC or CCOC are listed in Tables 8 and 9, respectively. The full list of deregulated lncRNAs according to each subtype can be found in the Supplementary Materials (Table S12).

Table 8.- Differentially expressed lncRNAs in high-grade serous ovarian cancer patients identified in two or three (*) studies.

HGSOC	
Upregulated lncRNA genes	**Downregulated lncRNA genes**
WT1-AS, PART1, ENSG00000255135*	*FAM155A-IT1, DLX6-AS1*

Table 9.- Differentially expressed lncRNAs in clear cell ovarian cancer patients identified in two, three (*), or four (in bold) studies.

CCOC	
Upregulated lncRNA genes	**Downregulated lncRNA genes**
SNHG12, ***LINC00472***, *C8orf31*, RBPMS-AS1, ENSG00000271992, ENSG00000259052, ENSG00000218416, ENSG00000253307, ENSG00000223786, CPNE8-AS1, ENSG00000224583, ENSG00000264596, FAM155A-IT1, ENSG00000274718, ENSG00000187185, ENSG00000253666, LINC01137, ENSG00000257681, LINC02765, ENSG00000257831, ENSG00000236283, ENSG00000260317, LINC01637, ENSG00000265625, PPP1R3B-DT, PCCA-DT, ENSG00000286546, LINC00598, LINC02435, ENSG00000249125*	*PART1, ZNF667-AS1, WT1-AS, HCP5, LINC01139, ENSG00000227733, TARID, EMX2OS, ENSG00000235560, PRKCQ-AS1, ENSG00000255135, PAXIP1-DT*

We performed two different multiple pairwise comparisons (up- and downregulated lncRNAs, separately) between the lists drawn for each subtype to identify true subtype-specific lncRNAs and exclude those present in more than one subtype. The results of these overlaps are shown in Figure 11. We found an *a priori* unexpected specificity between lncRNAs and histological subtypes of EOC. Surprisingly, only 1 out of the 418 upregulated and 3 out of the 467 downregulated lncRNAs in any subtype were deregulated in the same way in two different subtypes (included in the Supplementary Materials, Table S3), meaning that the remaining lncRNAs are potentially subtype-specific.

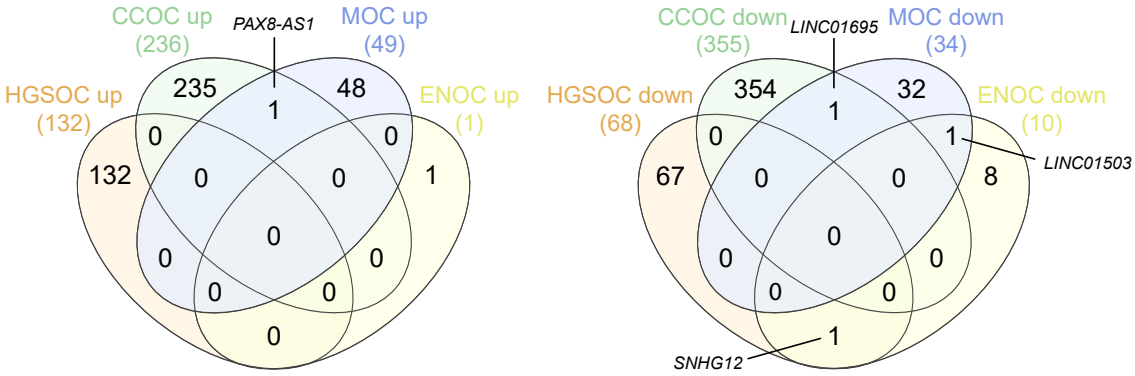

Figure 11.- Venn diagrams representing the intersections between the final lists of the upregulated (**left**) and downregulated (**right**) subtype-specific lncRNAs. HGSOC, high-grade serous ovarian carcinoma; CCOC, clear cell ovarian carcinoma; MOC, mucinous ovarian carcinoma; ENOC, endometrioid ovarian carcinoma. Diagrams were generated using interactivenn.net.

DISCUSSION

The lack of early detection methods for EOC and its consequent late diagnosis result in dramatic high mortality. We aimed to update the significance of putative lncRNA-based biomarkers in EOC in light of available studies combining gene expression and clinical data. As the first objective of our analysis, we sought to identify differentially expressed lncRNAs (either upregulated or downregulated) in EOC compared with healthy samples that could be identified as significant candidates for future experimental analysis and translation to clinical practice as diagnostic biomarkers. Data from 22 different cohorts of patients were included in this analysis. Indeed, lncRNA expression in these cohorts had been previously analyzed in some cases, but not all. The reanalysis of all of these available data revealed worthwhile information because it allowed us to bring to light available, but not evident, information. We found 247 upregulated and 243 downregulated lncRNAs (listed in Tables 1 and 2, respectively), 200 and 209 of which were not previously related to EOC, respectively. The most frequently upregulated lncRNAs were *RNF157-AS1* and *BBOX1-AS1*, both in 12 different studies, whereas *MAGI2-AS3* was the most frequently downregulated lncRNA, in 15 different studies. Validation of these novel EOC-related lncRNAs is supported by three pieces of evidence: First, the meta-analysis, applied to protein-coding genes across the same studies, rendered a group of genes that are well-known EOC markers as significantly

deregulated, including *CP* (Lee et al., 2004), *CD24* (Tarhriz et al., 2019), and *INAVA* (L. Zhao et al., 2020), upregulated in 18, 17, and 16 studies, respectively, as well as *AOX1* (L. Zhao et al., 2020) and *PDGFD* (C. Yang et al., 2019) downregulated in 16 and 13 studies, respectively. Second, our analysis also found other lncRNAs previously related to EOC (cited in the Supplementary Materials, Table S4). These include, among others, *RNF157-AS1* (P. Xu et al., 2023) and *UCA1* (Lin et al., 2019), which interact with HMGA1 and EZH2, and YAP, respectively, to regulate transcription; *BBOX1-AS1* (Yao et al., 2021), *DUXAP8* (L.-M. Li et al., 2021), *LINC01503* (Y. Li et al., 2021), *HAGLR* (also known as HOXD-AS1) (Y. Zhang et al., 2017), *LINC00665* (D. Xu et al., 2021) and *HAGLROS* (Zhu & Mei, 2021), which act as competing endogenous RNAs (ceRNAs) with miRNAs, affecting gene expression at the post-transcriptional level; and *MAGI2-AS2* (Gokulnath et al., 2019), *HAND2-AS1* (Gokulnath et al., 2020), *ZNF300P1* (Gloss et al., 2014), and *HYMAI* (Kamikihara et al., 2005), whose downregulation in EOC is explained by hypermethylation of the promoter. The third piece of evidence for the validation of our meta-analysis comes from the fact that 99 deregulated lncRNAs in EOC patients were also deregulated in EOC cell lines (Supplementary Materials, Table S4). The lncRNAs that showed significant upregulation, and which were more frequently found in different cohorts, but that had not been previously related to EOC diagnosis, were *ENSG00000187951*, *MIR205HG*, *ZNF232-AS1*, *ENSG00000285756*, *LINC01297*, *TFAP2A-AS1*, *LINC01977*, and *LINC01770*, as shown in Figure 2A. Some of them have been previously related to other cancer types. *MIR205HG* is the host gene for the microRNA miR-205 but, although originating from the same primary transcript through alternative splicing, its lncRNA and miRNA are functionally independent (Di Agostino et al., 2018; Du et al., 2019; Profumo et al., 2019). *MIR205HG* promotes lung squamous cell carcinoma (L. Liu et al., 2020), osteosarcoma (X. Wang et al., 2021), melanoma (J. Guo et al., 2021), cervical cancer (Y. Li et al., 2019; Yin et al., 2021), head and neck squamous carcinoma (Di Agostino et al., 2018) and esophageal squamous carcinoma (Hongle et al., 2020); however, in esophageal adenocarcinoma, it is downregulated and

hinders HNRNPA0 mRNA translation by interacting with LIN28A (X. Dong et al., 2022) and affecting the Hedgehog pathway (Song et al., 2021). *MIR205HG* also acts in physiological processes, such as in embryogenesis by regulating the transcription of Pit1, Zbtb20, prolactin, and growth hormone in the anterior pituitary in mouse models (Du et al., 2019); or in cell fate by preventing luminal differentiation of human prostate basal cells through the interferon pathway by forming a DNA:RNA triplex in the *Alu* regulatory elements in the proximal promoter of target genes (Bezzecchi et al., 2022; Profumo et al., 2019). *LINC01770* is upregulated in endometrial cancer in comparison with endometrial dysplasia tissues (Hao et al., 2023). *LINC01977* is upregulated and correlated with poor prognosis in lung adenocarcinoma (T. Zhang et al., 2022) and breast cancer (Z. Li et al., 2021); in lung adenocarcinoma, TGF-β derived from infiltrated tumor-associated macrophages (TAM2) activates SMAD3, which binds *LINC01977* to induce its nuclear transport, where it upregulates transcription by simultaneously binding the promoter and super-enhancer, facilitating the interaction between SMAD3 and CBP/P300 to activate ZEB1 transcription (T. Zhang et al., 2022). In breast cancer, *LINC01977* expression is also correlated with chemoresistance to doxorubicin by targeting the miR-212-3p/GOLM1 axis (Z. Li et al., 2021). *LINC01297* is upregulated in estrogen receptor (ER)-positive breast cancer, in comparison with ER-negative breast cancer (Van Grembergen et al., 2016) and lung adenocarcinoma (Hu et al., 2019); there is also a positive correlation between *LINC01297* and the expression of its nearby gene *LINC01296 expression*, which acts as an oncogene in bladder cancer (Seitz et al., 2017). Conversely, *ENSG00000285756* and *TFAP2A-AS1*, which were EOC-upregulated lncRNAs in our analysis, are downregulated in other cancer types. *ENSG00000285756* is downregulated in cervical cancer (L. Li et al., 2021) and *TFAP2A-AS1* is downregulated and correlated with a good prognosis in breast cancer, acting *in vitro* as a tumor suppressor by sponging miR-933 to modulate *SMAD2* mRNA stability (Zhou et al., 2019); *TFAP2A-AS1* is also transcriptionally activated by KLF15 and inhibits the proliferation and migration of gastric cancer cells by sponging miR-3657 to regulate

NISCH mRNA stability (X. Zhao et al., 2021). The lncRNAs that were more frequently downregulated in different cohorts, but that had not been previously related to EOC diagnosis, were *PGM5-AS1*, *ENSG00000267058*, *EPM2A-DT*, *NR2F1-AS1*, *KLF3-AS1*, *GLIDR*, *ERVK13-3*, and *CLN8-AS1*, as shown in Figure 2B. *PGM5-AS1* (*ENSG00000224958*) is downregulated in both EOC patients and EOC cell lines; it is also downregulated and negatively correlated with oxaliplatin resistance in colorectal cancer (Hui et al., 2022) but, on the other hand, it is upregulated and sponges miR-140-5p to prevent *FBN1* mRNA degradation in osteosarcoma (W. Liu et al., 2020). *KLF3-AS1* is downregulated in esophageal squamous cell carcinoma stem cells, promoting cell migration and invasion by being unable to sponge miR-185-5p, which induces KLF3 mRNA degradation, thereby preventing transcriptional repression of SOX2 and OCT4 by KLF3 (J.-Q. Liu et al., 2020), and acts as a competing endogenous tumor suppressor RNA in gastric cancer (H. Jiang et al., 2021) and osteosarcoma (C. Chen & Liu, 2022). Conversely, several lncRNAs that are downregulated in EOC are upregulated and stimulate cancer progression in other tissues. *NR2F1-AS1* is upregulated in non-small cell lung (Jin et al., 2021), thyroid (F. Guo et al., 2019), pancreatic (Luo et al., 2021), and hepatocellular (Huang et al., 2018) cancers; in pancreatic cancer, it is induced by hypoxia, its expression is positively correlated with the expression of its sense gene *NR2F1*, and they both trigger the AKT and mTOR pathways, promoting proliferation, migration, and invasion (Y. Liu et al., 2022). *NR2F1-AS1* is also upregulated in dormant breast cancer stem-like cells and increases tumor dissemination by recruiting PTBP1 to the mRNA of its sense gene (*NR2F1*), promoting its translation so that NR2F1 represses ΔNp63 transcription (Y. Liu et al., 2021). *GLIDR* is upregulated and promotes glioma (Yu et al., 2021), lung (Tai et al., 2021), and prostate (S. Li et al., 2023) cancers by acting as competing endogenous RNAs for miRNAs. *ERVK13-3* is upregulated in osteosarcoma (Xie et al., 2022).

Our second objective was to find differentially expressed lncRNAs showing a significant correlation with favorable or unfavorable prognosis. From our initial selection of studies from 46 different cohorts, only 11 contained information about death and relapse events over time. The analysis of these data rendered a limited amount of lncRNAs whose differential expression could be related to prognosis. Among them, high expression of *GUSBP11* and *MIR924HG* (underlined in Tables 3 and 4) was positively correlated with shorter OS and DFS, meaning a negative prognosis. In accordance with our data for EOC, high expression levels of *GUSBP11* are predicted to bind miR-22-3p to avoid CCN2A mRNA degradation, correlating to poor overall survival in hepatocellular carcinoma patients (S. Chen et al., 2022). Conversely, *GUSBP11* expression correlates with better prognosis in head and neck squamous cell carcinoma (Cao et al., 2017), bladder cancer (Cai et al., 2023), papillary renal cell carcinoma (Jia et al., 2022), and pancreatic adenocarcinoma (Lyu et al., 2023). Regarding *MIR924HG*, there is no information about it in the literature. However, miR-924, which is hosted in the *MIR924HG* locus, acts as a tumor suppressor in non-small cell lung carcinoma (H. Wang et al., 2020) and hepatocellular carcinoma (Fan et al., 2018). In our analysis, *AQP5-AS1* was associated with a more favorable prognosis due to its correlation with longer survival periods in different studies. There is no information regarding the antisense lncRNA *AQP5-AS1* in the literature, but the sense transcript encodes the protein AQP5, which is overexpressed in OC tissues (J.-H. Yang et al., 2006) and promotes proliferation and migration in OC (Yan et al., 2014); however, contradictory data can also be found, since high *AQP5* expression is correlated with a better prognosis in OC patients (Chetry et al., 2018).

The third objective was the identification of differentially expressed lncRNAs associated with metastasis in EOC. Seven studies included samples that allowed comparisons of (i) peritoneal solid metastasis versus cancer cells from the ascitic fluid, (ii) peritoneal solid metastasis versus primary tumor, and (iii) cancer cells from the ascitic fluid versus primary tumor. Upregulation of *LINC02544*, *LINC01235*, *HECW2-AS1*, and

MIR31HG in relation to this process was found from this meta-analysis and, since it has not been previously found in EOC, deserves special mention. Previous data about the influence of these lncRNAs in invasion or metastasis and unfavorable prognosis can be found in other cancers and reinforce our findings. *LINC02544* is overexpressed in lung squamous cell carcinoma patients with lymph node metastasis, and it promotes proliferation, migration, and invasion *in vitro* by sponging miR-138-5p, a potential target of E2F3 (W. Wei et al., 2022); increased expression of *LINC02544* has also been related to *in vitro* invasion and unfavorable prognosis in breast cancer (Z.-H. Guo et al., 2020). *LINC01235* is upregulated in gastric cancer patients *versus* healthy individuals and metastatic *versus* non-metastatic gastric cancer patients, promoting migration, invasion, and EMT, as well as negatively affecting prognosis (Tan et al., 2020; C. Zhang et al., 2021). *MIR31HG* has been associated with unfavorable prognosis in gastric cancer (Tu et al., 2020), lung adenocarcinoma (Mo et al., 2022), head and neck squamous cell carcinoma (Chang et al., 2021; R. Wang et al., 2018), colorectal cancer (J. Wang et al., 2022), and non-small cell lung carcinoma (S. Zheng et al., 2019).

The intersection of differentially expressed lncRNAs obtained in the three previous analyses (diagnosis, prognosis, and metastasis) highlighted the importance of two lncRNAs (*NR2F2-AS1* and *RPH3AL-AS1*) in EOC. *A priori*, we did not expect a large overlap between lncRNAs useful in diagnosis and prognosis, since lncRNAs discovered in each category may be regulating different phases and functions of oncogenesis. A greater overlap exists between metastasis and prognosis, since the functional relationship between metastasis and prognosis is very straightforward, and the presence of metastasis is usually associated with shorter survival times. *NR2F2-AS1* is upregulated in several malignancies, such as non-small cell lung cancer, clear cell renal cell carcinoma, and prostate, cervical, nasopharynx, and esophageal cancers, being considered an oncogene (Ghorbanzadeh et al., 2022), contrary to what we observed in EOC. Its gene product NR2F2 or COUP-TFII is highly expressed in the ovarian stroma

and is negligible in the ovarian epithelium, although *NR2F2* is downregulated at the mRNA level in OC tissues. NR2F2 expression increases in the epithelial component and is associated with shorter periods before recurrence (Hawkins et al., 2013). NR2F2 acts as an oncogene in other cancers, such as renal, prostate, or breast cancers (J. Zheng et al., 2016). *RPH3AL-AS1* is located within the cytoband 17p13.3, and its downregulation in EOC could be due to the high deletion frequency of this chromosomal region in OC patients (Phillips et al., 1996; Sakamoto et al., 1996).

Next, as a fourth objective, we aimed to identify lncRNAs related to standard chemotherapy resistance. Among the studies considered in this meta-analysis, there were only three studies containing information that allowed us to study this correlation. Although the results from our meta-analysis confirm the influence of two lncRNAs previously associated with resistance to chemotherapy in EOC, *WDFY3-AS2* (Wu et al., 2021), and *MALAT1* (Mao et al., 2021), and some new lncRNAs that were also detected, more studies are needed to validate these results.

Epithelial ovarian cancer can be further classified into five subtypes according to its histological structure: high-grade serous, low-grade serous, endometrioid, clear cell, and mucinous (Gilks & Prat, 2009). We found in our meta-analysis that the differential expression of lncRNAs is highly specific for the different subtypes, which can be used for diagnostic purposes.

One of the most interesting characteristics of lncRNAs is that they can be detected in tumor-derived small extracellular vesicles, as well as free molecules or protein-associated complexes circulating in the blood. The fact that circulating levels of some lncRNAs in serum or plasma samples can correlate to those found in tumor tissue increases their importance as biomarkers in liquid biopsy for EOC, with ongoing clinical trials (Salamini-Montemurri et al., 2020). There are examples of some lncRNAs identified in our meta-analysis that have been previously found in liquid biopsies. *HAND2-AS1*, which is downregulated in EOC tumors, as confirmed in 13 studies (Table 2), had been

also detected in blood plasma from triple-negative breast cancer patients (M. Wei et al., 2019). The expression of *SP2-AS1*, which was downregulated in eight studies (Table 2), was previously detected in blood and associated with the risk of endometriosis and endometrioid ovarian cancer (Mortlock et al., 2022). *UCA1,* which was upregulated in 10 EOC studies (Table 2), also showed increased levels in serum-derived exosomes from cisplatin-resistant OC patients (Z. Li et al., 2019) and plasma from colorectal cancer patients (M. Wang et al., 2021). *PGM5-AS1*, downregulated in tumor tissues from 12 EOC studies (Table 2), was also downregulated in plasma from colorectal cancer patients (M. Wang et al., 2021). The lncRNA *ESRG*, upregulated in eight EOC studies (Table 2), was detected in exosomes present in effusion supernatants from HGSOC (Filippov-Levy et al., 2018). *GUSBP11,* which was correlated with a poor prognosis in EOC (Tables 3 and 4, and Figure 4)*,* was upregulated in plasma from gastric cancer patients in comparison with healthy individuals (R. Zheng et al., 2019).

Finally, it is also important to remark that EOC is intrinsically associated with late diagnosis and, therefore, most of the studied samples included in this meta-analysis come from advanced stages of the disease, which implies that early-stage samples are underrepresented. Studies with larger cohort sizes and increased representation of samples from the initial stages of EOC, along with the use of sensitive, normalized, universally standardized, and reproducible techniques to detect circulating lncRNAs, are still needed to make possible the translation of these findings into the gynecological clinical setting.

According to GENCODE Release 43 (Frankish et al., 2021) the number of known lncRNA genes in the human genome so far is 19,928, which is slightly higher than the 19,393 protein-coding genes. Despite this large number, only a small proportion of lncRNAs have been associated with EOC, and with this study we have increased this number, with 1,631 new lncRNA genes. This effort has produced valuable information to take into account in future projects, since specific lncRNAs are associated with EOC for diagnosis (*ENSG00000187951*, *MIR205HG*, *ZNF232-AS1*, *ENSG00000285756*,

LINC01297, *TFAP2A-AS1*, *LINC01977*, *LINC01770*, which are upregulated; and *PGM5-AS1*, *ENSG00000267058*, *EPM2A-DT*, *NR2F1-AS1*, *KLF3-AS1*, *GLIDR*, *ERVK13-3*, *CLN8-AS1*, which are downregulated), prognosis (*GUSBP11*, *MIR924HG*, unfavorable; and *AQP5-AS1*, favorable), and metastasis (*LINC02544*, *LINC01235*, *HECW2-AS1*, and *MIR31HG*). Furthermore, the differential expression of lncRNAs is highly specific to the different subtypes, which can be used for diagnosis purposes.

SUPPLEMENTARY MATERIALS AVAILABILITY

Chapter 1 includes Supplementary Tables S1 to S12 and Supplementary Figure S1, which are contained in the electronic support attached to this Thesis.

REFERENCES

Barrett, T., Wilhite, S. E., Ledoux, P., Evangelista, C., Kim, I. F., Tomashevsky, M., Marshall, K. A., Phillippy, K. H., Sherman, P. M., Holko, M., Yefanov, A., Lee, H., Zhang, N., Robertson, C. L., Serova, N., Davis, S., & Soboleva, A. (2012). NCBI GEO: archive for functional genomics data sets—update. *Nucleic Acids Research*, *41*(D1), D991–D995. https://doi.org/10.1093/nar/gks1193

Bezzecchi, E., Pagani, G., Forte, B., Percio, S., Zaffaroni, N., Dolfini, D., & Gandellini, P. (2022). MIR205HG/LEADR Long Noncoding RNA Binds to Primed Proximal Regulatory Regions in Prostate Basal Cells Through a Triplex- and Alu-Mediated Mechanism. *Frontiers in Cell and Developmental Biology*, *10*. https://doi.org/10.3389/fcell.2022.909097

Bray, N. L., Pimentel, H., Melsted, P., & Pachter, L. (2016). Near-optimal probabilistic RNA-seq quantification. *Nature Biotechnology*, *34*(5), 525–527. https://doi.org/10.1038/nbt.3519

Cai, J., Xie, H., Yan, Y., Huang, Z., Tang, P., Cao, X., Wang, Z., Yang, C., Wen, J., Tan, M., Zhang, F., & Shen, B. (2023). A novel cuproptosis-related lncRNA signature predicts prognosis and therapeutic response in bladder cancer. *Frontiers in Genetics*, *13*. https://doi.org/10.3389/fgene.2022.1082691

Cao, W., Liu, J., Liu, Z., Wang, X., Han, Z.-G., Ji, T., Chen, W., & Zou, X. (2017). A three-lncRNA signature derived from the Atlas of ncRNA in cancer (TANRIC) database predicts the survival of patients with head and neck squamous cell carcinoma. *Oral Oncology*, *65*, 94–101. https://doi.org/10.1016/j.oraloncology.2016.12.017

Chang, K.-W., Hung, W.-W., Chou, C.-H., Tu, H.-F., Chang, S.-R., Liu, Y.-C., Liu, C.-J., & Lin, S.-C. (2021). LncRNA MIR31HG Drives Oncogenicity by Inhibiting the Limb-Bud and Heart Development Gene (LBH) during Oral Carcinoma. *International Journal of Molecular Sciences*, *22*(16), 8383. https://doi.org/10.3390/ijms22168383

Chen, C., & Liu, L. (2022). Silencing of lncRNA KLF3-AS1 represses cell growth in osteosarcoma via miR-338-3p/MEF2C axis. *Journal of Clinical Laboratory Analysis*, *36*(11), e24698. https://doi.org/10.1002/jcla.24698

Chen, Q., Xie, J., & Yang, Y. (2022). Long non-coding RNA NRSN2-AS1 facilitates

tumorigenesis and progression of ovarian cancer via miR-744-5p/PRKX axis. *Biology of Reproduction*, *106*(3), 526–539. https://doi.org/10.1093/biolre/ioab212

Chen, S., Zhao, Z., Wang, X., Zhang, Q., Lyu, L., & Tang, B. (2022). The Predictive Competing Endogenous RNA Regulatory Networks and Potential Prognostic and Immunological Roles of Cyclin A2 in Pan-Cancer Analysis. *Frontiers in Molecular Biosciences*, *9*. https://doi.org/10.3389/fmolb.2022.809509

Chen, Y., Bi, F., An, Y., & Yang, Q. (2019). Identification of pathological grade and prognosis-associated lncRNA for ovarian cancer. *Journal of Cellular Biochemistry*, *120*(9), 14444–14454. https://doi.org/10.1002/jcb.28704

Chetry, M., Li, S., Liu, H., Hu, X., & Zhu, X. (2018). Prognostic values of aquaporins mRNA expression in human ovarian cancer. *Bioscience Reports*, *38*(2). https://doi.org/10.1042/BSR20180108

Di Agostino, S., Valenti, F., Sacconi, A., Fontemaggi, G., Pallocca, M., Pulito, C., Ganci, F., Muti, P., Strano, S., & Blandino, G. (2018). Long Non-coding MIR205HG Depletes Hsa-miR-590-3p Leading to Unrestrained Proliferation in Head and Neck Squamous Cell Carcinoma. *Theranostics*, *8*(7), 1850–1868. https://doi.org/10.7150/thno.22167

Dong, H., Hong, S., Xu, X., Xiao, Y., Jin, L., & Xiong, M. (2010). Meta-analysis and Network Analysis of Five Ovarian Cancer Gene Expression Dataset. *2010 Third International Joint Conference on Computational Science and Optimization*, 242–246. https://doi.org/10.1109/CSO.2010.245

Dong, P., Xiong, Y., Konno, Y., Ihira, K., Kobayashi, N., Yue, J., & Watari, H. (2021). Long non-coding RNA DLEU2 drives EMT and glycolysis in endometrial cancer through HK2 by competitively binding with miR-455 and by modulating the EZH2/miR-181a pathway. *Journal of Experimental & Clinical Cancer Research*, *40*(1), 216. https://doi.org/10.1186/s13046-021-02018-1

Dong, X., Chen, X., Lu, D., Diao, D., Liu, X., Mai, S., Feng, S., & Xiong, G. (2022). LncRNA miR205HG hinders HNRNPA0 translation: anti-oncogenic effects in esophageal carcinoma. *Molecular Oncology*, *16*(3), 795–812. https://doi.org/10.1002/1878-0261.13142

Du, Q., Hoover, A. R., Dozmorov, I., Raj, P., Khan, S., Molina, E., Chang, T.-C., de la Morena, M. T., Cleaver, O. B., Mendell, J. T., & van Oers, N. S. C. (2019). MIR205HG Is a Long Noncoding RNA that Regulates Growth Hormone and Prolactin Production in the Anterior Pituitary. *Developmental Cell*, *49*(4), 618–631. https://doi.org/10.1016/j.devcel.2019.03.012

Fan, H., Lv, P., Mu, T., Zhao, X., Liu, Y., Feng, Y., Lv, J., Liu, M., & Tang, H. (2018). LncRNA n335586/miR-924/CKMT1A axis contributes to cell migration and invasion in hepatocellular carcinoma cells. *Cancer Letters*, *429*, 89–99. https://doi.org/10.1016/j.canlet.2018.05.010

Filippov-Levy, N., Cohen-Schussheim, H., Tropé, C. G., Hetland Falkenthal, T. E., Smith, Y., Davidson, B., & Reich, R. (2018). Expression and clinical role of long non-coding RNA in high-grade serous carcinoma. *Gynecologic Oncology*, *148*(3), 559–566. https://doi.org/10.1016/j.ygyno.2018.01.004

Frankish, A., Diekhans, M., Jungreis, I., Lagarde, J., Loveland, J. E., Mudge, J. M., Sisu, C., Wright, J. C., Armstrong, J., Barnes, I., Berry, A., Bignell, A., Boix, C., Carbonell Sala, S., Cunningham, F., Di Domenico, T., Donaldson, S., Fiddes, I. T., García Girón, C., … Flicek, P. (2021). GENCODE 2021. *Nucleic Acids Research*, *49*(D1), D916–D923. https://doi.org/10.1093/nar/gkaa1087

Fridley, B. L., Dai, J., Raghavan, R., Li, Q., Winham, S. J., Hou, X., Weroha, S. J., Wang, C., Kalli, K. R., Cunningham, J. M., Lawrenson, K., Gayther, S. A., & Goode, E. L. (2018). Transcriptomic Characterization of Endometrioid, Clear Cell, and High-Grade Serous Epithelial Ovarian Carcinoma. *Cancer Epidemiology, Biomarkers & Prevention*, *27*(9), 1101–1109. https://doi.org/10.1158/1055-9965.EPI-17-0728

Ghorbanzadeh, S., Poor-Ghassem, N., Afsa, M., Nikbakht, M., & Malekzadeh, K. (2022). Long non-coding RNA NR2F2-AS1: its expanding oncogenic roles in tumor progression. *Human Cell*, *35*(5), 1355–1363. https://doi.org/10.1007/s13577-022-00733-1

Gilks, C. B., & Prat, J. (2009). Ovarian carcinoma pathology and genetics: recent advances. *Human Pathology*, *40*(9), 1213–1223. https://doi.org/10.1016/j.humpath.2009.04.017

Gloss, B., Moran-Jones, K., Lin, V., Gonzalez, M., Scurry, J., Hacker, N. F., Sutherland, R. L., Clark, S. J., & Samimi, G. (2014). ZNF300P1 Encodes a lincRNA that regulates cell polarity and is epigenetically silenced in type II epithelial ovarian cancer. *Molecular Cancer*, *13*(1), 3. https://doi.org/10.1186/1476-4598-13-3

Goksuluk, D., Korkmaz, S., Zararsiz, G., & Karaagaoglu, A., E. (2016). easyROC: An Interactive Web-tool for ROC Curve Analysis Using R Language Environment. *The R Journal*, *8*(2), 213. https://doi.org/10.32614/RJ-2016-042

Gokulnath, P., de Cristofaro, T., Manipur, I., Di Palma, T., Soriano, A. A., Guarracino, M. R., & Zannini, M. (2019). Long Non-Coding RNA MAGI2-AS3 is a New Player with a Tumor Suppressive Role in High Grade Serous Ovarian Carcinoma. *Cancers*, *11*(12), 2008. https://doi.org/10.3390/cancers11122008

Gokulnath, P., de Cristofaro, T., Manipur, I., Di Palma, T., Soriano, A. A., Guarracino, M. R., & Zannini, M. (2020). Long Non-Coding RNA HAND2-AS1 Acts as a Tumor Suppressor in High-Grade Serous Ovarian Carcinoma. *International Journal of Molecular Sciences*, *21*(11), 4059. https://doi.org/10.3390/ijms21114059

Guo, F., Fu, Q., Wang, Y., & Sui, G. (2019). Long non-coding RNA NR2F1-AS1 promoted proliferation and migration yet suppressed apoptosis of thyroid cancer cells through regulating miRNA-338-3p/ CCND1 axis. *Journal of Cellular and Molecular Medicine*, *23*(9), 5907–5919. https://doi.org/10.1111/jcmm.14386

Guo, J., Gan, Q., Gan, C., Zhang, X., Ma, X., & Dong, M. (2021). LncRNA MIR205HG regulates melanomagenesis via the miR-299-3p/VEGFA axis. *Aging*, *13*(4), 5297–5311. https://doi.org/10.18632/aging.202450

Guo, Z.-H., Yao, L.-T., & Guo, A.-Y. (2020). Clinical and biological impact of LINC02544 expression in breast cancer after neoadjuvant chemotherapy. *European Review for Medical and Pharmacological Sciences*, *24*(20), 10573–10585.

Hao, C., Lin, S., Liu, P., Liang, W., Li, Z., & Li, Y. (2023). Potential serum metabolites and long-chain noncoding RNA biomarkers for endometrial cancer tissue. *Journal of Obstetrics and Gynaecology Research*, *49*(2), 725–743. https://doi.org/10.1111/jog.15494

Hawkins, S. M., Loomans, H. A., Wan, Y.-W., Ghosh-Choudhury, T., Coffey, D., Xiao, W., Liu, Z., Sangi-Haghpeykar, H., & Anderson, M. L. (2013). Expression and Functional Pathway Analysis of Nuclear Receptor NR2F2 in Ovarian Cancer. *The Journal of Clinical Endocrinology & Metabolism*, *98*(7), E1152–E1162. https://doi.org/10.1210/jc.2013-1081

Heberle, H., Meirelles, G. V., da Silva, F. R., Telles, G. P., & Minghim, R. (2015).

InteractiVenn: a web-based tool for the analysis of sets through Venn diagrams. *BMC Bioinformatics*, *16*(1), 169. https://doi.org/10.1186/s12859-015-0611-3

Hongle, L., Jia, J., Yang, L., Chu, J., Sheng, J., Wang, C., Meng, W., Jia, Z., Yin, H., Wan, J., & He, F. (2020). LncRNA MIR205HG Drives Esophageal Squamous Cell Carcinoma Progression by Regulating miR-214/SOX4 Axis. *OncoTargets and Therapy*, *13*, 13097–13109.

Hu, J., Wang, T., & Chen, Q. (2019). Competitive endogenous RNA network identifies four long non-coding RNA signature as a candidate prognostic biomarker for lung adenocarcinoma. *Translational Cancer Research*, *8*(4), 1046–1064. https://doi.org/10.21037/tcr.2019.06.09

Huang, H., Chen, J., Ding, C., Jin, X., Jia, Z., & Peng, J. (2018). LncRNA NR2F1-AS1 regulates hepatocellular carcinoma oxaliplatin resistance by targeting ABCC1 via miR-363. *Journal of Cellular and Molecular Medicine*, *22*(6), 3238–3245. https://doi.org/10.1111/jcmm.13605

Hui, B., Lu, C., Wang, J., Xu, Y., Yang, Y., Ji, H., Li, X., Xu, L., Wang, J., Tang, W., Wang, K., & Gu, Y. (2022). Engineered exosomes for co-delivery of PGM5-AS1 and oxaliplatin to reverse drug resistance in colon cancer. *Journal of Cellular Physiology*, *237*(1), 911–933. https://doi.org/10.1002/jcp.30566

Jia, Q., Liao, X., Zhang, Y., Xu, B., Song, Y., Bian, G., & Fu, X. (2022). Anti-Tumor Role of CAMK2B in Remodeling the Stromal Microenvironment and Inhibiting Proliferation in Papillary Renal Cell Carcinoma. *Frontiers in Oncology*, *12*. https://doi.org/10.3389/fonc.2022.740051

Jiang, H., Hu, K., Xia, Y., Liang, L., & Zhu, X. (2021). Long Noncoding RNA KLF3-AS1 Acts as an Endogenous RNA of miR-223 to Attenuate Gastric Cancer Progression and Chemoresistance. *Frontiers in Oncology*, *11*. https://doi.org/10.3389/fonc.2021.704339

Jiang, R., Zhang, H., Zhou, J., Wang, J., Xu, Y., Zhang, H., Gu, Y., Fu, F., Shen, Y., Zhang, G., Feng, L., Zhang, X., Chen, Y., & Shen, F. (2021). Inhibition of long non-coding RNA XIST upregulates microRNA-149-3p to repress ovarian cancer cell progression. *Cell Death & Disease*, *12*(2), 145. https://doi.org/10.1038/s41419-020-03358-0

Jin, L., Chen, C., Huang, L., Sun, Q., & Bu, L. (2021). Long noncoding RNA NR2F1-AS1 stimulates the tumorigenic behavior of non-small cell lung cancer cells by sponging miR-363-3p to increase SOX4. *Open Medicine*, *17*(1), 87–95. https://doi.org/10.1515/med-2021-0403

Kamikihara, T., Arima, T., Kato, K., Matsuda, T., Kato, H., Douchi, T., Nagata, Y., Nakao, M., & Wake, N. (2005). Epigenetic silencing of the imprinted geneZAC by DNA methylation is an early event in the progression of human ovarian cancer. *International Journal of Cancer*, *115*(5), 690–700. https://doi.org/10.1002/ijc.20971

Lee, C. M., Lo, H.-W., Shao, R.-P., Wang, S.-C., Xia, W., Gershenson, D. M., & Hung, M.-C. (2004). Selective Activation of Ceruloplasmin Promoter in Ovarian Tumors. *Cancer Research*, *64*(5), 1788–1793. https://doi.org/10.1158/0008-5472.CAN-03-2551

Li, H., Lei, Y., Li, S., Li, F., & Lei, J. (2022). LncRNA PART1 Stimulates the Development of Ovarian Cancer by Up-regulating RACGAP1 and RRM2. *Reproductive Sciences*, *29*(8), 2224–2235. https://doi.org/10.1007/s43032-022-00905-2

Li, L.-M., Hao, S.-J., Ni, M., Jin, S., & Tian, Y.-Q. (2021). DUXAP8 promotes the

proliferation and migration of ovarian cancer cells via down-regulating microRNA-29a-3p expression. *European Review for Medical and Pharmacological Sciences*, *25*, 1837–1844. https://doi.org/10.26355/eurrev_202102_25078

Li, L., Peng, Q., Gong, M., Ling, L., Xu, Y., & Liu, Q. (2021). Using lncRNA Sequencing to Reveal a Putative lncRNA-mRNA Correlation Network and the Potential Role of PCBP1-AS1 in the Pathogenesis of Cervical Cancer. *Frontiers in Oncology*, *11*. https://doi.org/10.3389/fonc.2021.634732

Li, P., Xu, H., Yang, L., Zhan, M., Shi, Y., Zhang, C., Gao, D., Gu, M., Chen, Y., & Wang, Z. (2022). E2F transcription factor 2-activated DLEU2 contributes to prostate tumorigenesis by upregulating serum and glucocorticoid-induced protein kinase 1. *Cell Death & Disease*, *13*(1), 77. https://doi.org/10.1038/s41419-022-04525-1

Li, S., Wang, Y., Cao, Q., Li, H., Zhao, Z., Wei, B., Yuan, H., Chen, Z., & Yang, S. (2023). GLIDR promotes the aggressiveness progression of prostate cancer cells by sponging miR-128–3p. *Pathology - Research and Practice*, *242*, 154343. https://doi.org/10.1016/j.prp.2023.154343

Li, W., Liu, Z., Liang, B., Chen, S., Zhang, X., Tong, X., Lou, W., Le, L., Tang, X., & Fu, F. (2018). Identification of core genes in ovarian cancer by an integrative meta-analysis. *Journal of Ovarian Research*, *11*(1), 94. https://doi.org/10.1186/s13048-018-0467-z

Li, Y., Wang, H., & Huang, H. (2019). Long non-coding RNA MIR205HG function as a ceRNA to accelerate tumor growth and progression via sponging miR-122–5p in cervical cancer. *Biochemical and Biophysical Research Communications*, *514*(1), 78–85. https://doi.org/10.1016/j.bbrc.2019.04.102

Li, Y., Zhai, Y., & Chen, Y. (2021). GATA1-induced upregulation of LINC01503 promotes carboplatin resistance in ovarian carcinoma by upregulating PD-L1 via sponging miR-766-5p. *Journal of Ovarian Research*, *14*(1), 108. https://doi.org/10.1186/s13048-021-00856-3

Li, Z., Li, Y., Wang, X., Liang, Y., Luo, D., Han, D., Li, C., Chen, T., Zhang, H., Liu, Y., Wang, Z., Chen, B., Wang, L., Zhao, W., & Yang, Q. (2021). LINC01977 Promotes Breast Cancer Progression and Chemoresistance to Doxorubicin by Targeting miR-212-3p/GOLM1 Axis. *Frontiers in Oncology*, *11*. https://doi.org/10.3389/fonc.2021.657094

Li, Z., Niu, H., Qin, Q., Yang, S., Wang, Q., Yu, C., Wei, Z., Jin, Z., Wang, X., Yang, A., & Chen, X. (2019). lncRNA UCA1 Mediates Resistance to Cisplatin by Regulating the miR-143/FOSL2-Signaling Pathway in Ovarian Cancer. *Molecular Therapy - Nucleic Acids*, *17*(September), 92–101. https://doi.org/10.1016/j.omtn.2019.05.007

Lin, X., Spindler, T. J., de Souza Fonseca, M. A., Corona, R. I., Seo, J. H., Dezem, F. S., Li, L., Lee, J. M., Long, H. W., Sellers, T. A., Karlan, B. Y., Noushmehr, H., Freedman, M. L., Gayther, S. A., & Lawrenson, K. (2019). Super-Enhancer-Associated LncRNA UCA1 Interacts Directly with AMOT to Activate YAP Target Genes in Epithelial Ovarian Cancer. *IScience*, *17*, 242–255. https://doi.org/10.1016/j.isci.2019.06.025

Liu, J.-Q., Deng, M., Xue, N.-N., Li, T.-X., Guo, Y.-X., Gao, L., Zhao, D., & Fan, R.-T. (2020). lncRNA KLF3-AS1 Suppresses Cell Migration and Invasion in ESCC by Impairing miR-185-5p-Targeted KLF3 Inhibition. *Molecular Therapy - Nucleic Acids*, *20*, 231–241. https://doi.org/10.1016/j.omtn.2020.01.020

Liu, L., Li, Y., Zhang, R., Li, C., Xiong, J., & Wei, Y. (2020). MIR205HG acts as a ceRNA to expedite cell proliferation and progression in lung squamous cell carcinoma via

targeting miR-299-3p/MAP3K2 axis. *BMC Pulmonary Medicine*, *20*(1), 163. https://doi.org/10.1186/s12890-020-1174-2

Liu, W., Liu, P., Gao, H., Wang, X., & Yan, M. (2020). Long non-coding RNA PGM5-AS1 promotes epithelial-mesenchymal transition, invasion and metastasis of osteosarcoma cells by impairing miR-140-5p-mediated FBN1 inhibition. *Molecular Oncology*, *14*(10), 2660–2677. https://doi.org/10.1002/1878-0261.12711

Liu, Y., Chen, S., Cai, K., Zheng, D., Zhu, C., Li, L., Wang, F., He, Z., Yu, C., & Sun, C. (2022). Hypoxia-induced long noncoding RNA NR2F1-AS1 maintains pancreatic cancer proliferation, migration, and invasion by activating the NR2F1/AKT/mTOR axis. *Cell Death & Disease*, *13*(3), 232. https://doi.org/10.1038/s41419-022-04669-0

Liu, Y., Zhang, P., Wu, Q., Fang, H., Wang, Y., Xiao, Y., Cong, M., Wang, T., He, Y., Ma, C., Tian, P., Liang, Y., Qin, L.-X., Yang, Q., Yang, Q., Liao, L., & Hu, G. (2021). Long non-coding RNA NR2F1-AS1 induces breast cancer lung metastatic dormancy by regulating NR2F1 and ΔNp63. *Nature Communications*, *12*(1), 5232. https://doi.org/10.1038/s41467-021-25552-0

Love, M. I., Huber, W., & Anders, S. (2014). Moderated estimation of fold change and dispersion for RNA-seq data with DESeq2. *Genome Biology*, *15*(12), 550. https://doi.org/10.1186/s13059-014-0550-8

Luo, D., Liu, Y., Li, Z., Zhu, H., & Yu, X. (2021). NR2F1-AS1 Promotes Pancreatic Ductal Adenocarcinoma Progression Through Competing Endogenous RNA Regulatory Network Constructed by Sponging miRNA-146a-5p/miRNA-877-5p. *Frontiers in Cell and Developmental Biology*, *9*. https://doi.org/10.3389/fcell.2021.736980

Lyu, H., Zhang, J., Wei, Q., Huang, Y., Zhang, R., Xiao, S., Guo, D., Chen, X.-Z., Zhou, C., & Tang, J. (2023). Identification of Wnt/β-Catenin- and Autophagy-Related lncRNA Signature for Predicting Immune Efficacy in Pancreatic Adenocarcinoma. *Biology*, *12*(2), 319. https://doi.org/10.3390/biology12020319

Ma, S.-Y., Wei, P., & Qu, F. (2019). KCNMA1-AS1 attenuates apoptosis of epithelial ovarian cancer cells and serves as a risk factor for poor prognosis of epithelial ovarian cancer. *European Review for Medical and Pharmacological Sciences*, *23*(11), 4629–4641. https://doi.org/10.26355/eurrev_201906_18041

Malek, E., Kim, B., & Driscoll, J. (2016). Identification of Long Non-Coding RNAs Deregulated in Multiple Myeloma Cells Resistant to Proteasome Inhibitors. *Genes*, *7*(10), 84. https://doi.org/10.3390/genes7100084

Mao, T.-L., Fan, M.-H., Dlamini, N., & Liu, C.-L. (2021). LncRNA MALAT1 Facilitates Ovarian Cancer Progression through Promoting Chemoresistance and Invasiveness in the Tumor Microenvironment. *International Journal of Molecular Sciences*, *22*(19), 10201. https://doi.org/10.3390/ijms221910201

Mo, X., Hu, D., Yang, P., Li, Y., Bashir, S., Nai, A., Ma, F., Jia, G., & Xu, M. (2022). A novel cuproptosis-related prognostic lncRNA signature and lncRNA MIR31HG/miR-193a-3p/TNFRSF21 regulatory axis in lung adenocarcinoma. *Frontiers in Oncology*, *12*. https://doi.org/10.3389/fonc.2022.927706

Mortlock, S., Corona, R. I., Kho, P. F., Pharoah, P., Seo, J.-H., Freedman, M. L., Gayther, S. A., Siedhoff, M. T., Rogers, P. A. W., Leuchter, R., Walsh, C. S., Cass, I., Karlan, B. Y., Rimel, B. J., Montgomery, G. W., Lawrenson, K., & Kar, S. P. (2022). A multi-level investigation of the genetic relationship between endometriosis and ovarian cancer histotypes. *Cell Reports Medicine*, *3*(3), 100542. https://doi.org/10.1016/j.xcrm.2022.100542

Mudunuri, U., Che, A., Yi, M., & Stephens, R. M. (2009). bioDBnet: the biological database network. *Bioinformatics*, *25*(4), 555–556. https://doi.org/10.1093/bioinformatics/btn654

Negi, A., Shukla, A., Jaiswar, A., Shrinet, J., & Jasrotia, R. S. (2022). Applications and challenges of microarray and RNA-sequencing. In *Bioinformatics* (pp. 91–103). Elsevier. https://doi.org/10.1016/B978-0-323-89775-4.00016-X

Phillips, N. J., Ziegler, M. R., Radford, D. M., Fair, K. L., Steinbrueck, T., Xynos, F. P., & Donis-Keller, H. (1996). Allelic deletion on chromosome 17p13.3 in early ovarian cancer. *Cancer Research*, *56*(3), 606–611. http://www.ncbi.nlm.nih.gov/pubmed/8564979

Pleasance, E., Bohm, A., Williamson, L. M., Nelson, J. M. T., Shen, Y., Bonakdar, M., Titmuss, E., Csizmok, V., Wee, K., Hosseinzadeh, S., Grisdale, C. J., Reisle, C., Taylor, G. A., Lewis, E., Jones, M. R., Bleile, D., Sadeghi, S., Zhang, W., Davies, A., … Laskin, J. (2022). Whole-genome and transcriptome analysis enhances precision cancer treatment options. *Annals of Oncology*, *33*(9), 939–949. https://doi.org/10.1016/j.annonc.2022.05.522

Profumo, V., Forte, B., Percio, S., Rotundo, F., Doldi, V., Ferrari, E., Fenderico, N., Dugo, M., Romagnoli, D., Benelli, M., Valdagni, R., Dolfini, D., Zaffaroni, N., & Gandellini, P. (2019). LEADeR role of miR-205 host gene as long noncoding RNA in prostate basal cell differentiation. *Nature Communications*, *10*(1), 307. https://doi.org/10.1038/s41467-018-08153-2

Ren, S., Zhang, Y., Yang, X., Li, X., Zheng, Y., Liu, Y., & Zhang, X. (2022). N6-methyladenine- induced LINC00667 promoted breast cancer progression through m6A/KIAA1429 positive feedback loop. *Bioengineered*, *13*(5), 13462–13473. https://doi.org/10.1080/21655979.2022.2077893

Sakamoto, T., Nomura, N., Mori, H., & Wake, N. (1996). Poor Correlation with Loss of Heterozygosity on Chromosome 17p and p53 Mutations in Ovarian Cancers. *Gynecologic Oncology*, *63*(2), 173–179. https://doi.org/10.1006/gyno.1996.0302

Salamini-Montemurri, M., Lamas-Maceiras, M., Barreiro-Alonso, A., Vizoso-Vázquez, Á., Rodríguez-Belmonte, E., Quindós-Varela, M., & Esperanza Cerdán, M. (2020). The challenges and opportunities of lncRNAs in ovarian cancer research and clinical use. *Cancers*, *12*(4), 1–25. https://doi.org/10.3390/cancers12041020

Seitz, A. K., Christensen, L. L., Christensen, E., Faarkrog, K., Ostenfeld, M. S., Hedegaard, J., Nordentoft, I., Nielsen, M. M., Palmfeldt, J., Thomson, M., Jensen, M. T. S., Nawroth, R., Maurer, T., Ørntoft, T. F., Jensen, J. B., Damgaard, C. K., & Dyrskjøt, L. (2017). Profiling of long non-coding RNAs identifies LINC00958 and LINC01296 as candidate oncogenes in bladder cancer. *Scientific Reports*, *7*(1), 395. https://doi.org/10.1038/s41598-017-00327-0

Shen, X., & Zhu, W. (2019). Long non-coding RNA LINC01627 is a prognostic risk factor for epithelial ovarian cancer. *Oncology Letters*, *18*(3), 2861–2868. https://doi.org/10.3892/ol.2019.10661

Song, J. H., Tieu, A. H., Cheng, Y., Ma, K., Akshintala, V. S., Simsek, C., Prasath, V., Shin, E. J., Ngamruengphong, S., Khashab, M. A., Abraham, J. M., & Meltzer, S. J. (2021). Novel Long Noncoding RNA miR205HG Functions as an Esophageal Tumor-Suppressive Hedgehog Inhibitor. *Cancers*, *13*(7), 1707. https://doi.org/10.3390/cancers13071707

Tai, G., Fu, H., Bai, H., Liu, H., Li, L., & Song, T. (2021). Long non-coding RNA GLIDR accelerates the tumorigenesis of lung adenocarcinoma by miR-1270/TCF12 axis.

Cell Cycle, *20*(17), 1653–1662. https://doi.org/10.1080/15384101.2021.1953754

Tan, Y.-E., Xing, Y., Ran, B.-L., Zhang, C., Pan, S.-W., An, W., Chen, Q.-C., & Xu, H.-M. (2020). LINC01235-TWIST2 feedback loop facilitates epithelial–mesenchymal transition in gastric cancer by inhibiting THBS2. *Aging*, *12*(24), 25060–25075. https://doi.org/10.18632/aging.103979

Tang, Z., Kang, B., Li, C., Chen, T., & Zhang, Z. (2019). GEPIA2: an enhanced web server for large-scale expression profiling and interactive analysis. *Nucleic Acids Research*, *47*(W1), W556–W560. https://doi.org/10.1093/nar/gkz430

Tarhriz, V., Bandehpour, M., Dastmalchi, S., Ouladsahebmadarek, E., Zarredar, H., & Eyvazi, S. (2019). Overview of CD24 as a new molecular marker in ovarian cancer. *Journal of Cellular Physiology*, *234*(3), 2134–2142. https://doi.org/10.1002/jcp.27581

Tu, C., Ren, X., He, J., Li, S., Qi, L., Duan, Z., Wang, W., & Li, Z. (2020). The predictive value of lncRNA MIR31HG expression on clinical outcomes in patients with solid malignant tumors. *Cancer Cell International*, *20*(1), 115. https://doi.org/10.1186/s12935-020-01194-y

Van Grembergen, O., Bizet, M., de Bony, E. J., Calonne, E., Putmans, P., Brohée, S., Olsen, C., Guo, M., Bontempi, G., Sotiriou, C., Defrance, M., & Fuks, F. (2016). Portraying breast cancers with long noncoding RNAs. *Science Advances*, *2*(9), e1600220. https://doi.org/10.1126/sciadv.1600220

Wang, H., Chen, X., Yang, B., Xia, Z., & Chen, Q. (2020). MiR-924 as a tumor suppressor inhibits non-small cell lung cancer by inhibiting RHBDD1/Wnt/β-catenin signaling pathway. *Cancer Cell International*, *20*(1), 491. https://doi.org/10.1186/s12935-020-01516-0

Wang, H., Fu, Z., Dai, C., Cao, J., Liu, X., Xu, J., Lv, M., Gu, Y., Zhang, J., Hua, X., Jia, G., Xu, S., Jia, X., & Xu, P. (2016). LncRNAs expression profiling in normal ovary, benign ovarian cyst and malignant epithelial ovarian cancer. *Scientific Reports*, *6*(1), 38983. https://doi.org/10.1038/srep38983

Wang, J., Liu, B., Cao, J., Zhao, L., & Wang, G. (2022). MIR31HG Expression Predicts Poor Prognosis and Promotes Colorectal Cancer Progression. *Cancer Management and Research*, *14*, 1973–1986. https://doi.org/10.2147/CMAR.S351928

Wang, J., Tian, Y., Zheng, H., Ding, Y., & Wang, X. (2019). An integrated analysis reveals the oncogenic function of lncRNA LINC00511 in human ovarian cancer. *Cancer Medicine*, *8*(6), 3026–3035. https://doi.org/10.1002/cam4.2171

Wang, M., Zhang, Z., Pan, D., Xin, Z., Bu, F., Zhang, Y., Tian, Q., & Feng, X. (2021). Circulating lncRNA UCA1 and lncRNA PGM5-AS1 act as potential diagnostic biomarkers for early-stage colorectal cancer. *Bioscience Reports*, *41*(7). https://doi.org/10.1042/BSR20211115

Wang, R., Ma, Z., Feng, L., Yang, Y., Tan, C., Shi, Q., Lian, M., He, S., Ma, H., & Fang, J. (2018). LncRNA MIR31HG targets HIF1A and P21 to facilitate head and neck cancer cell proliferation and tumorigenesis by promoting cell-cycle progression. *Molecular Cancer*, *17*(1), 162. https://doi.org/10.1186/s12943-018-0916-8

Wang, X., Yu, X., Long, X., & Pu, Q. (2021). MIR205 host gene (MIR205HG) drives osteosarcoma metastasis via regulating the microRNA 2114-3p (miR-2114-3p)/twist family bHLH transcription factor 2 (TWIST2) axis. *Bioengineered*, *12*(1), 1576–1586. https://doi.org/10.1080/21655979.2021.1920326

Wei, M., Liu, L., & Wang, Z. (2019). Long non-coding RNA heart and neural crest derivatives expressed 2-antisense RNA 1 overexpression inhibits the proliferation of cancer cells by reducing RUNX2 expression in triple-negative breast cancer. *Oncology Letters*, *18*(6), 6775–6780. https://doi.org/10.3892/ol.2019.11001

Wei, W., Xu, T., Zhang, Y., Huang, Y., & Wang, X. (2022). Upregulation of long noncoding RNA linc02544 and its association with overall survival rate and the influence on cell proliferation and migration in lung squamous cell carcinoma. *Discover Oncology*, *13*(1), 41. https://doi.org/10.1007/s12672-022-00501-5

Wu, Y., Wang, T., Xia, L., & Zhang, M. (2021). LncRNA WDFY3-AS2 promotes cisplatin resistance and the cancer stem cell in ovarian cancer by regulating hsa-miR-139-5p/SDC4 axis. *Cancer Cell International*, *21*(1), 284. https://doi.org/10.1186/s12935-021-01993-x

Xie, H., Dai, L., Ye, B., Chen, R., Wang, B., Zhang, N., Miao, H., & Liang, W. (2022). Long non-coding RNA ERVK13-1 aggravates osteosarcoma through the involvement of microRNA-873-5p/KLF5 axis. *Acta Biochimica Polonica*, *69*(4), 703–710. https://doi.org/10.18388/abp.2020_5809

Xu, D., Song, Q., Liu, Y., Chen, W., LU, L., Xu, M., Fang, X., Zhao, W., & Zhou, H. (2021). LINC00665 promotes Ovarian Cancer progression through regulating the miRNA-34a-5p/E2F3 axis. *Journal of Cancer*, *12*(6), 1755–1763. https://doi.org/10.7150/jca.51457

Xu, P., Xu, S., Pan, H., Dai, C., Xu, Y., Wang, L., Cong, Y., Zhang, H., Cao, J., Ge, L., & Jia, X. (2023). Differential effects of the LncRNA RNF157-AS1 on epithelial ovarian cancer cells through suppression of DIRAS3- and ULK1-mediated autophagy. *Cell Death & Disease*, *14*(2), 140. https://doi.org/10.1038/s41419-023-05668-5

Yan, C., Zhu, Y., Zhang, X., Chen, X., Zheng, W., & Yang, J. (2014). Down-regulated aquaporin 5 inhibits proliferation and migration of human epithelial ovarian cancer 3AO cells. *Journal of Ovarian Research*, *7*(1), 78. https://doi.org/10.1186/s13048-014-0078-2

Yang, C., Zhang, M., Cai, Y., Rong, Z., Wang, C., Xu, Z., Xu, H., Song, W., Hou, Y., & Lou, G. (2019). Platelet-derived growth factor-D expression mediates the effect of differentiated degree on prognosis in epithelial ovarian cancer. *Journal of Cellular Biochemistry*, *120*(5), 6920–6925. https://doi.org/10.1002/jcb.27432

Yang, J.-H., Shi, Y.-F., Cheng, Q., & Deng, L. (2006). Expression and localization of aquaporin-5 in the epithelial ovarian tumors. *Gynecologic Oncology*, *100*(2), 294–299. https://doi.org/10.1016/j.ygyno.2005.08.054

Yao, H., Chen, R., Yang, Y., & Jiang, J. (2021). LncRNA BBOX1-AS1 Aggravates the Development of Ovarian Cancer by Sequestering miR-361-3p to Augment PODXL Expression. *Reproductive Sciences*, *28*(3), 736–744. https://doi.org/10.1007/s43032-020-00366-5

Yin, L., Zhang, Y., & Zheng, L. (2021). Analysis of differentially expressed long non-coding RNAs revealed a pro-tumor role of MIR205HG in cervical cancer. *Molecular Medicine Reports*, *25*(2), 42. https://doi.org/10.3892/mmr.2021.12558

Yu, Q., Li, X., & Feng, T. (2021). GLIDR promotes the progression of glioma by regulating the miR-4677-3p/MAGI2 axis. *Experimental Cell Research*, *406*(1), 112726. https://doi.org/10.1016/j.yexcr.2021.112726

Zhang, C., Liang, Y., Zhang, C.-D., Pei, J.-P., Wu, K.-Z., Li, Y.-Z., & Dai, D.-Q. (2021). The novel role and function of LINC01235 in metastasis of gastric cancer cells by

inducing epithelial-mesenchymal transition. *Genomics*, *113*(3), 1504–1513. https://doi.org/10.1016/j.ygeno.2021.03.027

Zhang, T., Xia, W., Song, X., Mao, Q., Huang, X., Chen, B., Liang, Y., Wang, H., Chen, Y., Yu, X., Zhang, Z., Yang, W., Xu, L., Dong, G., & Jiang, F. (2022). Super-enhancer hijacking LINC01977 promotes malignancy of early-stage lung adenocarcinoma addicted to the canonical TGF-β/SMAD3 pathway. *Journal of Hematology & Oncology*, *15*(1), 114. https://doi.org/10.1186/s13045-022-01331-2

Zhang, X., Liu, G., Qiu, J., Zhang, N., Ding, J., & Hua, K. (2017). E2F1-regulated long non-coding RNA RAD51-AS1 promotes cell cycle progression, inhibits apoptosis and predicts poor prognosis in epithelial ovarian cancer. *Scientific Reports*, *7*(1), 4469. https://doi.org/10.1038/s41598-017-04736-z

Zhang, Y., Dun, Y., Zhou, S., & Huang, X.-H. (2017). LncRNA HOXD-AS1 promotes epithelial ovarian cancer cells proliferation and invasion by targeting miR-133a-3p and activating Wnt/β-catenin signaling pathway. *Biomedicine & Pharmacotherapy*, *96*, 1216–1221. https://doi.org/10.1016/j.biopha.2017.11.096

Zhao, L., Li, Y., Zhang, Z., Zou, J., Li, J., Wei, R., Guo, Q., Zhu, X., Chu, C., Fu, X., Yue, J., & Li, X. (2020). Meta-analysis based gene expression profiling reveals functional genes in ovarian cancer. *Bioscience Reports*, *40*(11). https://doi.org/10.1042/BSR20202911

Zhao, X., Chen, L., Wu, J., You, J., Hong, Q., & Ye, F. (2021). Transcription factor KLF15 inhibits the proliferation and migration of gastric cancer cells via regulating the TFAP2A-AS1/NISCH axis. *Biology Direct*, *16*(1), 21. https://doi.org/10.1186/s13062-021-00300-y

Zheng, J., Qin, W., Jiao, D., Ren, J., Wei, M., Shi, S., Xi, W., Wang, H., Yang, A.-G., Huan, Y., & Wen, W. (2016). Knockdown of COUP-TFII inhibits cell proliferation and induces apoptosis through upregulating BRCA1 in renal cell carcinoma cells. *International Journal of Cancer*, *139*(7), 1574–1585. https://doi.org/10.1002/ijc.30193

Zheng, R., Liang, J., Lu, J., Li, S., Zhang, G., Wang, X., Liu, M., Wang, W., Chu, H., Tao, G., Zhao, Q., Wang, M., Du, M., Qiang, F., & Zhang, Z. (2019). Genome-wide long non-coding RNAs identified a panel of novel plasma biomarkers for gastric cancer diagnosis. *Gastric Cancer*, *22*(4), 731–741. https://doi.org/10.1007/s10120-018-00915-7

Zheng, S., Zhang, X., Wang, X., & Li, J. (2019). MIR31HG promotes cell proliferation and invasion by activating the Wnt/β-catenin signaling pathway in non-small cell lung cancer. *Oncology Letters*, *17*(1), 221–229. https://doi.org/10.3892/ol.2018.9607

Zhou, B., Guo, H., & Tang, J. (2019). Long Non-Coding RNA TFAP2A-AS1 Inhibits Cell Proliferation and Invasion in Breast Cancer via miR-933/SMAD2. *Medical Science Monitor*, *25*, 1242–1253. https://doi.org/10.12659/MSM.912421

Zhu, L., & Mei, M. (2021). Interference of long non-coding RNA HAGLROS inhibits the proliferation and promotes the apoptosis of ovarian cancer cells by targeting miR-26b-5p. *Experimental and Therapeutic Medicine*, *22*(2), 879. https://doi.org/10.3892/etm.2021.10311

Chapter 2.

Identification of HMGB1/2-RNA interactions in ovarian cancer cell lines

INTRODUCTION

RNA-binding proteins (RBPs) are a class of proteins that bind to different types of RNA and play a crucial role in the regulation of gene expression. RPBs also affect the fate of the RNAs they bind within the cell by modulating their splicing, processing, stability, translation, and subcellular location (Glisovic et al., 2008). At the same time, bound RNAs can also impact the functions, stability, processing, and subcellular location of the RBPs, as it happens for instance with lncRNAs (Davidovich & Cech, 2015). These interactions can range from binary, a single RBP binding a single RNA, to the formation of complex structures involving multiple RBPs and RNA molecules, such as the spliceosome (Corley et al., 2020).

RBPs are characterized by presenting one or more RNA-binding domains (RBDs), which are structural motifs that specifically recognize and bind to RNA molecules. These domains typically have an evolutionarily conserved sequence and structural architecture that determine their RNA-binding specificity and affinity. The number of known RNA binding motifs in RBDs is rising and many are waiting to be discovered, but some are well-known such as RNA Recognition Motif, K-homology, Zinc Fingers, Double-stranded RNA-binding domain, Helicase (Lunde et al., 2007), and also HMG-box (Holmes et al., 2020) or intrinsically disordered regions (Corley et al., 2020).

There are several techniques available to study RNA-protein interactions that, depending on the research interest, can be classified as “protein-centered” and “RNA-centered” techniques, with low-throughput readouts such as RT-qPCR or western blot, or high-throughput readouts such as transcriptomics or proteomics, respectively.

For the protein-centric approach, the main methods to identify RNAs bound to a certain protein are RNA immunoprecipitation (RIP), cross-linking immunoprecipitation (CLIP) and derivatives, and proximity labeling assays.

RIP involves the immunoprecipitation (IP) of an RBP using specific antibodies, followed by the extraction and identification of associated RNA molecules. To maintain the integrity of native ribonucleoprotein complexes, these are purified using

physiological-like conditions. The degree of association between an RNA and the RBP of interest is determined by the enrichment of the RNA through target-specific immunoprecipitation, relative to a control unspecific immunoprecipitation. RIP is often coupled with techniques like microarrays, RNA sequencing, or RT-qPCR, known as RIP-chip (Keene et al., 2006), RIP-Seq (Zhao et al., 2010), or RIP-qPCR (Martindale et al., 2020), respectively.

CLIP is similar to RIP but with the addition of initial cell UV-crosslinking, partial RNase digestion after lysis, and high-stringency washes after the IP, which allow the fixation of RNPs, an increase of the signal-to-noise ratio, and the determination of the binding sequence, respectively (Ule et al., 2003). CLIP when subjected to high-throughput sequencing is termed HITS-CLIP (Licatalosi et al., 2008).

Efforts to narrow down the RNA binding site at single nucleotide resolution led to the development of photoactivatable ribonucleoside-enhanced CLIP (PAR-CLIP) (Hafner et al., 2010) and individual nucleotide resolution CLIP (iCLIP) (König et al., 2010). PAR-CLIP relies on the addition of nucleoside analogs, which cause transitions in the cDNA when crosslinked with a protein, and the final analysis of mutations in RNA-Seq, whereas iCLIP is based on the truncation of reverse transcription at the crosslink site. Library preparation in iCLIP and many other variants of the method use a cDNA circularization approach, whereas another variant known as enhanced CLIP (eCLIP) (Van Nostrand et al., 2017) uses a highly concentrated T4 RNA ligase 1 to ligate a DNA adapter to the 3′ ends of the cDNA (Hafner et al., 2021).

Proximity labeling techniques exploit the fusion of the RBP of interest with an engineered ascorbate peroxidase (APEX2) in the APEX-Seq method (Padrón et al., 2019), or adenosine deaminase (ADAR) in the TRIBE method (McMahon et al., 2016) to biotinylate or deaminate, respectively, RNA-binding partners in the vicinity, enabling their subsequent identification and characterization.

For the “RNA-centered” approach, the main methods to identify proteins bound to a certain RNA are biotinylated, S1-aptamer-fused, or biotinylated CRISPR-recognized RNA Pull-Down Assays, which are cell-free *in vitro*; besides, RNA-capture, organic phase separation, protein-mass shift, Trap-MS2, and RaPID proximity labeling method, which are carried out *in cellula,* are also useful techniques (Ramanathan et al., 2019).

There are also *in vitro* cell-free and low-throughput techniques used as a validation tool rather than a discovery approach suitable for both protein- and RNA-centric approaches, such as electrophoretic mobility shift assay (EMSA) or fluorescence anisotropy (FA), which rely on the change in migration or fluorescence polarization properties upon protein binding to a labeled RNA, respectively. As an example of *in silico* RBP-RNA interaction discovery, catRAPID predicts RNAs or RBPs at omic level using as an input the amino acid or nucleotide sequence, respectively (Agostini et al., 2013).

The HMGB proteins, which are altered in ovarian cancer, also have the ability to bind RNA, and in this chapter, various strategies are addressed to identify these RNAs, with a particular focus on lncRNAs capable of interacting with HMGB1 and HMGB2 in epithelial ovarian cancer cell lines.

MATERIALS AND METHODS

Cell culture

PEO1 and SKOV3 cell lines were obtained from the American Type Culture Collection (ATCC) and maintained at 37°C in 5% CO_2 in air in a humidified incubator in Roswell Park Memorial Institute (RPMI) 1610 medium (Lonza Biologics) supplemented with 10% heat-inactivated FBS (Gibco) and 1% penicillin-streptomycin (Gibco).

Native RIP-Seq

Experimental design.- The two RIP-Seq experiments were carried out using PEO1 and SKOV3 cancerous cell lines and comprised 12 samples each. The experiment performed using PEO1 consisted of 4 biological replicates with three conditions/antibodies each (anti-HMGB1, anti-HMGB2, and rabbit IgG isotype control).

The experiment with SKOV3 consisted of 3 biological replicates and, in addition to the conditions specified previously for PEO1, also included an input sample.

Antibody coupling to magnetic beads.- 25 µL of protein A-coated Dynabeads (Invitrogen) per immunoprecipitation, equivalent to 750 µg, were washed 3 times with ice-cold NT-2 buffer (50 mM Tris-HCl pH 7.4, 150 mM NaCl, 1 mM $MgCl_2$ and 0.05% NP-40), incubated with 5 µg of HMGB1 (ab18256, Abcam), HMGB2 (ab67282, Abcam), or Rabbit IgG isotype Control (02-6102, Thermo Fisher) antibodies for 20 min at room temperature (RT) in rotation and washed again twice with ice-cold NT-2 buffer. In order to crosslink the antibody to the beads, antibody-coupled beads were washed twice with 0.2 M Triethanolamine Buffer solution pH 8 (TEABS) (Sigma-Aldrich) and incubated with 0.2 M dimethyl pimelimidate (DMP) dihydrochloride dissolved in TEABS in rotation for 45 min at RT. The supernatant was discarded and beads were incubated with 50 mM Tris-HCl pH 7.4 in rotation at RT for 15 min to quench the crosslinking reaction. Beads were washed 3 times with NT-2 buffer and resuspended NT-2 buffer supplemented with 2 units/µL RiboLock RNase Inhibitor (Thermo Scientific), 1 mM dithiothreitol (DTT) and 15 mM EDTA pH 8.

Cell lysate preparation.- 5 or 2 150-mm Petri dishes of 70-80% cell confluence were used in each experiment for PEO1 or SKOV3, respectively. The medium was discarded and cells were carefully washed twice with ice-cold 1X PBS pH 7.4, detached by scraping, transferred to a 50 mL tube, and pelleted by centrifugation at 4°C 5,000 rpm for 5 min. The supernatant was discarded and the pellet was detached from the bottom of the tube by flicking on ice-cold polysome lysis buffer (PLB) (100 mM KCl, 5 mM $MgCl_2$, 10 mM HEPES-NaOH pH 7, 0.5% NP-40) supplemented with 0.2 units/µL RiboLock RNase Inhibitor (Thermo Scientific), 1 mM DTT, and 1X Pierce Protease Inhibitor were added to the pellet (6 mL or 360 µL for PEO1 or SKOV3 experiment, respectively), cells were carefully resuspended also by flicking and the mixture was incubated on ice for 20 min. To ensure good cell lysis, resuspended PEO1 cell lysate was transferred into a 7 mL Dounce homogenizer with a type B pestle, applying 40 passages and aliquoted in 2

mL tubes; resuspended SKOV3 cells were snap-frozen (-80°C), then thawed and vortexed. Lysates were finally centrifuged at 20,000 x *g* for 10 min at 4°C and supernatants were collected and transferred to a new tube.

Immunoprecipitation.- A 1% of the cell extract was kept as Input for use in western blot and another 1% was kept as RNA Input for sequencing when necessary. The remaining cell extract was divided into three tubes containing the HMGB1, HMGB2, and IgG isotype control antibodies previously coupled with Dynabeads, respectively, and incubated in rotation for 4 hours at 4°C. After the incubation, beads were washed 6 times with ice-cold NT-2 buffer, pipetting up and down for the PEO1 experiment, and 2 times 20 s and 4 times 2 min vortex for the SKOV3 experiment. Finally, washed beads were resuspended in NT-2 buffer, of which 20% was transferred to a new tube for checking by western blot the efficiency of immunoprecipitation.

RNA purification.- The remaining 80% of the beads and the SKOV3 Input were treated with DNase I, RNase-free (Thermo Scientific) at 37°C for 20 min with slight agitation. Beads were washed once with ice-cold NT-2 buffer and the supernatant was removed. The beads and the SKOV3 input were treated with 0.5 µg/µL Proteinase K (Invitrogen) and 0.1% SDS supplemented NT-2 buffer at 55°C for 25 min in agitation at 1,200 rpm. The beads supernatant was transferred into new 1.5 mL tubes, and the beads were added more NT-2.

Both IPs and Input were added the same volume of Acid-Phenol:Chloroform pH 4.5 (with IAA, 125:24:1) (Thermo Scientific), thoroughly inverted to mix, and centrifuged at 20,000 x *g* for 10 min. The upper phase was collected and transferred into new tubes and added 2.5 v/v ethanol 100%, 10% 3 M sodium acetate pH 5.2, and 1% glycoblue or glycogen for PEO1 and SKOV3, respectively. Tubes were mixed thoroughly and incubated at -80°C overnight. The day after, tubes were mixed by inversion and centrifuged at 20,000 x *g* for 30 min at 4°C. The supernatant was discarded, 75% ethanol was added to each tube and tubes were centrifuged again at 20,000 x *g* for 15 min at

4°C. The supernatant was discarded, the tubes were air-dried, and the pellets were resuspended in sterile distilled water. Immunoprecipitated RNA was quantified using Qubit 2.0 High Sensitivity RNA kit (Thermo Scientific), and control quality was evaluated using BioAnalyzer 2100 Eukaryote Total RNA Pico kit (Agilent).

RNA-Sequencing.- Immunoprecipitated RNA samples were sent to Centro Andaluz de Biología Molecular y Medicina Regenerativa (CABIMER, Seville) and processed by the Genomics Unit. All cDNA libraries were prepared using Illumina Stranded TOTAL RNA Preparation RIBO-ZERO PLUS kit, starting from 10 ng of IP RNA, including the step of ribosomal RNA depletion. RNA and cDNA libraries were quantified and quality-controlled using Qubit High Sensitivity and Bioanalyzer Eukaryote Total RNA Pico kits, respectively. The sequencing was performed in a NextSeq 500 (Illumina) equipment using 75 bp long and single-end reads and High Output kit Flowcell loaded at equimolar sample content, with an approximate depth of 33 million reads per sample.

RIP-seq analysis.- Fastq files from different lanes, which were quality-filtered and adapter-trimmed by CABIMER staff, corresponding to each sample were concatenated. Mapping, transcript quantification, and bam file generation were performed with STAR version 2.7.10b against the *Homo sapiens* genome (hg38 version). Bam index files were generated using samtools version 1.17. Bam files were converted into bigwig files using bamCoverage from Deeptools (Ramírez et al., 2016). RNA-Seq data were processed using RStudio (version 2022.12.0 Build 353), R (version 4.1.0), Bioconductor (version 3.14), and DESeq2 (version 1.34). Read counts were imported into RStudio using tximport and implemented into DESeq2 using the function DESeqDataSetFromMatrix. Gene filtering and normalization were carried out using DESeq2. Differential expression between specific antibody IPs and rabbit isotype IgG control or Input was run with DESeq2, and finally annotated by merging with the human genome information (hg38, GRCh38.p13) using RStudio (v4.1.0) merge function from data.table package. The statistical significance cutoff *p*-value was set as 0.05 and Log_2

(fold change) as 0.585. Gene ontology analyses were performed with the Clusterprofiler package and summarized (adjusted *p*-value < 0.05).

PEO1 eCLIP

HMGB1 and HMGB2 eCLIP experiments in the PEO1 cell line were carried out using the EclipseBIO RBP-eCLIP kit, which is based on (Blue et al., 2022; Van Nostrand et al., 2017), following their corresponding protocol (version 2.0). The experimental design comprised two biological replicates, i.e., two immunoprecipitations and two corresponding size-matched inputs, for each antibody, namely anti-HMGB1 (ab1825, Abcam) and anti-HMGB2 (ab67282, Abcam). IgG isotype control (02-6102, Thermo Scientific) control antibody was used for IP specificity validation.

The protocol for each biological replicate consisted of the following steps. Three 150 mm Petri dishes (80-90% confluence) were washed with cold 1x DPBS (14040133, Gibco) and exposed to 400 mJ/cm^2, λ=254 nm light in a UVP Crosslinker CL-3000 (Analytic Jena) to achieve the protein-nucleic acid crosslinking. Then, cells were detached by scraping, diluted in cold 1x DPBS to count cell density, spun in a refrigerated centrifuge, and resuspended in 1 mL of cold 1x DPBS to get 20x10^6 cells/tube, enough for one biological replicate. Later, cells were lysed in cold eCLIP Lysis Buffer (provided in the kit) supplemented with protease (78429, Thermo Scientific) and RNase inhibitors (provided in the kit) and sonicated in cold for 10 min (on/off cycles of 30 s) in a Bioruptor UCD-200 (Diagenode) equipment, setting the energy in “low” position to break up membranes and fragment nucleic acids. A 10 µL aliquot of each lysate was transferred to a new tube and treated with protease (provided in the kit) for 10 min at 37°C followed by 20 min at 50°C, both with mixing at 1,200 rpm, continued by a purification using Zymo RNA Clean & Concentrator Kit. The concentration and quality of the purified RNA from the aliquot were assessed using Agilent 4200 TapeStation equipment.

Lysates were digested with RNase I and DNase I and incubated overnight with magnetic beads previously coupled to HMGB1 or HMGB2 antibodies. An aliquot was

kept as “Input”, and the rest of the immunoprecipitated RNA was washed, repaired at the 3’ end by alkaline phosphatase and polynucleotide kinase, washed again, and ligated to a biotinylated adapter, followed by a third wash. After this, both IP and Inputs were loaded in three different polyacrylamide gels: one to detect immunoprecipitated protein, another to detect biotinylated pulled-down RNA, and the last one to purify RNA for sequencing.

The third gel was transferred to a nitrocellulose membrane and bands ranging from 25 kDa to 100 kDa, corresponding to each sample, were trimmed, and chopped into small pieces, transferred to tubes, and digested with Protease K. RNA was purified from them again with Zymo RNA Clean & Concentrator Kit. Input RNA was repaired, and the biotinylated adapter was ligated as it was done previously with IP samples. Later, all samples were retrotranscribed, followed by the ligation of a new ssDNA adapter. Ligated cDNA was measured by qPCR and the addition of sequencing indexes was carried out by standard PCR, adjusting the cycles accordingly to the qPCR results. The resulting libraries were purified using AMPure XP beads (A63881, Beckman Coulter) and agarose gel electrophoresis rescue, to be finally quantified using an Agilent 4200 TapeStation system. Libraries were sequenced in an Illumina NovaSeq 6000 sequencer with a depth of 25 million reads per sample, both IPs and Inputs.

This experiment was analyzed by Eclipsebio company (San Diego, United States of America) using a standard RBP-eCLIP pipeline (Blue et al., 2022). Briefly, raw sequencing reads were trimmed of unique molecular identifiers and adapters, filtered of repetitive elements such as rRNA, mapped to the reference genome, and filtered of PCR duplicates. Clusters (regions within the IP sample that contain a pileup of reads) were identified using the peak caller CLIPper (Ge et al., 2021) and normalized against the paired input sample. Each cluster was then normalized against the paired input sample, using a cutoff of Log_2 (fold change) ≥ 0.585 and -log10(*p*-value) ≥ 1.301.

Genome visualization

Coverage tracks were generated from bam files using the Integrative Genomics Viewer (IGV) from Broad Institute, version 2.14 (Thorvaldsdottir et al., 2013) (https://software.broadinstitute.org/software/igv/). Bigwig files for each condition corresponding were merged separating by positive and negative strands, using bigWigMerge and bedGraphToBigWig functions from UCSC tools (Kent et al., 2010).

Bioinformatic RNA interacting partners prediction

To predict lncRNAs binding to HMGB1 and HMGB2 we used the online tool catRAPID (http://s.tartaglialab.com/page/catrapid_group) (Armaos et al., 2021). Specifically, we used the options omics to compare protein(s) vs transcriptome, selecting long non-coding RNA transcriptome from *Homo sapiens*. The input amino acid FASTA sequences used were ENSP00000345347 and ENSP00000296503 for HMGB1 and HMGB2, respectively.

Western blot

Washed beads were resuspended into 40 µL 5X Laemmli buffer and boiled at 95°C for 10 min. Supernatants were directly loaded into the wells of 6%-10% polyacrylamide gels. After the run, the gel was transferred in semi-dry conditions into an activated PVDF membrane (Cytiva, 10600023), and blocked for 1 hour in 5% skimmed powdered milk in 0.1% Tween PBS (137 mM NaCl, 2.7 mM KCl, 10 mM Na_2HPO_4, 1.8 mM KH_2PO_4). Membranes were incubated overnight at 4°C in rotation with 1:1,000 dilution in the same powdered milk solution of HMGB1 (ab18256, Abcam) and HMGB2 (ab67282, Abcam) antibodies. Protein G, HRP conjugate (Millipore) was used as the secondary antibody. Images were obtained using BioRad Gel Doc XR+ equipment.

RESULTS AND DISCUSSION

After 50 years of their discovery, HMGB proteins have been widely studied regarding their ability to bind DNA and how they affect chromosomal architecture and modulate gene transcription (Joshi et al., 2012; Stros et al., 2009; Zirkel et al., 2018). In

contrast, collective evidence suggests that important HMGB functions within the cell are due to their interaction with RNAs (Castello et al., 2016), including lncRNAs (Sofiadis et al., 2021; Yamanaka et al., 2015), although this feature has been less explored. This study broadens the catalog of RNAs to which HMGB1 and HMGB2 bind in the context of epithelial ovarian cancer, not only increasing the complexity of the mechanism of action of these two proteins but also providing novel potential biomarkers for the disease based on the RNA interacting partners. To do so, we explored three different approaches described in this chapter, of which, one is computational and probabilistic - catRAPID algorithm - and the other two are experimental - RIP-Seq and eCLIP.

In silico analysis of HMGB1 and HMGB2 RNA interacting partners

As a preliminary search, we carried out an *in silico* analysis to predict which RNAs could interact with HMGB1 and/or HMGB2 by applying an algorithm known as catRAPID (Agostini et al., 2013), which relies on the biophysical properties, i.e. van der Waals, hydrogen bonding, and secondary structure propensities of RNAs and proteins (Bellucci et al., 2011). The “omics” option of this web-based tool uses the amino acid sequence of a protein as input to carry out multiple pairwise tests with the human transcriptome to calculate the protein-RNA interaction probability. The defining output parameter is the z-score, which consists in a normalization based on the standard deviations above the mean relative to the distribution of interaction prediction scores for high-confidence interactions in the algorithm training sets. The interaction probability ranges from strong positive prediction when the z-score is above 4, to weak positive prediction when the z-score is positive and close to 0, being the negative values neglectable (Lang et al., 2019). We obtained two lists of probable RNA interacting partners, one for HMGB1 and another for HMGB2, both comprised of 41,534 different genes, each gene corresponding to the transcript isoform with the highest interaction probability. We sorted each list by decreasing z-score and set a threshold of z-score ≥ 1, keeping 2,978 and 2,301 genes for HMGB1 and HMGB2, respectively, as seen in Figure 1.

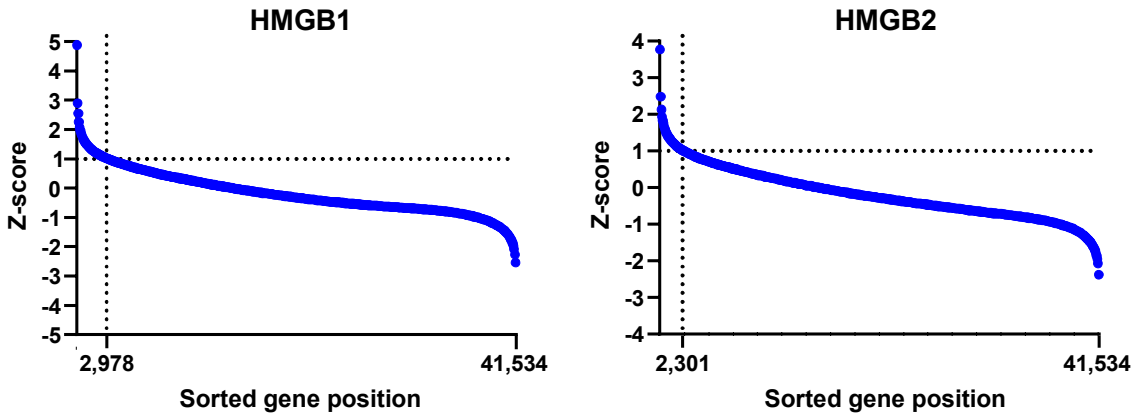

Figure 1.- Normalized interaction probability distribution from catRAPID algorithm. Z-score values for HMGB1 (**left**) and HMGB2 (**right**) are sorted in decreasing order. The dotted lines represent the z-score = 1 and the corresponding position from the sorted gene list.

The biotype frequencies from the selected and predicted interacting RNAs are very similar between HMGB1 and HMGB2, shown in Figure 2, being the protein-coding genes the most abundant, followed by lncRNAs and pseudogenes.

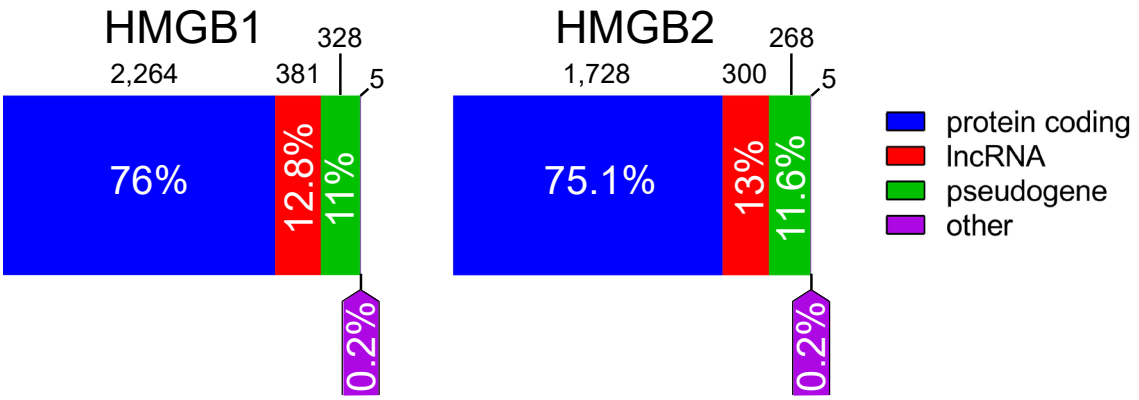

Figure 2.- Ensembl gene biotype frequencies of the selected genes from the prediction lists. The percentages inside the squares and the numbers above the squares represent the relative and the absolute frequency for each gene biotype, respectively.

Although genes are not identical if we compare the two lists, there is a high overlap in the general classification (Figure 3A) and also when compared by biotype (Figure 3B-D). Since this algorithm is based on the protein and RNA sequences, and HMGB1 and HMGB2 share >80% identity (Stros et al., 2009), it was expected to obtain overlapping results.

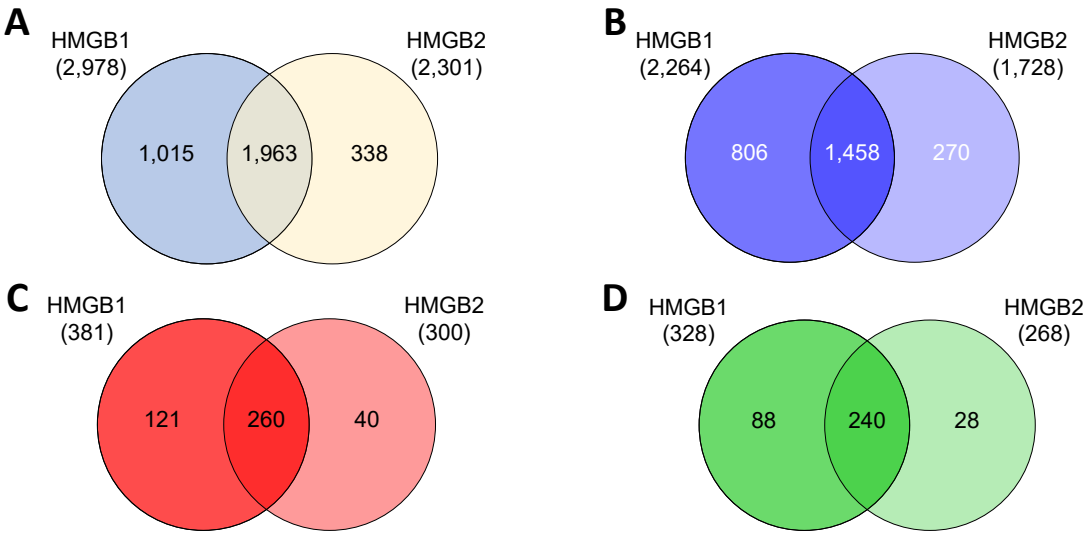

Figure 3.- Intersection between HMGB1 and HMGB2 selected and predicted RNA interacting partners. Overlap of the full list (**A**), protein-coding genes (**B**), lncRNAs (**C**), and pseudogenes (**D**).

Additionally, we decided to explore the biological functions that are related to the mRNAs predicted to interact with HMGB1 and HMGB2. We did three gene ontology (GO) analyses, one with HMGB1-exclusive mRNAs, one with HMGB2-exclusive mRNAs, and another one with mRNAs common for HMGB1 and HMGB2. The most representative and statistically significant GO terms are represented in Figure 4.

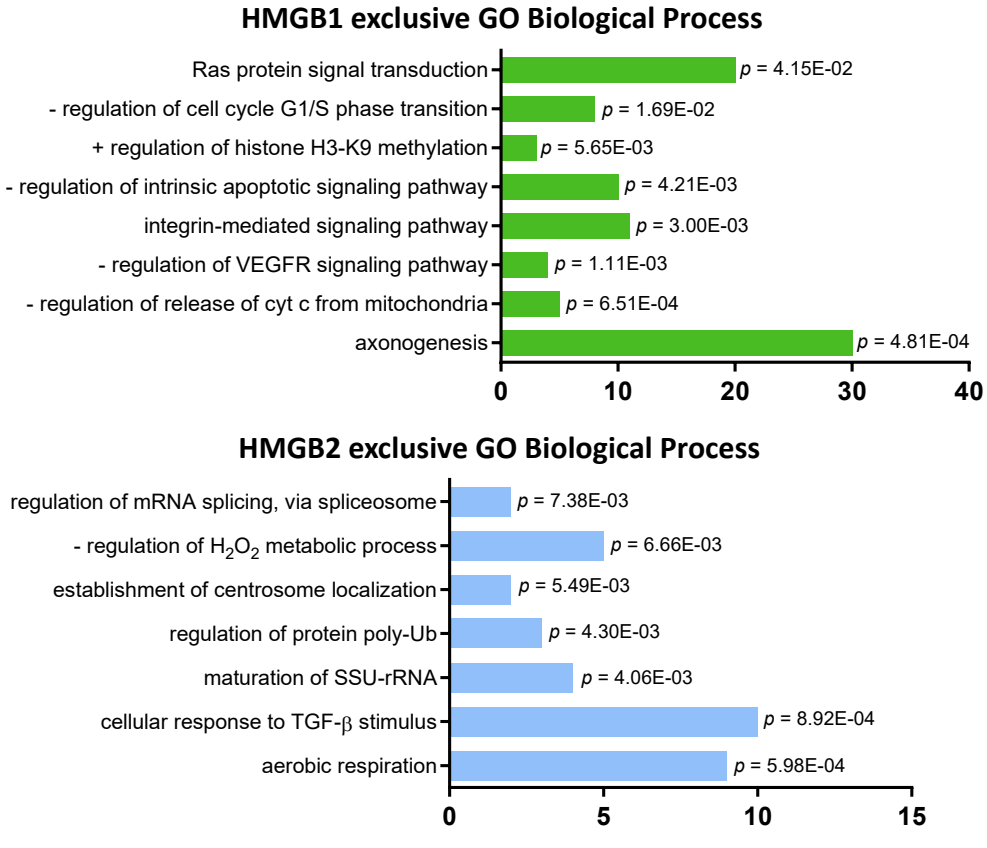

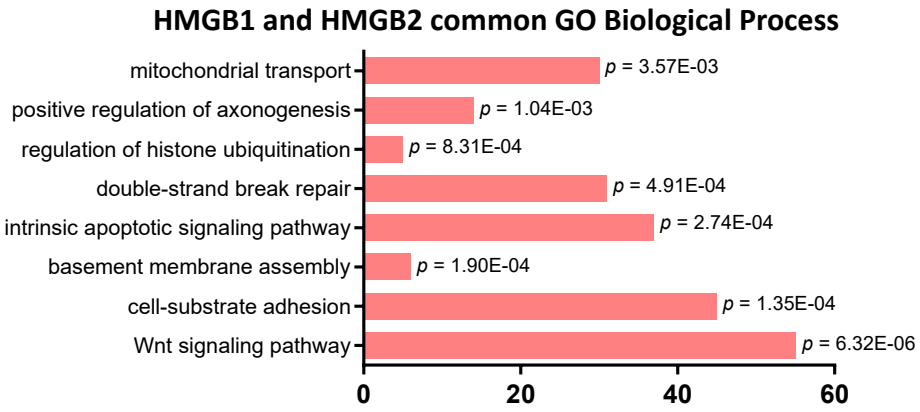

Figure 4.- Gene ontology enrichment analysis of predicted mRNA binding partners. Overrepresented gene ontology terms exclusive for HMGB1 (**top**), exclusive for HMGB2 (**middle**), and common for HMGB1 and HMGB2 (**bottom**). Values at the end of the bars correspond to the *p*-value. SSU, small subunit; Ub, ubiquitination.

Since the list with mRNAs common for HMGB1 and HMGB2 contains more elements, the enriched GO terms have a higher statistical significance.

Among the mRNAs that bind only to HMGB1 or those that bind to HMGB1 and HMGB2, in the GO-term analysis, we find common descriptors like “axonogenesis” and “positive regulation of axonogenesis”, which implies a cytoskeleton rearrangement also necessary in cancerous cells migration (Grelet et al., 2022; Yang et al., 2019), and terms such as “negative regulation of cytochrome c release” and “negative regulation of intrinsic apoptotic signaling pathway”, which are related with the avoidance of apoptosis, one of the cancer hallmarks (Hanahan & Weinberg, 2011). In the HMGB1-exclusive terms, we also find “G1/S cell cycle transition” in which a cell can transition to G0 and become arrested, leading to senescence, quiescence, or dormancy states that represent a cause of tumor relapse (Triana-Martínez et al., 2020). Several cellular signaling pathways commonly deregulated in cancer (Hanahan & Weinberg, 2011) are significant in the GO-term analysis; VEGFR, Ras, and integrin are found among RNAs binding to HMGB1, TGF-β response among those binding to HMGB2. Finally, HMGB1 and HMGB2 common terms include Wnt signaling pathway, DNA-repair, and terms related to the extracellular matrix, such as “basement membrane assembly” and “cell-substrate adhesion” also associated with cancer (Torgovnick & Schumacher, 2015; Z. Yuan et al., 2023; T. Zhan et al., 2017). In this analysis, we also find terms related to the regulation

of gene expression and metabolism, which are mechanisms causing functional or disease-related cellular changes. In the HMGB2-exclusive terms, we find RNA “small subunit maturation” and “splicing”, which are related to RNA processing, a previously described function for HMGB proteins (Bianco & Mohr, 2019). Histone post-translational modifications related terms are also found, corresponding to methylation in the HMGB1-exclusive subgroup, or ubiquitination among HMGB1 and HMGB2 common terms, but both affect the transcriptional regulation (Kouzarides, 2007). In the HMGB2-exclusive subgroup we find “reactive oxygen species metabolism”, “aerobic respiration” and “energy production”, all altered in the malignant transformation of cells (J. Kim et al., 2016).

Finally, we wanted to emphasize the lncRNAs with higher interaction probability with HMGB1 and/or HMGB2. Thus, we listed the ones with the highest z-score for each category in Table 1.

Table 1.- Top 25 z-score lncRNAs predicted to interact with HMGB1, HMGB2, or both. Z-scores from the middle column that are separated by a dash correspond to HMGB1 and HMGB2, respectively.

HMGB1 exclusive lncRNAs		**HMGB1 and HMGB2 common lncRNAs**		**HMGB2 exclusive lncRNAs**	
Gene symbol	**z-score**	**Gene symbol**	**z-score**	**Gene symbol**	**z-score**
ENSG00000255046	1.74	*DSCAM-AS1*	4.32 - 3.6	*LINC01122*	1.33
LINC03057	1.67	*LINC00621*	4.05 - 3	*GS1-24F4.2*	1.26
ODC1-DT	1.66	*ENSG00000261242*	3.68 - 3.03	*TOX-DT*	1.26
LINC01088	1.62	*CTC-338M12.4*	3.46 - 2.93	*LINC00211*	1.24
TTC39C-AS1	1.6	*ZNF503-AS2*	3.35 - 2.31	*ENSG00000230090*	1.24
ENSG00000256540	1.59	*MIR762HG*	3.27 - 1.97	*LINC02816*	1.23
ENSG00000229422	1.47	*ENSG00000254187*	3.21 - 2.3	*ENSG00000257711*	1.23
ENSG00000226445	1.45	*DENND5B-AS1*	3.02 - 2.84	*AGK-DT*	1.18
ENSG00000259011	1.4	*ENSG00000224905*	2.97 - 2.77	*LINC01293*	1.18
FKBP14-AS1	1.39	*LNCOG*	2.97 - 2.09	*RALY-AS1*	1.17
LINC02882	1.38	*TLE1-DT*	2.92 - 2.69	*LINC00051*	1.16
SGO1-AS1	1.38	*NCAM1-AS1*	2.91 - 2.15	*PRR29-AS1*	1.14
TMEM26-AS1	1.38	*NR2F2-AS1*	2.9 - 2.52	*ENSG00000254551*	1.14
PDE7B-AS1	1.37	*GAS5*	2.88 - 2.35	*ENSG00000282907*	1.13
ENSG00000227946	1.37	*OIP5-AS1*	2.87 - 2.78	*SPRY4-AS1*	1.1
CCDC144NL-AS1	1.35	*STEAP2-AS1*	2.86 - 2.45	*TNFRSF10A-DT*	1.1
C1QTNF7-AS1	1.33	*LRRC52-AS1*	2.86 - 2.3	*LINC00970*	1.08
ENSG00000232748	1.33	*ENSG00000248223*	2.84 - 2.22	*LINC02609*	1.08
LINC01770	1.32	*LINC01280*	2.82 - 2.58	*RFX3-AS1*	1.08
MYCNOS	1.32	*LARGE-AS1*	2.73 - 2.5	*ENSG00000237863*	1.08
ZBED5-AS1	1.32	*LINC00922*	2.7 - 2.25	*IKBKB-DT*	1.07
LINC00837	1.31	*ENSG00000232692*	2.69 - 2.24	*ENSG00000254528*	1.07
LINC02444	1.31	*LINC-PINT*	2.67 - 1.89	*ENSG00000241596*	1.07
LINC01018	1.3	*ENSG00000245261*	2.66 - 1.6	*ZCCHC14-DT*	1.06
ENSG00000229953	1.3	*ENSG00000265618*	2.63 - 2.27	*LINC01322*	1.04

We can draw from this *in silico* study that, despite the sequence similarities that occur between HMGB1 and HMGB2 proteins, the catRAPID algorithm is able to identify specific associations of different lncRNAs to each of them. However, only two, which are common to HMGB1 and HMGB2 (*DSCAM-AS1* and *LINC00621*) reach a z-score of 4 which would be desirable to select strong predicted interactions. The fact that the z-scores for interactions of the lncRNAs which are significative for HMGB1 and HMGB2 are two- or three-fold higher compared to the ones that are exclusive for each protein might indicate that the amino acids that bind to RNA are those that are evolutionarily conserved between them. Setting the threshold of z-score = 3, six lncRNA common to HMGB1 and HMGB2 remain, namely, *DSCAM-AS1*, *LINC00621*, *ENSG00000261242*, *CTC-338M12.4*, *ZNF503-AS2*, *MIR762HG*, of which there is only information in the literature for *DSCAM-AS1* and *LINC00621*.

DSCAM-AS1 is transcriptionally activated by estrogen and progesterone receptors and mediates tumor progression and tamoxifen resistance through the interaction with hnRNPL (Niknafs et al., 2016) to regulate alternative exon splicing and 3′-end usage (Elhasnaoui et al., 2020), and miR-130a/ESR1 axis (Yadav et al., 2022) in breast cancer. It is also involved in other cancer types such as non-small cell lung cancer, colorectal cancer, osteosarcoma, hepatocellular carcinoma, melanoma, and cervical cancer (Ghafouri-Fard et al., 2021).

LINC00621, which is activated by the FOXA2 transcription factor, is an important tumor-suppressive lncRNA in the squamous subtype of pancreatic ductal adenocarcinoma that is involved in maintaining a pro-epithelial state associated with favorable disease outcome (Dorn et al., 2020). On the contrary, FOXA1-activated *LINC00621* acts as an oncogene in lung adenocarcinoma by activating the TGF-β signaling pathway (Wei et al., 2023).

Additionally, some of these targets were found to be deregulated in the EOC patient studies from the diagnostic category (cancer vs. healthy) analyzed in Chapter 1

(shown in Chapter 1 Tables 1 and 2). From the HMGB1-exclusive lncRNAs, *LINC01770*, *MYCNOS*, and *LINC03057* were upregulated in 8 (GSE18520, GSE52037, GSE54388, GSE38666, GSE14407, GSE40595, GEPIA, and GSE190688), 5 (GSE14407, GSE38666, GSE137238, GSE52037, and GSE190688), and 3 (GSE119054, GEPIA, and GSE190688) studies, respectively, whereas *LINC01018* was downregulated in 4 studies (GSE29450, GEPIA, (H. Wang et al., 2016), and GSE119054). From the HMGB1 and HMGB2 common lncRNAs, *NR2F2-AS1* was downregulated in 4 studies (GEPIA, (H. Wang et al., 2016), GSE119054, and GSE190688), and *LNCOG* was upregulated in metastasis (Chapter 1 Table 5). From the HMGB2-exclusive lncRNAs, *TNFRSF10A-DT* and *RALY-AS1* are upregulated in 5 ((H. Wang et al., 2016), GSE137238, GEPIA, GSE119054, and GSE10971) and 4 (GSE18520, GSE40595, GSE38666, and (H. Wang et al., 2016)) studies, respectively, whereas *IRS4-AS1* is downregulated in 3 studies (GSE119054, GEPIA, and (H. Wang et al., 2016)).

RIP-Seq analysis of HMGB1 and HMGB2 RNA interacting partners

In an attempt to experimentally determine the RNA interactome of HMGB1 and HMGB2, we performed native RNA immunoprecipitation coupled with RNA Sequencing, also known as RIP-Seq (Zhao et al., 2010). This technique enables the detection of direct and indirect binders of a protein at a transcriptome-wide scale, as was previously commented in the introduction. We included in the experimental design of RIP analysis two EOC cell lines, PEO1 and SKOV-3, as they are, respectively, representative models of the high-grade serous (Beaufort et al., 2014) and clear cell EOC (Barnes et al., 2021), the first and second most frequent histological subtypes of EOC. However, as described below, from the performed RIP studies only the results from the PEO1 experiments had enough quality for performing further analysis.

- RIP-Seq in PEO1 cells

In the RIP-Seq experiments carried out in PEO1 cells, we first performed a series of immunoprecipitations (IPs) to set up conditions that were monitored by western blot, comparing the signals from inputs and IPs (Figure 5). In each biological replicate, one IP was carried out with HMGB1 antibody, another with HMGB2 antibody, and a third one with isotype IgG as a non-targeting, negative control. In most of the IPs, we confirmed the recovery of the protein target although with different efficiencies (Figure 5).

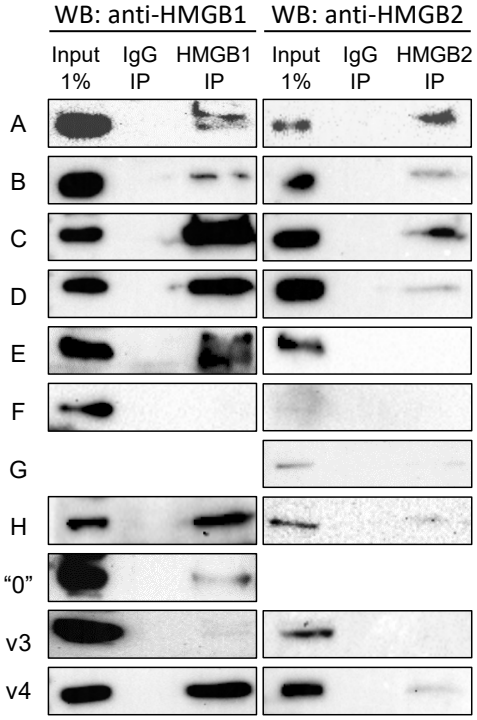

Figure 5.- Efficiency of HMGB1 and HMGB2 immunoprecipitation in PEO1 checked by western blot. A-H, 0, v3, and v4, represent the different immunoprecipitation attempts. Input consists of 1 % volume of protein extract; HMGB1 IP, HMGB2 IP, and IgG IP represent the 20 % eluate from beads after IP and washes.

After extraction of RNA from the IPs, RNA and contaminant DNA concentrations were measured using a Qubit 3.0 fluorometer with High Sensitivity kits (Data are available in Supplementary Materials Table S13). We also verified RNA quality with 2100 Bioanalyzer (Agilent) capillary electrophoresis, whose profiles can be found in Supplementary Materials Figure S2.

Based on the western blot results, RNA profiles, and concentration of all the samples, we chose the ones indicated in Table 2 to prepare cDNA libraries for RNA sequencing.

Table 2. Sample selection of RNAs extracted from IPs for cDNA libraries preparation and RNA-Sequencing.

	IgG IP	HMGB1 IP	HMGB2 IP
A	X	X	X
B		X	
C			X
D	X	X	
E			
F			
G			X
H	X	X	X
“0”	X		
v3			
v4			

Strand-specific library preparation and RNA sequencing conditions are described in the Material and Methods section. RNA-Seq was carried out after rRNA depletion also as indicated in the Material and Methods section. Generated fastq files were trimmed, QC filtered, mapped to the human genome (hg38), and quantified using STAR. Mapping summary statistics can be found in Supplementary Materials Table S14.

We used the STAR-generated counts as input for DESeq2 (Love et al., 2014) to obtain the differentially expressed genes (DEG) between the specific IPs (HMGB1 or HMGB2) *versus* the IgG control. A first discriminant analysis according to the transcriptomic profile of the 4 replicates showed some disagreements between different experimental conditions and sample grouping (data not shown). Because of this, we excluded sequencing data of IgG IP *H* and HMGB1 IP *D* to perform DEG analysis of HMGB1 *versus* IgG and also excluded IgG IP *H* and HMGB2 IP *H* to perform DEG analysis of HMGB2 *versus* IgG. Results of the discriminant analysis obtained after these exclusions show a closer grouping of samples within each condition and better separation between the two conditions (Figure 6).

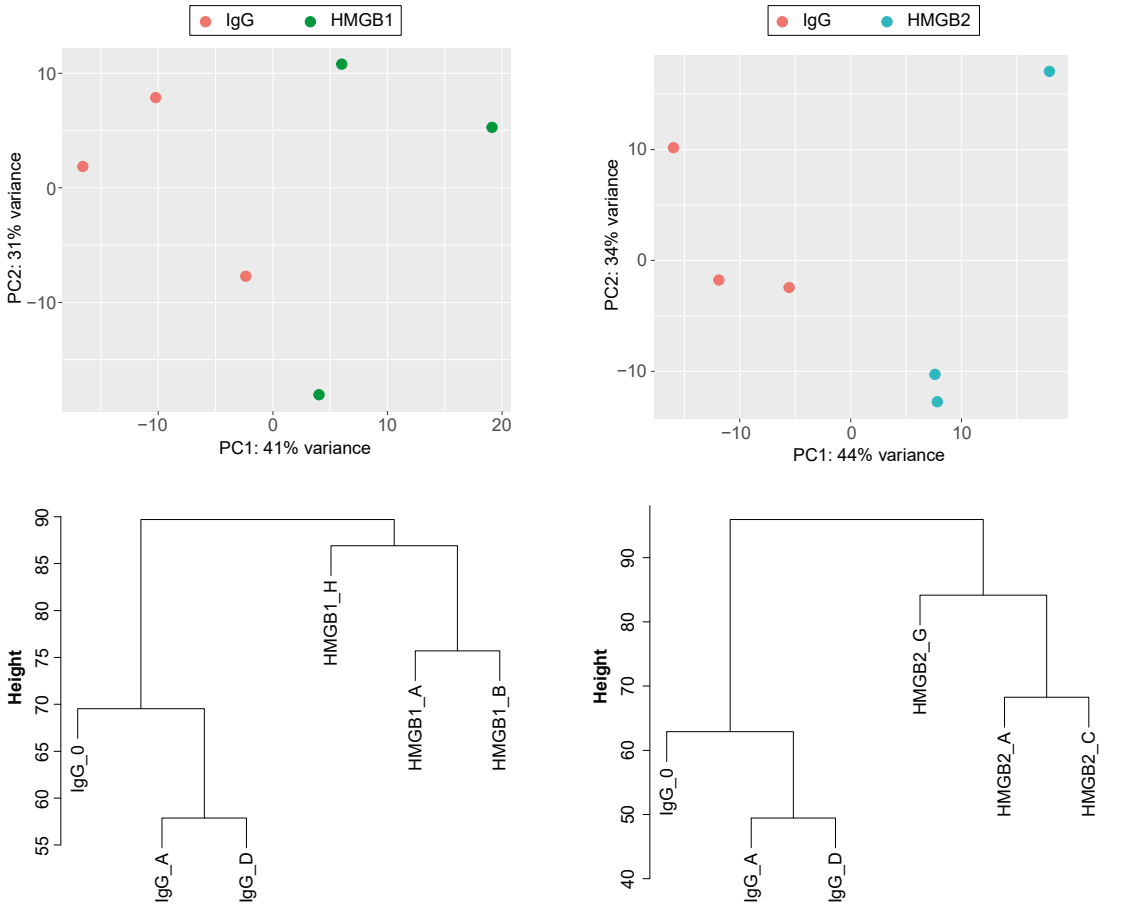

Figure 6.- Discriminant analysis of PEO1 RIP-Seq samples. Scatter plot from principal component analysis (**up**) and dendrogram from clustering analysis (**down**) for HMGB1 *versus* IgG (**left**) and HMGB2 *versus* IgG (**right**).

DESeq2 yielded 910 differentially expressed (enriched) RNAs for HMGB1 and 1,456 for HMGB2 when setting the *p*-value < 0.05 and Log_2 (Fold change) > 0.585 (equivalent to Fold change > 1.5). The full detailed lists are contained in Supplementary Materials Table S15. As shown in Figure 7, the vast majority (more than 90%) of the significantly enriched RNAs belong to protein-coding genes, whereas pseudogenes, followed by lncRNAs, and other biotypes represent a small proportion. Specifically, lncRNAs consist of 2% of the enriched genes, having 17 and 32 lncRNAs in HMGB1 and HMGB2 conditions, respectively.

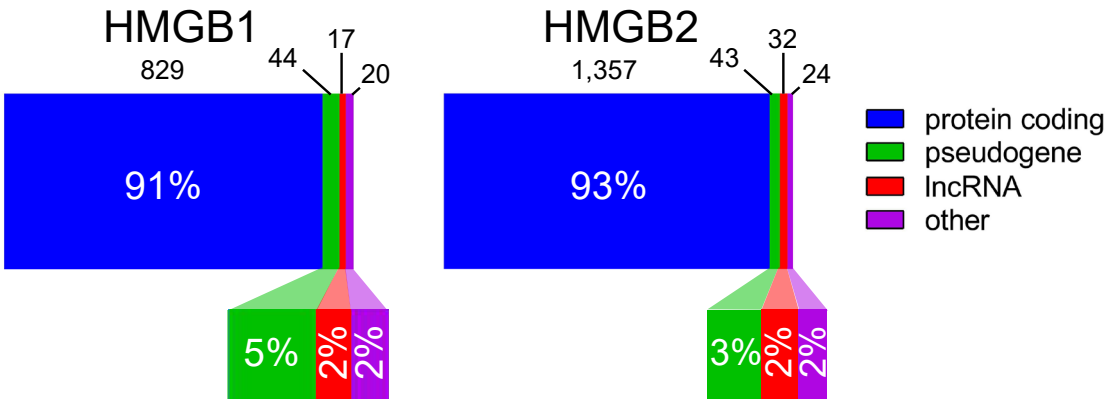

Figure 7.- RIP-Seq Ensembl gene biotype frequencies of the selected genes from enriched genes. The percentages inside the squares and the numbers above the squares represent the relative and the absolute frequency for each gene biotype, respectively.

The overlap between HMGB1 and HMGB2 lists identified 643 RNA targets that are shared between HMGB1 and HMGB2, of which 596 are mRNAs, 22 are pseudogenes, and 9 are lncRNAs (Figure 8).

Only some of these identified lncRNAs (Figure 8D) have been reported in the literature to be implicated in cancer. Specifically, *LINC01963* is enriched in HMGB1 but not in HMGB2. *LINC01963* is downregulated and inhibits the progression of pancreatic carcinoma by targeting miR-641/TMEFF2 (K. Li et al., 2020), however, it promotes chemoresistance to docetaxel by targeting miR-216b-5p/TrkB axis in prostate cancer (Xing et al., 2022).

Then *LINC00205*, *LINC00689*, *LINC00294*, *PSMG3-AS1*, *MIR663AHG*, *PINK1-AS*, *FAM225A*, and *FAM225B* are enriched in HMGB2 but not in HMGB1. *LINC00205* promotes lung cancer by recruiting FUS and stabilizing the mRNA of *CSDE1* in the cytoplasm (Xie & Guo, 2020); hepatoblastoma by regulating miR-154-3p/ROCK1 axis (G. Liu et al., 2022); gastric cancer by sponging miR-26a and upregulating its downstream targets HMGA2, EZH2, and USP15 (Huangfu et al., 2022); and hepatocellular carcinoma via miR-184/EPHX1 axis (Long et al., 2020) and miR-122-5p (L. Zhang, Wang, et al., 2019). *LINC00689* is upregulated and enhances proliferation and metastasis glioma by regulating miR-338-3p/PKM2 axis (X. Liu et al., 2019); prostate cancer via miR-496/CTNNB1 to activate Wnt pathway (L. Meng et al., 2020); triple-negative breast cancer through the miR-142-3p/USP6NL axis (T. Ma et al., 2020); and

gastric cancer via miR-526b-3p/ADAM9 axis (G. Yin et al., 2020). *LINC00294* is downregulated and inhibits glioma via miR-1278/NEFM (X. Zhou et al., 2020) and miR-21-5p/CASKIN1/cAMP (Dong et al., 2021) axes; and colorectal cancer through regulating miR-620/MKRN2 axis (Qi et al., 2023). However, it promotes cervical cancer, in which is induced by GRP78 (Qiu et al., 2020). *PSMG3-AS1* is upregulated in glioma and favors temozolomide resistance through c-Myc stabilization in the nucleus (L. Zhou et al., 2022). It is also upregulated in prostate cancer and downregulates miR-106b at transcriptional level by increasing DNA methylation (L. Zhang et al., 2023). *MIR663AHG* acts as a tumor suppressor in colon cancer through the sponging of the miRNA that hosts, miR663a and its precursor pre-miR663a, preventing the degradation of miR663a mRNA targets (H. Yuan et al., 2023). *PINK1-AS*, which is activated by MLK-1, is upregulated and promotes hepatocellular carcinoma by regulating the miR-34a-5p/ALDOA, and thus, glycolysis (J. Wang, Zhang, et al., 2022). *FAM225A* is upregulated and modulates the axis miR-326/PADI2 to promote proliferation and metastasis in gastric cancer (X. Ma et al., 2022). It drives nasopharyngeal carcinoma by two different described mechanisms: sponging miR-590-3p/miR-1275 leading to an upregulation of ITGB3 that triggers FAK/PI3K/Akt signaling (Z.-Q. Zheng et al., 2019), and stabilizing FUS to *CENP-N* mRNA to activate cGAS-STING signaling (Han et al., 2022). *FAM225A* promotes esophageal squamous cell carcinoma (Zhu et al., 2021), colorectal cancer (X. Zhang et al., 2020), and hepatocarcinoma (Y.-T. Liu et al., 2020) by regulating miR-197-5p/NONO, miR-613/NOTCH3, and miR-130a-5p/CCNG1 axes, respectively. *FAM225B* is correlated with poor prognosis in recurrent glioblastoma patients (J. Li et al., 2020) and promotes proliferation and metastasis in nasopharyngeal carcinoma by modulating the miR-613/CCND2 axis (Dai et al., 2022).

PRECSIT, also known as *LINC00346*, and *ZNF710-AS1* were previously related to cancer and are enriched in both HMGB1 and HMGB2 RIPs. *PRECSIT* is a p53-repressed lncRNA that activates STAT3 signaling and is upregulated in cutaneous

squamous cell carcinoma (Piipponen et al., 2020) and hepatocellular carcinoma (Y. Yin et al., 2020). In hepatocellular carcinoma, it was described to regulate the miR-542-3p/WDR18 axis to activate the Wnt/β-catenin pathway too (N. Zhang & Chen, 2020). It yields gemcitabine chemoresistance in pancreatic cancer by regulating miR-188-3p/BRD4 axis (Shi et al., 2019). *ZNF710-AS1* promotes cell proliferation and inhibits apoptosis of clear cell renal cell carcinoma by regulating in *cis* the expression of its sense transcript, *ZNF710* (G. Li et al., 2020).

Besides, when comparing with the studies of differential expression between EOC patients and healthy controls (diagnostic category in Chapter 1), we found that *ENSG00000250899* is upregulated in three studies (GSE119054, GEPIA, and GSE190688) and *PSMG3-AS1* is downregulated in three studies (GSE14407, GEPIA, and GSE10971), both shown in Chapter 1 Tables 1 and 2.

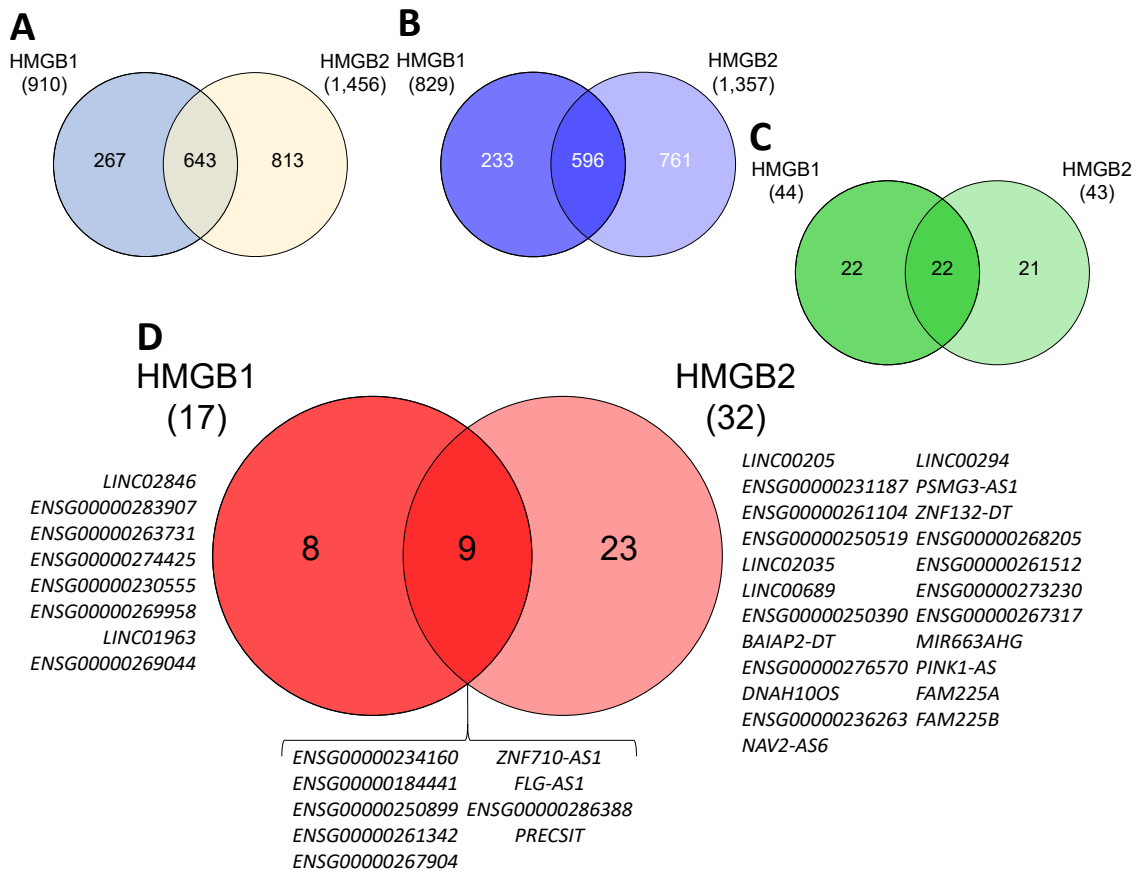

Figure 8.- Intersection between HMGB1 and HMGB2 RNAs obtained from PEO1 RIP-Seq analysis. Overlap of the full list (**A**), protein-coding genes (**B**), pseudogenes (**C**), and lncRNAs (**D**).

To gain knowledge on the processes related to the enriched mRNAs, we also performed three different gene ontology analyses from the genes in Figure 8B, including those enriched in HMGB1 but not in HMGB2 (233), in HMGB2 but not in HMGB1 (761), and those in common for the two proteins (596). The resulting GO terms are depicted in Figure 9.

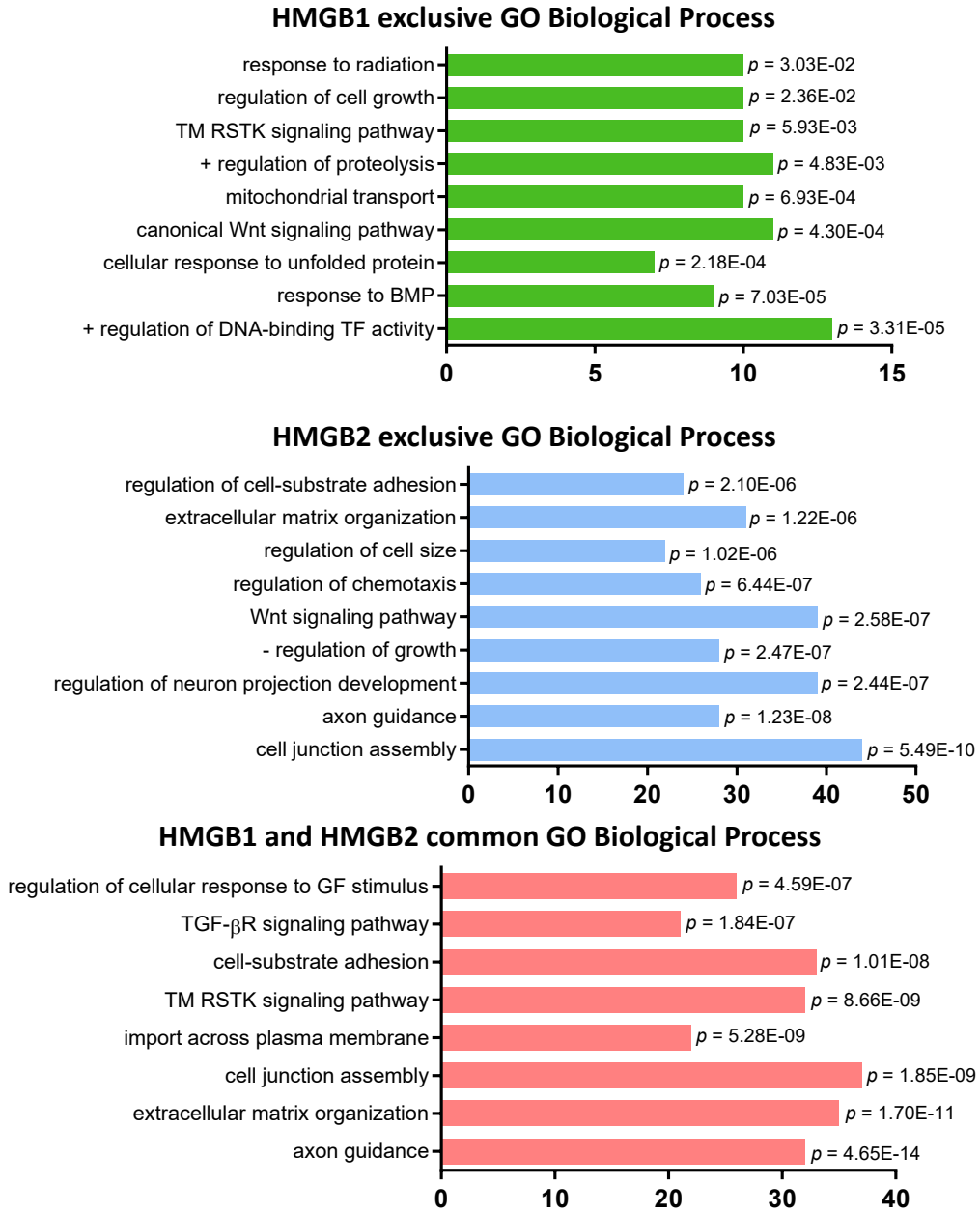

Figure 9.- Gene ontology enrichment analysis of PEO1 RIP-Seq enriched mRNA. Overrepresented gene ontology terms exclusive for HMGB1 (**top**), exclusive for HMGB2 (**middle**), and common for HMGB1 and HMGB2 (**bottom**). Values at the end of the bars correspond to the *p*-value.

Three signaling pathways relevant to cancer biology are significantly represented in the GO analysis, namely, Wnt, receptor tyrosine kinase, and TGF-β family. Also, extracellular matrix and cell-substrate adhesion are present, as well as “axon guidance”, “regulation of neuron projection development”, or “regulation of chemotaxis”, which are potentially related to invasion and EMT processes. In HMGB1-exclusive, DNA-binding activity is present, having a direct relation with the DNA chaperone, a function by which HMGB1 is mainly described in the literature (Osmanov et al., 2013). Additionally, there are terms involved in protein metabolism, including protein unfolding and degradation. There are also terms related to cell growth and proliferation, such as “regulation of cell size”, “regulation of cell growth”, and “regulation of cellular response to growth factor stimulus”, all of them intimately implicated in tumor growth. Finally, “response to radiation” could be related to radiotherapy resistance (L. Zhang, Shi, et al., 2019). Since the list with mRNAs exclusive for HMGB1 contains fewer elements (233) than the other two lists (596 and 761), it has less information and therefore the enriched GO terms have a lower statistical significance, i.e., higher *p*-value.

Finally, below are represented the coverage tracks of 10 lncRNAs (Figure 10) and 10 mRNAs (Figure 11) with some of the highest number of reads and statistical significance between the specific and unspecific IPs from the PEO1 RIP-Seq experiment, namely, *ENSG00000234160*, *ENSG00000250899*, *ENSG00000263731*, *LINC01963*, *PRECSIT*, *BAIAP2-DT*, *LINC00205*, *LINC00294*, *LINC02035*, and *SYT15-AS1*; and *COL4A2*, *IGFBP5*, *LAMB3*, *NOTCH2*, *THBS1*, *LAMA5*, *ITGA3*, *AGRN*, *PLXNB2*, and *CELSR2*.

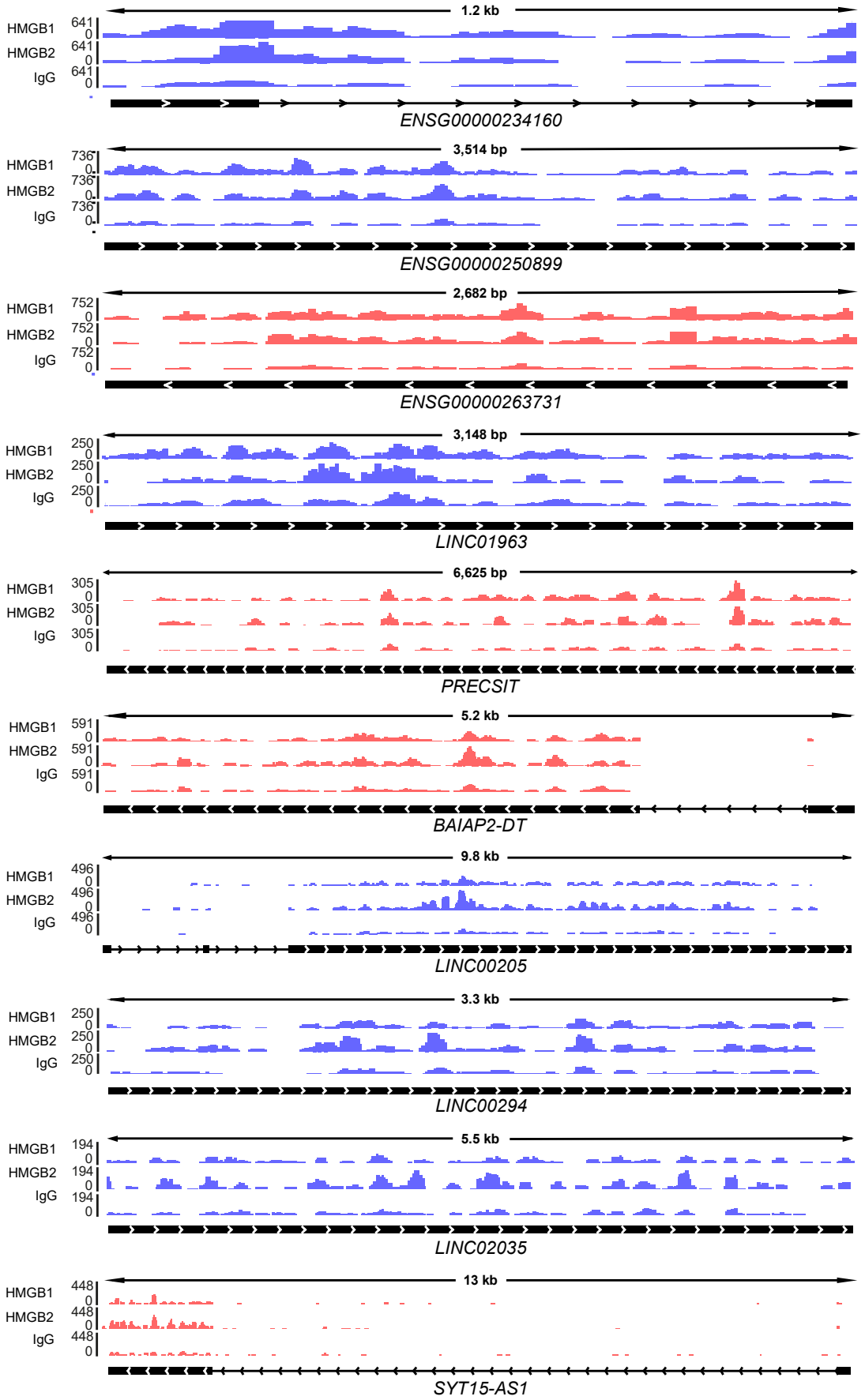

Figure 10.- Example coverage tracks for enriched lncRNAs in HMGB1 and/or HMGB2 IPs in PEO1 RIP-Seq experiment. Blue and red histograms represent merged reads in positive or negative strands, respectively. The numbers on the left side represent the coverage range for each gene.

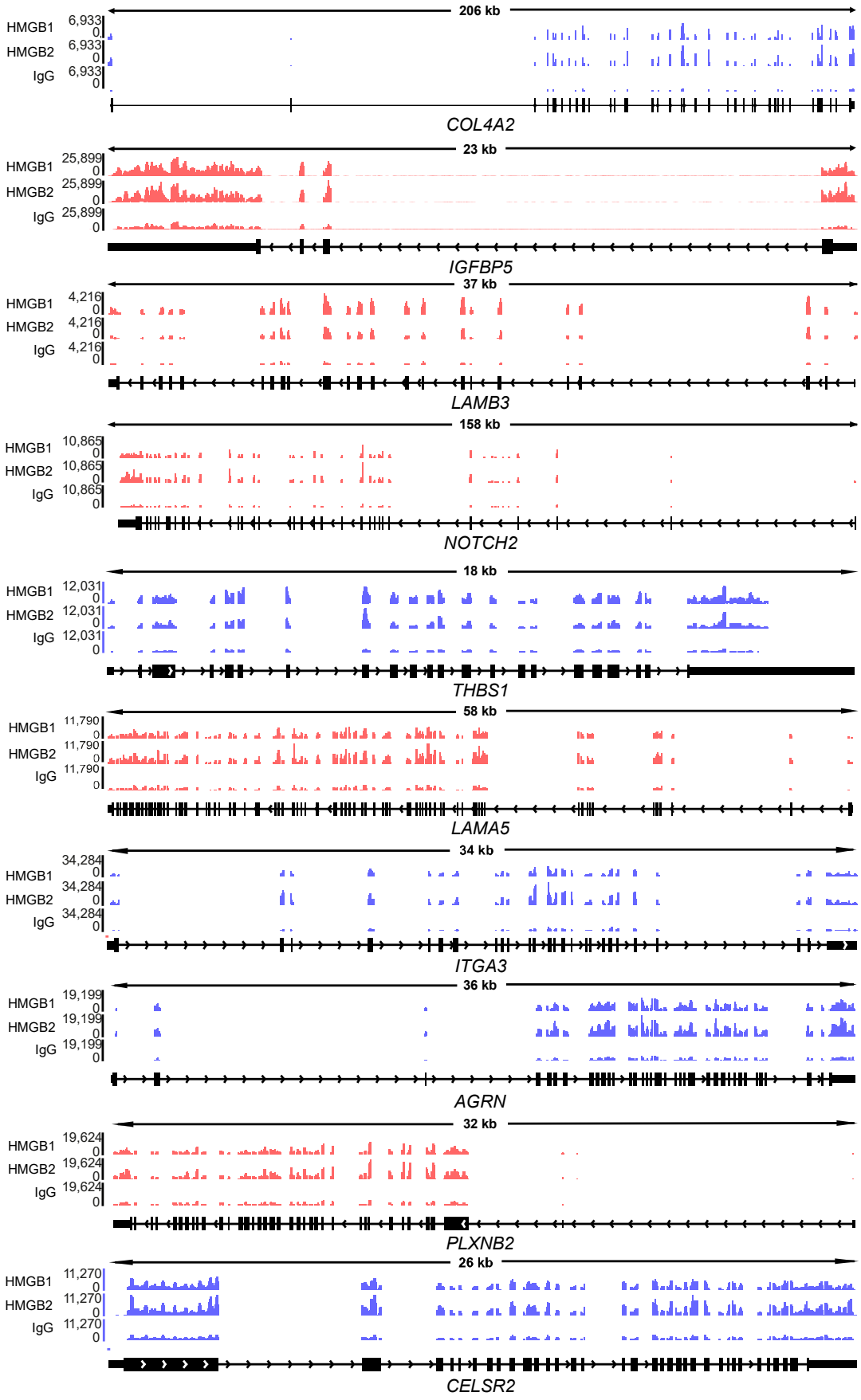

Figure 11.- Example coverage tracks for enriched mRNAs in HMGB1 and/or HMGB2 IPs in PEO1 RIP-Seq experiment. Blue and red histograms represent merged reads in positive or negative strands, respectively. The numbers on the left side represent the coverage range for each gene.

- RIP-Seq in SKOV3 cell line

We carried out the RIP-Seq in the SKOV3 cell line similarly to the previously described PEO1 cell line. A series of IPs were performed, and their efficiency was checked by western blot, as shown in Figure 12.

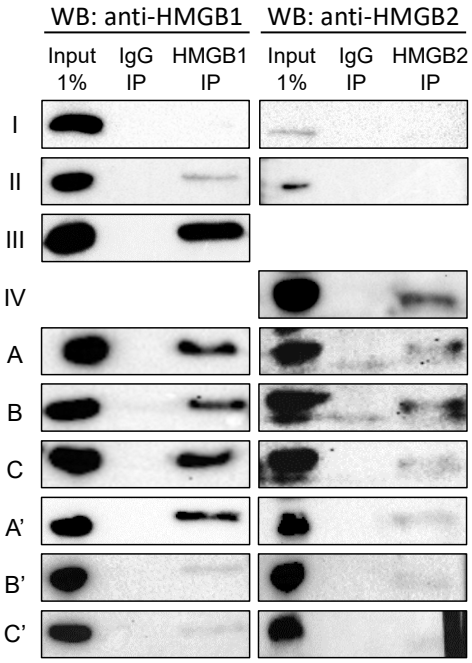

Figure 12.- HMGB1 and HMGB2 immunoprecipitation in SKOV3 efficiency checking by western blot. "30-3-2021"-C' represent the different immunoprecipitation attempts. Input consists of 1 % volume of protein extract; IP H1 and IP H2 (HMGB1 and HMGB2, respectively), as well as IP IgG, represent the 20 % eluate from beads after IP and washes.

RNA quality in all samples and the concentration of the purified RNA and contaminant DNA concentrations in the Inputs were assessed. Detailed information is shown in Supplementary Materials Table S16 and Figure S3, respectively.

Based on the western blot results and RNA profiles and concentration from all the samples, we chose Input, IP IgG, IP HMGB1, and IP HMGB2 from biological replicates *A*, *B*, and *C* to prepare cDNA libraries for RNA sequencing. We added 1 µL of 1:10,000 and 1 µL of 1:1,000 of ERCC RNA Spike-In Mix (4456740, Invitrogen) diluted in water to the IP and Input RNA samples, respectively, before library preparation to normalize and deconvolute all the dilutions and amplifications in the cDNA synthesis and sequencing process. We faced some adverse issues with the library preparation, as the libraries had abnormal size ranges and shapes (more than one peak or relative maximum fragment size), but we went on and sequenced them anyway.

Then, generated fastq files were trimmed, QC filtered, mapped, and quantified to the human genome (hg38) and ERCC92 spike in reference sequences using STAR. Mapping summary statistics can be found in Supplementary Materials Table S17. Unfortunately, all samples presented a very low uniquely mapped read percentage, ranging from 3.5% to 30.7%, except for sample IgG *A* which had 86%, meaning that the number of useful reads was very low. Due to this fact, we did not consider this data for further analysis.

eCLIP analysis of HMGB1 and HMGB2 RNA interacting partners in PEO1 cell line

During a three-month stay in a laboratory abroad funded by EMBO, I performed enhanced crosslinking immunoprecipitation (eCLIP) in the group of Myriam Gorospe (National Institute on Aging, Baltimore, United States of America). This method is based on RIP-Seq with the improvements of increased signal-to-noise ratio and specificity due to UV-crosslinking and harsher washes. Because of time limitations, we only assayed the PEO1 cell line, using the EclipseBIO RBP-eCLIP kit, which is based on previously published methods (Blue et al., 2022; Van Nostrand et al., 2017). The experimental design included two biological replicates, consisting of two immunoprecipitations and two corresponding size-matched inputs, performed independently for HMGB1 and HMGB2. Additionally, an unspecific IgG isotype control was used as a negative control for immunoprecipitation in parallel, but this sample was not taken further for library preparation and deep sequencing.

The protocol is specified in the Materials and Methods section, and some of the checkpoints through it are illustrated below. The first one was the assessment of crosslinked total RNA extracted from a 1% aliquot of the lysates as shown in Figure 13. This is crucial to add the right amount of RNase for fragmentation and obtaining the binding sites. Since the RNA was sonicated, the RNA integrity number (RIN) is not considered in this case.

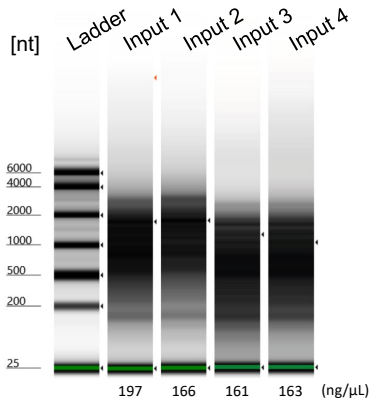

Figure 13.- RNA integrity and concentration assessment. Inputs 1 and 2 correspond to the lysate used for HMGB1 IPs, and inputs 3 and 4 to the lysate used for HMGB2 IPs.

The second checkpoint consisted in evaluating the efficiency of the IPs at protein and RNA levels by comparing the signal from the eluates of the specific and unspecific antibodies. For protein, we did a regular western blot, and for RNA, we did a northern blot probing the membrane with horseradish peroxidase-coupled streptavidin that binds to the biotinylated RNA, obtained in a previous step of the protocol. The result of these two blots is depicted in Figure 11. We cut the lane of each IP from 25 kDa, which corresponds to the molecular weight of HMGB1 and HMGB2, to 100 kDa (dotted square in Figure 14) as indicated in the protocol to purify RNA and continue with the next steps.

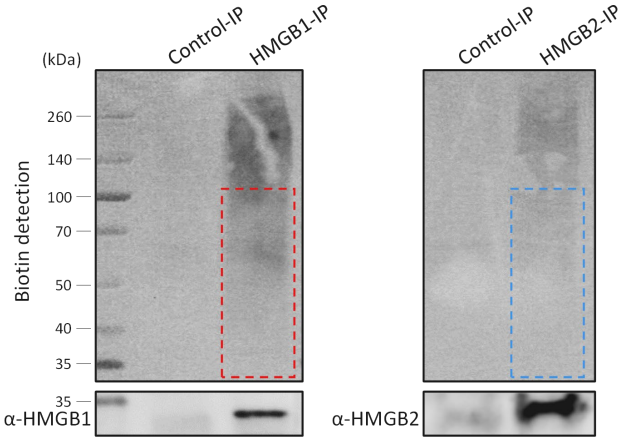

Figure 14.- Immunoprecipitation in PEO1 efficiency checking. The upper part represents the northern blot, and the lower part represents the western blot. The dotted squares represent the part of the membrane used to continue with the protocol.

The third checkpoint comprised quantification by qPCR of the amount of cDNA of the IPs and the Input (a 1:100 dilution for the Input according to the manufacturer's protocol) libraries to adjust the extra cycles of PCR performed for the index addition and minimize the unnecessary duplication of sequences, leaving more space (reads) for less abundant fragments. The results of this qPCR, together with the corresponding cycles are collected in Table 3.

Table 3.- Determination of index-addition PCR extra cycles.

	Sample	*Average Ct*	*Extra cycles*	*Total cycles*
HMGB1	Input 1 1:100	10	1	7
	Input 2 1:100	10	1	7
	IP 1	17	8	14
	IP 2	17	8	14
HMGB2	Input 1 1:100	11	2	8
	Input 2 1:100	11	2	8
	IP 1	16	7	13
	IP 2	17	8	14

The fourth and last checkpoint was the library purification by agarose gel rescue and assessment by capillary electrophoresis, depicted in Figure 15. The libraries were cut from 150 to 350 nucleotide sizes.

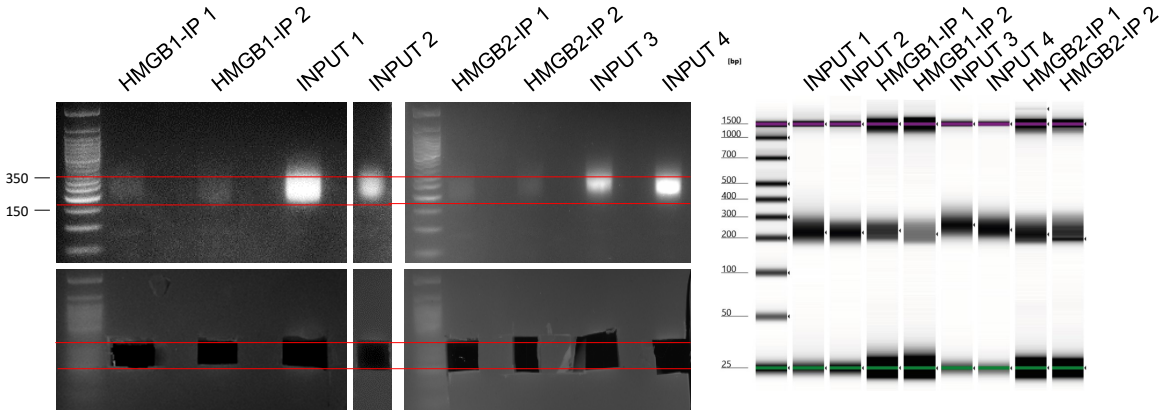

Figure 15.- Gel electrophoresis of the sequencing libraries. Agarose gel before and after cutting the band corresponding to the library size (left). Image of capillary electrophoresis after gel rescue and purification (right).

The analysis of sequencing libraries is described in the Materials and Methods section, and all the sequencing information and intermediate parameters from each step of this analysis can be found in Supplementary Materials Table S18.

Both the HMGB1 and HMGB2 IPs resulted in a lower-than-expected read number, with the main loss of reads coming from high mapping to repetitive element regions and an elevated duplication rate indicating low library complexity. However, this fact was not an obstacle to the further analysis of the experiment. One of these repetitive elements that is worth noting is 18S ribosomal RNA, since there is an enrichment in the IPs compared to the Input, as depicted in Table 4. This result matches the previous proteomic-based association of HMGB1 and HMGB2 with ribosome biogenesis proteins (Barreiro-Alonso et al., 2021).

Table 4.- 18S ribosomal RNA mapping statistics in the eCLIP experiment. RPM, reads per million mapped reads.

RNA18S	IP RPM	Input RPM	Fold Change
HMGB1 Rep1	254,683.926	159,333.183	1.598
HMGB1 Rep2	245,722.856	165,392.775	1.486
HMGB2 Rep1	205,197.758	132,191.158	1.552
HMGB2 Rep2	203,430.936	138,216.154	1.472

Peak calling analysis using CLIPper yielded 4,394 and 1,857 peaks in HMGB1 replicates while HMGB2 replicates generated 1,118 and 2,108 peaks, respectively, when setting Log_2 (fold change) ≥ 0.585 and *p*-value ≤ 0.05 as cutoff values. Table 4 shows the statistics about the identified peaks and the biotypes concerning the bound RNAs. All the identified peaks for HMGB1 and HMGB2 are listed in Supplementary Materials Table S19. From all the identified peaks, we kept those that are located within one gene only, represented in Table 5 by “unique target”, the ones located in regions from two or three different genes simultaneously (“2 overlapping” or “3 overlapping” in Table 4) were not considered for further analysis, as shown in Table 5.

Table 5.- Summary of the peak calling analysis from each eCLIP replicate for HMGB1 and HMGB2.

		HMGB1 Rep1	HMGB1 Rep2	HMGB2 Rep1	HMGB2 Rep2
Peaks	Total	4,394	1,857	1,118	2,108
	Unique target	4,272	1,814	1,072	2,052
	2 overlapping	114	43	40	53
	3 overlapping	8	0	6	3

Then, we calculated the relative proportion of the different gene elements in which the “unique target” peaks are located, plotted in Figure 15. In HMGB1, the most represented feature is coding sequence (CDS), followed by distal intron and noncoding exon (defined in Aspden et al. (2023)), whereas in HMGB2, most of the peaks fall inside distal introns, followed by noncoding exon, and distal intron from noncoding RNAs.

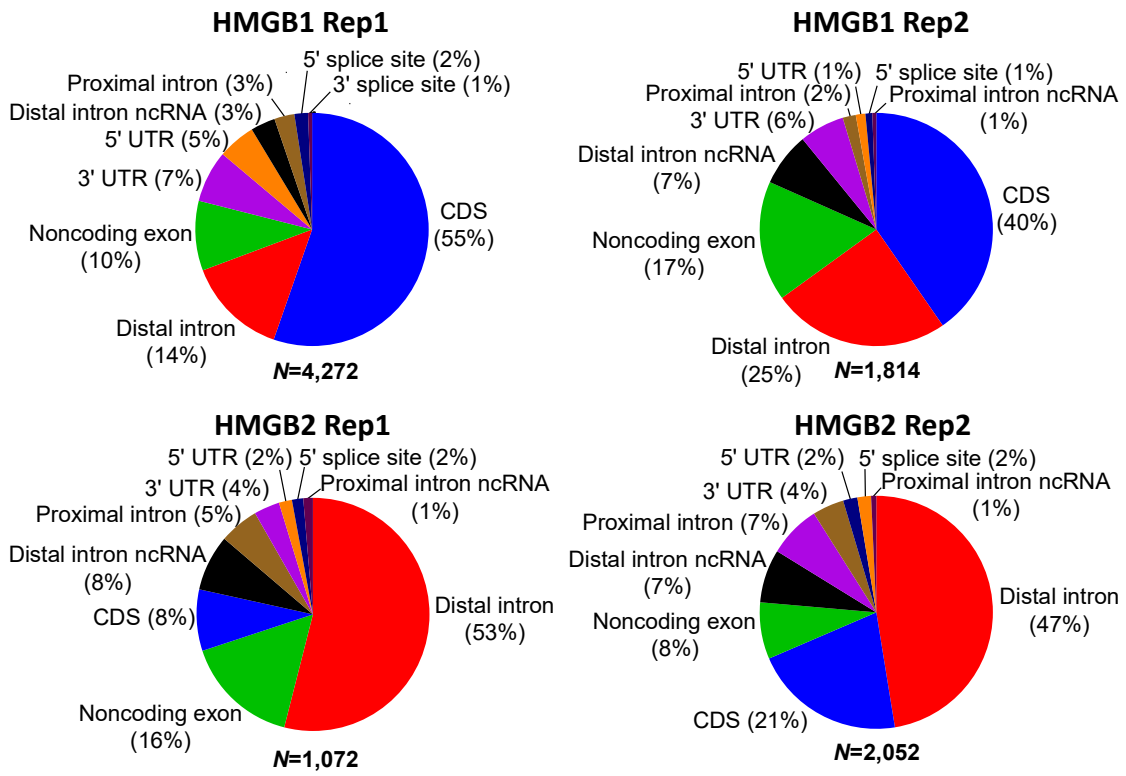

Figure 15.- The relative proportion of gene features. Upper pie charts correspond to HMGB1, and lower pie charts correspond to HMGB2, being the left-side ones replicate 1 and the right-side ones replicate 2. N, number of "unique target" peaks.

Once the unique target peaks were annotated, we obtained 2,361 and 919 genes for HMGB1 replicates and 407 and 821 genes for HMGB2 replicates. We also obtained the number of peaks per gene, sorted the genes in descending order of this value, and plotted them in Figure 16. For HMGB1, *KCNQ10T1*, *MALAT1*, *AHNAK*, *MT-RNR2*, or *PTPRN2*, and for HMGB2, *TRIO*, *MALAT1*, *SNHG14*, *EXT1*, *GPI*, or *ANKRD11*, correspond to the genes with the highest number of peaks in both replicates.

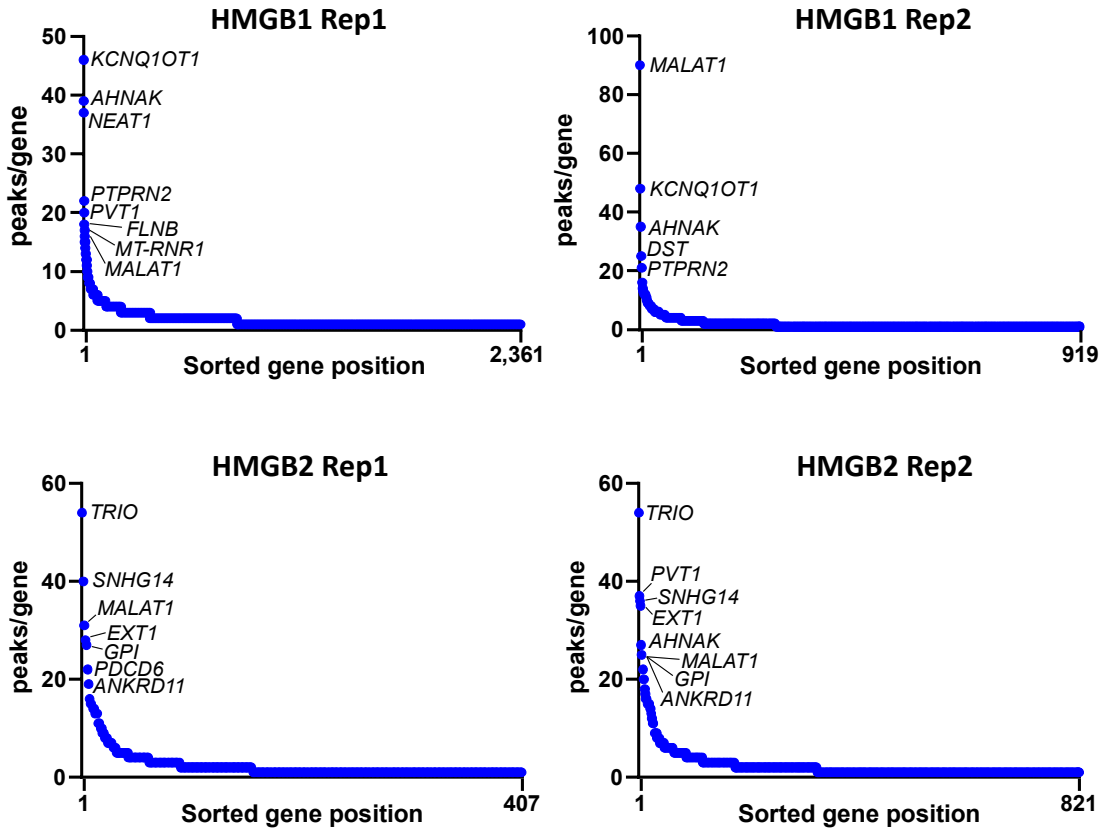

Figure 16.- The number of peaks per gene sorted in descending order.

The overlap between replicates yielded 584 and 285 consistently enriched RNAs for HMGB1 and HMGB2, respectively, as shown in Figure 17.

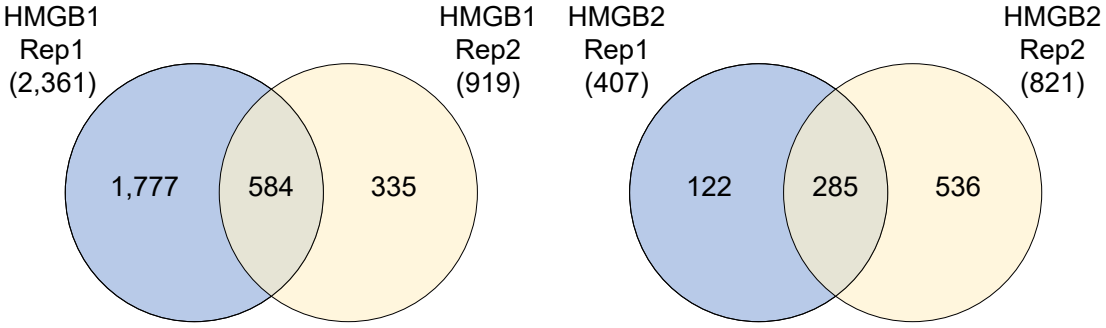

Figure 17.- Overlap between eCLIP replicates for HMGB1 and HMGB2.

The biotype frequencies of the genes in the intersection between replicates are shown in Figure 18. More than 80% of the significantly enriched RNAs belong to protein-coding genes, whereas snoRNAs, lncRNAs, pseudogenes, and other biotypes represent a small proportion. In contrast to catRAPID and RIP-Seq, in eCLIP small nucleolar RNAs are depicted with their own category as they comprise a relevant number of elements.

LncRNAs consisted of 6% and 8% of the enriched genes, having 34 and 18 lncRNAs in HMGB1 and HMGB2 conditions, respectively.

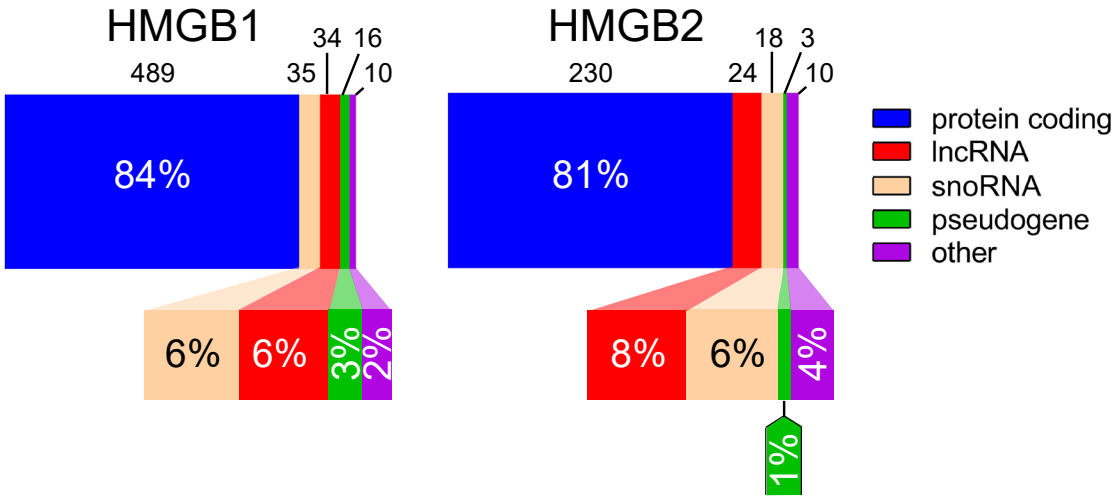

Figure 18.- eCLIP Ensembl gene biotype relative proportion of enriched genes. The numbers above the squares represent the absolute number for each gene biotype.

Again, we overlapped HMGB1 and HMGB2 gene lists and identified 132 RNA targets that are shared between HMGB1 and HMGB2, of which 93 are mRNAs, 16 are snoRNAs, and 16 are lncRNAs, whereas there is no intersection in pseudogenes (Figure 19). Among these lncRNAs, whose intersection and gene symbols are depicted in Figure 15E, many of them have been reported in the literature to be implicated in cancer. Specifically, *MIR31HG*, *HCG18*, *LINC00665*, *DUXAP8*, and *GMDS-DT* are enriched in HMGB1 but not in HMGB2 eCLIP. *MIR31HG* implications in cancer were already described in Chapter 1 (Chang et al., 2021; Mo et al., 2022; Tu et al., 2020; J. Wang, Liu, et al., 2022; R. Wang et al., 2018; S. Zheng et al., 2019) because we found it to be upregulated in metastatic EOC tissues in the meta-analysis (GSE73091 and GSE133296, and shown in Chapter 1 Table 5). *HCG18* has been already described to promote ovarian cancer by regulation of the miR-29a/TRAF4/5 axis and the activation of the NF-κβ pathway (F. Zhang et al., 2022). It regulates the miR-133b/FGFR1 axis to promote laryngeal and hypopharyngeal squamous cell carcinoma (Peng & Ge, 2021). It was found within cholangiocarcinoma to promote proliferation through the miR-424-5p/SOX9 axis to activate the PI3K/Akt pathway (Ni et al., 2023). *LINC00665* modulates breast (Ji et al., 2020), lung (Cong et al., 2019), and colorectal (Nan et al., 2022) cancer

by regulating the miR-379-5p/LIN28B, miR-98/AKR1B10-ERK, and miR-138-5p/SIN3A axes, respectively. *DUXAP8* promotes proliferation and prevents apoptosis by sponging miR590-5p (Q. Meng et al., 2020), and we found it to be upregulated in eleven studies from the diagnostic category and correlating with shorter overall survival in the meta-analysis from Chapter 1 (GSE54388, GSE18520, GSE137238, GSE14407, GSE29450, GSE40595, GSE38666, GEPIA, GSE10971, GSE23391, and GSE190688; GSE32062, and shown in Chapter 1 Tables 1 and 3). *GMDS-DT* is downregulated and related to poor prognosis in liver cancer (D. Wang et al., 2019). Despite not being related with cancer in the literature, we found *TPT1-AS1* to be downregulated in 4 studies from the diagnostic meta-analysis from Chapter 1 ((H. Wang et al., 2016), GSE40595, GEPIA, GSE119054 and shown in Chapter 1 Table 2).

SNHG14, *NUTM2B-AS1*, *LINC00910*, and *NUTM2A-AS1* were previously related to cancers and are enriched in HMGB2 but not in HMGB1 eCLIP. *SNHG14* promotes colorectal cancer (Ye et al., 2019) and hepatocellular carcinoma (Liao et al., 2021) through miR-32-5p/SKIL and miR-876-5p/SSR2 axes, respectively. *LINC00910* is activated by OCT1 in breast cancer (Harandi-Zadeh et al., 2021). *NUTM2A-AS1* promotes lung adenocarcinoma by regulating the miR-590-5p/METTL3 axis (J. Wang et al., 2021), and gastric cancer by regulating the miR396a/TET1/HIF1a/PD-L1 axis (J. Wang et al., 2020). Also, we found *NUTM2A-AS1* to be upregulated in three patient studies from the diagnostic category in Chapter 1 meta-analysis ((H. Wang et al., 2016), GSE66957, GSE10971, and shown in Chapter 1 Table 1). *NUTM2B-AS1* is downregulated in pituitary adenoma (Ghafouri-Fard et al., 2022) and cervical cancer (J. Zhan et al., 2022).

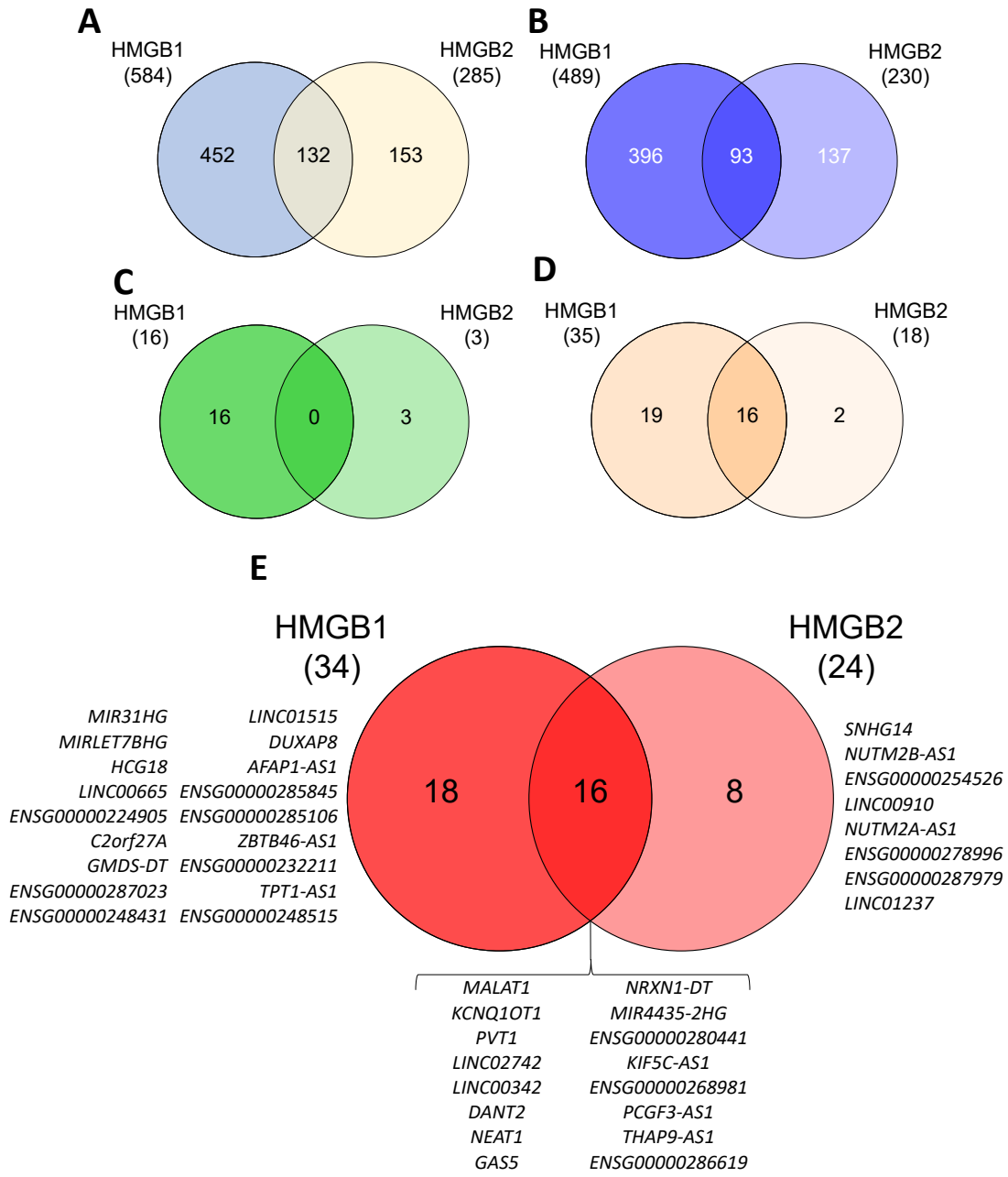

Figure 19.- Intersection between HMGB1 and HMGB2 RNAs obtained from PEO1 eCLIP analysis. Overlap of the full list (**A**), protein-coding genes (**B**), pseudogenes (**C**), snoRNAs (**D**), and lncRNAs (**E**).

MALAT1, PVT1, *LINC00342*, *NEAT1*, *GAS5*, *MIR4435-2HG*, and *THAP9-AS1* were previously related to cancers and are enriched in both HMGB1 and HMGB2 eCLIP experiments. *MALAT1* promotes metastasis, inflammation, and chemoresistance, while inhibiting apoptosis (Mao et al., 2021), as well as regulating RBFOX2-mediated alternative splicing in ovarian cancer (Gordon et al., 2019). *PVT1* is amplified in ovarian cancer and promotes proliferation and metastasis (Ding et al., 2019; Guan et al., 2007) by sponging miR-140 (Ding et al., 2019). It causes chemoresistance to doxorubicin

(Tabury et al., 2022) and platinum agents (Biomy et al., 2021) also in ovarian cancer. *LINC00342* is upregulated, associated with poor prognosis, and promotes non-small cell lung cancer by repressing p53 and PTEN expression (Tang et al., 2019). It also promotes colorectal cancer by modulating the miR-19a-3p/NPEPL1 and miR-545-5p/MDM2 axes (Miao et al., 2020; Shen et al., 2021). *NEAT1* promotes epithelial ovarian cancer by interacting with the RNA binding protein LIN28B (Yong et al., 2018), as well as by regulating the miR-365/FGF9 (J. Yuan et al., 2021), let-7 g/MEST/ATGL (L. Yin & Wang, 2021), and miR-1321/TJP3 (Luo et al., 2020) axes. *GAS5* hinders epithelial ovarian cancer by inhibiting inflammasome formation and pyroptosis (J. Li et al., 2018), regulating the miR-23a-WT1 axis (L. Zhou et al., 2023), and interacting with E2F4 (Long et al., 2019) and hnRNPK (T. Zhang et al., 2023) to regulate PARP1-associated MAPK and PI3K/AKT/mTOR pathways, respectively. *MIR4435-2HG* is upregulated and acts as an oncogene in several types of cancer by modulating Wnt and TGF-β1 pathways, as well as several miRNA/mRNA axes (M. Zhang et al., 2022). *THAP9-AS1* drives and is associated with poor prognosis in pancreatic ductal adenocarcinoma by sponging miR-484 and interacting with YAP (N. Li et al., 2020). It is also upregulated, associated with poor patient prognosis, and promotes hepatocellular carcinoma (Su et al., 2022). Additionally, we found *LINC00342* to be downregulated in 5 diagnostic studies from the meta-analysis carried out in Chapter 1 (GSE18520, GSE40595, GSE54388, GEPIA, GSE10971, and shown in Chapter 1 Table 2).

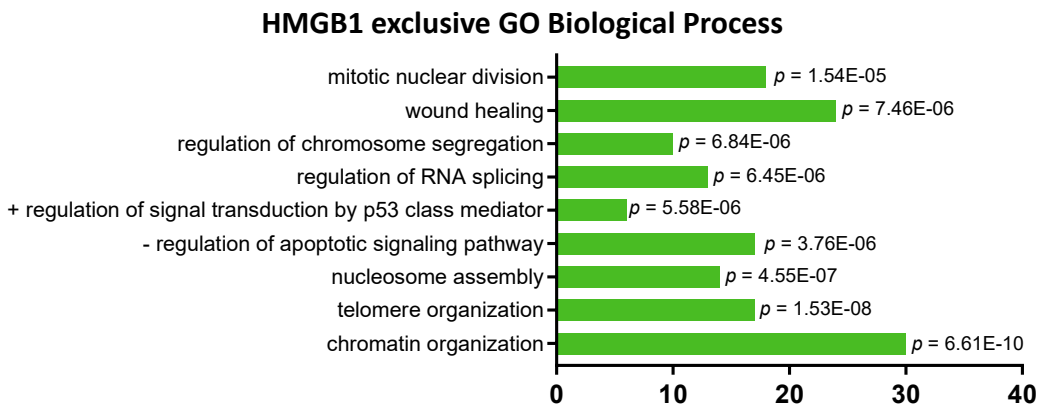

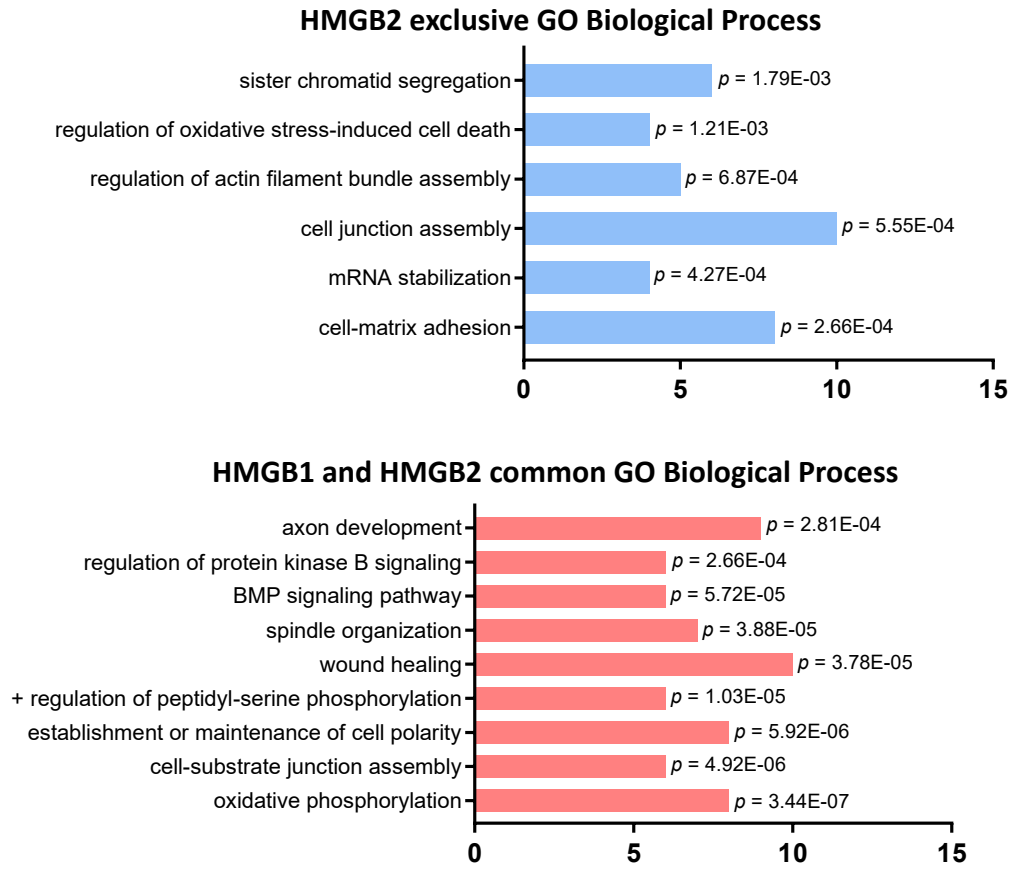

Figure 20.- Gene ontology enrichment analysis of PEO1 eCLIP enriched mRNA. Overrepresented gene ontology terms exclusive for HMGB1 (**top**), exclusive for HMGB2 (**middle**), and common for HMGB1 and HMGB2 (**bottom**). Values at the end of the bars correspond to the *p*-value.

In the GO-term analysis carried out for mRNAs, we find terms related to mitosis in the specific HMGB1 group, such as “mitotic nuclear division”, “regulation of chromosome segregation” and “sister chromatid segregation” in the specific HMGB2 group, or “spindle organization” in the HMGB1/HMGB2 common group, functions previously described for this proteins (Jia et al., 2019; Pallier et al., 2003). Also, terms related to migration and metastasis, such as “wound healing” in HMGB1, “regulation of actin filament bundle” in HMGB2, and “cell polarity” and “axon development” in HMGB1/HMGB2-common terms. In HMGB2-specific and HMGB1/2-common groups, there are terms associated with the extracellular matrix, such as “cell matrix adhesion” and “cell junction assembly”, or “cell substrate junction assembly”. Among specific HMGB1 terms, we find “nucleosome assembly” and “chromatin organization” that is one of the main functions of HMGB1 when it binds DNA (Gazzar et al., 2009; Ueda et al.,

2004), as well as “telomere organization”. In these three GO analyses there are several terms related to mitochondria, “positive regulation of apoptosis signaling pathway”, “oxidative phosphorylation”, and “regulation of oxidative stress-induced cell death”. In terms of signaling pathways, we found p53 in HMGB1-exclusive, and Bone Morphogenetic Protein (BMP) signaling and Protein Kinase B in HMGB1/HMGB2-common. BMPs are signaling molecules that belong to the TGF-β superfamily of proteins which are important in embryogenesis and development and also for the maintenance of adult tissue homeostasis, as well as related to cancerous processes (R. N. Wang et al., 2014).

Another research group tried to address the same question we asked, by carrying out sCLIP, a modification of iCLIP, to identify RNAs bound to HMGB1 and HMGB2 in the context of cellular senescence in IMR90 fibroblasts nuclei (Sofiadis et al., 2021). Fibroblasts are an essential component of the stroma and tumor microenvironment that are able to influence tumor characteristics and behavior. So, we speculated that, despite a difference in the genetic background and cellular context, some of the binding targets could be common in the two different approaches.

We overlapped the RNA binding targets from our eCLIP experiment and those from Sofiadis’ sCLIP experiment, as shown in Figure 21. We found commonalities between the two experiments, specifically, 352 and 80 targets in common for HMGB1 and HMGB2, respectively, of which 11 and 6 correspond to lncRNAs. The intersection for HMGB1 eCLIP targets is quite high, approximately 60%, although for HMGB2 is only 28%.

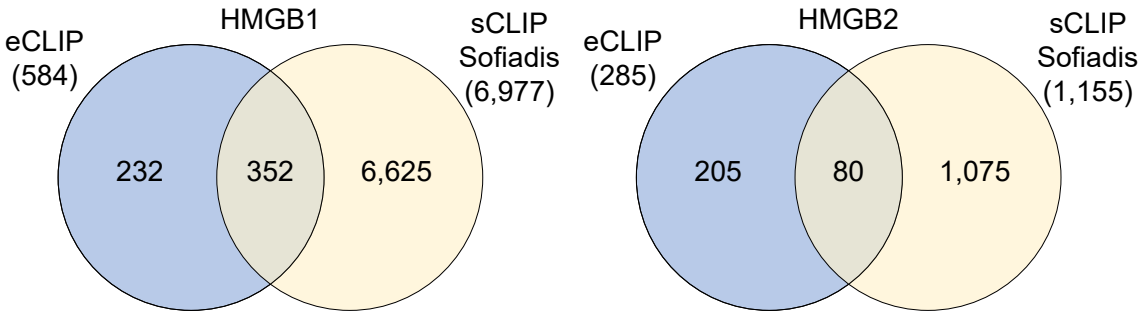

Figure 21.- Target overlap between eCLIP and sCLIP (Sofiadis et al., 2021) experiments.

These overlapping lncRNAs are *THAP9-AS1*, *TPT1-AS1*, *ENSG00000224905*, *GMDS-DT*, *LINC01515*, and *MIRLET7BHG* for HMGB1; *SNHG14* for HMGB2; and *GAS5*, *KCNQ1OT1*, *MALAT1*, *MIR4435-HG*, and *NEAT1* for both HMGB1 and HMGB2. We previously commented on their role in cancer for *THAP9-AS1*, *GMDS-DT*, *SNHG14*, *GAS5*, *MALAT1,* and *NEAT1*, therefore, their association with HMGB1 and HMGB2 in the sCLIP experiment supports the results we have obtained in eCLIP in the EOC model.

Finally, below are represented the coverage tracks of lncRNAs (Figure 22) and mRNAs (Figure 23) with the highest number of reads and statistical significance between the specific and unspecific IPs from the PEO1 eCLIP experiment, namely *GAS5*, *KCNQ1OT1*, *MALAT1*, *LINC00342*, *NEAT1*, and *NORAD* lncRNAs, and *IGFBP5*, *PKM*, *MYL6*, *SRRM2*, *VIM*, *AHNAK*, *FUS*, *CD53*, *ENO*, and *CCN1* mRNAs.

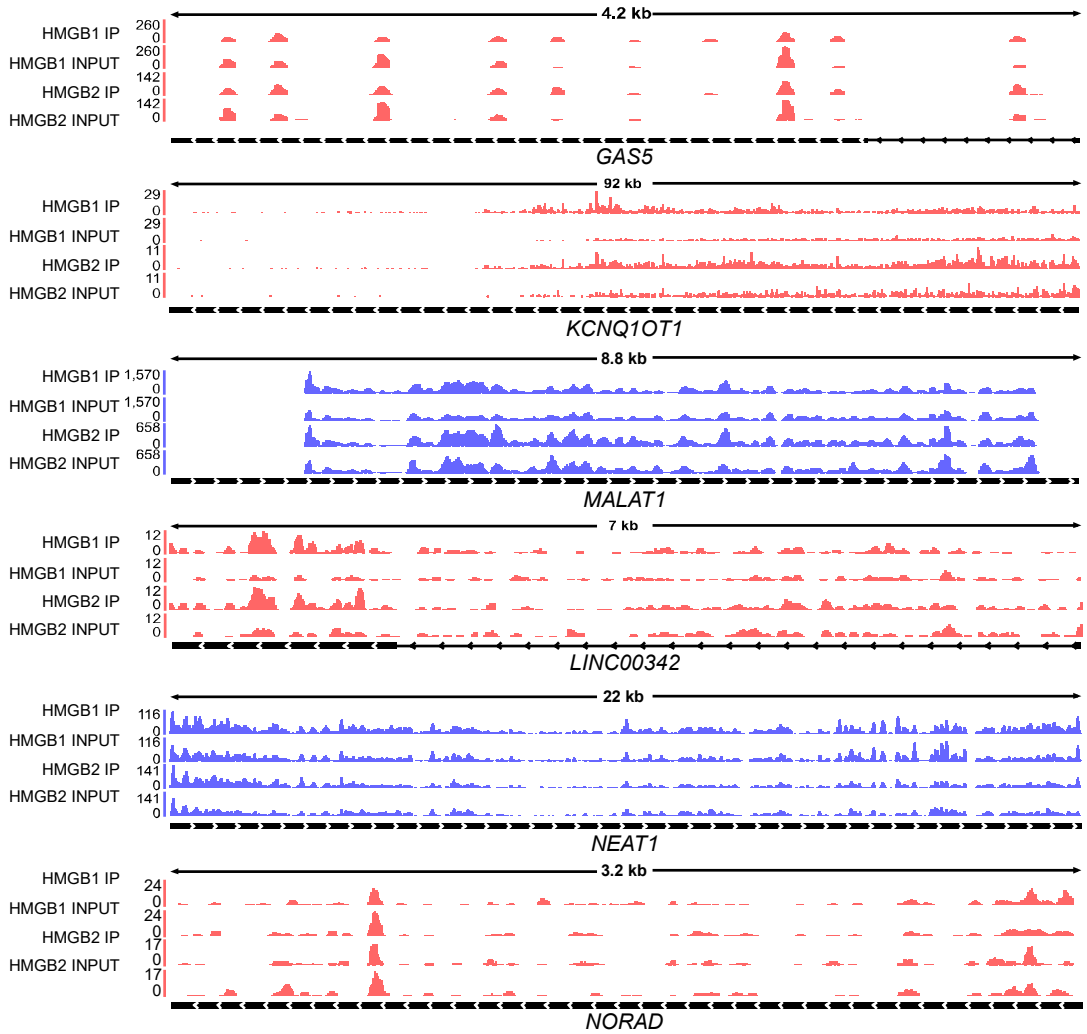

Figure 22.- Example coverage tracks for enriched lncRNAs in HMGB1 and/or HMGB2 IPs in the PEO1 eCLIP experiment. Blue and red histograms represent merged reads in positive or negative strands, respectively. The numbers on the left side represent the coverage range for each gene.

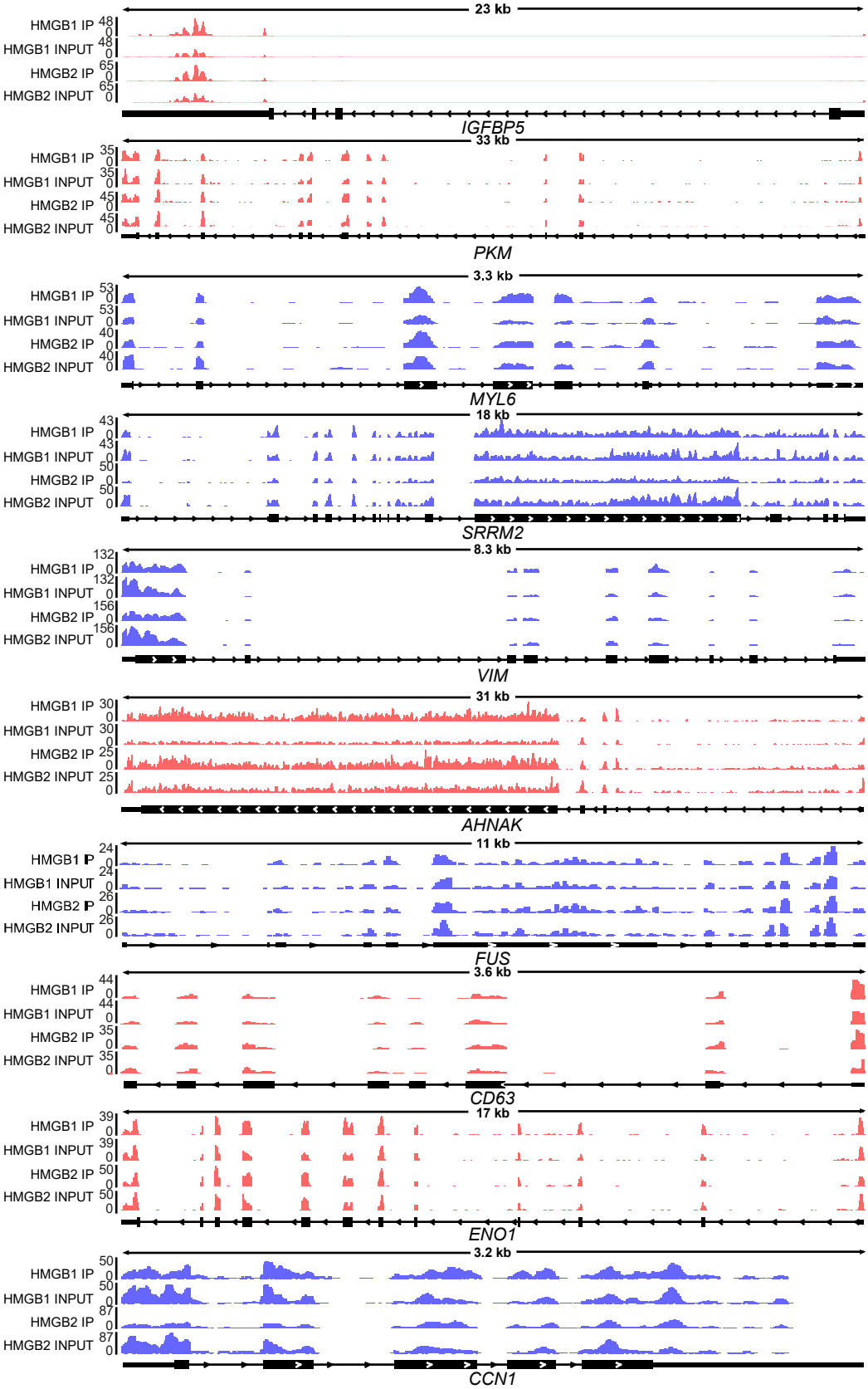

Figure 23.- Example coverage tracks for enriched mRNAs in HMGB1 and/or HMGB2 IPs in the PEO1 eCLIP experiment. Blue and red histograms represent merged reads in positive or negative strands, respectively. The numbers on the left side represent the coverage range for each gene.

Comparative of results obtained in this study by the different approaches

We overlapped the list of enriched RNAs identified by either RIP-Seq or eCLIP, in addition to the catRAPID-predicted RNA binders. We identified intersections in all the possible combinations within the results of the catRAPID algorithm, RIP-Seq, and eCLIP for HMGB1 and HMGB2, as shown in Figure 24.

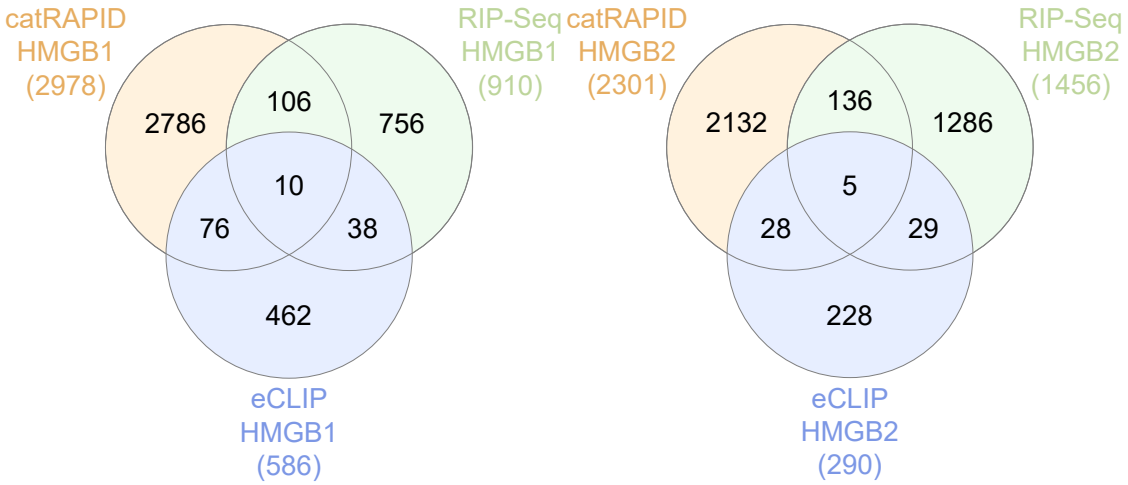

Figure 24.- Overall method comparison. HMGB1 (**left**) and HMGB2 (**right**).

When comparing the different methods, we obtained 10 and 5 mRNAs that are positive for binding for HMGB1 and HMGB2, respectively, in the three approaches. These RNAs are *PLXND1*, *LARGE1*, *EFNA5*, *CLCN7*, *AGRN*, *COL6A1*, *GCN1*, *COL1A1*, *ADAMTS1*, and *COL4A2*, for HMGB1, and *PLXND1*, *NEK6*, *DIP2C*, *VOPP1* and *C1S* for HMGB2. Due to their reproducibility across the three different approaches, these mRNAs could be of special interest for further analysis. Besides, several proteins encoded by these genes are cited in previous publications in the context of ovarian cancer. Plexin D1 (encoded by *PLXND1*) has been associated with tumor progression (Vivekanadhan & Mukhopadhyay, 2019) and its protein levels are upregulated in the blood of high-grade serous (HGSOC) EOC patients with poor prognosis (S. I. Kim et al., 2023). EFNA5 is overexpressed and is correlated with lower survival in HGSOC patients (Herath et al., 2006; Jukonen et al., 2021). There are three collagen mRNAs in the three analyses of HMGB1 binding RNAs. This family of proteins is the most abundant in the extracellular matrix and tumor microenvironment and is implicated in tumor fibrosis (Xu

et al., 2019); interestingly the three found in our analysis, namely, COL4A2, COL1A1, and COL6A1, have been previously related to ovarian cancer (Brown et al., 2015). NEK6 is a serine/threonine kinase whose expression is induced in mitosis as it mediates the establishment of the mitotic spindle by phosphorylating Eg5 (Rapley et al., 2008); it is overexpressed and correlated with poor prognosis and resistance to paclitaxel and carboplatin in serous ovarian cancer (Donato et al., 2015).

Other mRNAs that bind specifically to HMGB1 or HMGB2 have been previously related to other types of cancers. AGRN takes part in cell-to-matrix adhesion and it is upregulated and promotes metastasis in various human cancers, such as breast cancer, hepatocellular carcinoma, prostate cancer, oral squamous cell carcinoma, and rectal cancer (Z.-Q. Wang et al., 2021). LARGE1, also known as LARGE xylosyl- and glucuronyltransferase 1, belongs to the N-acetylglucosaminyl transferase protein family and it synthesizes the sugar chain of glycosphingolipids and glycoproteins (Peyrard et al., 1999); Downregulation of this protein was observed in aggressive non-small-cell lung cancer (Y. Liu et al., 2021), breast, and brain cancers (de Bernabé et al., 2009). ADAMTS1, harboring disintegrin and metalloproteinase activity, also acts as an inhibitor of angiogenesis by sequestering pro-angiogenic stimuli, e.g. vascular epithelial growth factor (VEGF), and preventing its interaction with its receptor (de Arao Tan et al., 2013); despite having anti-angiogenic properties, ADAMTS1 carries out pro-tumorigenic and metastatic functions by releasing peptides derived from the proteolysis, such as EGFR ligands that favor extracellular matrix remodeling in the bone to facilitate metastasis, as well as syndecan-4 or semaphorins that enhance migration (Wagstaff, 2011). DIP2C, disco-interacting protein 2 homolog C, is downregulated in breast cancer (J. Li et al., 2017), and its loss leads to EMT induction in a colorectal cancer cell line (Larsson et al., 2017). GCN1 (general control nonderepressible 1) is a ribosome collision sensor overexpressed in prostate cancer (Furnish et al., 2022). VOPP1, known as vesicular overexpressed in cancer pro-survival protein 1, is a protein component of the cytoplasmic

vesicle membranes that promotes tumor growth in breast cancer (Bonin et al., 2018) and also promotes esophageal squamous carcinoma (Baras et al., 2011). In clear cell renal carcinoma, C1S is associated with poor prognosis, promotes proliferation in cancer cell lines, and inhibits T cell activation in cocultures (Daugan et al., 2021); this protein is also elevated and promotes proliferation, cell death avoidance, angiogenesis, and ERK/Akt activation in cutaneous squamous cell carcinoma (Riihilä et al., 2020).

Despite in the previous chapter we were focused on lncRNAs, we also had information about protein-coding genes (data not shown), and, therefore, decided to check the deregulation status of these mRNAs in EOC patients. We found *COL4A2*, *PLXND1*, and *CLCN7* to be upregulated in 12, 10, and 7 studies, respectively, whereas *DIP2C* was downregulated in 9 diagnostic studies from Chapter 1. The rest of the commented mRNAs had ambiguous results as they were upregulated in some studies and downregulated in others from Chapter 1.

Unfortunately, there are no lncRNAs in the intersections of results obtained by the three approaches, although there are some in the pairwise comparisons between the catRAPID algorithm and RIP-Seq or the catRAPID algorithm and eCLIP. For HMGB1, *ZNF710-AS1*, *LINC02846* are present in catRAPID and RIP-Seq, and *GAS5*, *PCGF3-AS1*, and *ENSG00000224905* are included in catRAPID and eCLIP. For HMGB2, *ZNF710-AS1* and *SYT15-AS1* are present in catRAPID and RIP-Seq, and *GAS5*, *PCGF3-AS1*, and *SNHG14* are included in catRAPID and eCLIP. However, we did not find common lncRNAs in the results obtained by RIP-Seq and eCLIP. An explanation could be that crosslinking may enhance and fix transitory interactions that were not detected in RIP-Seq's native conditions. Besides, the antibody batches were different between the two experiments, as they were performed in two different laboratories, and this also adds a source of variability.

In summary, the results obtained reveal a set of mRNAs and lncRNAs that interact with HMGB1 and/or HMGB2 in the PEO1 cancerous cell line. This opens the way to future functional loss- and gain-of-function experiments in EOC cells for HMGB1/2 and the selected lncRNAs to establish common pathways and infer the specific regulatory model in which they take part. Also offers a panel of RNAs binding to HMGB1/2 to be determined in serum from EOC patients.

SUPPLEMENTARY MATERIALS AVAILABILITY

Chapter 2 includes Supplementary Tables S13 to S19 and Supplementary Figures S2 and S3, which are contained in the electronic support attached to this Thesis.

REFERENCES

Agostini, F., Zanzoni, A., Klus, P., Marchese, D., Cirillo, D., & Tartaglia, G. G. (2013). catRAPID omics: a web server for large-scale prediction of protein-RNA interactions. *Bioinformatics*, *29*(22), 2928–2930. https://doi.org/10.1093/bioinformatics/btt495

Armaos, A., Colantoni, A., Proietti, G., Rupert, J., & Tartaglia, G. G. (2021). cat RAPID omics v2.0 : going deeper and wider in the prediction of protein–RNA interactions. *Nucleic Acids Research*, *49*(W1), W72–W79. https://doi.org/10.1093/nar/gkab393

Aspden, J. L., Wallace, E. W. J., & Whiffin, N. (2023). Not all exons are protein coding: Addressing a common misconception. *Cell Genomics*, *3*(4), 100296. https://doi.org/10.1016/j.xgen.2023.100296

Baras, A. S., Solomon, A., Davidson, R., & Moskaluk, C. A. (2011). Loss of VOPP1 overexpression in squamous carcinoma cells induces apoptosis through oxidative cellular injury. *Laboratory Investigation*, *91*(8), 1170–1180. https://doi.org/10.1038/labinvest.2011.70

Barnes, B. M., Nelson, L., Tighe, A., Burghel, G. J., Lin, I.-H., Desai, S., McGrail, J. C., Morgan, R. D., & Taylor, S. S. (2021). Distinct transcriptional programs stratify ovarian cancer cell lines into the five major histological subtypes. *Genome Medicine*, *13*(1), 140. https://doi.org/10.1186/s13073-021-00952-5

Barreiro-Alonso, A., Lamas-Maceiras, M., Lorenzo-Catoira, L., Pardo, M., Yu, L., Choudhary, J. S., & Cerdán, M. E. (2021). HMGB1 Protein Interactions in Prostate and Ovary Cancer Models Reveal Links to RNA Processing and Ribosome Biogenesis through NuRD, THOC and Septin Complexes. *Cancers*, *13*(18), 4686. https://doi.org/10.3390/cancers13184686

Beaufort, C. M., Helmijr, J. C. A., Piskorz, A. M., Hoogstraat, M., Ruigrok-Ritstier, K., Besselink, N., Murtaza, M., van IJcken, W. F. J., Heine, A. A. J., Smid, M., Koudijs, M. J., Brenton, J. D., Berns, E. M. J. J., & Helleman, J. (2014). Ovarian Cancer Cell Line Panel (OCCP): Clinical Importance of In Vitro Morphological Subtypes. *PLoS ONE*, *9*(9), e103988. https://doi.org/10.1371/journal.pone.0103988

Bellucci, M., Agostini, F., Masin, M., & Tartaglia, G. G. (2011). Predicting protein associations with long noncoding RNAs. *Nature Methods*, *8*(6), 444–445. https://doi.org/10.1038/nmeth.1611

Bianco, C., & Mohr, I. (2019). Ribosome biogenesis restricts innate immune responses to virus infection and DNA. *ELife*, *8*. https://doi.org/10.7554/eLife.49551

Biomy, W. A. A., Mostafa, M. Y., EL-Khazragy, N. N., Ghonem, K. K. E., & Hewety, A. A. (2021). Long Non-Coding RNA- PVT1 in Ovarian Cancer as Predictors for Platinum Analogues Resistance. *QJM: An International Journal of Medicine*, *114*(Supplement_1). https://doi.org/10.1093/qjmed/hcab103.002

Blue, S. M., Yee, B. A., Pratt, G. A., Mueller, J. R., Park, S. S., Shishkin, A. A., Starner, A. C., Van Nostrand, E. L., & Yeo, G. W. (2022). Transcriptome-wide identification of RNA-binding protein binding sites using seCLIP-seq. *Nature Protocols*, *17*(5), 1223–1265. https://doi.org/10.1038/s41596-022-00680-z

Bonin, F., Taouis, K., Azorin, P., Petitalot, A., Tariq, Z., Nola, S., Bouteille, N., Tury, S., Vacher, S., Bièche, I., Rais, K. A., Pierron, G., Fuhrmann, L., Vincent-Salomon, A., Formstecher, E., Camonis, J., Lidereau, R., Lallemand, F., & Driouch, K. (2018). VOPP1 promotes breast tumorigenesis by interacting with the tumor suppressor WWOX. *BMC Biology*, *16*(1), 109. https://doi.org/10.1186/s12915-018-0576-6

Brown, C. W., Brodsky, A. S., & Freiman, R. N. (2015). Notch3 Overexpression Promotes Anoikis Resistance in Epithelial Ovarian Cancer via Upregulation of COL4A2. *Molecular Cancer Research*, *13*(1), 78–85. https://doi.org/10.1158/1541-7786.MCR-14-0334

Castello, A., Fischer, B., Frese, C. K., Horos, R., Alleaume, A.-M., Foehr, S., Curk, T., Krijgsveld, J., & Hentze, M. W. (2016). Comprehensive Identification of RNA-Binding Domains in Human Cells. *Molecular Cell*, *63*(4), 696–710. https://doi.org/10.1016/j.molcel.2016.06.029

Chang, K.-W., Hung, W.-W., Chou, C.-H., Tu, H.-F., Chang, S.-R., Liu, Y.-C., Liu, C.-J., & Lin, S.-C. (2021). LncRNA MIR31HG Drives Oncogenicity by Inhibiting the Limb-Bud and Heart Development Gene (LBH) during Oral Carcinoma. *International Journal of Molecular Sciences*, *22*(16), 8383. https://doi.org/10.3390/ijms22168383

Cong, Z., Diao, Y., Xu, Y., Li, X., Jiang, Z., Shao, C., Ji, S., Shen, Y., De, W., & Qiang, Y. (2019). Long non-coding RNA linc00665 promotes lung adenocarcinoma progression and functions as ceRNA to regulate AKR1B10-ERK signaling by sponging miR-98. *Cell Death & Disease*, *10*(2), 84. https://doi.org/10.1038/s41419-019-1361-3

Corley, M., Burns, M. C., & Yeo, G. W. (2020). How RNA-Binding Proteins Interact with RNA: Molecules and Mechanisms. *Molecular Cell*, *78*(1), 9–29. https://doi.org/10.1016/j.molcel.2020.03.011

Dai, W., Shi, Y., Hu, W., & Xu, C. (2022). Long noncoding RNA FAM225B facilitates proliferation and metastasis of nasopharyngeal carcinoma cells by regulating miR-613/CCND2 axis. *Bosnian Journal of Basic Medical Sciences*, *22*(1), 77–86. https://doi.org/10.17305/bjbms.2021.5691

Daugan, M. V., Revel, M., Russick, J., Dragon-Durey, M.-A., Gaboriaud, C., Robe-Rybkine, T., Poillerat, V., Grunenwald, A., Lacroix, G., Bougouin, A., Meylan, M., Verkarre, V., Oudard, S. M., Mejean, A., Vano, Y. A., Perkins, G., Validire, P., Cathelineau, X., Sanchez-Salas, R., … Roumenina, L. T. (2021). Complement

C1s and C4d as Prognostic Biomarkers in Renal Cancer: Emergence of Noncanonical Functions of C1s. *Cancer Immunology Research*, *9*(8), 891–908. https://doi.org/10.1158/2326-6066.CIR-20-0532

Davidovich, C., & Cech, T. R. (2015). The recruitment of chromatin modifiers by long noncoding RNAs: lessons from PRC2. *RNA*, *21*(12), 2007–2022. https://doi.org/10.1261/rna.053918.115

de Arao Tan, I., Ricciardelli, C., & Russell, D. L. (2013). The metalloproteinase ADAMTS1: A comprehensive review of its role in tumorigenic and metastatic pathways. *International Journal of Cancer*, *133*(10), 2263–2276. https://doi.org/10.1002/ijc.28127

de Bernabé, D. B.-V., Inamori, K., Yoshida-Moriguchi, T., Weydert, C. J., Harper, H. A., Willer, T., Henry, M. D., & Campbell, K. P. (2009). Loss of α-Dystroglycan Laminin Binding in Epithelium-derived Cancers Is Caused by Silencing of LARGE. *Journal of Biological Chemistry*, *284*(17), 11279–11284. https://doi.org/10.1074/jbc.C900007200

Ding, Y., Fang, Q., Li, Y., & Wang, Y. (2019). Amplification of lncRNA PVT1 promotes ovarian cancer proliferation by binding to miR-140. *Mammalian Genome*, *30*(7–8), 217–225. https://doi.org/10.1007/s00335-019-09808-1

Dong, X., Pi, Q., Yuemaierabola, A., Guo, W., & Tian, H. (2021). Silencing LINC00294 Restores Mitochondrial Function and Inhibits Apoptosis of Glioma Cells under Hypoxia via the miR-21-5p/CASKIN1/cAMP Axis. *Oxidative Medicine and Cellular Longevity*, *2021*, 1–21. https://doi.org/10.1155/2021/8240015

Dorn, A., Glaß, M., Neu, C. T., Heydel, B., Hüttelmaier, S., Gutschner, T., & Haemmerle, M. (2020). LINC00261 Is Differentially Expressed in Pancreatic Cancer Subtypes and Regulates a Pro-Epithelial Cell Identity. *Cancers*, *12*(5), 1227. https://doi.org/10.3390/cancers12051227

Elhasnaoui, J., Miano, V., Ferrero, G., Doria, E., Leon, A. E., Fabricio, A. S. C., Annaratone, L., Castellano, I., Sapino, A., & De Bortoli, M. (2020). DSCAM-AS1-Driven Proliferation of Breast Cancer Cells Involves Regulation of Alternative Exon Splicing and 3′-End Usage. *Cancers*, *12*(6), 1453. https://doi.org/10.3390/cancers12061453

Furnish, M., Boulton, D. P., Genther, V., Grofova, D., Ellinwood, M. L., Romero, L., Lucia, M. S., Cramer, S. D., & Caino, M. C. (2022). MIRO2 Regulates Prostate Cancer Cell Growth via GCN1-Dependent Stress Signaling. *Molecular Cancer Research*, *20*(4), 607–621. https://doi.org/10.1158/1541-7786.MCR-21-0374

Gazzar, M. El, Yoza, B. K., Chen, X., Garcia, B. A., Young, N. L., & McCall, C. E. (2009). Chromatin-Specific Remodeling by HMGB1 and Linker Histone H1 Silences Proinflammatory Genes during Endotoxin Tolerance. *Molecular and Cellular Biology*, *29*(7), 1959–1971. https://doi.org/10.1128/MCB.01862-08

Ge, X., Chen, Y. E., Song, D., McDermott, M., Woyshner, K., Manousopoulou, A., Wang, N., Li, W., Wang, L. D., & Li, J. J. (2021). Clipper: p-value-free FDR control on high-throughput data from two conditions. *Genome Biology*, *22*(1), 288. https://doi.org/10.1186/s13059-021-02506-9

Ghafouri-Fard, S., Khoshbakht, T., Taheri, M., & Ebrahimzadeh, K. (2021). A Review on the Carcinogenic Roles of DSCAM-AS1. *Frontiers in Cell and Developmental Biology*, *9*. https://doi.org/10.3389/fcell.2021.758513

Ghafouri-Fard, S., Safarzadeh, A., Akhavan-Bahabadi, M., Hussen, B. M., Taheri, M.,

& Dilmaghani, N. A. (2022). Expression pattern of non-coding RNAs in non-functioning pituitary adenoma. *Frontiers in Oncology*, *12*. https://doi.org/10.3389/fonc.2022.978016

Glisovic, T., Bachorik, J. L., Yong, J., & Dreyfuss, G. (2008). RNA-binding proteins and post-transcriptional gene regulation. *FEBS Letters*, *582*(14), 1977–1986. https://doi.org/10.1016/j.febslet.2008.03.004

Gordon, M. A., Babbs, B., Cochrane, D. R., Bitler, B. G., & Richer, J. K. (2019). The long non-coding RNA MALAT1 promotes ovarian cancer progression by regulating RBFOX2-mediated alternative splicing. *Molecular Carcinogenesis*, *58*(2), 196–205. https://doi.org/10.1002/mc.22919

Grelet, S., Fréreux, C., Obellianne, C., Noguchi, K., Howley, B. V, Dalton, A. C., & Howe, P. H. (2022). TGFβ-induced expression of long noncoding lincRNA Platr18 controls breast cancer axonogenesis. *Life Science Alliance*, *5*(2), e202101261. https://doi.org/10.26508/lsa.202101261

Guan, Y., Kuo, W.-L., Stilwell, J. L., Takano, H., Lapuk, A. V., Fridlyand, J., Mao, J.-H., Yu, M., Miller, M. A., Santos, J. L., Kalloger, S. E., Carlson, J. W., Ginzinger, D. G., Celniker, S. E., Mills, G. B., Huntsman, D. G., & Gray, J. W. (2007). Amplification of PVT1 Contributes to the Pathophysiology of Ovarian and Breast Cancer. *Clinical Cancer Research*, *13*(19), 5745–5755. https://doi.org/10.1158/1078-0432.CCR-06-2882

Hafner, M., Katsantoni, M., Köster, T., Marks, J., Mukherjee, J., Staiger, D., Ule, J., & Zavolan, M. (2021). CLIP and complementary methods. *Nature Reviews Methods Primers*, *1*(1), 20. https://doi.org/10.1038/s43586-021-00018-1

Hafner, M., Landthaler, M., Burger, L., Khorshid, M., Hausser, J., Berninger, P., Rothballer, A., Ascano, M., Jungkamp, A.-C., Munschauer, M., Ulrich, A., Wardle, G. S., Dewell, S., Zavolan, M., & Tuschl, T. (2010). Transcriptome-wide Identification of RNA-Binding Protein and MicroRNA Target Sites by PAR-CLIP. *Cell*, *141*(1), 129–141. https://doi.org/10.1016/j.cell.2010.03.009

Han, J.-B., Wang, Y., Yang, R., Xu, Y., Li, F., & Jia, Y. (2022). LncRNA FAM225A activates the cGAS-STING signaling pathway by combining FUS to promote CENP-N expression and regulates the progression of nasopharyngeal carcinoma. *Pathology - Research and Practice*, *236*, 154005. https://doi.org/10.1016/j.prp.2022.154005

Hanahan, D., & Weinberg, R. A. (2011). Hallmarks of Cancer: The Next Generation. *Cell*, *144*(5), 646–674. https://doi.org/10.1016/j.cell.2011.02.013

Harandi-Zadeh, S., Boycott, C., Beetch, M., Yang, T., Martin, B. J. E., Ren, K., Kwasniak, A., Dupuis, J. H., Lubecka, K., Yada, R. Y., Howe, L. J., & Stefanska, B. (2021). Pterostilbene Changes Epigenetic Marks at Enhancer Regions of Oncogenes in Breast Cancer Cells. *Antioxidants*, *10*(8), 1232. https://doi.org/10.3390/antiox10081232

Herath, N. I., Spanevello, M. D., Sabesan, S., Newton, T., Cummings, M., Duffy, S., Lincoln, D., Boyle, G., Parsons, P. G., & Boyd, A. W. (2006). Over-expression of Eph and ephrin genes in advanced ovarian cancer: ephrin gene expression correlates with shortened survival. *BMC Cancer*, *6*(1), 144. https://doi.org/10.1186/1471-2407-6-144

Holmes, Z. E., Hamilton, D. J., Hwang, T., Parsonnet, N. V., Rinn, J. L., Wuttke, D. S., & Batey, R. T. (2020). The Sox2 transcription factor binds RNA. *Nature Communications*, *11*(1), 1805. https://doi.org/10.1038/s41467-020-15571-8

Huangfu, L., Fan, B., Wang, G., Gan, X., Tian, S., He, Q., Yao, Q., Shi, J., Li, X., Du, H., Gao, X., Xing, X., & Ji, J. (2022). Novel prognostic marker LINC00205 promotes tumorigenesis and metastasis by competitively suppressing miRNA-26a in gastric cancer. *Cell Death Discovery*, *8*(1), 5. https://doi.org/10.1038/s41420-021-00802-8

Ji, W., Diao, Y.-L., Qiu, Y.-R., Ge, J., Cao, X.-C., & Yu, Y. (2020). LINC00665 promotes breast cancer progression through regulation of the miR-379-5p/LIN28B axis. *Cell Death & Disease*, *11*(1), 16. https://doi.org/10.1038/s41419-019-2213-x

Jia, L., Song, H., Fan, W., Song, Y., Wang, G., Li, X., He, Y., & Yao, A. (2019). The association between high mobility group box 1 chromatin protein and mitotic chromosomes in glioma cells. *Oncology Letters*, *19*(1), 745–752. https://doi.org/10.3892/ol.2019.11170

Joshi, S. R., Sarpong, Y. C., Peterson, R. C., & Scovell, W. M. (2012). Nucleosome dynamics: HMGB1 relaxes canonical nucleosome structure to facilitate estrogen receptor binding. *Nucleic Acids Research*, *40*(20), 10161–10171. https://doi.org/10.1093/nar/gks815

Jukonen, J., Moyano-Galceran, L., Höpfner, K., Pietilä, E. A., Lehtinen, L., Huhtinen, K., Gucciardo, E., Hynninen, J., Hietanen, S., Grénman, S., Ojala, P. M., Carpén, O., & Lehti, K. (2021). Aggressive and recurrent ovarian cancers upregulate ephrinA5, a non-canonical effector of EphA2 signaling duality. *Scientific Reports*, *11*(1), 8856. https://doi.org/10.1038/s41598-021-88382-6

Keene, J. D., Komisarow, J. M., & Friedersdorf, M. B. (2006). RIP-Chip: the isolation and identification of mRNAs, microRNAs and protein components of ribonucleoprotein complexes from cell extracts. *Nature Protocols*, *1*(1), 302–307. https://doi.org/10.1038/nprot.2006.47

Kent, W. J., Zweig, A. S., Barber, G., Hinrichs, A. S., & Karolchik, D. (2010). BigWig and BigBed: enabling browsing of large distributed datasets. *Bioinformatics*, *26*(17), 2204–2207. https://doi.org/10.1093/bioinformatics/btq351

Kim, J., Kim, J., & Bae, J.-S. (2016). ROS homeostasis and metabolism: a critical liaison for cancer therapy. *Experimental & Molecular Medicine*, *48*(11), e269–e269. https://doi.org/10.1038/emm.2016.119

Kim, S. I., Hwangbo, S., Dan, K., Kim, H. S., Chung, H. H., Kim, J.-W., Park, N. H., Song, Y.-S., Han, D., & Lee, M. (2023). Proteomic Discovery of Plasma Protein Biomarkers and Development of Models Predicting Prognosis of High-Grade Serous Ovarian Carcinoma. *Molecular & Cellular Proteomics*, *22*(3), 100502. https://doi.org/10.1016/j.mcpro.2023.100502

König, J., Zarnack, K., Rot, G., Curk, T., Kayikci, M., Zupan, B., Turner, D. J., Luscombe, N. M., & Ule, J. (2010). iCLIP reveals the function of hnRNP particles in splicing at individual nucleotide resolution. *Nature Structural & Molecular Biology*, *17*(7), 909–915. https://doi.org/10.1038/nsmb.1838

Kouzarides, T. (2007). Chromatin Modifications and Their Function. *Cell*, *128*(4), 693–705. https://doi.org/10.1016/j.cell.2007.02.005

Lang, B., Armaos, A., & Tartaglia, G. G. (2019). RNAct: Protein–RNA interaction predictions for model organisms with supporting experimental data. *Nucleic Acids Research*, *47*(D1), D601–D606. https://doi.org/10.1093/nar/gky967

Larsson, C., Ali, M. A., Pandzic, T., Lindroth, A. M., He, L., & Sjöblom, T. (2017). Loss of DIP2C in RKO cells stimulates changes in DNA methylation and epithelial-

mesenchymal transition. *BMC Cancer*, *17*(1), 1–12. https://doi.org/10.1186/s12885-017-3472-5

Li, G., Xie, M., Huang, Z., Li, H., Li, P., Zhang, Z., Ding, Y., Jia, Z., & Yang, J. (2020). Overexpression of antisense long non-coding RNA ZNF710-AS1-202 promotes cell proliferation and inhibits apoptosis of clear cell renal cell carcinoma via regulation of ZNF710 expression. *Molecular Medicine Reports*. https://doi.org/10.3892/mmr.2020.11032

Li, J., Ping, J. L., Ma, B., Chen, Y. R., & Li, L. Q. (2017). DIP2C expression in breast cancer and its clinical significance. *Pathology - Research and Practice*, *213*(11), 1394–1399. https://doi.org/10.1016/j.prp.2017.09.007

Li, J., Yang, C., Li, Y., Chen, A., Li, L., & You, Z. (2018). LncRNA GAS5 suppresses ovarian cancer by inducing inflammasome formation. *Bioscience Reports*, *38*(2), 1–11. https://doi.org/10.1042/BSR20171150

Li, J., Zhang, Q., Ge, P., Zeng, C., Lin, F., Wang, W., & Zhao, J. (2020). FAM225B Is a Prognostic lncRNA for Patients with Recurrent Glioblastoma. *Disease Markers*, *2020*, 1–7. https://doi.org/10.1155/2020/8888085

Li, K., Han, H., Gu, W., Cao, C., & Zheng, P. (2020). Long non-coding RNA LINC01963 inhibits progression of pancreatic carcinoma by targeting miR-641/TMEFF2. *Biomedicine & Pharmacotherapy*, *129*, 110346. https://doi.org/10.1016/j.biopha.2020.110346

Li, N., Yang, G., Luo, L., Ling, L., Wang, X., Shi, L., Lan, J., Jia, X., Zhang, Q., Long, Z., Liu, J., Hu, W., He, Z., Liu, H., Liu, W., & Zheng, G. (2020). lncRNA THAP9-AS1 Promotes Pancreatic Ductal Adenocarcinoma Growth and Leads to a Poor Clinical Outcome via Sponging miR-484 and Interacting with YAP. *Clinical Cancer Research*, *26*(7), 1736–1748. https://doi.org/10.1158/1078-0432.CCR-19-0674

Liao, Z., Zhang, H., Su, C., Liu, F., Liu, Y., Song, J., Zhu, H., Fan, Y., Zhang, X., Dong, W., Chen, X., Liang, H., & Zhang, B. (2021). Long noncoding RNA SNHG14 promotes hepatocellular carcinoma progression by regulating miR-876-5p/SSR2 axis. *Journal of Experimental & Clinical Cancer Research*, *40*(1), 36. https://doi.org/10.1186/s13046-021-01838-5

Licatalosi, D. D., Mele, A., Fak, J. J., Ule, J., Kayikci, M., Chi, S. W., Clark, T. A., Schweitzer, A. C., Blume, J. E., Wang, X., Darnell, J. C., & Darnell, R. B. (2008). HITS-CLIP yields genome-wide insights into brain alternative RNA processing. *Nature*, *456*(7221), 464–469. https://doi.org/10.1038/nature07488

Liu, G., Zhu, Q., Wang, H., Zhou, J., & Jiang, B. (2022). Long non-coding RNA Linc00205 promotes hepatoblastoma progression through regulating microRNA-154-3p/Rho-associated coiled-coil Kinase 1 axis via mitogen-activated protein kinase signaling. *Aging*, *14*(4), 1782–1796. https://doi.org/10.18632/aging.203902

Liu, X., Zhu, Q., Guo, Y., Xiao, Z., Hu, L., & Xu, Q. (2019). LncRNA LINC00689 promotes the growth, metastasis and glycolysis of glioma cells by targeting miR-338-3p/PKM2 axis. *Biomedicine & Pharmacotherapy*, *117*, 109069. https://doi.org/10.1016/j.biopha.2019.109069

Liu, Y.-T., Liu, G.-Q., & Huang, J.-M. (2020). FAM225A promotes sorafenib resistance in hepatocarcinoma cells through modulating miR-130a-5p–CCNG1 interaction network. *Bioscience Reports*, *40*(12). https://doi.org/10.1042/BSR20202054

Liu, Y., Huang, S., Kuang, M., Wang, H., & Xie, Q. (2021). High LARGE1 Expression May Predict Benefit from Adjuvant Chemotherapy in Resected Non-Small-Cell

Lung Cancer. *Pharmacogenomics and Personalized Medicine*, *14*, 87–99. https://doi.org/10.2147/PGPM.S271516

Long, X., Li, Q., Zhi, L., Li, J., & Wang, Z. (2020). LINC00205 modulates the expression of EPHX1 through the inhibition of miR-184 in hepatocellular carcinoma as a ceRNA. *Journal of Cellular Physiology*, *235*(3), 3013–3021. https://doi.org/10.1002/jcp.29206

Long, X., Song, K., Hu, H., Tian, Q., Wang, W., Dong, Q., Yin, X., & Di, W. (2019). Long non-coding RNA GAS5 inhibits DDP-resistance and tumor progression of epithelial ovarian cancer via GAS5-E2F4-PARP1-MAPK axis. *Journal of Experimental & Clinical Cancer Research*, *38*(345), 1–16. https://doi.org/10.1186/s13046-019-1329-2

Love, M. I., Huber, W., & Anders, S. (2014). Moderated estimation of fold change and dispersion for RNA-seq data with DESeq2. *Genome Biology*, *15*(12), 550. https://doi.org/10.1186/s13059-014-0550-8

Lunde, B. M., Moore, C., & Varani, G. (2007). RNA-binding proteins: modular design for efficient function. *Nature Reviews Molecular Cell Biology*, *8*(6), 479–490. https://doi.org/10.1038/nrm2178

Luo, M., Zhang, L., Yang, H., Luo, K., & Qing, C. (2020). Long non-coding RNA NEAT1 promotes ovarian cancer cell invasion and migration by interacting with miR-1321 and regulating tight junction protein 3 expression. *Molecular Medicine Reports*, *22*(4), 3429–3439. https://doi.org/10.3892/mmr.2020.11428

Ma, T., Liu, H., Liu, Y., Liu, T., Wang, H., Qiao, F., Song, L., & Zhang, L. (2020). USP6NL mediated by LINC00689/miR-142-3p promotes the development of triple-negative breast cancer. *BMC Cancer*, *20*(1), 998. https://doi.org/10.1186/s12885-020-07394-z

Ma, X., Wang, G., Fan, H., Li, Z., Chen, W., Xiao, J., Ni, P., Liu, K., Shen, K., Wang, Y., Xu, Z., & Yang, L. (2022). Long noncoding RNA FAM225A promotes the malignant progression of gastric cancer through the miR-326/PADI2 axis. *Cell Death Discovery*, *8*(1), 20. https://doi.org/10.1038/s41420-021-00809-1

Mao, T.-L., Fan, M.-H., Dlamini, N., & Liu, C.-L. (2021). LncRNA MALAT1 Facilitates Ovarian Cancer Progression through Promoting Chemoresistance and Invasiveness in the Tumor Microenvironment. *International Journal of Molecular Sciences*, *22*(19), 10201. https://doi.org/10.3390/ijms221910201

Martindale, J., Gorospe, M., & Idda, M. (2020). Ribonucleoprotein Immunoprecipitation (RIP) Analysis. *BIO-PROTOCOL*, *10*(2). https://doi.org/10.21769/BioProtoc.3488

McMahon, A. C., Rahman, R., Jin, H., Shen, J. L., Fieldsend, A., Luo, W., & Rosbash, M. (2016). TRIBE: Hijacking an RNA-Editing Enzyme to Identify Cell-Specific Targets of RNA-Binding Proteins. *Cell*, *165*(3), 742–753. https://doi.org/10.1016/j.cell.2016.03.007

Meng, L., Li, Z., Chen, Y., Liu, D., & Liu, Z. (2020). LINC00689 promotes prostate cancer progression via regulating miR-496/CTNNB1 to activate Wnt pathway. *Cancer Cell International*, *20*(1), 215. https://doi.org/10.1186/s12935-020-01280-1

Meng, Q., Li, Z., Pan, J., & Sun, X. (2020). Long noncoding RNA DUXAP8 regulates proliferation and apoptosis of ovarian cancer cells via targeting miR-590-5p. *Human Cell*, *33*(4), 1240–1251. https://doi.org/10.1007/s13577-020-00398-8

Miao, Z., Liu, S., Xiao, X., & Li, D. (2020). LINC00342 regulates cell proliferation, apoptosis, migration and invasion in colon adenocarcinoma via miR-545-

5p/MDM2 axis. *Gene*, *743*, 144604. https://doi.org/10.1016/j.gene.2020.144604

Mo, X., Hu, D., Yang, P., Li, Y., Bashir, S., Nai, A., Ma, F., Jia, G., & Xu, M. (2022). A novel cuproptosis-related prognostic lncRNA signature and lncRNA MIR31HG/miR-193a-3p/TNFRSF21 regulatory axis in lung adenocarcinoma. *Frontiers in Oncology*, *12*. https://doi.org/10.3389/fonc.2022.927706

Nan, S., Zhang, S., Jin, R., & Wang, J. (2022). LINC00665 up-regulates SIN3A expression to modulate the progression of colorectal cancer via sponging miR-138-5p. *Cancer Cell International*, *22*(1), 51. https://doi.org/10.1186/s12935-021-02176-4

Ni, Q., Zhang, H., Shi, X., & Li, X. (2023). Exosomal lncRNA HCG18 contributes to cholangiocarcinoma growth and metastasis through mediating miR-424-5p/SOX9 axis through PI3K/AKT pathway. *Cancer Gene Therapy*, *30*(4), 582–595. https://doi.org/10.1038/s41417-022-00500-2

Niknafs, Y. S., Han, S., Ma, T., Speers, C., Zhang, C., Wilder-Romans, K., Iyer, M. K., Pitchiaya, S., Malik, R., Hosono, Y., Prensner, J. R., Poliakov, A., Singhal, U., Xiao, L., Kregel, S., Siebenaler, R. F., Zhao, S. G., Uhl, M., Gawronski, A., … Feng, F. Y. (2016). The lncRNA landscape of breast cancer reveals a role for DSCAM-AS1 in breast cancer progression. *Nature Communications*, *7*(1), 12791. https://doi.org/10.1038/ncomms12791

Osmanov, T., Ugrinova, I., & Pasheva, E. (2013). The chaperone like function of the nonhistone protein HMGB1. *Biochemical and Biophysical Research Communications*, *432*(2), 231–235. https://doi.org/10.1016/j.bbrc.2013.02.008

Padrón, A., Iwasaki, S., & Ingolia, N. T. (2019). Proximity RNA Labeling by APEX-Seq Reveals the Organization of Translation Initiation Complexes and Repressive RNA Granules. *Molecular Cell*, *75*(4), 875-887.e5. https://doi.org/10.1016/j.molcel.2019.07.030

Pallier, C., Scaffidi, P., Chopineau-Proust, S., Agresti, A., Nordmann, P., Bianchi, M. E., & Marechal, V. (2003). Association of Chromatin Proteins High Mobility Group Box (HMGB) 1 and HMGB2 with Mitotic Chromosomes. *Molecular Biology of the Cell*, *14*(8), 3414–3426. https://doi.org/10.1091/mbc.e02-09-0581

Peng, H., & Ge, P. (2021). Long non-coding RNA HCG18 facilitates the progression of laryngeal and hypopharyngeal squamous cell carcinoma by upregulating FGFR1 via miR-133b. *Molecular Medicine Reports*, *25*(2), 46. https://doi.org/10.3892/mmr.2021.12562

Peyrard, M., Seroussi, E., Sandberg-Nordqvist, A.-C., Xie, Y.-G., Han, F.-Y., Fransson, I., Collins, J., Dunham, I., Kost-Alimova, M., Imreh, S., & Dumanski, J. P. (1999). The human LARGE gene from 22q12.3-q13.1 is a new, distinct member of the glycosyltransferase gene family. *Proceedings of the National Academy of Sciences*, *96*(2), 598–603. https://doi.org/10.1073/pnas.96.2.598

Piipponen, M., Nissinen, L., Riihilä, P., Farshchian, M., Kallajoki, M., Peltonen, J., Peltonen, S., & Kähäri, V.-M. (2020). p53-Regulated Long Noncoding RNA PRECSIT Promotes Progression of Cutaneous Squamous Cell Carcinoma via STAT3 Signaling. *The American Journal of Pathology*, *190*(2), 503–517. https://doi.org/10.1016/j.ajpath.2019.10.019

Qi, P., Yexie, Z., Xue, C., Huang, G., Zhao, Z., & Zhang, X. (2023). LINC00294/miR-620/MKRN2 axis provides biomarkers and negatively regulates malignant progression in colorectal carcinoma. *Human & Experimental Toxicology*, *42*, 096032712311675. https://doi.org/10.1177/09603271231167577

Qiu, J., Zhou, S., Cheng, W., & Luo, C. (2020). LINC00294 induced by GRP78 promotes cervical cancer development by promoting cell cycle transition. *Oncology Letters*, *20*(5), 1–1. https://doi.org/10.3892/ol.2020.12125

Ramanathan, M., Porter, D. F., & Khavari, P. A. (2019). Methods to study RNA–protein interactions. *Nature Methods*, *16*(3), 225–234. https://doi.org/10.1038/s41592-019-0330-1

Ramírez, F., Ryan, D. P., Grüning, B., Bhardwaj, V., Kilpert, F., Richter, A. S., Heyne, S., Dündar, F., & Manke, T. (2016). deepTools2: a next generation web server for deep-sequencing data analysis. *Nucleic Acids Research*, *44*(W1), W160–W165. https://doi.org/10.1093/nar/gkw257

Riihilä, P., Viiklepp, K., Nissinen, L., Farshchian, M., Kallajoki, M., Kivisaari, A., Meri, S., Peltonen, J., Peltonen, S., & Kähäri, V. -M. (2020). Tumour-cell-derived complement components C1r and C1s promote growth of cutaneous squamous cell carcinoma. *British Journal of Dermatology*, *182*(3), 658–670. https://doi.org/10.1111/bjd.18095

Shen, P., Qu, L., Wang, J., Ding, Q., Zhou, C., Xie, R., Wang, H., & Ji, G. (2021). LncRNA LINC00342 contributes to the growth and metastasis of colorectal cancer via targeting miR-19a-3p/NPEPL1 axis. *Cancer Cell International*, *21*(1), 105. https://doi.org/10.1186/s12935-020-01705-x

Shi, W., Zhang, C., Ning, Z., Hua, Y., Li, Y., Chen, L., Liu, L., Chen, Z., & Meng, Z. (2019). Long non-coding RNA LINC00346 promotes pancreatic cancer growth and gemcitabine resistance by sponging miR-188-3p to derepress BRD4 expression. *Journal of Experimental & Clinical Cancer Research*, *38*(1), 60. https://doi.org/10.1186/s13046-019-1055-9

Sofiadis, K., Josipovic, N., Nikolic, M., Kargapolova, Y., Übelmesser, N., Varamogianni-Mamatsi, V., Zirkel, A., Papadionysiou, I., Loughran, G., Keane, J., Michel, A., Gusmao, E. G., Becker, C., Altmüller, J., Georgomanolis, T., Mizi, A., & Papantonis, A. (2021). HMGB1 coordinates SASP-related chromatin folding and RNA homeostasis on the path to senescence. *Molecular Systems Biology*, *17*(6), 1–17. https://doi.org/10.15252/msb.20209760

Stros, M., Polanska, E., Struncova, S., & Pospisilova, S. (2009). HMGB1 and HMGB2 proteins up-regulate cellular expression of human topoisomerase II. *Nucleic Acids Research*, *37*(7), 2070–2086. https://doi.org/10.1093/nar/gkp067

Su, Y., Xie, R., & Xu, Q. (2022). LncRNA THAP9-AS1 highly expressed in tissues of hepatocellular carcinoma and accelerates tumor cell proliferation. *Clinics and Research in Hepatology and Gastroenterology*, *46*(10), 102025. https://doi.org/10.1016/j.clinre.2022.102025

Tabury, K., Monavarian, M., Listik, E., Shelton, A. K., Choi, A. S., Quintens, R., Arend, R. C., Hempel, N., Miller, C. R., Györrfy, B., & Mythreye, K. (2022). PVT1 is a stress-responsive lncRNA that drives ovarian cancer metastasis and chemoresistance. *Life Science Alliance*, *5*(11), e202201370. https://doi.org/10.26508/lsa.202201370

Tang, H., Zhao, L., Li, M., Li, T., & Hao, Y. (2019). Investigation of LINC00342 as a poor prognostic biomarker for human patients with non–small cell lung cancer. *Journal of Cellular Biochemistry*, *120*(4), 5055–5061. https://doi.org/10.1002/jcb.27782

Thorvaldsdottir, H., Robinson, J. T., & Mesirov, J. P. (2013). Integrative Genomics Viewer (IGV): high-performance genomics data visualization and exploration.

Briefings in Bioinformatics, *14*(2), 178–192. https://doi.org/10.1093/bib/bbs017

Torgovnick, A., & Schumacher, B. (2015). DNA repair mechanisms in cancer development and therapy. *Frontiers in Genetics*, *6*. https://doi.org/10.3389/fgene.2015.00157

Triana-Martínez, F., Loza, M. I., & Domínguez, E. (2020). Beyond Tumor Suppression: Senescence in Cancer Stemness and Tumor Dormancy. *Cells*, *9*(2), 346. https://doi.org/10.3390/cells9020346

Tu, C., Ren, X., He, J., Li, S., Qi, L., Duan, Z., Wang, W., & Li, Z. (2020). The predictive value of lncRNA MIR31HG expression on clinical outcomes in patients with solid malignant tumors. *Cancer Cell International*, *20*(1), 115. https://doi.org/10.1186/s12935-020-01194-y

Ueda, T., Chou, H., Kawase, T., Shirakawa, H., & Yoshida, M. (2004). Acidic C-Tail of HMGB1 Is Required for Its Target Binding to Nucleosome Linker DNA and Transcription Stimulation. *Biochemistry*, *43*(30), 9901–9908. https://doi.org/10.1021/bi035975l

Ule, J., Jensen, K. B., Ruggiu, M., Mele, A., Ule, A., & Darnell, R. B. (2003). CLIP Identifies Nova-Regulated RNA Networks in the Brain. *Science*, *302*(5648), 1212–1215. https://doi.org/10.1126/science.1090095

Van Nostrand, E. L., Nguyen, T. B., Gelboin-Burkhart, C., Wang, R., Blue, S. M., Pratt, G. A., Louie, A. L., & Yeo, G. W. (2017). Robust, Cost-Effective Profiling of RNA Binding Protein Targets with Single-end Enhanced Crosslinking and Immunoprecipitation (seCLIP). In *Methods in Molecular Biology* (pp. 177–200). https://doi.org/10.1007/978-1-4939-7204-3_14

Vivekanadhan, S., & Mukhopadhyay, D. (2019). Divergent roles of Plexin D1 in cancer. *Biochimica et Biophysica Acta (BBA) - Reviews on Cancer*, *1872*(1), 103–110. https://doi.org/10.1016/j.bbcan.2019.05.004

Wagstaff, L. (2011). The roles of ADAMTS metalloproteinases in tumorigenesis and metastasis. *Frontiers in Bioscience*, *16*(1), 1861. https://doi.org/10.2741/3827

Wang, D., Du, X., Bai, T., Chen, M., Chen, J., Liu, J., Li, L., Li, H., & Zhang, C. (2019). Decreased Expression of Long Non-Coding RNA GMDS Divergent Transcript (GMDS-DT) is a Potential Biomarker for Poor Prognosis of Hepatocellular Carcinoma. *Medical Science Monitor*, *25*, 6221–6229. https://doi.org/10.12659/MSM.917663

Wang, H., Fu, Z., Dai, C., Cao, J., Liu, X., Xu, J., Lv, M., Gu, Y., Zhang, J., Hua, X., Jia, G., Xu, S., Jia, X., & Xu, P. (2016). LncRNAs expression profiling in normal ovary, benign ovarian cyst and malignant epithelial ovarian cancer. *Scientific Reports*, *6*(1), 38983. https://doi.org/10.1038/srep38983

Wang, J., Liu, B., Cao, J., Zhao, L., & Wang, G. (2022). MIR31HG Expression Predicts Poor Prognosis and Promotes Colorectal Cancer Progression. *Cancer Management and Research*, *14*, 1973–1986. https://doi.org/10.2147/CMAR.S351928

Wang, J., Yu, Z., Wang, J., Shen, Y., Qiu, J., & Zhuang, Z. (2020). LncRNA NUTM2A-AS1 positively modulates TET1 and HIF-1A to enhance gastric cancer tumorigenesis and drug resistance by sponging miR-376a. *Cancer Medicine*, *9*(24), 9499–9510. https://doi.org/10.1002/cam4.3544

Wang, J., Zha, J., & Wang, X. (2021). Knockdown of lncRNA NUTM2A-AS1 inhibits lung adenocarcinoma cell viability by regulating the miR-590-5p/METTL3 axis.

Oncology Letters, *22*(5), 798. https://doi.org/10.3892/ol.2021.13059

Wang, J., Zhang, H.-M., Dai, Z.-T., Huang, Y., Liu, H., Chen, Z., Wu, Y., & Liao, X.-H. (2022). MKL-1-induced PINK1-AS overexpression contributes to the malignant progression of hepatocellular carcinoma via ALDOA-mediated glycolysis. *Scientific Reports*, *12*(1), 21283. https://doi.org/10.1038/s41598-022-24023-w

Wang, R., Ma, Z., Feng, L., Yang, Y., Tan, C., Shi, Q., Lian, M., He, S., Ma, H., & Fang, J. (2018). LncRNA MIR31HG targets HIF1A and P21 to facilitate head and neck cancer cell proliferation and tumorigenesis by promoting cell-cycle progression. *Molecular Cancer*, *17*(1), 162. https://doi.org/10.1186/s12943-018-0916-8

Wang, R. N., Green, J., Wang, Z., Deng, Y., Qiao, M., Peabody, M., Zhang, Q., Ye, J., Yan, Z., Denduluri, S., Idowu, O., Li, M., Shen, C., Hu, A., Haydon, R. C., Kang, R., Mok, J., Lee, M. J., Luu, H. L., & Shi, L. L. (2014). Bone Morphogenetic Protein (BMP) signaling in development and human diseases. *Genes & Diseases*, *1*(1), 87–105. https://doi.org/10.1016/j.gendis.2014.07.005

Wang, Z.-Q., Sun, X.-L., Wang, Y.-L., & Miao, Y.-L. (2021). Agrin promotes the proliferation, invasion and migration of rectal cancer cells via the WNT signaling pathway to contribute to rectal cancer progression. *Journal of Receptors and Signal Transduction*, *41*(4), 363–370. https://doi.org/10.1080/10799893.2020.1811325

Wei, J., Yu, H., Liu, T., Wang, Z., Lang, C., & Pan, Y. (2023). FOXA1-induced LINC00621 promotes lung adenocarcinoma progression via activating the TGF-β signaling pathway. *Thoracic Cancer*, *14*(21), 2026–2037. https://doi.org/10.1111/1759-7714.14986

Xie, P., & Guo, Y. (2020). LINC00205 promotes malignancy in lung cancer by recruiting FUS and stabilizing CSDE1. *Bioscience Reports*, *40*(10). https://doi.org/10.1042/BSR20190701

Xing, Z., Li, S., Xing, J., Yu, G., Wang, G., & Liu, Z. (2022). Silencing of LINC01963 enhances the chemosensitivity of prostate cancer cells to docetaxel by targeting the miR-216b-5p/TrkB axis. *Laboratory Investigation*, *102*(6), 602–612. https://doi.org/10.1038/s41374-022-00736-4

Xu, S., Xu, H., Wang, W., Li, S., Li, H., Li, T., Zhang, W., Yu, X., & Liu, L. (2019). The role of collagen in cancer: from bench to bedside. *Journal of Translational Medicine*, *17*(1), 309. https://doi.org/10.1186/s12967-019-2058-1

Yadav, N., Sunder, R., Desai, S., Dharavath, B., Chandrani, P., Godbole, M., & Dutt, A. (2022). Progesterone modulates the DSCAM-AS1/miR-130a/ESR1 axis to suppress cell invasion and migration in breast cancer. *Breast Cancer Research*, *24*(1), 97. https://doi.org/10.1186/s13058-022-01597-x

Yamanaka, Y., Faghihi, M. A., Magistri, M., Alvarez-Garcia, O., Lotz, M., & Wahlestedt, C. (2015). Antisense RNA Controls LRP1 Sense Transcript Expression through Interaction with a Chromatin-Associated Protein, HMGB2. *Cell Reports*, *11*(6), 967–976. https://doi.org/10.1016/j.celrep.2015.04.011

Yang, D., Qu, F., Cai, H., Chuang, C.-H., Lim, J. S., Jahchan, N., Grüner, B. M., S Kuo, C., Kong, C., Oudin, M. J., Winslow, M. M., & Sage, J. (2019). Axon-like protrusions promote small cell lung cancer migration and metastasis. *ELife*, *8*. https://doi.org/10.7554/eLife.50616

Ye, T., Zhang, N., Wu, W., Yang, B., Wang, J., Huang, W., & Tang, D. (2019). SNHG14 promotes the tumorigenesis and metastasis of colorectal cancer through

miR-32-5p/SKIL axis. *In Vitro Cellular & Developmental Biology - Animal*, *55*(10), 812–820. https://doi.org/10.1007/s11626-019-00398-5

Yin, G., Tian, P., BuHe, A., Yan, W., Li, T., & Sun, Z. (2020). LncRNA LINC00689 Promotes the Progression of Gastric Cancer Through Upregulation of ADAM9 by Sponging miR-526b-3p. *Cancer Management and Research*, *12*, 4227–4239. https://doi.org/10.2147/CMAR.S231042

Yin, L., & Wang, Y. (2021). Long non-coding RNA NEAT1 facilitates the growth, migration, and invasion of ovarian cancer cells via the let-7 g/MEST/ATGL axis. *Cancer Cell International*, *21*(1), 437. https://doi.org/10.1186/s12935-021-02018-3

Yin, Y., Zheng, W., Zhang, X., Chen, Y., & Tuo, Y. (2020). LINC00346 promotes hepatocellular carcinoma progression via activating the JAK-STAT3 signaling pathway. *Journal of Cellular Biochemistry*, *121*(1), 735–742. https://doi.org/10.1002/jcb.29319

Yong, W., Yu, D., Jun, Z., Yachen, D., Weiwei, W., Midie, X., Xingzhu, J., & Xiaohua, W. (2018). Long noncoding RNA NEAT1, regulated by LIN28B, promotes cell proliferation and migration through sponging miR-506 in high-grade serous ovarian cancer. *Cell Death & Disease*, *9*(9), 861. https://doi.org/10.1038/s41419-018-0908-z

Yuan, H., Ren, Q., Du, Y., Ma, Y., Gu, L., Zhou, J., Tian, W., & Deng, D. (2023). LncRNA miR663AHG represses the development of colon cancer in a miR663a-dependent manner. *Cell Death Discovery*, *9*(1), 220. https://doi.org/10.1038/s41420-023-01510-1

Yuan, J., Yi, K., & Yang, L. (2021). LncRNA NEAT1 promotes proliferation of ovarian cancer cells and angiogenesis of co-incubated human umbilical vein endothelial cells by regulating FGF9 through sponging miR-365. *Medicine*, *100*(3), e23423. https://doi.org/10.1097/MD.0000000000023423

Yuan, Z., Li, Y., Zhang, S., Wang, X., Dou, H., Yu, X., Zhang, Z., Yang, S., & Xiao, M. (2023). Extracellular matrix remodeling in tumor progression and immune escape: from mechanisms to treatments. *Molecular Cancer*, *22*(1), 48. https://doi.org/10.1186/s12943-023-01744-8

Zhan, J., Yang, F., Ge, C., & Yu, X. (2022). Multi-Omics Approaches Identify Necroptosis-Related Prognostic Signature and Associated Regulatory Axis in Cervical Cancer. *International Journal of General Medicine*, *15*, 4937–4948. https://doi.org/10.2147/IJGM.S366925

Zhan, T., Rindtorff, N., & Boutros, M. (2017). Wnt signaling in cancer. *Oncogene*, *36*(11), 1461–1473. https://doi.org/10.1038/onc.2016.304

Zhang, F., Luo, B.-H., Wu, Q.-H., Li, Q.-L., & Yang, K.-D. (2022). LncRNA HCG18 upregulates TRAF4/TRAF5 to facilitate proliferation, migration and EMT of epithelial ovarian cancer by targeting miR-29a/b. *Molecular Medicine*, *28*(1), 2. https://doi.org/10.1186/s10020-021-00415-y

Zhang, L., Chen, Y., Wang, Z., & Xia, Q. (2023). LncRNA PSMG3-AS1 is upregulated in prostate carcinoma and downregulates miR-106b through DNA methylation. *Systems Biology in Reproductive Medicine*, *69*(4), 264–270. https://doi.org/10.1080/19396368.2023.2187269

Zhang, L., Shi, H., Chen, H., Gong, A., Liu, Y., Song, L., Xu, X., You, T., Fan, X., Wang, D., Cheng, F., & Zhu, H. (2019). Dedifferentiation process driven by radiotherapy-induced HMGB1/TLR2/YAP/HIF-1α signaling enhances pancreatic

cancer stemness. *Cell Death & Disease*, *10*(10), 724. https://doi.org/10.1038/s41419-019-1956-8

Zhang, L., Wang, Y., Sun, J., Ma, H., & Guo, C. (2019). LINC00205 promotes proliferation, migration and invasion of HCC cells by targeting miR-122-5p. *Pathology - Research and Practice*, *215*(9), 152515. https://doi.org/10.1016/j.prp.2019.152515

Zhang, M., Yu, X., Zhang, Q., Sun, Z., He, Y., & Guo, W. (2022). MIR4435-2HG: A newly proposed lncRNA in human cancer. *Biomedicine & Pharmacotherapy*, *150*, 112971. https://doi.org/10.1016/j.biopha.2022.112971

Zhang, N., & Chen, X. (2020). A positive feedback loop involving the LINC00346/β-catenin/MYC axis promotes hepatocellular carcinoma development. *Cellular Oncology*, *43*(1), 137–153. https://doi.org/10.1007/s13402-019-00478-4

Zhang, T., Leng, Y., Duan, M., Li, Z., Ma, Y., Huang, C., Shi, Q., Wang, Y., Wang, C., Liu, D., Zhao, X., Cheng, S., Liu, A., Zhou, Y., Liu, J., Pan, Z., Zhang, H., Shen, L., & Zhao, H. (2023). LncRNA GAS5-hnRNPK axis inhibited ovarian cancer progression via inhibition of AKT signaling in ovarian cancer cells. *Discover Oncology*, *14*(1), 157. https://doi.org/10.1007/s12672-023-00764-6

Zhang, X., Shi, H., Yao, J., Li, Y., Gao, B., Zhang, Y., Wang, C., Zhou, H., & Zhang, L. (2020). FAM225A facilitates colorectal cancer progression by sponging miR-613 to regulate NOTCH3. *Cancer Medicine*, *9*(12), 4339–4349. https://doi.org/10.1002/cam4.3053

Zhao, J., Ohsumi, T. K., Kung, J. T., Ogawa, Y., Grau, D. J., Sarma, K., Song, J. J., Kingston, R. E., Borowsky, M., & Lee, J. T. (2010a). Genome-wide Identification of Polycomb-Associated RNAs by RIP-seq. *Molecular Cell*, *40*(6), 939–953. https://doi.org/10.1016/j.molcel.2010.12.011

Zhao, J., Ohsumi, T. K., Kung, J. T., Ogawa, Y., Grau, D. J., Sarma, K., Song, J. J., Kingston, R. E., Borowsky, M., & Lee, J. T. (2010b). Genome-wide Identification of Polycomb-Associated RNAs by RIP-seq. *Molecular Cell*, *40*(6), 939–953. https://doi.org/10.1016/j.molcel.2010.12.011

Zheng, S., Zhang, X., Wang, X., & Li, J. (2019). MIR31HG promotes cell proliferation and invasion by activating the Wnt/β-catenin signaling pathway in non-small cell lung cancer. *Oncology Letters*, *17*(1), 221–229. https://doi.org/10.3892/ol.2018.9607

Zheng, Z.-Q., Li, Z.-X., Zhou, G.-Q., Lin, L., Zhang, L.-L., Lv, J.-W., Huang, X.-D., Liu, R.-Q., Chen, F., He, X.-J., Kou, J., Zhang, J., Wen, X., Li, Y.-Q., Ma, J., Liu, N., & Sun, Y. (2019). Long Noncoding RNA FAM225A Promotes Nasopharyngeal Carcinoma Tumorigenesis and Metastasis by Acting as ceRNA to Sponge miR-590-3p/miR-1275 and Upregulate ITGB3. *Cancer Research*, *79*(18), 4612–4626. https://doi.org/10.1158/0008-5472.CAN-19-0799

Zhou, L., Huang, X., Zhang, Y., Wang, J., Li, H., & Huang, H. (2022). PSMG3-AS1 enhances glioma resistance to temozolomide via stabilizing c-Myc in the nucleus. *Brain and Behavior*, *12*(5). https://doi.org/10.1002/brb3.2531

Zhou, L., Jiang, H., Lin, L., Li, Y., & Li, J. (2023). lncRNA GAS5 suppression of the malignant phenotype of ovarian cancer via the miR-23a-WT1 axis. *Annals of Translational Medicine*, *11*(2), 119–119. https://doi.org/10.21037/atm-22-6394

Zhou, X., Lv, L., Zhang, Z., Wei, S., & Zheng, T. (2020). LINC00294 negatively modulates cell proliferation in glioma through a neurofilament medium-mediated

pathway via interacting with miR-1278. *The Journal of Gene Medicine*, *22*(10). https://doi.org/10.1002/jgm.3235

Zhu, P., Huang, H., Gu, S., Liu, Z., Zhang, X., Wu, K., Lu, T., Li, L., Dong, C., Zhong, C., & Zhou, Y. (2021). Long Noncoding RNA FAM225A Promotes Esophageal Squamous Cell Carcinoma Development and Progression via Sponging MicroRNA-197-5p and Upregulating NONO. *Journal of Cancer*, *12*(4), 1073–1084. https://doi.org/10.7150/jca.51292

Zirkel, A., Nikolic, M., Sofiadis, K., Mallm, J.-P., Brackley, C. A., Gothe, H., Drechsel, O., Becker, C., Altmüller, J., Josipovic, N., Georgomanolis, T., Brant, L., Franzen, J., Koker, M., Gusmao, E. G., Costa, I. G., Ullrich, R. T., Wagner, W., Roukos, V., … Papantonis, A. (2018). HMGB2 Loss upon Senescence Entry Disrupts Genomic Organization and Induces CTCF Clustering across Cell Types. *Molecular Cell*, *70*(4), 730-744.e6. https://doi.org/10.1016/j.molcel.2018.03.030

Chapter 3.

Effects of HMGB1 and HMGB2 on the transcriptome of an ovarian cancer cell line

INTRODUCTION

The precise regulation of gene expression is essential for living organisms (Orphanides & Reinberg, 2002). One of the key players in this process is the HMGB (High Mobility Group Box) family of proteins. These proteins, discovered due to their abundance in the nucleus and ability to bind DNA (Goodwin & Johns, 1973), have been shown to play multifaceted roles in chromatin organization, modulation of gene transcription, and response to various biological cues (Reeves, 2015).

Initially considered as proteins whose main function was to stabilize DNA structure, HMGB proteins have emerged as key regulators of gene expression. Although their affinity for DNA is undeniable, it has been discovered that these proteins can participate in cell signaling (Huttunen et al., 2002; Park et al., 2006) and collaborate in the formation of transcription complexes (Rowell et al., 2012; Zwilling et al., 1995). This functional duality allows them to interact dynamically with chromatin, influencing the accessibility of transcription factors to critical gene regions.

In this chapter, we explore how HMGB1 and HMGB2 impact gene expression at the transcriptomic level in the PEO1 EOC cell line by performing RNA sequencing of siRNA-mediated knockdown and control conditions, with special interest in lncRNAs. Silencing of HMGB1 and HMGB2 could lead to changes in the transcription of specific genes and ultimately to alterations in the cellular pathways regulated by these genes. Therefore, the knockdown of these proteins is expected to reveal crucial information about their role in the finely tuned coordination of gene expression. This approach not only shows the consequences directly mediated by HMGB1 and HMGB2, but also the indirect effects of the regulatory networks in which their targets are involved; for instance, by regulating other transcription factors or lncRNAs. Within the gene regulation landscape, lncRNAs emerge as essential yet largely unexplored regulators due to their previous consideration of “junk” DNA (H. Wang et al., 2020). We pay particular attention to the modulation of lncRNAs in response to HMGB1 and HMGB2 knockdown. By analyzing how these lncRNAs respond to a decrease in the levels of these proteins, we

can predict their potential involvement in HMGB1 and HMGB2-mediated gene expression regulation. The findings of this study not only enrich our understanding of how these regulatory proteins modulate lncRNA expression but also shed light on new layers of complexity in the regulation of gene expression in EOC.

MATERIALS AND METHODS

Cell culture

The PEO1 cell line was obtained from the American Type Culture Collection (ATCC) and maintained at 37°C in 5% CO_2 in air in a humidified incubator in Roswell Park Memorial Institute (RPMI) 1610 medium (Lonza Biologics) supplemented with 10% heat-inactivated FBS (Gibco) and 1% penicillin-streptomycin (Gibco).

siRNA and plasmid transfection

PEO1 cells were transfected with a pool of four small interfering (si)RNA oligonucleotides targeting HMGB1 (L-018981-00-0005: 5'-CAAACUCAUUCAUUAGUCA-3'; 5'-CAAAGCAUGGGAUUAUUAG-3'; 5'-CCACUUACAUUUACAAACU-3'; and 5'- CGAAAUAAUUGUUGUUCUG-3'), and HMGB2 (L-011689-00-0005: 5'-GCAAAGAAAUUGGGUGAAA-3'; 5'-GAACAUCGCCCAAAGAUCA-3'; 5'- GAAUAAAUGGCUAUCCUUU-3'; and 5'-GAAGAAGAACGAACCAGAA-3'), as well as a pool of non-targeting sequences as a control (D-001810-10-05: 5'-UGGUUUACAUGUCGACUAA-3'; 5'-UGGUUUACAUGUUGUGUGA-3'; 5'-UGGUUUACAUGUUUUCUGA-3'; and 5'-UGGUUUACAUGUUUUCCUA-3'). 250,000 cells were plated per well in a 6-well plate the day before the transfection. SiRNAs and Lipofectamine 2000 were diluted separately with Opti-MEM (Gibco), incubated for 5 min at room temperature (RT), then mixed and incubated for 20 min at RT. The mixture was added to each well containing 2 mL of RPMI 1610 medium (Lonza) supplemented with FBS, having a final siRNA concentration of 50 nM. 48 hours after the transfection, cells were collected for protein and RNA extraction.

Protein extraction

Cells were detached by trypsinization, washed twice with cold 1X DPBS, and pelleted (500 x *g*, 5 min, 4°C). An equivalent volume of RIPA buffer supplemented with protease inhibitor (78429, Thermo Scientific) was added to the pellet, pipetted up and down, and incubated for 5 min on ice. Then samples were sonicated in cold for 10 min (on/off cycles of 30 s) in a Bioruptor UCD-200 (Diagenode) equipment, setting the energy in a "low" position sonicator. Lysates were centrifuged at 12.000 x *g*, 10 min, 4°C, and supernatants with the soluble protein extract were transferred to new tubes. Protein concentration was determined with bicinchoninic acid (BCA) assay (23227, Thermo Scientific) by interpolation using a bovine serum albumin standard curve of known protein concentrations.

Western blot

Equal amounts of total protein were subjected to 10% SDS-PAGE. The gel was transferred in semi-dry conditions into an activated PVDF membrane (Cytiva, 10600023), and blocked for 1 hour in 5% skimmed powdered milk in 0.1% Tween PBS (137 mM NaCl, 2.7 mM KCl, 10 mM Na_2HPO_4, 1.8 mM KH_2PO_4). Membranes were incubated overnight at 4°C in rotation in a 1:1,000 dilution of HMGB1 (ab18256, Abcam), HMGB2 (ab67282, Abcam), or β-actin (sc-47778, Santa Cruz) antibodies in the same powdered milk solution. Protein G, HRP conjugate (Millipore) was used as the secondary antibody. Images were obtained using Gel Doc XR+ equipment (BioRad).

RNA extraction and RT-qPCR

Total RNA for checking the silencing and RNA-Seq was extracted using a Direct-zol RNA miniprep kit (R2053, Zymo Research). 1 µg of RNA was converted in cDNA using Maxima Reverse Transcriptase kit (EP0741, Thermo Scientific), and then 15 ng of cDNA were added in each qPCR reaction using Luna qPCR Master Mix (M3003S, New England BioLabs). The primers used are the following: HMGB1-F, 5'-TCAAAGGAGAACATCCTGGCC-3'; HMGB1-R, 5'-GCTTGTCATCTGCAGCAGTGTT-

3'; HMGB2-F, 5'-GAGCAGTCAGCCAAAGATAAAC-3'; HMGB2-R 5'-TCCTGCTTCACTTTTGCCCTT-3'; ACTB-F, 5'-GATGAGATTGGCATGGCTTT-3'; and ACTB-R, 5'-CACCTTCACCGTTCCAGTTT-3'.

RNA-Sequencing

The quality and quantity of RNA were checked using Agilent RNA Screen Tape on the Agilent TapeStation. 150 ng of high-quality RNA (RNA Integrity Number ≥ 8.8) was used for sequencing library preparation using the Illumina TruSeq Stranded Total RNA Library prep kit according to the manufacturer's protocol (Illumina, Cat# 20020598). Briefly, after rRNA depletion and cDNA generation, the cDNAs were subjected to the 3' End Adenylation, the Adapter Ligation, and purified with AMPure beads (Beckman, Cat#A63881). The products were size selected with SPRIselect beads (Beckman, Cat#B23318) adding an equivalent volume to discard fragments shorter than 150 nucleotides. Then selected cDNAs were enriched by PCR and purified again with SPRIselect beads to generate final libraries. The quality and quantity of sequencing libraries were checked using Agilent DNA 1000 Screen Tape on the Agilent TapeStation. Paired-end sequencing was performed for ~110 cycles with an Illumina NovaSeq 6000 sequencer with a depth of 200 million reads. Filtered and adapter-trimmed reads were mapped and quantified using with STAR version 2.7.10b against the *Homo sapiens* genome (hg38 version). Differentially expressed genes were obtained using DESeq2 (Love et al., 2014) as described in previous chapters. Novel transcripts that do not have yet a gene symbol are identified by their Ensembl Gene ID.

Gene set enrichment analysis

We used the normalized counts from DESeq2 along with their Ensembl Gene IDs as input for Gene Set Enrichment Analysis software from UC San Diego and Broad Institute (Mootha et al., 2003; Subramanian et al., 2005). We separately compared siHMGB1 and siHMGB2 vs. siControl, using "Human_Ensembl_Gene_ID_ MSigDB.2023.1.Hs.chip" as chip platform, and hallmark (h.all.v2023.1.Hs.symbols.gmt)

or ontology (c5.go.bp.v2023.1.Hs.symbols.gmt) as gene sets; we selected permutation type = gene_set, and the remaining options were left by default.

Heatmap and bar plots

Heatmaps were elaborated with the “Expression” option of the online tool Heatmapper (Babicki et al., 2016), using normalized reads as input. The hierarchical clustering and the distance measurement were performed using average linkage and Pearson methods, respectively. Bar plots were created with GraphPad Prism version 8.0.2.

RESULTS

HMGB1 and HMGB2 knockdown verification

A standard small interfering RNA-mediated transient knockdown strategy was performed to study the transcriptional effects of HMGB1 and HMGB2 at the transcriptional level in the PEO1 epithelial ovarian cancer cell line. Specifically, three biological replicates, namely *A*, *B*, and *C*, were included, as depicted in Figure 1. Although knockdown efficiency was higher in HMGB2, with a 90% decrease in expression, in comparison with HMGB1, which had around 75% reduction at protein and mRNA levels, both knockdowns are biologically and statistically significant in comparison with the siControl.

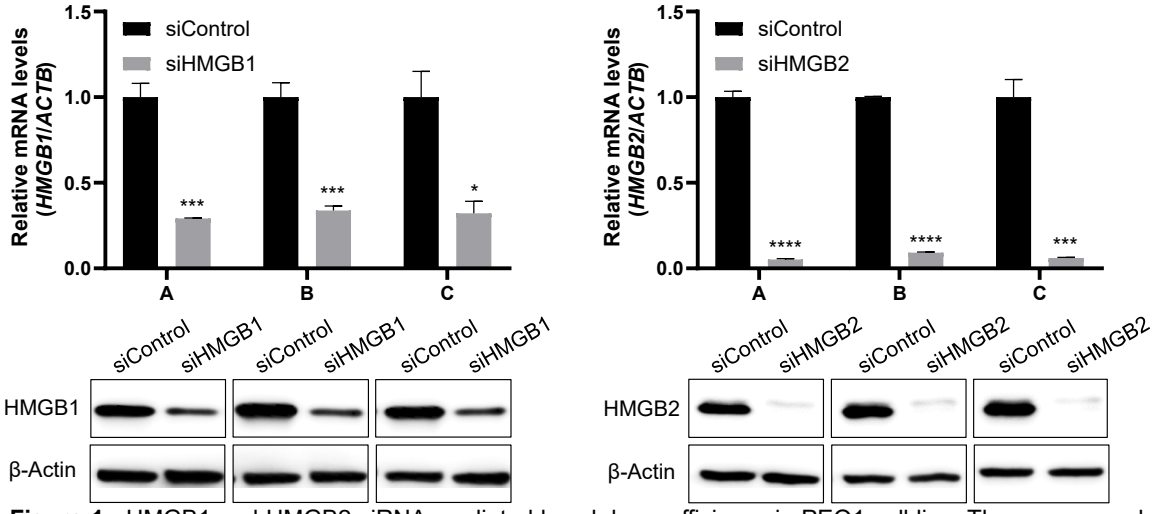

Figure 1.- HMGB1 and HMGB2 siRNA-mediated knockdown efficiency in PEO1 cell line. The upper panel consists of the mRNA levels measured by RT-qPCR using 15 ng of cDNA. The lower panel shows the protein levels in a western blot, loading 30 µg of total protein. Error bars represent the standard deviation of the mean. * $p < 0.05$, *** $p > 0.001$, **** $p > 0.0001$.

Differentially expressed genes upon HMGB1 and HMGB2 knockdown

Reads were mapped to the human genome (hg38) and two differential gene expression analyses with DESeq2 separately were carried out: one comparing siHMGB1 *versus* control and another comparing siHMGB2 *versus* control. A summary of mapping process can be found in Supplementary Materials Table S20. Selecting $|\text{Log}_2$ (Fold change)| ≥ 0.585 and *p*-value < 0.05 as cutoff values, these analyses yielded 189 upregulated and 66 downregulated genes when silencing HMGB1 (of which 68 and 18 are lncRNAs, respectively, 86 in total), whereas 480 upregulated and 421 downregulated genes were obtained when silencing HMGB2 (of which 139 and 43 are lncRNAs, respectively, 182 in total), as shown in Figure 2. The full list of the differentially expressed genes can be found in Supplementary Materials Table S21.

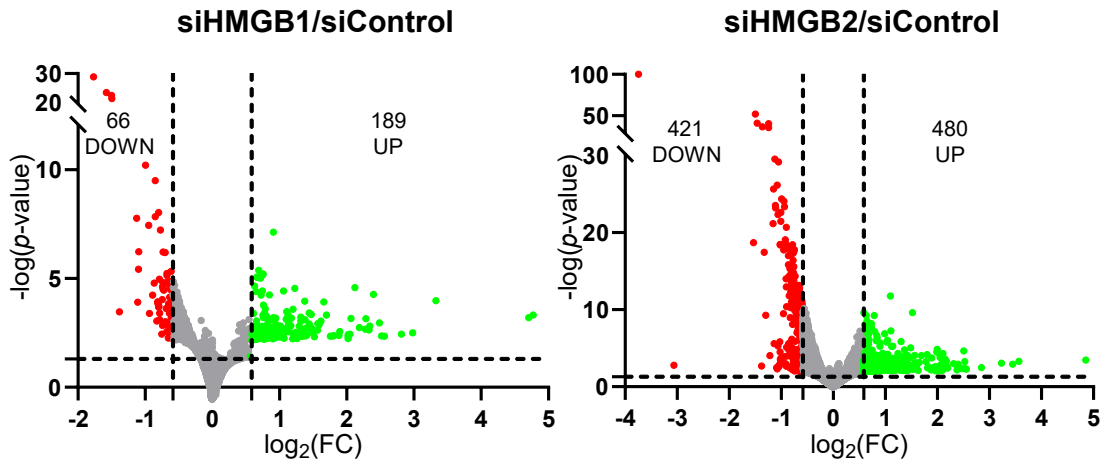

Figure 2.- Volcano plot of deregulated genes upon knockdown in PEO1 cell line measured by RNA-Seq. The horizontal dotted line represents the significance threshold of -log(p-value) = 1.301 (which is equivalent to *p*-value = 0.05). Vertical dotted lines represent the fold change threshold of $\log_2$(FC) = 0.585 and -0.585 (which is equivalent to FC = 1.5). FC, fold change.

There are 18 upregulated and 4 downregulated lncRNAs which are regulated by HMGB1 and also by HMGB2. *ENSG00000263164*, *ENSG00000273199*, *ENSG00000260254*, *LINC02128*, *ENSG00000287514*, *LINC00840*, *ENSG00000258464*, *LINC03010*, *ENSG00000264673*, *ENSG00000237530*, *ENSG00000270002*, *LINC02423*, *ENSG00000286550*, *ENSG00000254160*, *ENSG00000223884*, *KAZN-AS1*, *ENSG00000259881*, and *ENSG00000277997* are upregulated, whereas *ENSG00000269399*, *ENSG00000264895*, *SMC2-DT*, and *HIF1A-AS3* are downregulated when the levels of either HMGB1 or HMGB2 are decreased.

The most relevant data were plotted in two heatmaps (Figure 3) to represent the clustering of the deregulated lncRNAs, their relative expression levels, as well as the reproducibility across the three replicates for each condition. The lncRNAs depicted in each heatmap include 86 lncRNAs deregulated after HMGB1 silencing or HMGB2 silencing with the lowest *p*-value. Upregulated and downregulated genes are clearly clustered in two differentiated groups.

Figure 3.- Expression heatmaps of the lncRNAs deregulated in HMGB1 or HMGB2 knockdown in the PEO1 cell line. HMGB1 heatmap (**left**) and HMGB2 heatmap (**right**). Green intensity and red intensity represent increased and decreased normalized expression values, respectively.

Gene set enrichment analysis

We analyzed the pathways and processes in which HMGB1 and HMGB2 take part in epithelial ovarian cancer cells, so we used the mapped reads of the two comparisons as input for Gene set enrichment analysis software (Mootha et al., 2003; Subramanian et al., 2005). We used two molecular signature databases in both cases: “hallmark gene sets”, represented in Figure 4 and Figure 6, and “GO biological process”, represented in Figure 5 and Figure 7.

In the hallmarks analyses, we found the term “coagulation” enriched in siHMGB1, “myogenesis” in siHMGB2, as well as “KRAS signaling down” in both siHMGB1 and siHMGB2 in comparison to the control condition. On the contrary, hallmarks enriched in control include “TNFα via NF-κβ” when compared to siHMGB1, “TGF-β signaling” when compared to siHMGB2, and “G2 to mitosis checkpoint”, “E2F targets”, “MYC targets”, “mitotic spindle”, “protein secretion”, “MTORC1 signaling pathway”, “oxidative phosphorylation”, “unfolded protein response”, and “DNA repair”, when compared to either siHMGB1 or siHMGB2.

Regarding GO biological process analyses, we observed “plasma membrane fusion”, “leukotriene biosynthetic process”, and “superoxide anion generation” enriched in siHMGB1. The term “phagocytosis recognition” was enriched in siHMGB2. The term “G-protein coupled receptor signaling coupled to cyclic nucleotide secondary messenger” was enriched in both siHMGB1 and siHMGB2. On the other hand, we found “sister chromatid segregation”, “ribosome biogenesis”, “RNA localization”, “RNA splicing” or “mRNA processing”, “regulation of telomere maintenance” or “regulation of telomere maintenance organization” that are enriched in the control condition in comparison to siHMGB1 or siHMGB2, whereas “cytoplasmic translation”, “tRNA modification”, and “cell cycle checkpoint” were enriched specifically only when comparing the control *versus* siHMGB2.

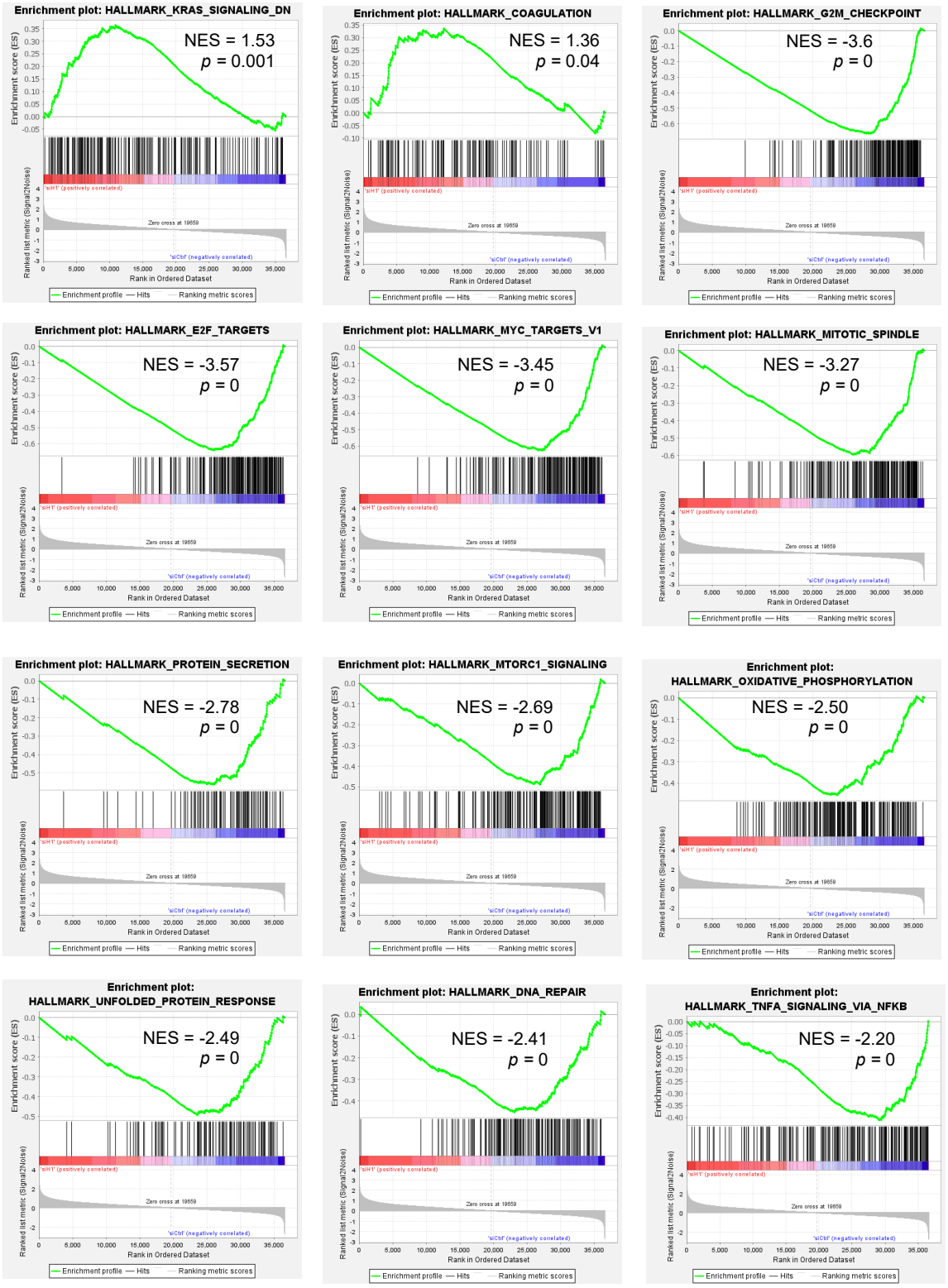

Figure 4.- Gene set enrichment analysis human hallmarks for HMGB1. NES, normalized enrichment score; *p*, *p*-value.

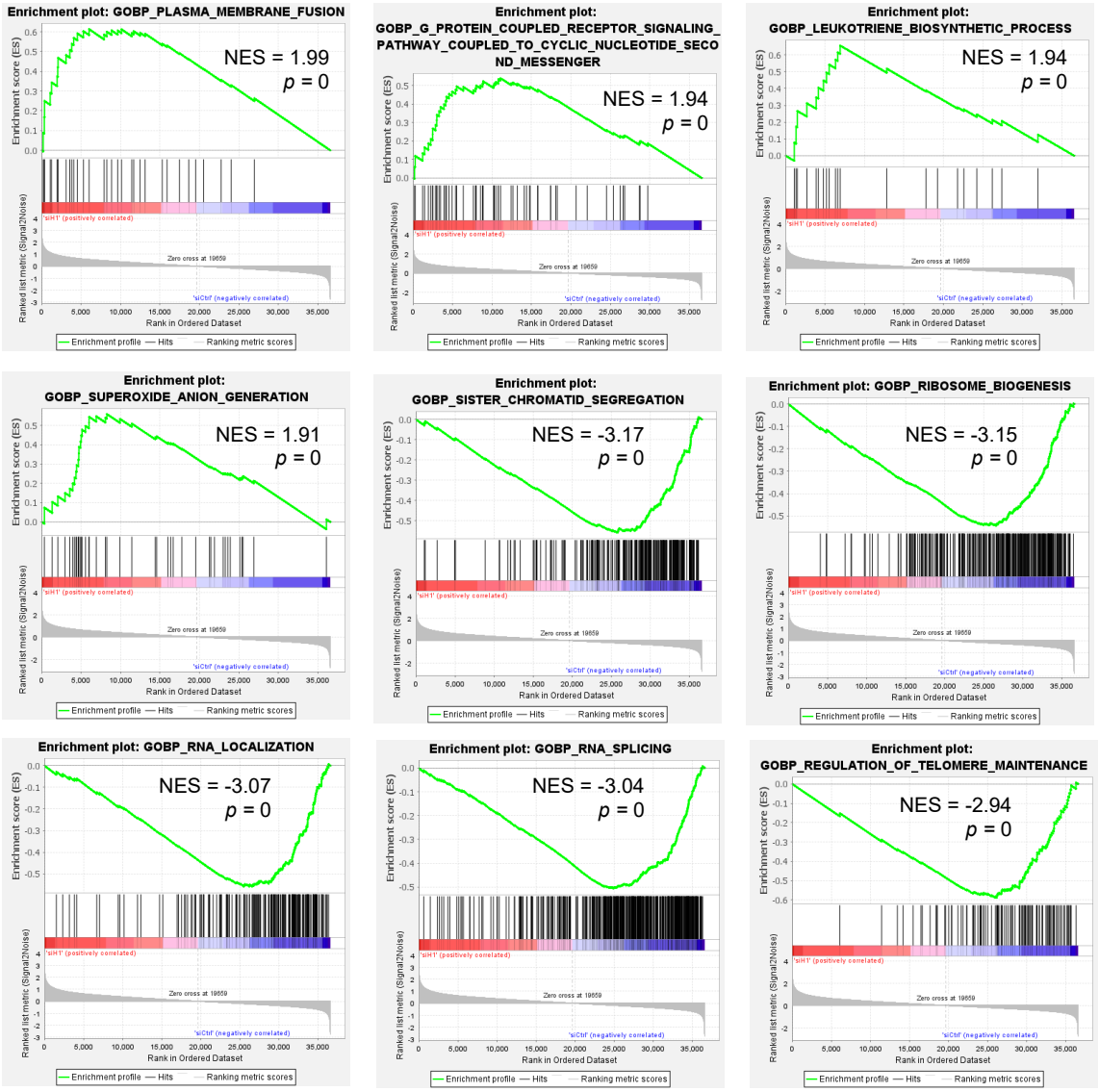

Figure 5.- Gene set enrichment analysis gene ontology biological process for HMGB1. NES, normalized enrichment score; *p*, *p*-value.

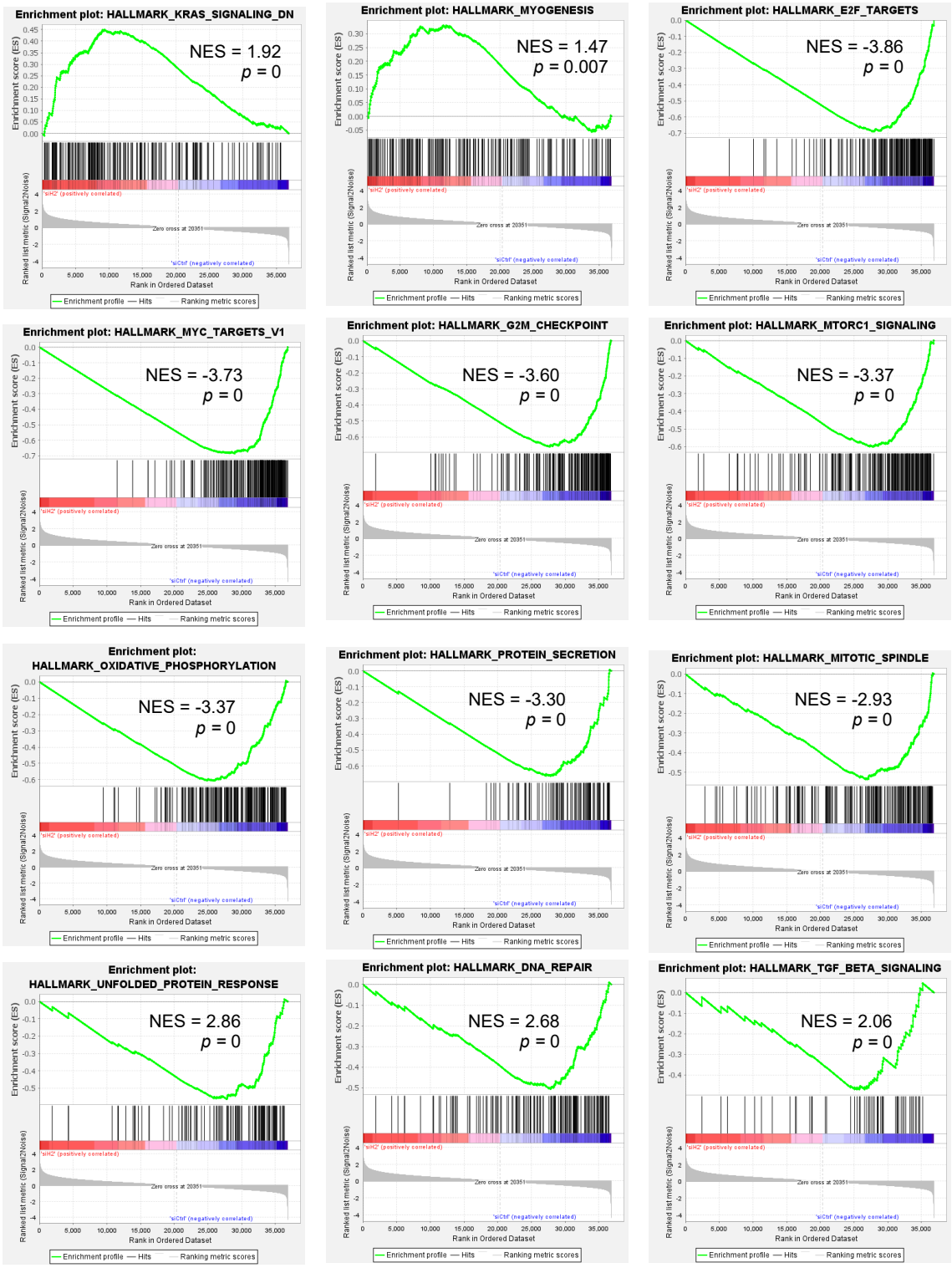

Figure 6.- Gene set enrichment analysis human hallmarks for HMGB2. NES, normalized enrichment score; *p*, *p*-value.

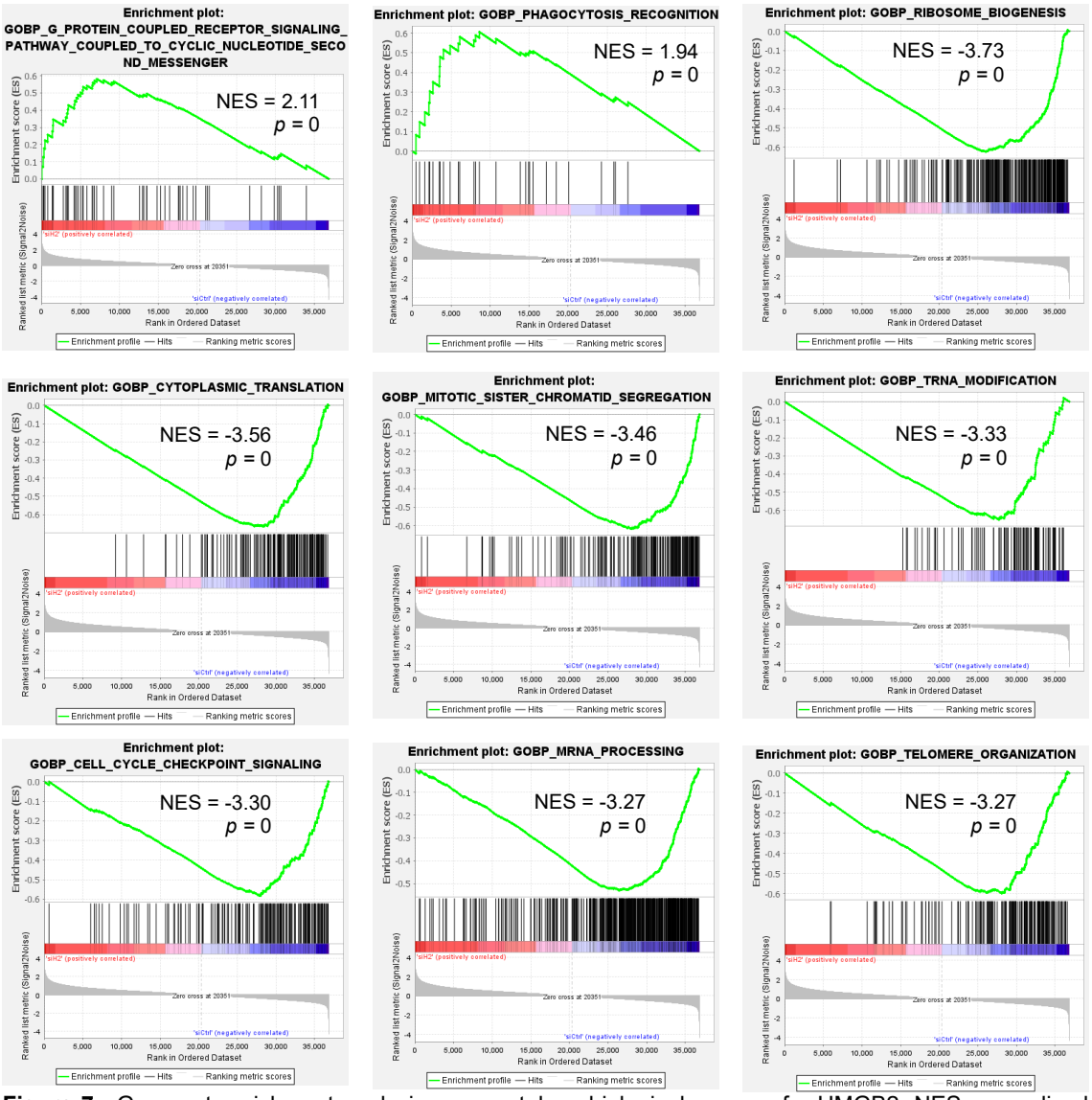

Figure 7.- Gene set enrichment analysis gene ontology biological process for HMGB2. NES, normalized enrichment score; *p*, *p*-value.

DISCUSSION

In this chapter, we present the effects observed on the transcriptome of the high-grade serous epithelial ovarian cancer cell line PEO1, in an siRNA-mediated loss-of-function model of HMGB1 and HMGB2 proteins. After successfully obtaining the knockdown in triplicates and proceeding with library preparation, sequencing, and data analysis, the identification of lncRNAs regulated by HMGB1 and/or HMGB2, as well as their connections with EOC, found in the literature or previous chapters of this Thesis, are discussed. Besides, these data also contribute to increasing our knowledge about the control that HMGB1 and HMGB2 exert in the regulation of biological functions and signaling pathways in this model.

The functions of lncRNAs that are deregulated in the siHMGB1 and siHMGB2 PEO1 models

The vast majority of the deregulated lncRNAs found in this model had not been previously related to EOC, although they had been previously related to other cancer types or diseases.

Among those upregulated in siHMGB1, we found *STARD13-AS* and *SIRLNT*. *STARD13-AS* suppresses proliferation and metastasis in colorectal cancer (Yang et al., 2019). *SIRLNT*, also known as lncRNA-PRLB, promotes breast cancer by regulating the miR-4766-5p/SIRT1 axis (Liang et al., 2018).

Eight of those lncRNAs upregulated in siHMGB2, *LINC00964*, *MIAT*, *LINC00668*, *LINC01108*, *LINC00654*, *CTBP1-AS*, *DBH-AS1*, and *CARMN*, were described in other cancers. *LINC00964* is upregulated in the plasma of head and neck squamous cell carcinoma patients compared with those in volunteers without the disease (Yao et al., 2018). The lncRNA *MIAT* (Myocardial Infarction Associated Transcript) has been associated with multiple types of cancers, including gastric, liver, colorectal, esophageal, pancreatic, breast, cervical, lung, among others, showing oncogenic properties (Da et al., 2020). *LINC00668* promotes colorectal (Yan et al., 2019) and non-small cell lung (An et al., 2019) cancers by regulating miR-188-5p/USP47 and miR-193a/KLF7 axes, respectively, as well as breast cancer by interacting with the protein SND1 (Qian et al., 2020). *LINC01108*, also known as *lncRNA-ES1*, promotes breast cancer progression by downregulating OCT4 and SOX2 leading to a decrease in the levels of their targets miR-302 and miR-106b (Keshavarz & Asadi, 2019). *LINC00654* is implicated in sorafenib resistance by recruiting STAT3 to activate SLC7A11 transcription thereby inhibiting ferroptosis in hepatocellular carcinoma (Peng et al., 2023). *CTBP1-AS* is responsive to androgens and promotes prostate cancer by recruiting PSF to the promoter of its sense transcript and repressing in *cis* its transcription (Takayama et al., 2013). *DBH-AS1* promotes diffuse large B-cell lymphoma by interacting with BUD13 to stabilize FN1 mRNA (Song et al., 2020), and hepatocellular carcinoma by activating mitogen-activated

protein kinase signaling (Huang et al., 2015). LncRNA *CARMN* (Cardiac Mesoderm Enhancer-Associated) overexpression correlates with improved prognosis and chemosensitivity of triple-negative breast cancer via acting as miR143-3p host gene, which will sponge MCM5, and inhibiting DNA replication (Sheng et al., 2021). It also inhibits cervical cancer cell growth by sponging miR-92a-3p to prevent the degradation of BTG2 mRNA and ultimately affects the Wnt/β-catenin pathway (L. Wang et al., 2023). The fusion transcript *CARMN-NOTCH2* leads to high NOTCH2 expression in glomus tumors of the upper digestive tract (Girard et al., 2021).

We also found in the literature information about *ADIRF-AS1*, *SFTA1P*, *MIR23AHG*, *MIR503HG*, and *ZNF674-AS1*, which are downregulated in siHMGB1. The circadian clock-regulated lncRNA *ADIRF-AS1* (Adipogenesis Regulatory Factor antisense 1) promotes clear cell carcinoma by binding the PBRM1-containing PBAF complex as well as affecting the extracellular matrix (Brooks et al., 2022). *ADIRF-AS1* also promotes oncogenic phenotypes *in vitro* and *in vivo* by sponging miR-761 to upregulate IRS1 in a model of osteosarcoma (Xu et al., 2022). Additionally, it is upregulated in non-small-cell lung carcinoma (Yu et al., 2015) and its expression is also correlated with poor prognosis in osteosarcoma and colorectal cancer (Lu et al., 2021; Xu et al., 2022). The pseudogene-derived lncRNA *SFTA1P* (Surfactant Associated 1) is upregulated in lung cancers (Du et al., 2020), affecting the survival of lung squamous cell carcinoma (Xiong et al., 2019); mechanistically, *SFTA1P* mediates positive feedback regulation of the Hippo-YAP/TAZ signaling pathway in a TEAD-dependent manner to promote non-small cell lung cancer (Zhu et al., 2021). It also contributes to cervical cancer progression by interaction with PTBP1 to facilitate TPM4 mRNA degradation (Luo et al., 2022). Oppositely, *SFTA1P* plays a tumor-suppressive role in gastric cancer by inhibiting cell proliferation, migration, and invasion (Ma et al., 2018). The lncRNA miR-23A host gene, *MIR23AHG*, which is downregulated upon HMGB1 knockdown, was discovered to affect migration in a lung cancer model using a CRISPR-mediated

knockout library (Esposito et al., 2022). *MIR503HG* acts as a tumor suppressor in triple-negative breast cancer by regulating miR-224-5p/HOXA9 axis (S.-M. Wang et al., 2021), whereas it acts as an oncogene in non-small cell lung cancer by regulating miR-489-3p and miR-625-5p (Dao et al., 2020). *ZNF674-AS1* acts as a tumor suppressor in the thyroid (Le et al., 2022), gastric (Ye & Wang, 2022), non-small cell lung (Y. Liu et al., 2021), and hepatic (Li et al., 2022) cancers.

The only lncRNA downregulated in siHMGB2 that was reported in the literature was *CHASERR*. Also known as *LINC01578*, it affects the radiation resistance of lung cancer cells by regulating microRNA-216b-5p/TBL1XR1 axis (P. Wang et al., 2022) and drives colon cancer metastasis through a positive feedback loop with the NF-κβ/YY1 axis (J. Liu et al., 2020).

Among lncRNAs deregulated in our model, only two had been previously related to ovarian cancer. *MIR503HG*, which is downregulated in siHMGB1, acts as a tumor suppressor in ovarian cancer by interacting with SPI1 to prevent TMEFF1 transcription (Tian et al., 2022). *HIF1A-AS3*, downregulated in siHMGB1 and siHMGB2, is induced in hypoxia, regulates its sense transcript HIF1A by *cis* regulation in endothelial cells (Downes et al., 2023), and promotes ovarian cancer progression through its binding to YBX1, resulting in p21 and AJAP1 transcriptions suppression (Xie et al., 2023).

Comparison of the lncRNAs regulated by HMGB1 and/or HMGB2 in PEO1 with data described in previous chapters

The results from this study were compared with those from the other two previous chapters, deregulated lncRNAs arising from the meta-analysis from EOC patient cohorts described in Chapter 1, and lncRNAs identified in the HMGB1-HMGB2 RNA interactome described in Chapter 2.

We found several concordances between the data obtained in the transcriptome of siHMGB1 and siHMGB2 in the PEO1 cell line and transcriptome analyses from EOC

patients studied in Chapter 1. Downregulation as a consequence of the knockdown of HMGB proteins and upregulation in EOC patients is expected for those lncRNAs positively involved in carcinogenesis and whose expression is induced by HMGB1 or HMGB2. *ENSG00000269399*, which is downregulated in both siHMGB1 and siHMGB2, is upregulated in three patient cohorts from the diagnostic category (GSE190688, GSE119054, and GSE137238, and shown in Chapter 1 Table 1). *ENSG00000272990*, which is downregulated in siHMGB2, is also upregulated in peritoneal metastasis when compared to the primary tumor (GSE137237 and shown in Supplementary Materials Table S8).

The overlap between the lncRNA genes identified in the HMGB1/2 RNA interactome (Chapter 2) and lncRNAs whose transcription is regulated by HMGB1 and/or HMGB2 (this chapter) is low. Indeed, physical and genetic interactions might be alternative forms by which HMGB proteins and related lncRNAs control cellular functions. *LINC03013* (upregulated in siHMGB1), *MIR503HG* (downregulated in siHMGB1), and *ENSG00000259881* (upregulated in siHMGB1 and siHMGB2) are present in the catRAPID candidates as possible interactors with HMGB1, whereas *DSP-AS1* (downregulated in siHMGB2) and *LINC02981* (upregulated in siHMGB2) are present in the catRAPID candidates as possible interactors with HMGB2. Finally, from the experimental approaches, we only found *ENSG00000287023*, downregulated in siHMGB2, enriched in the HMGB1 eCLIP experiment.

A transcriptomic view of HMGB1 and HMGB2 functions in the siHMGB1 and siHMGB2 PEO1 model

We pursued to find out in which pathways HMGB1 and HMGB2 are involved in this particular cell model and genetic background. For this purpose, we analyzed the RNA-Seq counts with the Gene Set Enrichment Analysis tool using human hallmarks (Liberzon et al., 2015) and gene ontology (Ashburner et al., 2000) biological processes from the Human Molecular Signatures Database (MSigDB).

From the hallmark gene sets, it turns out that the proto-oncogene KRAS has a G-quadruplex within its promoter and HMGB1 has been described to bind and stabilize it (Amato et al., 2018). Considering that biological data showed that the silencing of HMGB1 increases *KRAS* expression (Amato et al., 2018), our results showing that KRAS down-regulated target genes are enriched in the siHMGB1 condition support the hypothesis that HMGB1 negatively regulates KRAS transcription. This model could also apply to HMGB2 as it has been also described to interact with G-quadruplex (Zhang et al., 2021), and “KRAS signaling” is also enriched in siHMGB2. The ability of HMGB1 and HMGB2 to recognize G-quadruplexes is directly related to “telomere maintenance” or “telomere organization”, hallmarks that are enriched in the control condition when compared to either siHMGB1 or siHMGB2, as telomeres also present G-quadruplexes (Amato et al., 2019; Kučírek et al., 2019). The maintenance of telomeres, of which the telomerase enzyme is responsible, is essential for cancer cells to overcome replicative senescence and gain replicative immortality (H.-C. Fan et al., 2021), one of the hallmarks of cancer (Hanahan & Weinberg, 2011).

The finding of the enriched hallmark “superoxide anion generation” in the control condition in comparison with siHMGB1, supports previous data describing that extracellular HMGB1 increases reactive oxygen species (ROS) through the interaction with TLR4 to trigger MyD88-IRAK4-p38 and Akt signaling pathways and eventually inhibiting NAD(P)H oxidase (J. Fan et al., 2007). Additionally, three cysteine residues enable HMGB1 and HMGB2 to get oxidized or reduced depending on the redox state of the cell (reviewed by Barreiro-Alonso et al., 2016).

Regarding other hallmarks, “coagulation“, which is enriched in siHMGB1, could be of interest for further studies because of its relationship with immune checkpoint inhibitors, since coagulation factors, such as tissue factor or Factor X induce immune evasion, whereas the anticoagulant rivaroxaban increases infiltration and improves anti-PD-1 therapy (Bauer et al., 2022). The “myogenesis” hallmark, which is enriched in

siHMGB2, could be relevant in the study of the molecular mechanisms causing cachexia, which consists on muscle loss due to impairment and wasting of myogenesis, a process mediated by chemokines derived from the tumor microenvironment like CXCL1 (Hogan et al., 2018).

Other hallmarks are also related to known HMGB functions or cancer. “G2/M phase” and “E2F targets” are enriched in control versus siHMGB1 or siHMGB2. HMGB1 interacts with retinoblastoma protein to repress E2F and cyclin A transcription repression in breast cancer to suppress growth and increase radiosensitivity (Jiao et al., 2007). Also, decreased gene expression was observed for Tc1d8, cyclin B3, Rb1, cyclin A1, E2f2, and Bub1, which are crucial regulators of cell cycle progression, especially in the G1/S and G2/M phases, in HMGB2 knockout mouse liver cells (Yano et al., 2022).

In the analysis of GO terms related to biological processes, we found the “RNA processing” and “ribosome biogenesis”, which are enriched in the control condition in comparison to siHMGB1 or siHMGB2. These results are in accordance with previous data from our laboratory based on proteomic approaches, which linked the HMGB1 interactome to the NuRD, THOC, and septin complexes (Barreiro-Alonso et al., 2021). Also supporting these results, HMGB2 expression was described to be induced after nucleolar stress, a situation in which ribosomal gene transcription is repressed (Bianco & Mohr, 2019). In connection with the mitotic spindle biological process, HMGB1 and HMGB2 interact through their HMG box domains with the mitotic spindle in cervical cancer or glioma cells (Jia et al., 2019; Pallier et al., 2003).

Altogether, the results drawn from this chapter broadened the scope of regulatory targets and processes in which HMGB1 and/or HMGB2 are involved in the context of epithelial ovarian cancer, particularly in high-grade serous, as the cell line used belongs to this histological subtype. However, the precise mechanism by which all these features take place is still yet to be determined in future studies.

SUPPLEMENTARY MATERIALS AVAILABILITY

Chapter 3 includes Supplementary Tables S20 and S21, which are contained in the electronic support attached to this Thesis.

REFERENCES

Amato, J., Cerofolini, L., Brancaccio, D., Giuntini, S., Iaccarino, N., Zizza, P., Iachettini, S., Biroccio, A., Novellino, E., Rosato, A., Fragai, M., Luchinat, C., Randazzo, A., & Pagano, B. (2019). Insights into telomeric G-quadruplex DNA recognition by HMGB1 protein. *Nucleic Acids Research*, *47*(18), 9950–9966. https://doi.org/10.1093/nar/gkz727

Amato, J., Madanayake, T. W., Iaccarino, N., Novellino, E., Randazzo, A., Hurley, L. H., & Pagano, B. (2018). HMGB1 binds to the KRAS promoter G-quadruplex: a new player in oncogene transcriptional regulation? *Chemical Communications*, *54*(68), 9442–9445. https://doi.org/10.1039/C8CC03614D

An, Y., Shang, Y., Xu, Z., Zhang, Q., Wang, Z., Xuan, W., & Zhang, X. (2019). STAT3-induced long noncoding RNA LINC00668 promotes migration and invasion of non-small cell lung cancer via the miR-193a/KLF7 axis. *Biomedicine & Pharmacotherapy*, *116*, 109023. https://doi.org/10.1016/j.biopha.2019.109023

Ashburner, M., Ball, C. A., Blake, J. A., Botstein, D., Butler, H., Cherry, J. M., Davis, A. P., Dolinski, K., Dwight, S. S., Eppig, J. T., Harris, M. A., Hill, D. P., Issel-Tarver, L., Kasarskis, A., Lewis, S., Matese, J. C., Richardson, J. E., Ringwald, M., Rubin, G. M., & Sherlock, G. (2000). Gene Ontology: tool for the unification of biology. *Nature Genetics*, *25*(1), 25–29. https://doi.org/10.1038/75556

Babicki, S., Arndt, D., Marcu, A., Liang, Y., Grant, J. R., Maciejewski, A., & Wishart, D. S. (2016). Heatmapper: web-enabled heat mapping for all. *Nucleic Acids Research*, *44*(W1), W147–W153. https://doi.org/10.1093/nar/gkw419

Barreiro-Alonso, A., Lamas-Maceiras, M., Lorenzo-Catoira, L., Pardo, M., Yu, L., Choudhary, J. S., & Cerdán, M. E. (2021). HMGB1 Protein Interactions in Prostate and Ovary Cancer Models Reveal Links to RNA Processing and Ribosome Biogenesis through NuRD, THOC and Septin Complexes. *Cancers*, *13*(18), 4686. https://doi.org/10.3390/cancers13184686

Barreiro-Alonso, A., Lamas-Maceiras, M., Rodríguez-Belmonte, E., Vizoso-Vázquez, Á., Quindós, M., & Cerdán, M. E. (2016). High Mobility Group B Proteins, Their Partners, and Other Redox Sensors in Ovarian and Prostate Cancer. *Oxidative Medicine and Cellular Longevity*, *2016*, 1–17. https://doi.org/10.1155/2016/5845061

Bauer, A. T., Gorzelanny, C., Gebhardt, C., Pantel, K., & Schneider, S. W. (2022). Interplay between coagulation and inflammation in cancer: Limitations and therapeutic opportunities. *Cancer Treatment Reviews*, *102*, 102322. https://doi.org/10.1016/j.ctrv.2021.102322

Bianco, C., & Mohr, I. (2019). Ribosome biogenesis restricts innate immune responses to virus infection and DNA. *ELife*, *8*. https://doi.org/10.7554/eLife.49551

Brooks, R., Monzy, J., Aaron, B., Zhang, X., Kossenkov, A., Hayden, J., Keeney, F., Speicher, D. W., Zhang, L., & Dang, C. V. (2022). Circadian lncRNA ADIRF-AS1 binds PBAF and regulates renal clear cell tumorigenesis. *Cell Reports*, *41*(3), 111514. https://doi.org/10.1016/j.celrep.2022.111514

Da, C., Gong, C.-Y., Nan, W., Zhou, K.-S., WU, Z.-L., & Zhang, H.-H. (2020). The role of long non-coding RNA MIAT in cancers. *Biomedicine & Pharmacotherapy*, *129*, 110359. https://doi.org/10.1016/j.biopha.2020.110359

Dao, R., Wudu, M., Hui, L., Jiang, J., Xu, Y., Ren, H., & Qiu, X. (2020). Knockdown of lncRNA MIR503HG suppresses proliferation and promotes apoptosis of non-small cell lung cancer cells by regulating miR-489-3p and miR-625-5p. *Pathology - Research and Practice*, *216*(3), 152823. https://doi.org/10.1016/j.prp.2020.152823

Downes, N., Niskanen, H., Tomas-Bosch, V., Taipale, M., Godiwala, M., Väänänen, M.-A., Turunen, T. A., Aavik, E., Laham-Karam, N., Ylä-Herttuala, S., & Kaikkonen, M. U. (2023). Hypoxic regulation of hypoxia inducible factor 1 alpha via antisense transcription. *Journal of Biological Chemistry*, 105291. https://doi.org/10.1016/j.jbc.2023.105291

Du, D., Shen, X., Zhang, Y., Yin, L., Pu, Y., & Liang, G. (2020). Expression of long non-coding RNA SFTA1P and its function in non-small cell lung cancer. *Pathology - Research and Practice*, *216*(9), 153049. https://doi.org/10.1016/j.prp.2020.153049

Esposito, R., Polidori, T., Meise, D. F., Pulido-Quetglas, C., Chouvardas, P., Forster, S., Schaerer, P., Kobel, A., Schlatter, J., Kerkhof, E., Roemmele, M., Rice, E. S., Zhu, L., Lanzós, A., Guillen-Ramirez, H. A., Basile, G., Carrozzo, I., Vancura, A., Ullrich, S., … Johnson, R. (2022). Multi-hallmark long noncoding RNA maps reveal non-small cell lung cancer vulnerabilities. *Cell Genomics*, *2*(9), 100171. https://doi.org/10.1016/j.xgen.2022.100171

Fan, H.-C., Chang, F.-W., Tsai, J.-D., Lin, K.-M., Chen, C.-M., Lin, S.-Z., Liu, C.-A., & Harn, H.-J. (2021). Telomeres and Cancer. *Life*, *11*(12), 1405. https://doi.org/10.3390/life11121405

Fan, J., Li, Y., Levy, R. M., Fan, J. J., Hackam, D. J., Vodovotz, Y., Yang, H., Tracey, K. J., Billiar, T. R., & Wilson, M. A. (2007). Hemorrhagic Shock Induces NAD(P)H Oxidase Activation in Neutrophils: Role of HMGB1-TLR4 Signaling. *The Journal of Immunology*, *178*(10), 6573–6580. https://doi.org/10.4049/jimmunol.178.10.6573

Girard, N., Marin, C., Hélias-Rodzewicz, Z., Villa, C., Julié, C., Lajarte-Thirouard, A., Beauce, S. M., Lagorce-Pages, C., Renaud, F., Cazals-Hatem, D., Guedj, N., Cros, J., Raffin-Sanson, M., Selves, J., Terris, B., Fléjou, J., Garchon, H., Coindre, J., & Emile, J. (2021). CARMN-NOTCH2 fusion transcript drives high NOTCH2 expression in glomus tumors of the upper digestive tract. *Genes, Chromosomes and Cancer*, *60*(11), 723–732. https://doi.org/10.1002/gcc.22981

Goodwin, G. H., & Johns, E. W. (1973). Isolation and Characterisation of Two Calf-Thymus Chromatin Non-Histone Proteins with High Contents of Acidic and Basic Amino Acids. *European Journal of Biochemistry*, *40*(1), 215–219. https://doi.org/10.1111/j.1432-1033.1973.tb03188.x

Hanahan, D., & Weinberg, R. A. (2011). Hallmarks of Cancer: The Next Generation. *Cell*, *144*(5), 646–674. https://doi.org/10.1016/j.cell.2011.02.013

Hogan, K. A., Cho, D. S., Arneson, P. C., Samani, A., Palines, P., Yang, Y., & Doles, J. D. (2018). Tumor-derived cytokines impair myogenesis and alter the skeletal muscle immune microenvironment. *Cytokine*, *107*, 9–17. https://doi.org/10.1016/j.cyto.2017.11.006

Huang, J., Ren, T., Cao, S., Zheng, S., Hu, X., Hu, Y., Lin, L., Chen, J., Zheng, L., & Wang, Q. (2015). HBx-related long non-coding RNA DBH-AS1 promotes cell proliferation and survival by activating MAPK signaling in hepatocellular carcinoma. *Oncotarget*, *6*(32), 33791–33804.

https://doi.org/10.18632/oncotarget.5667

Huttunen, H. J., Fages, C., Kuja-Panula, J., Ridley, A. J., & Rauvala, H. (2002). Receptor for advanced glycation end products-binding COOH-terminal motif of amphoterin inhibits invasive migration and metastasis. *Cancer Research*, *62*(16), 4805–4811. http://www.ncbi.nlm.nih.gov/pubmed/12183440

Jia, L., Song, H., Fan, W., Song, Y., Wang, G., Li, X., He, Y., & Yao, A. (2019). The association between high mobility group box 1 chromatin protein and mitotic chromosomes in glioma cells. *Oncology Letters*, *19*(1), 745–752. https://doi.org/10.3892/ol.2019.11170

Jiao, Y., Wang, H., & Fan, S. (2007). Growth suppression and radiosensitivity increase by HMGB1 in breast cancer. *Acta Pharmacologica Sinica*, *28*(12), 1957–1967. https://doi.org/10.1111/j.1745-7254.2007.00669.x

Keshavarz, M., & Asadi, M. H. (2019). Long non-coding RNA ES1 controls the proliferation of breast cancer cells by regulating the Oct4/Sox2/miR-302 axis. *The FEBS Journal*, *286*(13), 2611–2623. https://doi.org/10.1111/febs.14825

Kučírek, M., Bagherpoor, A. J., Jaroš, J., Hampl, A., & Štros, M. (2019). HMGB2 is a negative regulator of telomerase activity in human embryonic stem and progenitor cells. *The FASEB Journal*, *33*(12), 14307–14324. https://doi.org/10.1096/fj.201901465RRR

Le, F., Li, H.-M., Lv, Q.-L., Chen, J.-J., Lin, Q.-X., Ji, Y.-L., & Yi, B. (2022). lncRNA ZNF674-AS1 inhibits the migration, invasion and epithelial-mesenchymal transition of thyroid cancer cells by modulating the miR-181a/SOCS4 axis. *Molecular and Cellular Endocrinology*, *544*, 111551. https://doi.org/10.1016/j.mce.2021.111551

Li, D., Xie, Y., Sun, J., Zhang, L., & Jiang, W. (2022). LncRNA ZNF674-AS1 Hinders Proliferation and Invasion of Hepatic Carcinoma Cells through the Glycolysis Pathway. *Journal of Oncology*, *2022*, 1–9. https://doi.org/10.1155/2022/8063382

Liang, Y., Song, X., Li, Y., Sang, Y., Zhang, N., Zhang, H., Liu, Y., Duan, Y., Chen, B., Guo, R., Zhao, W., Wang, L., & Yang, Q. (2018). A novel long non-coding RNA-PRLB acts as a tumor promoter through regulating miR-4766-5p/SIRT1 axis in breast cancer. *Cell Death & Disease*, *9*(5), 563. https://doi.org/10.1038/s41419-018-0582-1

Liberzon, A., Birger, C., Thorvaldsdóttir, H., Ghandi, M., Mesirov, J. P., & Tamayo, P. (2015). The Molecular Signatures Database Hallmark Gene Set Collection. *Cell Systems*, *1*(6), 417–425. https://doi.org/10.1016/j.cels.2015.12.004

Liu, J., Zhan, Y., Wang, J., Wang, J., Guo, J., & Kong, D. (2020). Long noncoding RNA LINC01578 drives colon cancer metastasis through a positive feedback loop with the NF-κB/YY1 axis. *Molecular Oncology*, *14*(12), 3211–3233. https://doi.org/10.1002/1878-0261.12819

Liu, Y., Huang, R., Xie, D., Lin, X., & Zheng, L. (2021). ZNF674-AS1 antagonizes miR-423-3p to induce G0/G1 cell cycle arrest in non-small cell lung cancer cells. *Cellular & Molecular Biology Letters*, *26*(1), 6. https://doi.org/10.1186/s11658-021-00247-y

Love, M. I., Huber, W., & Anders, S. (2014). Moderated estimation of fold change and dispersion for RNA-seq data with DESeq2. *Genome Biology*, *15*(12), 550. https://doi.org/10.1186/s13059-014-0550-8

Lu, Y., Wang, W., Liu, Z., Ma, J., Zhou, X., & Fu, W. (2021). Long non-coding RNA

profile study identifies a metabolism-related signature for colorectal cancer. *Molecular Medicine*, *27*(1), 83. https://doi.org/10.1186/s10020-021-00343-x

Luo, A., Lan, X., Qiu, Q., Zhou, Q., Li, J., Wu, M., Liu, P., Zhang, H., Lu, B., Lu, Y., & Lu, W. (2022). LncRNA SFTA1P promotes cervical cancer progression by interaction with PTBP1 to facilitate TPM4 mRNA degradation. *Cell Death & Disease*, *13*(11), 936. https://doi.org/10.1038/s41419-022-05359-7

Ma, H., Ma, T., Chen, M., Zou, Z., & Zhang, Z. (2018). The pseudogene-derived long non-coding RNA SFTA1P suppresses cell proliferation, migration, and invasion in gastric cancer. *Bioscience Reports*, *38*(2). https://doi.org/10.1042/BSR20171193

Mootha, V. K., Lindgren, C. M., Eriksson, K.-F., Subramanian, A., Sihag, S., Lehar, J., Puigserver, P., Carlsson, E., Ridderstråle, M., Laurila, E., Houstis, N., Daly, M. J., Patterson, N., Mesirov, J. P., Golub, T. R., Tamayo, P., Spiegelman, B., Lander, E. S., Hirschhorn, J. N., … Groop, L. C. (2003). PGC-1α-responsive genes involved in oxidative phosphorylation are coordinately downregulated in human diabetes. *Nature Genetics*, *34*(3), 267–273. https://doi.org/10.1038/ng1180

Orphanides, G., & Reinberg, D. (2002). A Unified Theory of Gene Expression. *Cell*, *108*(4), 439–451. https://doi.org/10.1016/S0092-8674(02)00655-4

Pallier, C., Scaffidi, P., Chopineau-Proust, S., Agresti, A., Nordmann, P., Bianchi, M. E., & Marechal, V. (2003). Association of Chromatin Proteins High Mobility Group Box (HMGB) 1 and HMGB2 with Mitotic Chromosomes. *Molecular Biology of the Cell*, *14*(8), 3414–3426. https://doi.org/10.1091/mbc.e02-09-0581

Park, J. S., Gamboni-Robertson, F., He, Q., Svetkauskaite, D., Kim, J.-Y., Strassheim, D., Sohn, J.-W., Yamada, S., Maruyama, I., Banerjee, A., Ishizaka, A., & Abraham, E. (2006). High mobility group box 1 protein interacts with multiple Toll-like receptors. *American Journal of Physiology-Cell Physiology*, *290*(3), C917–C924. https://doi.org/10.1152/ajpcell.00401.2005

Peng, H., Xu, A., Sun, C., Tong, F., Kang, X., Zhou, H., Kang, J., Li, X., Han, Y., Xue, C., Tang, C., Fang, L., Du, Y., Han, J., & Sun, D. (2023). LINC00654 confers sorafenib resistance by suppressing ferroptosis via STAT3-mediated transcriptional activation of SLC7A11 in hepatocellular carcinoma. *Colloids and Surfaces A: Physicochemical and Engineering Aspects*, *669*, 131458. https://doi.org/10.1016/j.colsurfa.2023.131458

Qian, W., Zhu, Y., Wu, M., Guo, Q., Wu, Z., Lobie, P. E., & Zhu, T. (2020). Linc00668 Promotes Invasion and Stem Cell-Like Properties of Breast Cancer Cells by Interaction With SND1. *Frontiers in Oncology*, *10*. https://doi.org/10.3389/fonc.2020.00088

Reeves, R. (2015). High mobility group (HMG) proteins: Modulators of chromatin structure and DNA repair in mammalian cells. *DNA Repair*, *36*, 122–136. https://doi.org/10.1016/j.dnarep.2015.09.015

Rowell, J. P., Simpson, K. L., Stott, K., Watson, M., & Thomas, J. O. (2012). HMGB1-Facilitated p53 DNA Binding Occurs via HMG-Box/p53 Transactivation Domain Interaction, Regulated by the Acidic Tail. *Structure*, *20*(12), 2014–2024. https://doi.org/10.1016/j.str.2012.09.004

Sheng, X., Dai, H., Du, Y., Peng, J., Sha, R., Yang, F., Zhou, L., Lin, Y., Xu, S., Wu, Y., Yin, W., & Lu, J. (2021). LncRNA CARMN overexpression promotes prognosis and chemosensitivity of triple negative breast cancer via acting as miR143-3p host gene and inhibiting DNA replication. *Journal of Experimental & Clinical Cancer Research*, *40*(1), 205. https://doi.org/10.1186/s13046-021-02015-4

Song, Y., Gao, F., Peng, Y., & Yang, X. (2020). Long non-coding RNA DBH-AS1 promotes cancer progression in diffuse large B-cell lymphoma by targeting FN1 via RNA-binding protein BUD13. *Cell Biology International*, *44*(6), 1331–1340. https://doi.org/10.1002/cbin.11327

Subramanian, A., Tamayo, P., Mootha, V. K., Mukherjee, S., Ebert, B. L., Gillette, M. A., Paulovich, A., Pomeroy, S. L., Golub, T. R., Lander, E. S., & Mesirov, J. P. (2005). Gene set enrichment analysis: A knowledge-based approach for interpreting genome-wide expression profiles. *Proceedings of the National Academy of Sciences*, *102*(43), 15545–15550. https://doi.org/10.1073/pnas.0506580102

Takayama, K., Horie-Inoue, K., Katayama, S., Suzuki, T., Tsutsumi, S., Ikeda, K., Urano, T., Fujimura, T., Takagi, K., Takahashi, S., Homma, Y., Ouchi, Y., Aburatani, H., Hayashizaki, Y., & Inoue, S. (2013). Androgen-responsive long noncoding RNA CTBP1-AS promotes prostate cancer. *The EMBO Journal*, *32*(12), 1665–1680. https://doi.org/10.1038/emboj.2013.99

Tian, J., Yang, L., Wang, Z., & Yan, H. (2022). MIR503HG impeded ovarian cancer progression by interacting with SPI1 and preventing TMEFF1 transcription. *Aging*, *14*(13), 5390–5405. https://doi.org/10.18632/aging.204147

Wang, H., Su, H., & Tan, Y. (2020). UNC5B-AS1 promoted ovarian cancer progression by regulating the H3K27me on NDRG2 via EZH2. *Cell Biology International*, *44*(4), 1028–1036. https://doi.org/10.1002/cbin.11300

Wang, L., Zhao, H., Fang, Y., Yuan, B., Guo, Y., & Wang, W. (2023). LncRNA CARMN inhibits cervical cancer cell growth via the miR-92a-3p/BTG2 /Wnt/β-catenin axis. *Physiological Genomics*, *55*(1), 1–15. https://doi.org/10.1152/physiolgenomics.00088.2022

Wang, P., Ke, L., Cai, C., & Dong, F. (2022). LINC01578 affects the radiation resistance of lung cancer cells through regulating microRNA-216b-5p/TBL1XR1 axis. *Bioengineered*, *13*(4), 10721–10733. https://doi.org/10.1080/21655979.2022.2051881

Wang, S.-M., Pang, J., Zhang, K.-J., Zhou, Z.-Y., & Chen, F.-Y. (2021). lncRNA MIR503HG inhibits cell proliferation and promotes apoptosis in TNBC cells via the miR-224-5p/HOXA9 axis. *Molecular Therapy - Oncolytics*, *21*, 62–73. https://doi.org/10.1016/j.omto.2021.03.009

Xie, W., Wang, W., Meng, S., Wu, X., Liu, X., Liu, Y., Kang, X., Su, Y., Lv, X., Guo, L., & Wang, C. (2023). A novel hypoxia-stimulated lncRNA HIF1A-AS3 binds with YBX1 to promote ovarian cancer tumorigenesis by suppressing p21 and AJAP1 transcription. *Molecular Carcinogenesis*. https://doi.org/10.1002/mc.23620

Xiong, Y., Zhang, X., Lin, Z., Xiong, A., Xie, S., Liang, J., & Zhang, W. (2019). SFTA1P, LINC00968, GATA6-AS1, TBX5-AS1, and FEZF1-AS1 are crucial long non-coding RNAs associated with the prognosis of lung squamous cell carcinoma. *Oncology Letters*, *18*(4), 3985–3993. https://doi.org/10.3892/ol.2019.10744

Xu, L., Tan, Y., Xu, F., & Zhang, Y. (2022). Long noncoding RNA ADIRF antisense RNA 1 upregulates insulin receptor substrate 1 to decrease the aggressiveness of osteosarcoma by sponging microRNA-761. *Bioengineered*, *13*(2), 2028–2043. https://doi.org/10.1080/21655979.2021.2019872

Yan, S., Yue, Y., Wang, J., Li, W., Sun, M., Gu, C., & Zeng, L. (2019). LINC00668 promotes tumorigenesis and progression through sponging miR-188–5p and regulating USP47 in colorectal cancer. *European Journal of Pharmacology*, *858*,

172464. https://doi.org/10.1016/j.ejphar.2019.172464

Yang, B., Zhou, S.-N., Tan, J.-N., Huang, J., Chen, Z.-T., Zhong, G.-Y., & Han, F.-H. (2019). Long Non-Coding RNA STARD13-AS Suppresses Cell Proliferation And Metastasis In Colorectal Cancer. *OncoTargets and Therapy*, *12*, 9309–9318. https://doi.org/10.2147/OTT.S217094

Yano, K., Choijookhuu, N., Ikenoue, M., Fidya, Fukaya, T., Sato, K., Lee, D., Taniguchi, N., Chosa, E., Nanashima, A., & Hishikawa, Y. (2022). Spatiotemporal expression of HMGB2 regulates cell proliferation and hepatocyte size during liver regeneration. *Scientific Reports*, *12*(1), 11962. https://doi.org/10.1038/s41598-022-16258-4

Yao, Y., Chen, X., Lu, S., Zhou, C., Xu, G., Yan, Z., Yang, J., Yu, T., Chen, W., Qian, Y., Ding, S., Tang, J., Chen, Y., & Zhang, Y. (2018). Circulating Long Noncoding RNAs as Biomarkers for Predicting Head and Neck Squamous Cell Carcinoma. *Cellular Physiology and Biochemistry*, *50*(4), 1429–1440. https://doi.org/10.1159/000494605

Ye, K., & Wang, Y. (2022). Long non-coding RNA ZNF674-AS1 antagonizes oxaliplatin resistance of gastric cancer via regulating EZH2-mediated methylation of CHST7. *Aging*, *14*(13), 5523–5536. https://doi.org/10.18632/aging.204165

Yu, H., Xu, Q., Liu, F., Ye, X., Wang, J., & Meng, X. (2015). Identification and Validation of Long Noncoding RNA Biomarkers in Human Non–Small-Cell Lung Carcinomas. *Journal of Thoracic Oncology*, *10*(4), 645–654. https://doi.org/10.1097/JTO.0000000000000470

Zhang, X., Spiegel, J., Martínez Cuesta, S., Adhikari, S., & Balasubramanian, S. (2021). Chemical profiling of DNA G-quadruplex-interacting proteins in live cells. *Nature Chemistry*, *13*(7), 626–633. https://doi.org/10.1038/s41557-021-00736-9

Zhu, B., Finch-Edmondson, M., Leong, K. W., Zhang, X., V., M., Lin, Q. X. X., Lee, Y., Ng, W. T., Guo, H., Wan, Y., Sudol, M., & DasGupta, R. (2021). LncRNA SFTA1P mediates positive feedback regulation of the Hippo-YAP/TAZ signaling pathway in non-small cell lung cancer. *Cell Death Discovery*, *7*(1), 369. https://doi.org/10.1038/s41420-021-00761-0

Zwilling, S., König, H., & Wirth, T. (1995). High mobility group protein 2 functionally interacts with the POU domains of octamer transcription factors. *The EMBO Journal*, *14*(6), 1198–1208. https://doi.org/10.1002/j.1460-2075.1995.tb07103.x

Concluding remarks

Regarding objective 1, to identify the deregulated lncRNAs in epithelial ovarian cancer patients from gene expression profiling studies, the following conclusions can be drawn:

- The lncRNAs *ENSG00000187951*, *MIR205HG*, *ZNF232-AS1*, *ENSG00000285756*, *LINC01297*, *TFAP2A-AS1*, *LINC01977*, and *LINC01770*, which are upregulated; and *PGM5-AS1*, *ENSG00000267058*, *EPM2A-DT*, *NR2F1-AS1*, *KLF3-AS1*, *GLIDR*, *ERVK13-3*, and *CLN8-AS1*, which are downregulated, have diagnostic value in epithelial ovarian cancer patients.
- High expression of the lncRNAs *GUSBP11* and *MIR924HG* correlates with unfavorable EOC patient prognosis, whereas high expression of the lncRNA *AQP5-AS1* correlates with favorable EOC patient prognosis.
- The lncRNAs *NR2F2-AS1* and *RPH3AL-AS1* are probable tumor suppressors in EOC.
- There is an *a priori* unexpected specificity between lncRNAs deregulation and histological subtypes of EOC.

Regarding objective 2, to analyze the RNA interactome of HMGB1 and HMGB2 in epithelial ovarian cancer cell lines, the following conclusions can be drawn:

- HMGB1 interacts with the lncRNAs *ZNF710-AS1*, *LINC02846*, *GAS5*, *PCGF3-AS1*, and *ENSG00000224905*; and HMGB2 interacts with the lncRNAs *ZNF710-AS1*, *SYT15*-AS1, *GAS5*, *PCGF3-AS1*, and *SNHG14*, as supported by one computational approach (catRAPID algorithm) and one experimental approach (either RIP-Seq or eCLIP).
- Eleven of the lncRNAs that we identified by RIP-Seq to interact with HMGB1 and/or HMGB2 in cell line PEO1 were not previously related to this epithelial ovarian cancer, although are known to be involved in other types of cancer.
- Among the lncRNAs interacting partners of HMGB1 and/or HMGB2 identified after UV-crosslinking in PEO1 cell line, *THAP9-AS1*, *TPT1-AS1*,

ENSG00000224905, *GMDS-DT*, *LINC01515*, *MIRLET7BHG*, *SNHG14*, *GAS5*, *KCNQ1OT1*, *MALAT1*, *MIR4435-HG*, and *NEAT1* are also present in the HMGB1/2 RNA interactome performed in human fibroblasts by Sofiadis et al. (2021).

- HMGB1 and HMGB2 are also able to bind mRNAs and, remarkably, those whose protein products take part in processes related to the extracellular matrix, axonogenesis-like cell migration, or Wnt signaling pathway, among others.
- *PLXND1*, *LARGE1*, *EFNA5*, *CLCN7*, *AGRN*, *COL6A1*, *GCN1*, *COL1A1*, *ADAMTS1*, and *COL4A2* mRNAs, as well as *PLXND1*, *NEK6*, *DIP2C*, *VOPP1*, and *C1S* mRNAs, bind HMGB1 and HMGB2, respectively, with high confidence as validated by three different approaches, catRAPID algorithm, RIP-Seq, and eCLIP.

Regarding objective 3, to study the effects of silencing HMGB1 and HMGB2 at the transcriptomic level in the EOC cell line PEO1, the following conclusions can be drawn:

- A decrease in HMGB1 or HMGB2 levels leads to a deregulation in lncRNAs previously associated with several cancer types, such as *STARD13-AS*, *SIRLNT*, *ADIRF-AS1*, *SFTA1P*, *MIR23AHG*, *MIR503HG*, and *ZNF674-AS1*, in the case of siHMGB1; *LINC00964*, *MIAT*, *LINC00668*, *LINC01108*, *LINC00654*, *CTBP1-AS*, *DBH-AS1*, *CARMN*, and *CHASERR* in the case of siHMGB2; and *HIF1A-AS3* in the case of either siHMGB1 or siHMGB2, of which *MIR503HG* and *HIF1A-AS3* in particular with ovarian cancer.
- Knocking down of HMGB1 or HMGB2 reveals a great overlap in the regulation of the expression pattern of the two proteins, with enrichment in genes related to KRAS signaling, MTORC1, E2F, or MYC targets, cell cycle progression, chromosomal segregation, ribosome biogenesis, RNA processing, and DNA repair.

Appendix
Resumen

1.- Introducción

El cáncer de ovario es una enfermedad que consiste en el crecimiento descontrolado de las células de este órgano y sus zonas adyacentes, que son capaces de invadir y colonizar otros órganos, siendo la segunda causa más común de muerte por cáncer ginecológico a nivel mundial (Centers for Disease and Control Prevention, 2022; Sung et al., 2021; World Health Organization, 2023). Según el tipo celular donde se origine, se clasifica en estromal, germinal o epitelial (Sankaranarayanan & Ferlay, 2006), y a su vez este último, el cáncer epitelial de ovario (EOC), que es el más frecuente y estudiado, se puede subdividir en cinco subtipos, denominados seroso de alto grado, seroso de bajo grado, endometrioide, de células claras y mucinoso (Gilks & Prat, 2009). Debido a su carácter asintomático durante las primeras etapas, el diagnóstico suele darse cuando la enfermedad ya está avanzada, resultando en un mal pronóstico, mientras que, un diagnóstico temprano hace que el pronóstico sea mucho mejor (Reid et al., 2017). Desafortunadamente, no existen biomarcadores de diagnóstico temprano efectivos y aprobados para la práctica clínica (Ueland, 2017).

Los ARN largos no codificantes (lncRNAs) son transcritos de más de 200 nucleótidos que, presumiblemente, no codifican para proteínas y por ello se ignoraron durante años, hasta que se demostró que son capaces de regular la expresión génica a nivel transcripcional, post-transcripcional, traduccional y post-traduccional (Wang & Chang, 2011). Es por esto por lo que han adquirido una gran importancia debido a sus profundas implicaciones en la fisiología y homeostasis celular, así como en distintas enfermedades, incluido el cáncer de ovario, condición en la que se ha demostrado que son capaces de controlar la proliferación celular, ciclo celular, varios tipos de muerte celular, migración, invasión, transición epitelio-mesénquima, metástasis, angiogénesis, metabolismo celular, inflamación e inmunomodulación (revisado en Salamini-Montemurri et al., 2020).

Las proteínas *High mobility group B* (HMGB) son una familia de proteínas eucariotas altamente conservadas que se caracterizan por la presencia de uno o más

dominios llamados *HMG-box*, que consisten cada uno de ellos en 3 hélices alfa plegadas en forma de L (Weir et al., 1993). De las cuatro proteínas HMGB canónicas en humanos, HMGB1, HMGB2, HMGB3 y HMGB4, nos centramos en HMGB1 y HMGB2, que constan de dos dominios HMG-box y una cola acídica C-terminal y tienen altos niveles de expresión de forma ubicua en muchos tejidos en los organismos pluricelulares (Štros, 2010). Se consideran proteínas de la cromatina no histónicas, ya que se encuentran en alta proporción en el núcleo donde actúan en la reparación, recombinación y como chaperonas del ADN o cofactores transcripcionales (Reeves, 2015), aunque también son capaces de translocarse al citoplasma donde modulan procesos como autofagia (Tang et al., 2010), apoptosis (Gnanasekar et al., 2009; Yang et al., 2020) o morfología mitocondrial (Tang et al., 2011). También actúan como sensores de especies reactivas de oxígeno (Tang et al., 2011) o ácidos nucleicos inmunogénicos (Yanai et al., 2009). Incluso pueden liberarse al espacio extracelular, donde actúan como alarminas para promover la inflamación (Andersson et al., 2018; Starkova et al., 2023). HMGB1 y HMGB2 participan en funciones tanto fisiológicas como patológicas, incluyendo varios tipos de cáncer, siendo capaces de promover proliferación, migración, invasión, transición epitelio-mesénquima, tolerancia a especies reactivas de oxígeno, evasión de apoptosis, inmunosupresión y resistencia a quimioterápicos (revisado en Barreiro-Alonso et al., 2016). Los niveles de estas proteínas aumentan entre 3 y 4,5 veces en pacientes con cáncer de ovario (Cámara-Quílez et al., 2020) y se asocian con un mal pronóstico (H. Li et al., 2018; Machado et al., 2017).

Se ha demostrado tanto *in vitro* como *in vivo* que las proteínas HMGB son capaces de unirse a distintos tipos de ARN (Arimondo et al., 2000; Bell et al., 2008; Choi et al., 2020; Yanai et al., 2009), incluidos lncRNAs, y que dicha interacción modula las funciones de estas proteínas. Por ejemplo, existen lncRNAs antisentido que reclutan a HMGB1 y HMGB2 para regular la transcripción de sus transcritos codificantes asociados, es decir, regulación en *cis*, actuando sobre la cromatina y/o reclutando

factores transcripcionales (Ma et al., 2017; Saayman et al., 2016; Yamanaka et al., 2015). Los lncRNAs también pueden regular la localización subcelular de estas proteínas, promoviendo o inhibiendo su presencia en el núcleo donde llevan a cabo su función reguladora de la transcripción o de reparación de ADN (Han et al., 2019; Huang et al., 2022; S. Li et al., 2020; Lou et al., 2021). La interacción con lncRNAs puede a su vez favorecer la estabilidad de HMGB1 o HMGB2, al evitar su ubiquitinación y posterior degradación (Gao et al., 2017). Por último, HMGB1 y HMGB2 también se unen a ARN mensajeros para regular su *splicing* (Sofiadis et al., 2021).

2.- Objetivos

Está descrito que las proteínas HMGB1 y HMGB2 y los lncRNAs están implicados en el inicio y progresión del cáncer, incluido el cáncer epitelial de ovario. El objetivo general de esta tesis doctoral es identificar lncRNAs que estén desregulados en cáncer epitelial de ovario y/o asociados con HMGB1 y/o HMGB2 para así identificar nuevos biomarcadores diagnósticos y dianas terapéuticas. Por este motivo, establecemos los siguientes objetivos:

1) Identificar los lncRNAs desregulados en pacientes con cáncer epitelial de ovario a partir de estudios del transcriptoma.
2) Analizar el interactoma de ARN de las proteínas HMGB1 y HMGB2 en líneas celulares de cáncer de ovario epitelial.
3) Estudiar los efectos del silenciamiento de las proteínas HMGB1 y HMGB2 a nivel del transcriptoma en la línea celular de cáncer de ovario epitelial PEO1.

3.- Metodología

Para identificar lncRNAs desregulados en pacientes con cáncer de ovario epitelial se llevó a cabo un metaanálisis de transcriptomas de muestras de mujeres con la enfermedad y mujeres sanas, realizados por diferentes grupos de investigación y disponibles en las bases de datos en línea. Tras una búsqueda en bases de datos donde

se recogen transcriptomas de pacientes de EOC y controles sanas, descargamos los archivos de intensidades, en el caso de estudios basados en microchips de expresión, y los archivos de recuento de lecturas mapeadas, en el caso de los estudios basados en secuenciación masiva de ARN. También descargamos los archivos de recuento de lecturas mapeadas de los estudios basados en secuenciación masiva de ARN para un panel de líneas celulares de ovario (57 cancerosas y 1 no cancerosa) como método de validación. Teniendo en cuenta la información clínica que proporcionaban los 46 estudios seleccionados, los agrupamos en cinco categorías que permitieran encontrar genes diferencialmente expresados asociados a diagnóstico, metástasis, resistencia a quimioterapia o subtipo histológico, y adicionalmente supervivencia. Analizamos individualmente la expresión diferencial de genes en los distintos grupos de cada categoría con las herramientas BRB-ArrayTools (https://brb.nci.nih.gov/BRB-ArrayTools/ desarrollada por el Dr. Richard Simon y su equipo), para los microchips de expresión, y DESeq2 (Love et al., 2014), para la secuenciación masiva de ARN. Tras anotar los genes con identificadores de *Ensembl*, comparamos las listas de cada categoría e hicimos recuento del número de estudios en los que aparecía cada gen de lncRNAs, así como si había un aumento o disminución de expresión en la comparativa.

El interactoma de ARN de las proteínas HMGB1 y HMGB2 se llevó a cabo mediante tres aproximaciones distintas. La primera de ellas consistió en la utilización del algoritmo catRAPID (http://service.tartaglialab.com/page/catrapid_group_old (Agostini et al., 2013)), que utiliza la secuencia de aminoácidos de la proteína de interés, en este caso, de HMGB1 y HMGB2, como punto de partida y que compara cada una de las proteínas problema con todos los transcritos, procedan tanto de genes codificantes como no codificantes. Estas comparaciones duales, proteína-RNA transcrito, permiten calcular la probabilidad de interacción con cada isoforma de cada gen, basándose en propiedades biofísicas de ambas moléculas. Las otras dos aproximaciones utilizadas son de carácter experimental, llevando a cabo las técnicas denominadas RIP-Seq, por

las siglas en inglés de inmunoprecipitación de ARN acoplada a secuenciación masiva (Zhao et al., 2010), y eCLIP, por las siglas en inglés de inmunoprecipitación con entrecruzamiento mejorado (Van Nostrand et al., 2017). Se utilizó como modelo de estudio la línea celular PEO1, que es representativa del subtipo seroso de alto grado (Beaufort et al., 2014). Estas dos técnicas presentan diferencias entre sí, pero se basan en la realización de un enriquecimiento de la proteína de interés basado en anticuerpos acoplados a nanopartículas magnéticas, proceso conocido como inmunoprecipitación, para finalmente purificar y secuenciar los ARN asociados a éstas. En eCLIP, las células antes de ser lisadas para proceder con la inmunoprecipitación son expuestas a radiación ultravioleta de 254 nm de longitud de onda para producir entrecruzamientos covalentes entre las moléculas y así estabilizar las uniones entre proteínas y ARN, lo que permite hacer lavados fuertes para eliminar uniones inespecíficas, en comparación con RIP-Seq donde no se lleva a cabo dicho entrecruzamiento y las uniones se deben únicamente a fuerzas intermoleculares no covalentes más débiles. Además, en eCLIP el lisado con las proteínas entrecruzadas se trata con una ARNasa para digerir las regiones donde el ácido nucleico no está interactuando con la proteína. Una vez realizada la secuenciación masiva del ADN complementario obtenido a partir del ARN inmunoprecipitado, el análisis de RIP-Seq se llevó a cabo mediante la búsqueda genes expresados diferencialmente, nuevamente con la herramienta DESeq2 comparando las inmunoprecipitaciones específicas con otras llevadas a cabo con un anticuerpo inespecífico control. En el análisis de los datos de eCLIP se utilizó un algoritmo llamado *peak calling* con la herramienta CLIPper (https://github.com/YeoLab/clipper (Ge et al., 2021), que analiza la forma de la distribución de las lecturas a lo largo del genoma en busca de enriquecimientos respecto a un ARN total denominado como *input*.

Finalmente, se silenciaron mediante ARN pequeño de interferencia (siRNA) los ARN mensajeros de HMGB1 y HMGB2. Tras una validación del silenciamiento mediante RT-qPCR y Western blot, se prepararon las librerías de ADN complementario y se llevó

a cabo la secuenciación masiva. Una vez mapeadas las lecturas, se determinaron los genes expresados diferencialmente con la herramienta DESeq2 y se estudiaron los conjuntos de genes asociados a distintos procesos biológicos utilizando el software *Gene set enrichment analysis* (Mootha et al., 2003; Subramanian et al., 2005) utilizando los conjuntos de genes denominados *hallmarks* y *gene ontology biological process*.

4.- Resultados

4.1 Identificación de lncRNAs desregulados en cáncer de ovario epitelial basada en un metaanálisis de transcriptomas

Encontramos inicialmente 63 estudios transcriptómicos, descartamos 17 por no cumplir con los requisitos establecidos, y los 46 restantes los agrupamos en cinco categorías como se ha comentado en la metodología.

En la categoría de diagnóstico, analizamos 22 estudios diferentes y obtuvimos 247 y 243 lncRNAs cuyos niveles estaban elevados o disminuidos, respectivamente, en tejido canceroso frente a tejido sano en al menos 3 estudios diferentes, de los cuales, 42 y 57, respectivamente, replicaban su comportamiento en líneas celulares de cáncer de ovario. Los lncRNAs que aumentaban su expresión en mayor número de estudios fueron *RNF157-AS1* y *BBOX1-AS1*, ambos en 12 estudios diferentes, mientras que *MAGI2-AS3* fue el que en más estudios disminuía su expresión, concretamente en 15 estudios diferentes. Este análisis nos permitió encontrar lncRNAs que no habían sido relacionados previamente con cáncer de ovario epitelial; *ENSG00000187951*, *MIR205HG*, *ZNF232-AS1*, *ENSG00000285756*, *LINC01297*, *TFAP2A-AS1*, *LINC01977* y *LINC01770* aumentaban su expresión en EOC; *PGM5-AS1*, *ENSG00000267058*, *EPM2A-DT*, *NR2F1-AS1*, *KLF3-AS1*, *GLIDR*, *ERVK13-3* y *CLN8-AS1*, disminuían su expresión en EOC.

En la categoría de pronóstico, analizamos 11 estudios diferentes e identificamos lncRNAs cuya alta expresión estaba asociada a mayor supervivencia (123 lncRNAs) y/o período libre de enfermedad (125 lncRNAs). Por otra parte, también identificamos

lncRNAs cuya alta expresión estaba asociada a menor supervivencia (32 lncRNAs) y período libre de enfermedad (34 lncRNAs). Los más significativos teniendo en cuenta la supervivencia son: *RNF157-AS1* y *AQP5-AS1* (alta expresión asociada a buen pronóstico), y *CRNDE* y *ZFAS1* (alta expresión asociada a mal pronóstico). *MALAT1* (alta expresión asociada a mal pronóstico) está asociado a período libre de enfermedad. De los lncRNAs previamente no relacionados con cáncer de ovario epitelial, la expresión de *GUSBP11* y *MIR924HG* tienen correlación positiva con pronóstico desfavorable, mientras que la de *AQP5-AS1* con pronóstico favorable.

En la categoría de metástasis, analizamos 7 estudios y encontramos 287 lncRNAs cuya expresión incrementa y 287 lncRNAs cuya expresión disminuye en metástasis peritoneal sólida respecto a células cancerosas del líquido ascítico o tumor primario, o en células cancerosas del líquido ascítico respecto al tumor primario. Algunos de ellos se consideran como más significativos (30 y 8, respectivamente) por estar desregulados en dos o tres estudios independientes. Estos resultados se replican también en el estudio con líneas celulares para 8 lncRNAs de cada grupo. También encontramos 26 lncRNAs cuyos niveles aumentan o disminuyen en células cancerosas del líquido ascítico pero que no varían sus niveles si se compara tumor primario y metástasis sólida en peritoneo. Cabe destacar que *LINC02544*, *LINC01235*, *HECW2-AS1* y *MIR31HG* están elevados en metástasis y no se habían relacionado previamente con EOC.

Al solapar los lncRNAs identificados en los estudios de las categorías denominadas como de diagnóstico, pronóstico y metástasis, identificamos a *NR2F2-AS1* y *RPH3AL-AS1* como posibles supresores de tumores al verse reducidos sus niveles en tejidos cancerosos frente a sanos, en metástasis frente a tumor primario, además de estar asociados con buen pronóstico.

En los 3 estudios analizados, pertenecientes a la categoría de resistencia a quimioterapia, identificamos 6 lncRNAs que incrementaban su expresión y 9 que la disminuían en pacientes que no respondían al tratamiento estándar.

Por último, el análisis de 6 estudios, con información adicional sobre del subtipo histológico diagnosticado, mostró 5 lncRNAs desregulados en el subtipo seroso de alto grado y 41 en el subtipo de célula clara en dos o más estudios diferentes. Al realizar la intersección de las listas de los lncRNAs desregulados en los diferentes subtipos de EOC (expresión elevada o disminuida por separado), observamos muy escaso solapamiento; concretamente de un lncRNA común a dos estudios en el caso de los lncRNA de expresión elevada en EOC, y tres lncRNA comunes en el caso de los de expresión disminuida.

4.2 Identificación de interacciones HMGB1/2-ARN en líneas celulares de cáncer de ovario epitelial

A partir del algoritmo de predicción de interacción catRAPID, obtuvimos una lista de 2978 genes para HMGB1 y 2301 genes para HMGB2 con valor normalizado de interacción mayor o igual a 1, donde 75% correspondía a genes codificantes, 13% a lncRNAs y 12% a pseudogenes; 1963 eran comunes a ambas proteínas. La lista de HMGB1 contenía 381 lncRNAs y la de HMGB2 contenía 300, existiendo 260 en común. Los dos lncRNAs con mayor probabilidad de interacción tanto para HMGB1 como para HMGB2 son *DSCAM-AS1* y *LINC00621* y estaban previamente asociados a otros tipos de cáncer. El análisis de ontologías génicas en el grupo de los genes codificantes arrojó términos relacionados con la axonogénesis, la regulación negativa de la apoptosis, la ruta de señalización Wnt, el procesamiento de ARN o la modificación postraduccional de histonas.

Los datos de RIP Seq a partir de tres réplicas biológicas de los ARN inmunoprecipitados con anticuerpos dirigidos a HMGB1 o HMGB2 en la línea PEO1 de cáncer de ovario resultó en la identificación de 910 y 1456 ARN enriquecidos para

HMGB1 y HMGB2, respectivamente, con una proporción relativa del 92% de genes codificantes, 4% de pseudogenes, 2% de lncRNAs y el 2% de otros tipos de ARN. Identificamos 8 lncRNAs presentes en el inmunoprecipitado de HMGB1, pero no en el de HMGB2. Entre ellos, *LINC01963* había sido previamente relacionados con cáncer. También identificamos 23 lncRNAs presentes en el inmunoprecipitado de HMGB2, pero no en el de HMGB1; de estos, *LINC00205*, *LINC00689*, *LINC00294*, *PSMG3-AS1*, *MIR663AHG*, *PINK1-AS*, *FAM225A* y *FAM225B* habían sido previamente relacionados con cáncer. También identificamos 9 lncRNAs presentes tanto en los inmunoprecipitados de HMGB1 como en los de HMGB2, de los cuales *PRECSIT* y *ZNF710-AS1* habían sido previamente relacionados con cáncer. También analizamos las ontologías génicas de los ARNm que nos proporcionaron términos (GO-terms) enriquecidos y relacionados con la matriz extracelular, guía de axón, regulación de la quimiotaxis, unión a ADN, metabolismo de proteínas, respuesta a estímulo de crecimiento o respuesta a radiación.

La técnica eCLIP, llevada a cabo con la línea celular PEO1, resultó en un enriquecimiento de ARN ribosomal 18S en los inmunoprecipitados de HMGB1 y HMGB2, respecto del *input*. También se identificaron más de mil picos (secuencias enriquecidas) que se ubican en su mayoría en regiones codificantes para los inmunoprecipitados de HMGB1 o en el intrón distal para los de HMGB2. De todos los genes asociados a los picos identificados solamente confirmamos 584 para HMGB1 y 285 para HMGB2 que fueran estadísticamente significativos en las dos réplicas independientes realizadas. De estos más del 80% eran ARN mensajeros, en torno al 7% lncRNAs y snoRNAs (*small nucleolar RNAs)*, en torno al 2% pseudogenes y el porcentaje restante otros tipos de ARN. De los 34 lncRNAs identificados por interaccionar con HMGB1 y los 24 identificados por interaccionar con HMGB2 en eCLIP, 16 son comunes a ambas proteínas. Varios de estos lncRNAs han sido relacionados previamente con cáncer, como: *MIR31HG*, *HCG18*, *LINC00665*, *DUXAP8* y *GMDS-DT*, los cuales co-inmunoprecipitan con HMGB1, pero no con HMGB2; *SNHG14*, *NUTM2B-*

AS1, *LINC00910* y *NUTM2A-AS1* que inmunoprecipitan con HMGB2, pero no con HMGB1; y *MALAT1, PVT1*, *LINC00342*, *NEAT1*, *GAS5*, *MIR4435-2HG* y *THAP9-AS1*, que están presentes en los experimentos de eCLIP de HMGB1 y HMGB2. Finalmente, se hizo un análisis de la ontología génica para los ARN mensajeros y se identificaron términos enriquecidos relacionados con la segregación de cromosomas, la migración celular, la matriz extracelular, el ensamblaje de nucleosomas, la fosforilación oxidativa, la regulación de la apoptosis y muerte celular inducida por estrés, así como señalización de p53, proteína morfogénica ósea y proteína quinasa B.

4.3 Efectos de HMGB1 y HMGB2 sobre el transcriptoma de la línea de cáncer de ovario epitelial PEO1

Llevamos a cabo una transfección de siRNA para HMGB1 y HMGB2 en la línea celular PEO1 y, tras comprobar que el silenciamiento se había producido satisfactoriamente a nivel de ARN mensajero y de proteína, realizamos la secuenciación masiva del ARN. El análisis de este experimento resultó en la identificación de 189 genes que aumentan su expresión tras el silenciamiento de HMGB1 y 66 genes que la disminuyen (de los cuales 68 y 18 son lncRNAs, respectivamente) en el silenciamiento de HMGB1. Tras el silenciamiento de HMGB2 se identificaron 480 genes de expresión incrementada y 421 genes que disminuyen su expresión (de los cuales 139 y 43 son lncRNAs, respectivamente). Hay 18 lncRNAs que incrementan su expresión y 4 que la disminuyen tanto por el silenciamiento de HMGB1 como por el de HMGB2.

Adicionalmente, analizamos los datos de secuenciación masiva utilizando *Gene Set Enrichment Analysis* para identificar a partir de los genes desregulados las rutas y los procesos celulares (*hallmarks* y ontologías génicas) en los que intervienen HMGB1 y HMGB2 en cáncer de ovario epitelial. Dentro de los *hallmarks*, encontramos enriquecidos los términos “coagulación” en el silenciamiento de HMGB1, y “miogénesis” en el silenciamiento de HMGB2, así como “genes que disminuyen su expresión por la activación de KRAS” en el silenciamiento de HMGB1 y HMGB2. Por el contrario, otros

términos más enriquecidos en el control incluyen “TNFα vía NF-κβ” respecto a siHMGB1 o “señalización TGF-β” respecto a siHMGB2. Los términos “punto de control G2/M”, “dianas de E2F”, “dianas de MYC”, “huso mitótico”, “secreción de proteínas”, “ruta de señalización de MTORC1”, “fosforilación oxidativa”, “respuesta a proteínas desplegadas” y “reparación de ADN” están enriquecidos en el control tanto al comparar con siHMGB1 como con siHMGB2.

En cuanto a las ontologías génicas de procesos biológicos, observamos que “fusión de membrana plasmática”, “proceso biosintético de leucotrieno” y “generación de anión superóxido” estaban enriquecidos en el silenciamiento de HMGB1; mientras que “reconocimiento de fagocitosis” estaba enriquecido en el silenciamiento de HMGB2. Los términos “señalización del receptor asociado a proteína G acoplado a nucleótido cíclico como segundo mensajero” está enriquecido en el silenciamiento de HMGB1 y también en el de HMGB2. Por otro lado, encontramos “segregación de cromátidas hermanas”, “biogénesis de ribosomas”, “localización de ARN”, “*splicing* de ARN” o “procesamiento de ARN mensajero” y “regulación del mantenimiento de los telómeros” enriquecidos en el silenciamiento control respecto al silenciamiento de HMGB1 y de HMGB2, mientras que “traducción citoplasmática”, “modificación del ARN transferente” y “punto de control del ciclo celular” estaban enriquecidas únicamente frente al silenciamiento de HMGB2.

5.- Conclusiones

En lo relativo al primer objetivo, identificar los lncRNAs desregulados en pacientes con cáncer epitelial de ovario a partir de estudios del transcriptoma, se obtuvieron las siguientes conclusiones:

- Los lncRNAs *ENSG00000187951*, *MIR205HG*, *ZNF232-AS1*, *ENSG00000285756*, *LINC01297*, *TFAP2A-AS1*, *LINC01977* y *LINC01770*, cuyos niveles están elevados; y *PGM5-AS1*, *ENSG00000267058*, *EPM2A-DT*, *NR2F1-AS1*, *KLF3-AS1*, *GLIDR*, *ERVK13-3* y *CLN8-AS1*, cuyos niveles están

disminuidos, aportan valor diagnóstico en pacientes con cáncer de ovario epitelial.

- Niveles altos de expresión de los lncRNAs *GUSBP11* y *MIR924HG* tienen correlación positiva con pronóstico desfavorable de pacientes con cáncer de ovario epitelial, mientras que niveles altos de expresión del lncRNA *AQP5-AS1* la tienen con pronóstico favorable en pacientes con cáncer de ovario epitelial.
- Los lncRNAs *NR2F2-AS1* y *RPH3AL-AS1* son posibles supresores de tumores en cáncer de ovario epitelial.
- Hay una especificidad *a priori* inesperada en la desregulación de lncRNAs entre los 5 subtipos histológicos de cáncer de ovario epitelial.

Respecto al segundo objetivo, analizar el interactoma de ARN de las proteínas HMGB1 y HMGB2 en líneas celulares de cáncer de ovario epitelial, se obtuvieron las siguientes conclusiones en la línea PEO1:

- HMGB1 interactúa con los lncRNAs *ZNF710-AS1*, *LINC02846*, *GAS5*, *PCGF3-AS1* y *ENSG00000224905*. HMGB2 interactúa con los lncRNAs *ZNF710-AS1*, *SYT15*-AS1, *GAS5*, *PCGF3-AS1* y *SNHG14*. Estos datos están respaldados por una aproximación computacional (algoritmo catRAPID) y una aproximación experimental (RIP-Seq o eCLIP).
- Once de los lncRNAs que identificamos por RIP-Seq que interaccionan con HMGB1 y/o HMGB2 en la línea celular PEO1 no estaban previamente relacionados con cáncer de ovario epitelial, pero sí que se conocía su relación con otros tipos de cáncer.
- De los lncRNAs que interaccionan con HMGB1 y/o HMGB2 identificados tras el entrecruzamiento de radiación ultravioleta en la línea celular PEO1, *THAP9-AS1*, *TPT1-AS1*, *ENSG00000224905*, *GMDS-DT*, *LINC01515*, *MIRLET7BHG*, *SNHG14*, *GAS5*, *KCNQ1OT1*, *MALAT1*, *MIR4435-HG*, y *NEAT1* también fueron

identificados en el interactoma de HMGB1/2 realizado en fibroblastos humanos por Sofiadis y colaboradores (2021).

- HMGB1 y HMGB2 son capaces de unirse con ARN mensajeros y, particularmente, con aquellos cuyos productos proteicos participan en procesos relacionados con la matriz extracelular, axonogénesis (similar a migración celular) o señalización de la ruta Wnt, entre otros.
- Los ARN mensajeros *PLXND1*, *LARGE1*, *EFNA5*, *CLCN7*, *AGRN*, *COL6A1*, *GCN1*, *COL1A1*, *ADAMTS1* y *COL4A2*, así como *PLXND1*, *NEK6*, *DIP2C*, *VOPP1* y *C1S* que se unen a HMGB1 y HMGB2 respectivamente, han sido validados por tres aproximaciones distintas, el algoritmo catRAPID, RIP-Seq y eCLIP.

En cuanto al tercer objetivo, estudiar los efectos del silenciamiento de las proteínas HMGB1 y HMGB2 a nivel del transcriptoma en la línea celular de cáncer de ovario epitelial PEO1, se obtuvieron las siguientes conclusiones:

- Un descenso en los niveles de HMGB1 o HMGB2 dio lugar a la desregulación de lncRNAs asociados previamente a varios tipos de cáncer, como *STARD13-AS*, *SIRLNT*, *ADIRF-AS1*, *SFTA1P*, *MIR23AHG*, *MIR503HG* y *ZNF674-AS1*, en el caso de siHMGB1; *LINC00964*, *MIAT*, *LINC00668*, *LINC01108*, *LINC00654*, *CTBP1-AS*, *DBH-AS1*, *CARMN* y *CHASERR* en el caso de siHMGB2; y *HIF1A-AS3* tanto en el caso de siHMGB1 como de siHMGB2. De ellos, *MIR503HG* y *HIF1A-AS3* habían sido ya previamente asociados a cáncer de ovario.
- El silenciamiento de HMGB1 o HMGB2 revela un gran solapamiento en el patrón de regulación de expresión mediado por las dos proteínas, con un enriquecimiento en genes relacionados con la señalización de KRAS, las dianas de MTORC1, E2F o MYC, progresión del ciclo celular, segregación cromosómica, biogénesis de ribosomas, procesamiento de ARN y reparación de ADN.

6.- Referencias

Agostini, F., Zanzoni, A., Klus, P., Marchese, D., Cirillo, D., & Tartaglia, G. G. (2013). catRAPID omics: a web server for large-scale prediction of protein-RNA interactions. *Bioinformatics*, *29*(22), 2928–2930. https://doi.org/10.1093/bioinformatics/btt495

Andersson, U., Yang, H., & Harris, H. (2018). High-mobility group box 1 protein (HMGB1) operates as an alarmin outside as well as inside cells. *Seminars in Immunology*, *38*, 40–48. https://doi.org/10.1016/j.smim.2018.02.011

Arimondo, P. B., Gelus, N., Hamy, F., Payet, D., Travers, A., & Bailly, C. (2000). The chromosomal protein HMG-D binds to the TAR and RBE RNA of HIV-1. *FEBS Letters*, *485*(1), 47–52. https://doi.org/10.1016/S0014-5793(00)02183-9

Barreiro-Alonso, A., Lamas-Maceiras, M., Rodríguez-Belmonte, E., Vizoso-Vázquez, Á., Quindós, M., & Cerdán, M. E. (2016). High Mobility Group B Proteins, Their Partners, and Other Redox Sensors in Ovarian and Prostate Cancer. *Oxidative Medicine and Cellular Longevity*, *2016*, 1–17. https://doi.org/10.1155/2016/5845061

Beaufort, C. M., Helmijr, J. C. A., Piskorz, A. M., Hoogstraat, M., Ruigrok-Ritstier, K., Besselink, N., Murtaza, M., van IJcken, W. F. J., Heine, A. A. J., Smid, M., Koudijs, M. J., Brenton, J. D., Berns, E. M. J. J., & Helleman, J. (2014). Ovarian Cancer Cell Line Panel (OCCP): Clinical Importance of In Vitro Morphological Subtypes. *PLoS ONE*, *9*(9), e103988. https://doi.org/10.1371/journal.pone.0103988

Bell, A. J., Chauhan, S., Woodson, S. A., & Kallenbach, N. R. (2008). Interactions of recombinant HMGB proteins with branched RNA substrates. *Biochemical and Biophysical Research Communications*, *377*(1), 262–267. https://doi.org/10.1016/j.bbrc.2008.09.131

Cámara-Quílez, M., Barreiro-Alonso, A., Rodríguez-Bemonte, E., Quindós-Varela, M., Cerdán, M. E., & Lamas-Maceiras, M. (2020). Differential Characteristics of HMGB2 Versus HMGB1 and their Perspectives in Ovary and Prostate Cancer. *Current Medicinal Chemistry*, *27*(20), 3271–3289. https://doi.org/10.2174/0929867326666190123120338

Centers for Disease and Control Prevention. (2022). *Basic Information About Ovarian Cancer*. https://www.cdc.gov/cancer/ovarian/basic_info/index.htm

Choi, M., Jeong, H., Kim, S., Kim, M., Lee, M., & Rhim, T. (2020). Targeted delivery of Chil3/Chil4 siRNA to alveolar macrophages using ternary complexes composed of HMG and oligoarginine micelles. *Nanoscale*, *12*(2), 933–943. https://doi.org/10.1039/C9NR06382J

Gao, D., Lv, A., Li, H.-P., Han, D.-H., & Zhang, Y.-P. (2017). LncRNA MALAT-1 Elevates HMGB1 to Promote Autophagy Resulting in Inhibition of Tumor Cell Apoptosis in Multiple Myeloma. *Journal of Cellular Biochemistry*, *118*(10), 3341–3348. https://doi.org/10.1002/jcb.25987

Ge, X., Chen, Y. E., Song, D., McDermott, M., Woyshner, K., Manousopoulou, A., Wang, N., Li, W., Wang, L. D., & Li, J. J. (2021). Clipper: p-value-free FDR control on high-throughput data from two conditions. *Genome Biology*, *22*(1), 288. https://doi.org/10.1186/s13059-021-02506-9

Gilks, C. B., & Prat, J. (2009). Ovarian carcinoma pathology and genetics: recent advances. *Human Pathology*, *40*(9), 1213–1223. https://doi.org/10.1016/j.humpath.2009.04.017

Gnanasekar, M., Thirugnanam, S., & Ramaswamy, K. (2009). Short hairpin RNA (shRNA) constructs targeting high mobility group box-1 (HMGB1) expression leads to inhibition of prostate cancer cell survival and apoptosis. *International Journal of Oncology*, *34*(2), 425–431. https://doi.org/10.3892/ijo_00000166

Han, Q., Xu, L., Lin, W., Yao, X., Jiang, M., Zhou, R., Sun, X., & Zhao, L. (2019). Long noncoding RNA CRCMSL suppresses tumor invasive and metastasis in colorectal carcinoma through nucleocytoplasmic shuttling of HMGB2. *Oncogene*, *38*(16), 3019–3032. https://doi.org/10.1038/s41388-018-0614-4

Huang, G., Xiang, Z., Wu, H., He, Q., Dou, R., Yang, C., Song, J., Huang, S., Wang, S., & Xiong, B. (2022). The lncRNA SEMA3B-AS1/HMGB1/FBXW7 Axis Mediates the Peritoneal Metastasis of Gastric Cancer by Regulating BGN Protein Ubiquitination. *Oxidative Medicine and Cellular Longevity*, *2022*(4), 1–26. https://doi.org/10.1155/2022/5055684

Li, H., Zhang, H., & Wang, Y. (2018). Centromere protein U facilitates metastasis of ovarian cancer cells by targeting high mobility group box 2 expression. *Am J Cancer Res*, *8*(5), 835–851. www.ajcr.us/

Li, S., Chen, S., Wang, B., Zhang, L., Su, Y., & Zhang, X. (2020). The long noncoding RNA LINC00341 suppresses colorectal carcinoma by preventing cell migration and apoptosis. *Cell Biochemistry and Function*, *38*(3), 266–274. https://doi.org/10.1002/cbf.3473

Lou, M.-M., Tang, X.-Q., Wang, G.-M., He, J., Luo, F., Guan, M.-F., Wang, F., Zou, H., Wang, J.-Y., Zhang, Q., Xu, M.-J., Shi, Q.-L., Shen, L.-B., Ma, G.-M., Wu, Y., Zhang, Y.-Y., Liang, A., Wang, T.-H., Xiong, L.-L., … Wang, W.-Y. (2021). Long noncoding RNA BS-DRL1 modulates the DNA damage response and genome stability by interacting with HMGB1 in neurons. *Nature Communications*, *12*(1), 4075. https://doi.org/10.1038/s41467-021-24236-z

Love, M. I., Huber, W., & Anders, S. (2014). Moderated estimation of fold change and dispersion for RNA-seq data with DESeq2. *Genome Biology*, *15*(12), 550. https://doi.org/10.1186/s13059-014-0550-8

Ma, S., Ming, Z., Gong, A.-Y., Wang, Y., Chen, X., Hu, G., Zhou, R., Shibata, A., Swanson, P. C., & Chen, X.-M. (2017). A long noncoding RNA, lincRNA-Tnfaip3, acts as a coregulator of NF-κB to modulate inflammatory gene transcription in mouse macrophages. *The FASEB Journal*, *31*(3), 1215–1225. https://doi.org/10.1096/fj.201601056R

Machado, L. R., Moseley, P. M., Moss, R., Deen, S., Nolan, C., Spendlove, I., Ramage, J. M., Chan, S. Y., & Durrant, L. G. (2017). High mobility group protein B1 is a predictor of poor survival in ovarian cancer. *Oncotarget*, *8*(60), 101215–101223. https://doi.org/10.18632/oncotarget.20538

Mootha, V. K., Lindgren, C. M., Eriksson, K.-F., Subramanian, A., Sihag, S., Lehar, J., Puigserver, P., Carlsson, E., Ridderstråle, M., Laurila, E., Houstis, N., Daly, M. J., Patterson, N., Mesirov, J. P., Golub, T. R., Tamayo, P., Spiegelman, B., Lander, E. S., Hirschhorn, J. N., … Groop, L. C. (2003). PGC-1α-responsive genes involved in oxidative phosphorylation are coordinately downregulated in human diabetes. *Nature Genetics*, *34*(3), 267–273. https://doi.org/10.1038/ng1180

Reeves, R. (2015). High mobility group (HMG) proteins: Modulators of chromatin structure and DNA repair in mammalian cells. *DNA Repair*, *36*, 122–136. https://doi.org/10.1016/j.dnarep.2015.09.015

Reid, B. M., Permuth, J. B., & Sellers, T. A. (2017). Epidemiology of ovarian cancer: a

review. *Cancer Biology & Medicine*, *14*(1), 9–32. https://doi.org/10.20892/j.issn.2095-3941.2016.0084

Saayman, S. M., Ackley, A., Burdach, J., Clemson, M., Gruenert, D. C., Tachikawa, K., Chivukula, P., Weinberg, M. S., & Morris, K. V. (2016). Long Non-coding RNA BGas Regulates the Cystic Fibrosis Transmembrane Conductance Regulator. *Molecular Therapy*, *24*(8), 1351–1357. https://doi.org/10.1038/mt.2016.112

Salamini-Montemurri, M., Lamas-Maceiras, M., Barreiro-Alonso, A., Vizoso-Vázquez, Á., Rodríguez-Belmonte, E., Quindós-Varela, M., & Esperanza Cerdán, M. (2020). The challenges and opportunities of lncRNAs in ovarian cancer research and clinical use. *Cancers*, *12*(4), 1–25. https://doi.org/10.3390/cancers12041020

Sankaranarayanan, R., & Ferlay, J. (2006). Worldwide burden of gynaecological cancer: The size of the problem. *Best Practice & Research Clinical Obstetrics & Gynaecology*, *20*(2), 207–225. https://doi.org/10.1016/j.bpobgyn.2005.10.007

Sofiadis, K., Josipovic, N., Nikolic, M., Kargapolova, Y., Übelmesser, N., Varamogianni-Mamatsi, V., Zirkel, A., Papadionysiou, I., Loughran, G., Keane, J., Michel, A., Gusmao, E. G., Becker, C., Altmüller, J., Georgomanolis, T., Mizi, A., & Papantonis, A. (2021). HMGB1 coordinates SASP-related chromatin folding and RNA homeostasis on the path to senescence. *Molecular Systems Biology*, *17*(6), 1–17. https://doi.org/10.15252/msb.20209760

Starkova, T., Polyanichko, A., Tomilin, A. N., & Chikhirzhina, E. (2023). Structure and Functions of HMGB2 Protein. *International Journal of Molecular Sciences*, *24*(9), 8334. https://doi.org/10.3390/ijms24098334

Štros, M. (2010). HMGB proteins: Interactions with DNA and chromatin. *Biochimica et Biophysica Acta (BBA) - Gene Regulatory Mechanisms*, *1799*(1–2), 101–113. https://doi.org/10.1016/j.bbagrm.2009.09.008

Subramanian, A., Tamayo, P., Mootha, V. K., Mukherjee, S., Ebert, B. L., Gillette, M. A., Paulovich, A., Pomeroy, S. L., Golub, T. R., Lander, E. S., & Mesirov, J. P. (2005). Gene set enrichment analysis: A knowledge-based approach for interpreting genome-wide expression profiles. *Proceedings of the National Academy of Sciences*, *102*(43), 15545–15550. https://doi.org/10.1073/pnas.0506580102

Sung, H., Ferlay, J., Siegel, R. L., Laversanne, M., Soerjomataram, I., Jemal, A., & Bray, F. (2021). Global Cancer Statistics 2020: GLOBOCAN Estimates of Incidence and Mortality Worldwide for 36 Cancers in 185 Countries. *CA: A Cancer Journal for Clinicians*, *71*(3), 209–249. https://doi.org/10.3322/caac.21660

Tang, D., Kang, R., Livesey, K. M., Cheh, C.-W., Farkas, A., Loughran, P., Hoppe, G., Bianchi, M. E., Tracey, K. J., Zeh, H. J., & Lotze, M. T. (2010). Endogenous HMGB1 regulates autophagy. *Journal of Cell Biology*, *190*(5), 881–892. https://doi.org/10.1083/jcb.200911078

Tang, D., Kang, R., Zeh, H. J., & Lotze, M. T. (2011). High-Mobility Group Box 1, Oxidative Stress, and Disease. *Antioxidants & Redox Signaling*, *14*(7), 1315–1335. https://doi.org/10.1089/ars.2010.3356

Ueland, F. (2017). A Perspective on Ovarian Cancer Biomarkers: Past, Present and Yet-To-Come. *Diagnostics*, *7*(1), 14. https://doi.org/10.3390/diagnostics7010014

Van Nostrand, E. L., Nguyen, T. B., Gelboin-Burkhart, C., Wang, R., Blue, S. M., Pratt, G. A., Louie, A. L., & Yeo, G. W. (2017). Robust, Cost-Effective Profiling of RNA Binding Protein Targets with Single-end Enhanced Crosslinking and Immunoprecipitation (seCLIP). In *Methods in Molecular Biology* (pp. 177–200).

https://doi.org/10.1007/978-1-4939-7204-3_14

Wang, K. C., & Chang, H. Y. (2011). Molecular Mechanisms of Long Noncoding RNAs. *Molecular Cell*, *43*(6), 904–914. https://doi.org/10.1016/j.molcel.2011.08.018

Weir, H. M., Kraulis, P. J., Hill, C. S., Raine, A. R., Laue, E. D., & Thomas, J. O. (1993). Structure of the HMG box motif in the B-domain of HMG1. *The EMBO Journal*, *12*(4), 1311–1319. https://doi.org/10.1002/j.1460-2075.1993.tb05776.x

World Health Organization. (2023). *Cancer*. https://www.who.int/health-topics/cancer

Yamanaka, Y., Faghihi, M. A., Magistri, M., Alvarez-Garcia, O., Lotz, M., & Wahlestedt, C. (2015). Antisense RNA Controls LRP1 Sense Transcript Expression through Interaction with a Chromatin-Associated Protein, HMGB2. *Cell Reports*, *11*(6), 967–976. https://doi.org/10.1016/j.celrep.2015.04.011

Yanai, H., Ban, T., Wang, Z., Choi, M. K., Kawamura, T., Negishi, H., Nakasato, M., Lu, Y., Hangai, S., Koshiba, R., Savitsky, D., Ronfani, L., Akira, S., Bianchi, M. E., Honda, K., Tamura, T., Kodama, T., & Taniguchi, T. (2009). HMGB proteins function as universal sentinels for nucleic-acid-mediated innate immune responses. *Nature*, *462*(7269), 99–103. https://doi.org/10.1038/nature08512

Yang, S., Ye, Z., Wang, Z., & Wang, L. (2020). High mobility group box 2 modulates the progression of osteosarcoma and is related with poor prognosis. *Annals of Translational Medicine*, *8*(17), 1082–1082. https://doi.org/10.21037/atm-20-4801

Zhao, J., Ohsumi, T. K., Kung, J. T., Ogawa, Y., Grau, D. J., Sarma, K., Song, J. J., Kingston, R. E., Borowsky, M., & Lee, J. T. (2010). Genome-wide Identification of Polycomb-Associated RNAs by RIP-seq. *Molecular Cell*, *40*(6), 939–953. https://doi.org/10.1016/j.molcel.2010.12.011

Supplementary material list

Chapter 1. Identification of lncRNAs deregulated in epithelial ovarian cancer based on a gene expression profiling meta-analysis.

Supplementary Table S1.xlsx

Supplementary Table S2.xlsx

Supplementary Table S3.xlsx

Supplementary Table S4.xlsx

Supplementary Table S5.xlsx

Supplementary Table S6.xlsx

Supplementary Table S7.xlsx

Supplementary Table S8.xlsx

Supplementary Table S9.xlsx

Supplementary Table S10.xlsx

Supplementary Table S11.xlsx

Supplementary Table S12.xlsx

Supplementary Figure S1.pdf

Chapter 2. Identification of HMGB1/2-RNA interactions in ovarian cancer cell lines.

Supplementary Materials Table S13.xlsx

Supplementary Materials Table S14.xlsx

Supplementary Materials Table S15.xlsx

Supplementary Materials Table S16.xlsx

Supplementary Materials Table S17.xlsx

Supplementary Materials Table S18.xlsx

Supplementary Materials Table S19.xlsx

Supplementary Materials Figure S2 & S3.pdf

Supplementary material list

Chapter 3. Effects of HMGB1 and HMGB2 on the transcriptome of an ovarian cancer cell line.

Supplementary Materials Table S1.xlsx

Supplementary Materials Table S2.xlsx